Understanding biodiversity and resilience of forest ecosystems using integrated remote sensing and trait-based approaches

A thesis submitted for the degree of Doctor of Philosophy

Xiongjie Deng

Supervisors: Dr Jesús Aguirre-Gutiérrez and Professor Yadvinder Malhi

School of Geography and the Environment

University of Oxford

Trinity Term 2025

若升高，必自下。

若陟遐，必自迩。

——《尚书·商书·太甲下》

Ruò Shēng Gāo, Bì Zì Xià.

Ruò Zhì Xiá, Bì Zì Ěr.

--Shàng Shū, Shāng Shū, Tài Jiǎ Xià

To rise high, one must begin from below.

To reach far, one must start from nearby.

--Book of Documents, Book of Shang, Taijia Part III

Abstract

Forests play a critical role in regulating climate, cycling nutrients, and providing habitat for a large proportion of global biodiversity. In addition, they contribute essential ecosystem services, such as carbon sequestration, water regulation, and the provision of resources for human livelihoods. Understanding the biodiversity of forest ecosystems is key to assessing their capacity to maintain these functions, especially as biodiversity strongly influences ecosystem resilience and productivity.

However, these vital forest ecosystems face severe threats from anthropogenic activities, including deforestation, land-use change, and climate change. These pressures have intensified the frequency of extreme weather events, such as droughts and heatwaves. Such disturbances pose a significant risk to the long-term stability and resilience of forest ecosystems, challenging their ability to provide these functions and services.

Functional trait ecology offers a powerful framework for understanding how forests respond to these pressures. Plant functional traits include morphological, physiological, and phenological characteristics that govern growth, survival, and reproduction, they determine species' responses to stress and influence key ecosystem processes such as productivity, nutrient cycling, and recovery after disturbance. By focusing on the composition, diversity, and redundancy of these traits, this thesis moves beyond species-level assessments to explore the mechanisms underpinning forest resilience and to inform more effective conservation and management strategies in the context of global change. However, measuring these traits in the field is time-consuming, labour-intensive, and spatially limited, which hinders our ability to assess ecosystem properties at landscape to global scales.

This limitation can be overcome by integrating *in-situ* trait data with advanced remote sensing technologies to investigate how functional trait composition, diversity, and redundancy affect the resilience of tropical and temperate forests, as well as to explore their spatial distribution and patterns of variation across geographical and environmental gradients. Remote sensing is increasingly central to ecological research, and it enables trait estimation and ecosystem monitoring over large spatial scales with high temporal resolution. This thesis leverages multi-source remotely sensed data including passive imagery and active data from multi-scale platforms such as close-range devices, drones, and satellites. By combining these data with environmental variables and employing machine learning and deep learning algorithms, this research explores spatial patterns of forest functional composition, diversity,

and redundancy, and evaluates their ecological significance across a range of biomes. The work is organised into three interconnected studies.

The first study (**Chapter 4**) develops and validates methods for mapping and predicting 15 functional traits at a pan-tropical scale. It demonstrates how combining multi-source remotely sensed data with machine learning and deep learning algorithms can improve predictions of these traits across tropical forests and identifies key predictors for trait prediction and assesses their relative contributions across different trait groups, which establishes a robust methodology for the subsequent analyses.

The second study (**Chapter 5**) focuses on temperate forests across a large latitudinal and environmental gradient from 30°S to 53°S in South America. It maps functional trait composition, diversity, and redundancy, identifies key environmental drivers, and highlights potential "resilience hotspots" where high functional diversity and redundancy co-occur, suggesting a greater capacity to withstand environmental pressures.

The third study (**Chapter 6**) examines the role of plant functional trait diversity and redundancy in modulating forest carbon resilience to extreme drought events in Mexico. Using long-term forest inventory data from 2007 to 2021, this study assesses how initial levels of functional diversity and redundancy affect forest responses to prolonged and severe drought. The trait-based perspective provides new insights into the mechanisms that support ecosystem stability during climatic extremes.

Together, these three studies contribute to a deeper understanding of how functional traits mediate the structure, function, and resilience of forest ecosystems across different biomes and environmental contexts. By combining trait-based ecology with advanced remote sensing and computational approaches, this thesis advances both theoretical and applied dimensions of ecological research. It offers scalable tools and empirical evidence to support biodiversity conservation, ecosystem monitoring, and climate adaptation planning in a rapidly changing world.

Acknowledgements

First and foremost, I owe my deepest gratitude to my parents. As《诗经》(*Shī Jīng*, The Book of Songs: The Ancient Chinese Classic of Poetry) says:

"哀哀父母，生我劬劳。"

(*Āi Āi Fù Mǔ, Shēng Wǒ Qú Láo.*)

"How constant is the sorrow of our parents, who gave us life and raised us with toil."

"父兮生我，母兮鞠我。拊我畜我，长我育我，顾我复我，出入腹我。欲报之德。昊天罔极！"

(*Fù Xī Shēng Wǒ, Mǔ Xī Jū Wǒ. Fǔ Wǒ Xù Wǒ, Zhǎng Wǒ Yù Wǒ, Gù Wǒ Fù Wǒ, Chū Rù Fù Wǒ. Yù Bào Zhī Dé. Hào Tiān Wǎng Jí!*)

"My father and my mother gave me life and nurtured me. They comforted me, fed me, raised me, and taught me. They looked after me, protected me, and carried me in their arms wherever they went. If I would repay their kindness, it is as boundless as the sky!" This ancient verse barely captures what my parents have always given me. Their constant support has been the foundation of my academic journey, a journey that has taken me from an underprivileged and remote region in western China to leading universities for my undergraduate and master's degrees, and ultimately, to the University of Oxford for my DPhil.

This journey has been paved with their enormous sacrifices. During my doctoral study in the UK, my father underwent two major surgeries in 2022, and my mother had operations on both eyes in 2025. Despite their health struggles, they have never wavered in their encouragement and love. I carry a profound sense of guilt for not being by their side during these difficult times, yet in every conversation, they brushed aside their own hardships and offered only encouragement and reassurance. I also carry with me the loving memory of my grandfather, who had always hoped to see me achieve more but sadly passed away just one year before I left China, his absence has been a quiet grief throughout this journey. It was their collective dream and support that lifted me to where I am today, and for this, my gratitude is indeed as boundless as the sky.

I would like to express my heartfelt appreciation to my two supervisors, Dr Jesús Aguirre-Gutiérrez and Professor Yadvinder Malhi. Dr Jesús Aguirre-Gutiérrez provided hands-on guidance throughout the research process and helped me sharpen my thinking and analytical

approach. My gratitude to Professor Yadvinder Malhi is equally profound. As a leading expert in the field, Professor Yadvinder Malhi yet has always found time to offer me high-level academic direction and, most touchingly, personal care and encouragement. As a Chinese student adjusting to doctoral life in a foreign country, I occasionally felt isolated; yet every year, Professor Yadvinder Malhi warmly invited lab members to his home for holiday celebrations. A particular moving memory I will never forget happened at a conference on Latin America-related research held at the University of Leeds in March 2023. I was the only person present who spoke neither Spanish nor Portuguese. When a presenter mentioned they would speak in Spanish due to not feeling fluent in English, and others agreed it was fine, Professor Yadvinder Malhi immediately added, "If we want to switch to Chinese, we have a candidate for that too." Later that evening, when we raised our glasses to toast, others said "cheers" in English or Spanish or Portuguese, he also turned to me and said "干杯" (pronounced "*Gān Bēi*") and confirmed with me if he had pronounced it correctly. That moment made me feel deeply included and respected, and it meant more than I can ever express in words.

My heartfelt thanks also go to my college advisor, Dr Hugo Slim, and his wife Asma. Their kindness has been a comforting light throughout my time in Oxford. Every year, Dr Hugo Slim would personally drive me to his home to celebrate Christmas Day with his family and invited me to enjoy the serene English summers at his house. The thoughtful Christmas gifts they chose for me each year made me feel truly at home in a foreign land. Furthermore, I struggled frequently with severe dental pain and was unable to register with any NHS dental clinics due to overcapacity in Oxford. On multiple occasions, Dr Hugo Slim went out of his way to help me find timely and affordable treatment, which eased a major burden during my studies. For their warmth and support, I am truly grateful.

My sincere thanks also go to members of the research lab. I would especially like to thank Dr Huanyuan Zhang-Zheng, Dr Nicola Stevens, Dr Eleanor Thomson, Dr Felipe Ribeiro Martello, Dr Milton Barbosa, and Mr Haoran Wu, for their insightful discussions and help with my research. In particular, I am grateful to Dr Huanyuan Zhang-Zheng, a former DPhil student and current postdoctoral fellow in the lab, whom I still prefer to call 师兄 (*Shī Xiōng*), a term meaning senior male colleague or, more intuitively, academic elder brother, despite local customs of addressing each other by name. This term carries a sense of respect, closeness, and kinship that I deeply value. On my very first day in the UK, he picked me up, welcomed me to his home for dinner, and even provided food and supplies during the initial days when I had no

bank card or local access. Thanks to him, my transition was far smoother and warmer than I ever expected.

I also wish to express my gratitude to Professor Zhenfeng Shao and Professor Deren Li from China. They were the ones who wholeheartedly supported my ambition to pursue a doctorate abroad. Throughout my DPhil studies, they have continued to be a source of encouragement and have maintained a collaborative relationship with me. Their academic guidance on Chapter 4 of my thesis was invaluable. Their sustained belief in my potential has been a powerful motivating force.

Last but not least, I am deeply grateful to the China Oxford Scholarship Fund (Pay It Forward Award) and Blackfriars Hall, Oxford, for their generous support throughout my doctoral studies.

Table of Contents

Outputs of doctorate

My second paper has been published in *International Journal of Applied Earth Observation and Geoinformation*:

Deng, X.[*], Carvajal, D., Urrutia-Jalabert, R., Machida, W., Rosen, A., Zhang-Zheng, H., Galbraith, D., Díaz, D., Malhi, Y., & Aguirre-Gutiérrez, J. (2025). Quantifying the functional composition and potential resilience hotspots across a large latitudinal and environmental gradient in South American forests. *International Journal of Applied Earth Observation and Geoinformation*, 142, 104704. https://doi.org/10.1016/j.jag.2025.104704

During my DPhil, I was involved in the following papers and monograph chapter:

(1) Aguirre-Gutiérrez, J., Rifai, S. W., **Deng, X.**, ter Steege, H., Thomson, E., Corral-Rivas, J. J., Guimaraes, A. F., Muller, S., Klipel, J., Fauset, S., Resende, A. F., Wallin, G., Joly, C. A., Abernethy, K., Adu-Bredu, S., Alexandre Silva, C., de Oliveira, E. A., Almeida, D. R. A., Alvarez-Davila, E., … Malhi, Y. (2025). Canopy functional trait variation across Earth's tropical forests. *Nature*, 1–8. https://doi.org/10.1038/s41586-025-08663-2

(2) Zhang-Zheng, H., **Deng, X.**, Aguirre-Gutiérrez, J., Stocker, B. D., Thomson, E., Ding, R., Adu-Bredu, S., Duah-Gyamfi, A., Gvozdevaite, A., Moore, S., Oliveras Menor, I., Prentice, I. C., & Malhi, Y. (2024). Why models underestimate West African tropical forest primary productivity. *Nature Communications*, 15(1), 9574. https://doi.org/10.1038/s41467-024-53949-0

(3) Zhang-Zheng, H., Adu-Bredu, S., Duah-Gyamfi, A., Moore, S., Addo-Danso, S. D., Amissah, L., Valentini, R., Djagbletey, G., Anim-Adjei, K., Quansah, J., Sarpong, B., Owusu-Afriyie, K., Gvozdevaite, A., Tang, M., Ruiz-Jaen, M. C., Ibrahim, F., Girardin, C. A. J., Rifai, S., Dahlsjö, C. A. L., Riutta, T., **Deng, X.**, Sun, Y., Prentice, I. C., Oliveras Menor, I., & Malhi, Y. (2024). Contrasting carbon cycle along tropical forest aridity gradients in West Africa and Amazonia. *Nature Communications*, 15(1), 3158. https://doi.org/10.1038/s41467-024-47202-x

(4) Malhi, Y., Christmann, T., **Deng, X.**, Zhang-Zheng, H., Moore, S., & Riutta, T. (2024). Forest carbon budgets and climate change. In *Routledge Handbook of Forest Ecology* (2nd ed.). Routledge.

(5) Chen, J., Shao, Z., **Deng, X.**, Huang, X., & Dang, C. (2023). Vegetation as the catalyst for water circulation on global terrestrial ecosystem. *Science of The Total Environment*, 895, 165071. https://doi.org/10.1016/j.scitotenv.2023.165071

List of abbreviations

AGC: Aboveground carbon

ALE: Alerce Costero

A_{max}: Light-saturated maximum rates of net photosynthesis at saturated CO_2 (2000 ppm CO_2)

Aopt: Photosynthesis rate at optimum temperature

A_{sat}: Light-saturated rates of net photosynthesis at ambient CO_2 concentration (400 ppm CO_2)

AVIRIS: Airborne Visible/Infrared Imaging Spectrometer

BIEN: Botanical Information and Ecology Network

BWD: Branch wood density

C: Carbon

Ca: Calcium

CAB: Las Cabras

COR: Correntoso

CWM: Community-weighted mean

CWV: Community-weighted variance

DBH: Diameter at breast height

DEM: Digital elevation model

DW: Dry weight

ECOSTRESS: ECOsystem Spaceborne Thermal Radiometer Experiment on Space Station

ESI: Evaporative stress index

ET: Evapotranspiration

FD: Functional diversity

FDis: Functional dispersion

FRed/FR: Functional redundancy

FW: Fresh weight

GEDI: Global Ecosystem Dynamics Investigation

GEE: Google Earth Engine

GEM: Global Ecosystems Monitoring

GFCH: Global Forest Canopy Height

K: Potassium

LA: Leaf area

LDMC: Leaf dry matter content

LiDAR: Light detection and ranging

LMA: Leaf mass per area

MAG: Magallanes National Reserve

MCWD: Maximum climatological water deficit

Mg: Magnesium

MLP: Multilayer Perceptron

MONAFOR: Monitoreo Nacional Forestal network

MSAVI: Modified soil-adjusted vegetation index

N: Nitrogen

NDRE: Normalised difference red-edge index

NDVI: Normalised difference vegetation index

NIR: Near-infrared

P: Phosphorus

P50: Water potential at which 50% of hydraulic conductivity is lost

P88: Water potential at which 88% of hydraulic conductivity is lost

R^2: Coefficient of determination

RAD: Radal 7 Tazas

Radar: Radio detection and ranging

RF: Random forests

RMSE: Root mean square error

SAR: Synthetic aperture radar

SAVI: Soil-adjusted vegetation index

SLA: Specific leaf area

SM50: Hydraulic safety margin P50

SM88: Hydraulic safety margin P88

SPT: San Pablo de Tregua

SRTM: Shuttle Radar Topography Mission

SWIR: Shortwave infrared

T50: Temperature at which the maximum quantum yield of the photosystem II declines to 50%

TmaxL: Temperature at carbon compensation point

TNRS: Taxonomic Name Resolution Service

Topt: Temperature of optimum photosynthesis

TRA: Trapananda National Reserve

TspanL: Breadth of temperature optimum

TWD: Trunk wood density

VPD: Vapour pressure deficit

WPmd: Minimum water potential (midday water potential at the driest month)

WUE: Water use efficiency

Abbreviations of organisations

ESA: European Space Agency

NASA: National Aeronautics and Space Administration

USGS: United States Geological Survey

List of figures

Chapter 1

Chapter 3

Chapter 4

Fig. S4.13. Distribution and variation patterns of A_{sat} at continental and pan-tropical scales.

Fig. S4.14. Distribution and variation patterns of leaf carbon (C) content at continental and pan-tropical scales.

Fig. S4.15. Distribution and variation patterns of leaf calcium (Ca) content at continental and pan-tropical scales.

Fig. S4.16. Distribution and variation patterns of leaf dry mass (DM) at continental and pan-tropical scales.

Fig. S4.17. Distribution and variation patterns of leaf fresh mass (FM) at continental and pan-tropical scales.

Fig. S4.18. Distribution and variation patterns of leaf potassium (K) content at continental and pan-tropical scales.

Fig. S4.19. Distribution and variation patterns of leaf water content (LWC) at continental and pan-tropical scales.

Fig. S4.20. Distribution and variation patterns of leaf nitrogen (N) content at continental and pan-tropical scales.

Fig. S4.21. Distribution and variation patterns of leaf phosphorus (P) content at continental and pan-tropical scales.

Fig. S4.22. Distribution and variation patterns of specific leaf area (SLA) at continental and pan-tropical scales.

Fig. S4.23. Distribution and variation patterns of leaf thickness at continental and pan-tropical scales.

Fig. S4.24. Distribution and variation patterns of wood density (WD) at continental and pan-tropical scales.

Fig. S4.25. Stacked bar plot for the importance of each variable for predicting each of the functional trait.

Fig. S4.26. Density distribution plot of vapour pressure deficit for each sampling country where plant functional traits were collected.

Chapter 5

Fig. 5.4. Mean variable importance of input data groups for predicting community-weighted mean (CWM) and community-weighted variance (CWV) of the four categories of functional traits.

Fig. 5.5. Mean variable importance of input data groups for predicting functional diversity (FDis) and redundancy (FRed) of the four categories of functional traits.

Supplementary figures:

Fig. S5.1. Trait within-category correlation.

Fig. S5.2. Input band within-category correlation.

Fig. S5.3. Distribution maps of CWM of FW, DW, LA, and SLA.

Fig. S5.4. Distribution maps of CWM of TWD, N, P, and Ca.

Fig. S5.5. Distribution maps of CWM of Mg, P50, P88, and WPmd.

Fig. S5.6. Distribution maps of CWM of TmaxL, TspanL, Topt, and T50.

Fig. S5.7. Distribution maps of CWV of FW, DW, LA, and SLA.

Fig. S5.8. Distribution maps of CWV of TWD, N, P, and Ca.

Fig. S5.9. Distribution maps of CWV of Mg, P50, P88, and WPmd.

Fig. S5.10. Distribution maps of CWV of TmaxL, TspanL, Topt, and T50.

Fig. S5.11. Distribution maps of FDis of morphological, nutrients, hydraulic, and photosynthetic traits.

Fig. S5.12. Distribution maps of FRed of morphological, nutrients, hydraulic, and photosynthetic traits.

Fig. S5.13. The contribution of each variable in predicting morphological traits.

Fig. S5.14. The contribution of each variable in predicting nutrient traits.

Fig. S5.15. The contribution of each variable in predicting hydraulic traits.

Fig. S5.16. The contribution of each variable in predicting photosynthetic traits.

Chapter 6

Fig. S6.9. Interaction effects between predictors on the change rate of carbon gains in temperate forest.

Fig. S6.10. Interaction effects between predictors on the change rate of carbon losses in temperate forest.

Fig. 6.S11. Heatmap of pairwise correlation between predictors.

List of tables

Chapter 2

Chapter 4

Chapter 5

Table 5.1. Latitudinal patterns of functional diversity (FDis) and functional redundancy (FRed), and corresponding ecological interpretation in South American temperate forests.

Supplementary tables:

Table S5.1. Total tree species richness and relative abundance (estimated from basal area) at each site.

Table S5.2. Information on plot locations, elevations, and sizes.

Table S5.3. Description of all morphological traits measured and calculated in Chile and the reasons why they were measured in this study.

Table S5.4. Description of all leaf nutrients measured in Chile and the reasons why they were measured in this study.

Table S5.5. Description of all hydraulic traits measured in Chile and the reasons why they were measured in this study.

Table S5.6. Description of all photosynthetic traits measured in Chile and the reasons why they were measured in this study.

Table S5.7. Description of multispectral images collected for each plot.

Table S5.8. Description of LiDAR data collected for each plot.

Table S5.9. Vegetation indices generated from spectral bands.

Table S5.10. Model performance for mapping the two community-weighted moments of morphological traits.

Table S5.11. Model performance for mapping the two community-weighted moments of nutrient traits.

Table S5.12. Model performance for mapping the two community-weighted moments of hydraulic traits.

Table S5.13. Model performance for mapping the two community-weighted moments of photosynthetic traits.

Table S5.14. Model performance for assessing the four groups of FDis and FRed.

Chapter 1 Introduction

1.1. Background

Forests, particularly tropical and temperate ecosystems, are among the most biodiverse and productive ecosystems on Earth (Cooper et al., 2024; Malhi et al., 2011). Together, they cover nearly 2.48 billion hectares or ~61% of total forest area (~19% of the planet's land area) (*Global Forest Resources Assessment 2020*, 2020) but contribute more than 60% of global terrestrial productivity and harbour over half of global biodiversity (Malhi et al., 2021; Pillay et al., 2022). Beyond their ecological functions, forests also provide a wide range of ecosystem services critical for global ecological stability and human well-being (Brockerhoff et al., 2017; Pan et al., 2011). These services include carbon sequestration (Brockerhoff et al., 2017; Oliver et al., 2015), water regulation (Seidl et al., 2019), nutrient cycling (Negi, 2022), and the provision of resources for human livelihoods (Langat et al., 2016; Oldekop et al., 2020). The diversity of plant species in these forests underpins the resilience of the ecosystem (Oliver et al., 2015) and enhances its capacity to adapt to and recover from disturbances such as climate change (Forzieri et al., 2022), extreme weather events (D'Andrea et al., 2021), and anthropogenic pressures (Forzieri et al., 2022; Guz & and Kulakowski, 2020). By supporting a wide range of functional traits among their species, tropical and temperate forests provide ecological "insurance" against changing conditions, making them invaluable for understanding biodiversity and ecosystem resilience (Bello et al., 2021; Gladstone-Gallagher et al., 2019; Oliver et al., 2015; Tilman et al., 2014).

1.1.1. Trait-based ecology: A functional perspective

The study of plant functional traits, often termed trait-based ecology, has emerged as a central framework for understanding the mechanisms governing plant community assembly, ecosystem functioning, and responses to environmental change (Lavorel & Garnier, 2002; McGill et al., 2006; Violle et al., 2007). Violle et al. (2007) defined a trait as "any morphological, physiological or phenological feature measurable at the individual level, from the cell to the whole organism", and emphasised that for a trait to be considered truly functional, it must "impact fitness (of an individual) indirectly via its effects on growth, reproduction and survival". Thus, in essence, functional traits can be summarised as the morpho-physio-phenological characteristics of organisms that influence their performance (growth, survival, reproduction) and, consequently, their fitness (Violle et al., 2007). These functional traits

reflect fundamental trade-offs in resource acquisition, utilisation, and conservation strategies evolved by plants in response to abiotic and biotic pressures (Sterck et al., 2011). Furthermore, from the perspective of functional ecology, they are pivotal as they mechanistically underpin both species' contributions to ecosystem properties and services, and their tolerance of environmental stressors and disturbances (Díaz et al., 2013; Suding et al., 2008).

Unlike species-based approaches, which focus on the identity of the organism and abundance of species (Gagic et al., 2015; Zakharova et al., 2019), trait-based approaches analyse species' functional roles and how these influence ecological processes (Laughlin, 2014). This framework is particularly valuable in diverse and complex systems like tropical and temperate forests, where the vast number of species and complicated interactions make it challenging to predict ecosystem dynamics using traditional species-level studies alone (Swenson & Rubio, 2025; Zakharova et al., 2019).

Plant functional traits relevant to forest ecosystems can be broadly grouped into morphological, leaf nutrient and related physiological, and phenological categories. Morphological traits refer to physical structures that influence plant form and resource acquisition strategies (Freschet et al., 2018; Hanley et al., 2007). Leaf nutrients and related physiological traits encompass both the chemical composition of leaf tissues, such as concentrations of nitrogen, phosphorus, and potassium, and associated traits like photosynthetic traits (e.g., photosynthetic rates) and hydraulic traits (e.g., water potential and hydraulic conductivity), which are linked to carbon assimilation and drought tolerance (Domec et al., 2017; Gessler et al., 2017; Guadarrama-Escobar et al., 2024). Although the broader category of physiological traits includes multiple dimensions, this thesis primarily focuses on leaf nutrients, which are assessed in all three studies (**Chapters 4**, **5**, and **6**), photosynthetic traits are included in **Chapters 4** and **5**, and hydraulic traits are examined specifically in **Chapter 5**. Finally, phenological traits capture the seasonal timing of key life cycle events (Post et al., 2008), including timing of leaf emergence, leaf lifespan, and time of flowering and fruit development.

To scale from individual plants to entire ecosystems, these traits are commonly characterised using community-level metrics that describe the functional structure of the community. The community-weighted mean (CWM) of a trait reflects the dominant functional strategy within a community (Bruelheide et al., 2018; Enquist et al., 2015; Muscarella & Uriarte, 2016). Complementing this, metrics of functional diversity (FD), such as functional dispersion (FDis), quantify the value, range, and distribution of traits present (Díaz & Cabido,

2001; Laliberté & Legendre, 2010). Finally, functional redundancy (FRed) measures the degree of overlap in functional roles among species (Rosenfeld, 2002), providing crucial insight into a community's potential stability and resilience to species loss (Biggs et al., 2020). These metrics can be quantified by related formulations (see **Section 3.3. Calculating functional trait composition, diversity, and redundancy, and carbon resilience** for details).

The comprehensive assessment of these community-level trait metrics (CWM, CWV, FDis, and FRed) is crucial for evaluating ecosystem responses to environmental drivers, disturbances, and for predicting changes in ecosystem functioning and stability (Bruelheide et al., 2018; Díaz, Lavorel, McINTYRE, et al., 2007; Oliver et al., 2015; Tilman et al., 2014). However, obtaining such comprehensive trait information across extensive spatial scales and through time using traditional field-based measurements presents considerable logistical and financial challenges (Wang & Gamon, 2019; Zheng et al., 2022). This challenge necessitates the exploration of alternative methodologies capable of providing spatially contiguous and temporally repeatable observations of vegetation functional characteristics.

1.1.2. Remote sensing for forest monitoring and trait estimation

Whilst traditional field-based ecological surveys are fundamental for characterising vegetation functional traits, they are inherently time- and resource-demanding (Wang & Gamon, 2019) and share the challenges outlined above. In addition, outcomes from traditional field surveys can be context-dependent, varying with environmental conditions and spatial scales (Gaston, 2000; Palmer et al., 2002; Wang & Gamon, 2019), and may be influenced by human bias (Asner et al., 2015; Lõhmus et al., 2018; Thomson et al., 2021). Remote sensing, the science of acquiring information about the Earth's surface without direct physical contact (Cavender-Bares et al., 2020), offers powerful tools to address these challenges by providing spatially contiguous and temporally repeatable observations across various scales, which allows to monitor the vast and often inaccessible regions of tropical and temperate forests and to quantify the spatial and temporal dynamics of their functional characteristics (Asner et al., 2015, 2017; Cavender-Bares et al., 2022; Helfenstein et al., 2022; Knyazikhin et al., 2013; Schneider et al., 2017).

The progression of remote sensing in forest ecology has been driven by advancements in sensor technology, analytical methods, and the integration of remotely sensed data with ecological theories. Several types of remotely sensed data are particularly relevant for

characterising forest functional trait composition, diversity, and redundancy, and they can be broadly categorised into passive and active systems (Kavzoglu et al., 2024). Passive sensors detect naturally reflected or emitted electromagnetic radiation from the Earth's surface, primarily solar radiation (Tedesco, 2015), whereas active sensors provide their own source of illumination and measure the backscattered signal (Tedesco, 2015). Passive sensors, ranging from multispectral to hyperspectral, are primarily sensitive to the biochemical properties of vegetation (Pandey et al., 2017), such as leaf pigments, water content, and chemical constituents, which are key components of many functional traits. Active sensors offer complementary information, particularly for characterising leaf chemical, physiological, and plant structural information (Cavender-Bares et al., 2020; Ollinger, 2011). For instance, light detection and ranging (LiDAR) directly measures the three-dimensional structure of the forest canopy (Calders et al., 2014; Goodwin et al., 2006), while synthetic aperture radar (SAR) is sensitive to forest structure, biomass, and moisture content (Inoue et al., 2014; Pourshamsi et al., 2021), with the unique ability to penetrate clouds (Mermoz et al., 2015).

The utility of these sensors is further expanded by the variety of platforms on which they can be deployed, each offering different advantages in terms of spatial coverage, resolution, and revisit frequency. These sensors range from satellites with global and repetitive coverage, to airborne systems with flexible and high-resolution mapping, and drones with on-demand and ultra-high-resolution data for local-scale studies. Crucially, the most comprehensive characterisation of forest ecosystems often arises from the integration of these different data types (data fusion) (Mohammadpour & Viegas, 2022; Torabzadeh et al., 2014). The ability to map plant functional traits and estimate functional diversity and redundancy through remote sensing enables the exploration of ecological patterns and processes at unprecedented spatial and temporal scales, offering vital data for biodiversity monitoring, ecosystem modelling, and informed conservation planning (Jetz et al., 2016; Wang & Gamon, 2019).

1.2. Knowledge gaps and key challenges

Despite significant advancements in trait-based ecology and remote sensing technologies, several critical challenges persist in accurately monitoring and understanding the functional dynamics of forest ecosystems, particularly at large spatial scales and in the context of global

environmental change. This thesis aims to fill in the following knowledge gaps and overcome the several key challenges:

(1) Improving large-scale trait prediction and optimising data integration and analytical approaches: While remote sensing shows promise for trait estimation, the accuracy and reliability of predicting a comprehensive set of functional traits (morphology, nutrients, photosynthesis, etc.) across large and heterogeneous landscapes like the pan-tropics remain a significant challenge (Aguirre-Gutiérrez et al., 2025; Zheng et al., 2022). There is a need to systematically evaluate the combined utility of multi-source remotely sensed data (spectral, SAR, and LiDAR) from multiple platforms (close-range sensing, drone, and satellite) and advanced modelling techniques (machine learning and deep learning) for this purpose, and to identify the relative contributions of different data and environmental variables such as climate, soil properties, and topography (Aguirre-Gutiérrez et al., 2025; Durán et al., 2019). In addition, the integration of diverse datasets and the application of appropriate analytical methods require careful evaluation to maximise predictive accuracy and ecological insight. Determining which combinations of data and methods are most effective for specific traits or ecological questions is an ongoing research frontier (Cavender-Bares et al., 2020; Wang & Gamon, 2019).

(2) Characterising functional trait composition, diversity, redundancy, and their drivers in diverse ecosystems: Accurately inferring functional trait composition, diversity, and redundancy across broad environmental gradients is pivotal for understanding how forest ecosystems respond to ongoing environmental change (Cavender-Bares et al., 2022; Schneider et al., 2017). Understanding how these functional attributes are shaped by key environmental drivers is essential for identifying areas of high ecological resilience or vulnerability (Biggs et al., 2020; Hisano et al., 2024; Oliver et al., 2015; Tavares et al., 2023). By identifying the environmental gradients that most strongly shape functional diversity and redundancy, we can locate ecosystems that are particularly sensitive to change, as well as those that may serve as refugia or resilience hotspots under future climate scenarios (Oliver et al., 2015; Trew & Maclean, 2021). This is particularly important in biodiverse and climatically variable regions, where management and conservation strategies must be informed by an understanding of how trait-based functional patterns interact with environmental pressures (Díaz et al., 2013; Díaz, Lavorel, De Bello, et al., 2007).

(3) Linking functional diversity and redundancy to forest resilience under climate change: Forest ecosystems globally face increasing threats from climate change, including more frequent and severe climatic stress events such as drought (Allen et al., 2010; Malhi et

al., 2020). A critical research problem is to understand the overall resilience of these ecosystems-their ability to withstand and recover from such disturbances. Within this broader context of ecosystem resilience, the mechanisms by which functional diversity influences specific processes, such as forest carbon stocks and dynamics (gains, losses, and net sink), are not fully understood (Brienen et al., 2015; Hubau et al., 2020; Maia et al., 2020; Sullivan et al., 2020). This is particularly essential regarding the differential roles of various trait dimensions (e.g., morphological traits, nutrients, and hydraulic traits) in conferring resilience to the carbon cycle (Hisano et al., 2024; Sakschewski et al., 2016; Tavares et al., 2023). Investigating these relationships in forests is critical for forecasting overall ecosystem stability and the future of forest carbon sinks under climate change (Hubau et al., 2020).

1.3. Research questions and hypotheses

The overarching aim of this doctoral research is to quantify and model functional trait composition, diversity, and redundancy in tropical and temperate forests, and to assess how these trait metrics influence ecosystem stability under environmental stress. Specifically, this thesis addresses the following research questions:

(1) To what extent does integrating multi-sensor remotely sensed data with environmental variables improve the prediction of key leaf functional traits across pan-tropical forests? Which data sources and algorithms provide the highest predictive accuracy and best identify the primary drivers of trait distribution and variation?

(2) How accurately can combined *in-situ* measurements and remote sensing estimate functional trait composition, diversity, and redundancy across South American temperate forests? Which environmental factors most strongly shape these functional attributes along large latitudinal and environmental gradients?

(3) How do initial levels of functional diversity and redundancy influence forest carbon stability in Mexico?

Correspondingly, I hypothesised:

(1) Integrating spectral, SAR, and LiDAR data with environmental variables will improve the accuracy of predicting multiple functional traits across tropical forests, compared to using spectral data alone. Deep learning algorithms such as Multilayer Perceptron (MLP) are expected to outperform machine learning algorithms such as Random forests (RF) for most

traits, and spectral data will contribute most strongly to predictions of biochemical traits, while SAR and LiDAR provide complementary structural information for morphological traits.

(2) Combining *in-situ* trait measurements with multi-source remote sensing will yield accurate estimates of functional trait composition, diversity, and redundancy in South American temperate forests. Hydrological stress is hypothesised to be the primary environmental filter shaping functional diversity and redundancy at large scales, while other environmental variables modulate local-scale patterns. High functional diversity and redundancy are expected to enhance the stability of ecosystem functions by providing complementary and overlapping trait strategies that buffer against the loss of individual species under environmental stress. In this context, stability serves as an operational measure of resilience without assuming a static baseline.

(3) Forest communities that start with higher functional trait diversity and redundancy exhibit greater carbon stability or accumulation under ongoing climate stress.

1.4. Significance and expected contributions

This thesis is expected to make significant scientific contributions to the fields of plant functional ecology, remote sensing of vegetation, biodiversity science, and climate change ecology.

First, this thesis will provide a comprehensive assessment of the capabilities and limitations of combining multi-sensor remotely sensed data for mapping multiple plant functional traits across extensive and critical forest biomes. The findings will inform the development of more accurate and robust operational trait monitoring systems (**Research questions 1** and **2**, **Chapters 4** and **5**). In addition, the comparative evaluation of different remotely sensed data combinations and analytical techniques (machine learning versus deep learning) for trait prediction will offer valuable guidance for future research in trait-based ecology and ecological remote sensing (**Research question 1**, **Chapter 4**).

Second, the research will yield novel insights into the spatial distribution of functional diversity and redundancy in South American temperate forests, identifying key environmental drivers and highlighting areas of potential ecological resilience. This contributes to a better understanding of biodiversity-environment relationships in understudied regions. Furthermore, the outputs of this research, including maps of functional trait composition, diversity, and redundancy, and an improved understanding of resilience mechanisms, can directly inform

evidence-based conservation strategies, sustainable forest management practices, and policies aimed at mitigating climate change impacts on forest ecosystems (**Research question 2**, **Chapter 5**).

Finally, by examining the interplay between functional diversity and redundancy, climatic stressors, and carbon stocks and carbon dynamics in both temperate and tropical forests in Mexico, this thesis will enhance understanding of the mechanisms by which biodiversity can influence ecosystem stability and carbon sequestration capacity in a changing climate. This is critical for predicting the future of global carbon sinks (**Research question 3**, **Chapter 6**).

1.5. Thesis outline

This thesis is structured into seven main chapters:

Chapter 1 Introduction (This Chapter): Provides the general background, defines the research questions and corresponding hypotheses, outlines the aims and objectives, gives an overview of the methodological approach, and states the significance and expected contributions of the thesis.

Chapter 2 Literature review: Reviews key concepts and background relevant to this thesis. It begins with an overview of temperate and tropical forests, highlighting the ecological significance and climate challenges of Chilean and Mexican forests. It then introduces core ideas in functional ecology, including trait definitions, community structure, biodiversity-function relationships, and ecosystem resilience. The chapter also outlines developments in ecological remote sensing, covering data types, platforms, and their use in monitoring forest traits and biodiversity. It concludes by identifying research gaps and positioning the thesis within this emerging field.

Chapter 3 Overview of methods: Outlines the methodological framework used throughout the thesis. It begins by introducing the study sites spanning temperate and tropical forests. The following section details the functional trait measurements, remotely sensed data, and relevant environmental variables used in the analyses. The chapter then explains how functional trait composition, diversity, redundancy, and carbon resilience are quantified. Finally, it describes the modelling approaches applied to relate biodiversity metrics and environmental factors to forest function and resilience.

Chapter 4 Multimodal remote sensing fusion for functional trait estimation across tropical forests: comparing machine learning and deep learning approaches (Paper 1): Addresses **Research question 1**, focusing on the prediction of 15 leaf morphological, nutrient, and photosynthetic traits in tropical forests using combined spectral, SAR, and LiDAR data with Random forests (RF) and Multilayer Perceptron (MLP) algorithms. This chapter evaluates predictive accuracies and identifies key drivers of trait distribution and variation, and tests if the MLP deep learning algorithm will outperform the RF machine learning algorithm.

Chapter 5 Quantifying the functional composition and potential resilience hotspots across a large latitudinal and environmental gradient in South American forests (Paper 2): Addresses **Research question 2**, investigating the distribution and variation patterns of functional trait composition, diversity, and redundancy across a latitudinal gradient in South American temperate forests in Chile. It identifies key environmental drivers (hydrological stress and soil properties) of these functional metrics, maps areas of potential resilience (between ~35°S and ~42°S, coinciding with Valdivian rainforests) where both functional diversity and redundancy are high, and explores sustainable conservation strategies tailored to regions with varying patterns of functional diversity and redundancy.

Chapter 6 Trait-based analysis of Mexican forest resilience to extreme climate change (Paper 3): Addresses **Research question 3**, utilising repeated forest inventory data to investigate how functional diversity and redundancy in morphological and nutrient traits interact with climatic stressors to affect temporal changes in aboveground carbon stocks and carbon dynamics. It specifically examines how different dimensions of functional diversity and redundancy influence forest carbon dynamics across temperate and tropical forests of Mexico. The analysis highlights contrasting roles of these functional dimensions: while high initial morphological FD tends to enhance carbon stability and buffer against increasing drought severity in temperate forests, high nutrient FD is often associated with reduced resilience. The chapter further discusses how these trait-climate interactions vary across forest types and environmental gradients, providing insights into the mechanisms underpinning forest carbon resilience under intensifying climate extremes.

The structure and interconnection among the three core papers of this thesis are illustrated in Fig. 1.1. Please note that **Chapters 4**, **5**, and **6** are formatted in accordance with the guidelines of the peer-reviewed journals in which the studies have been accepted, are currently under review, or are being prepared for submission.

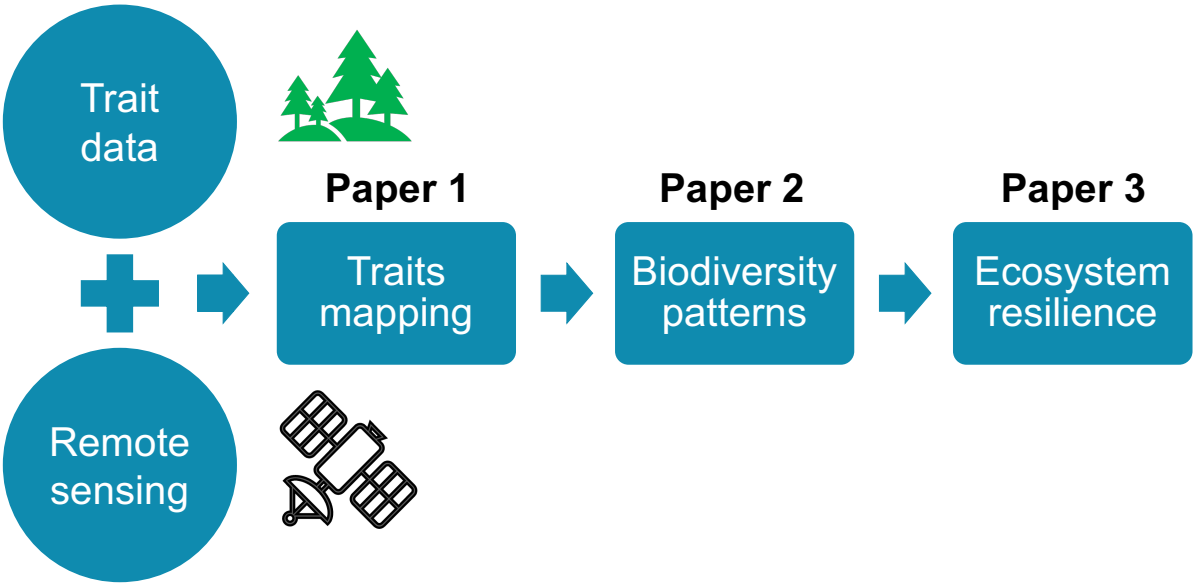

Fig. 1.1. Structure and interconnection among the three core papers of this thesis. Papers1 to 3 are presented in Chapters 4 to 6 of this thesis.

Chapter 7 Synthesis and conclusion: This concluding chapter synthesises the principal findings from **Chapters 4**, **5**, and **6**. It discusses their collective implications for understanding forest functional ecology and resilience in the context of global environmental change, revisits the main research questions, acknowledges limitations, and proposes avenues for future research.

1.6. References

Aguirre-Gutiérrez, J., Rifai, S. W., Deng, X., ter Steege, H., Thomson, E., Corral-Rivas, J. J., Guimaraes, A. F., Muller, S., Klipel, J., Fauset, S., Resende, A. F., Wallin, G., Joly, C. A., Abernethy, K., Adu-Bredu, S., Alexandre Silva, C., de Oliveira, E. A., Almeida, D. R. A., Alvarez-Davila, E., … Malhi, Y. (2025). Canopy functional trait variation across Earth's tropical forests. *Nature*, 1–8. https://doi.org/10.1038/s41586-025-08663-2

Allen, C. D., Macalady, A. K., Chenchouni, H., Bachelet, D., McDowell, N., Vennetier, M., Kitzberger, T., Rigling, A., Breshears, D. D., Hogg, E. H. (Ted), Gonzalez, P., Fensham, R., Zhang, Z., Castro, J., Demidova, N., Lim, J.-H., Allard, G., Running, S. W., Semerci, A., & Cobb, N. (2010). A global overview of drought and heat-induced tree mortality reveals emerging climate change risks for forests. *Forest Ecology and Management*, *259*(4), 660–684. https://doi.org/10.1016/j.foreco.2009.09.001

Asner, G. P., Martin, R. E., Anderson, C. B., & Knapp, D. E. (2015). Quantifying forest canopy traits: Imaging spectroscopy versus field survey. *Remote Sensing of Environment*, *158*, 15–27. https://doi.org/10.1016/j.rse.2014.11.011

Asner, G. P., Martin, R. E., Knapp, D. E., Tupayachi, R., Anderson, C. B., Sinca, F., Vaughn, N. R., & Llactayo, W. (2017). Airborne laser-guided imaging spectroscopy to map forest trait diversity and guide conservation. *Science*, *355*(6323), 385–389. https://doi.org/10.1126/science.aaj1987

Bello, F. de, Lavorel, S., Hallett, L. M., Valencia, E., Garnier, E., Roscher, C., Conti, L., Galland, T., Goberna, M., Májeková, M., Montesinos-Navarro, A., Pausas, J. G., Verdú, M., E-Vojtkó, A., Götzenberger, L., & Lepš, J. (2021). Functional trait effects on ecosystem stability: Assembling the jigsaw puzzle. *Trends in Ecology & Evolution*, *36*(9), 822–836. https://doi.org/10.1016/j.tree.2021.05.001

Biggs, C. R., Yeager, L. A., Bolser, D. G., Bonsell, C., Dichiera, A. M., Hou, Z., Keyser, S. R., Khursigara, A. J., Lu, K., Muth, A. F., Negrete Jr., B., & Erisman, B. E. (2020). Does functional redundancy affect ecological stability and resilience? A review and meta-analysis. *Ecosphere*, *11*(7), e03184. https://doi.org/10.1002/ecs2.3184

Brienen, R. J. W., Phillips, O. L., Feldpausch, T. R., Gloor, E., Baker, T. R., Lloyd, J., Lopez-Gonzalez, G., Monteagudo-Mendoza, A., Malhi, Y., Lewis, S. L., Vásquez Martinez, R., Alexiades, M., Álvarez Dávila, E., Alvarez-Loayza, P., Andrade, A., Aragão, L. E. O. C., Araujo-Murakami, A., Arets, E. J. M. M., Arroyo, L., … Zagt, R. J. (2015). Long-term decline of the Amazon carbon sink. *Nature*, *519*(7543), 344–348. https://doi.org/10.1038/nature14283

Brockerhoff, E. G., Barbaro, L., Castagneyrol, B., Forrester, D. I., Gardiner, B., González-Olabarria, J. R., Lyver, P. O., Meurisse, N., Oxbrough, A., Taki, H., Thompson, I. D., van der Plas, F., & Jactel, H. (2017). Forest biodiversity, ecosystem functioning and the provision of ecosystem services. *Biodiversity and Conservation*, *26*(13), 3005–3035. https://doi.org/10.1007/s10531-017-1453-2

Bruelheide, H., Dengler, J., Purschke, O., Lenoir, J., Jiménez-Alfaro, B., Hennekens, S. M., Botta-Dukát, Z., Chytrý, M., Field, R., Jansen, F., Kattge, J., Pillar, V. D., Schrodt, F., Mahecha, M. D., Peet, R. K., Sandel, B., van Bodegom, P., Altman, J., Alvarez-Dávila, E., … Jandt, U. (2018). Global trait–environment relationships of plant communities. *Nature Ecology & Evolution*, *2*(12), 1906–1917. https://doi.org/10.1038/s41559-018-0699-8

Calders, K., Armston, J., Newnham, G., Herold, M., & Goodwin, N. (2014). Implications of sensor configuration and topography on vertical plant profiles derived from terrestrial LiDAR. *Agricultural and Forest Meteorology*, *194*, 104–117. https://doi.org/10.1016/j.agrformet.2014.03.022

Cavender-Bares, J., Gamon, J. A., & Townsend, P. A. (Eds.). (2020). *Remote Sensing of Plant Biodiversity*. Springer International Publishing. https://doi.org/10.1007/978-3-030-33157-3

Cavender-Bares, J., Schneider, F. D., Santos, M. J., Armstrong, A., Carnaval, A., Dahlin, K. M., Fatoyinbo, L., Hurtt, G. C., Schimel, D., Townsend, P. A., Ustin, S. L., Wang, Z., & Wilson, A. M. (2022). Integrating remote sensing with ecology and evolution to advance biodiversity conservation. *Nature Ecology & Evolution*, *6*(5), 506–519. https://doi.org/10.1038/s41559-022-01702-5

Cooper, D. L. M., Lewis, S. L., Sullivan, M. J. P., Prado, P. I., ter Steege, H., Barbier, N., Slik, F., Sonké, B., Ewango, C. E. N., Adu-Bredu, S., Affum-Baffoe, K., de Aguiar, D. P. P., Ahuite Reategui, M. A., Aiba, S.-I., Albuquerque, B. W., de Almeida Matos, F. D., Alonso, A., Amani, C. A., do Amaral, D. D., … Zent, S. (2024). Consistent patterns of common species across tropical tree communities. *Nature*, *625*(7996), 728–734. https://doi.org/10.1038/s41586-023-06820-z

D'Andrea, E., Scartazza, A., Battistelli, A., Collalti, A., Proietti, S., Rezaie, N., Matteucci, G., & Moscatello, S. (2021). Unravelling resilience mechanisms in forests: Role of non-structural carbohydrates in responding to extreme weather events. *Tree Physiology*, *41*(10), 1808–1818. https://doi.org/10.1093/treephys/tpab044

Díaz, S., Lavorel, S., De Bello, F., Quétier, F., Grigulis, K., & Robson, T. M. (2007). Incorporating plant functional diversity effects in ecosystem service assessments. *Proceedings of the National Academy of Sciences*, *104*(52), 20684–20689.

Díaz, S., Lavorel, S., McINTYRE, S., Falczuk, V., Casanoves, F., Milchunas, D. G., Skarpe, C., Rusch, G., Sternberg, M., Noy-Meir, I., Landsberg, J., Zhang, W., Clark, H., & Campbell, B. D. (2007). Plant trait responses to grazing – a global synthesis. *Global Change Biology*, *13*(2), 313–341. https://doi.org/10.1111/j.1365-2486.2006.01288.x

Díaz, S., Purvis, A., Cornelissen, J. H. C., Mace, G. M., Donoghue, M. J., Ewers, R. M., Jordano, P., & Pearse, W. D. (2013). Functional traits, the phylogeny of function, and ecosystem service vulnerability. *Ecology and Evolution*, *3*(9), 2958–2975. https://doi.org/10.1002/ece3.601

Díaz, S., & Cabido, M. (2001). Vive la différence: Plant functional diversity matters to ecosystem processes. *Trends in Ecology & Evolution*, *16*(11), 646–655.

Domec, J.-C., Smith, D. D., & McCulloh, K. A. (2017). A synthesis of the effects of atmospheric carbon dioxide enrichment on plant hydraulics: Implications for whole-plant water use efficiency and resistance to drought. *Plant, Cell & Environment*, *40*(6), 921–937. https://doi.org/10.1111/pce.12843

Durán, S. M., Martin, R. E., Díaz, S., Maitner, B. S., Malhi, Y., Salinas, N., Shenkin, A., Silman, M. R., Wieczynski, D. J., Asner, G. P., Bentley, L. P., Savage, V. M., & Enquist, B. J. (2019). Informing trait-based ecology by assessing remotely sensed functional diversity across a broad tropical temperature gradient. *Science Advances*, *5*(12), eaaw8114. https://doi.org/10.1126/sciadv.aaw8114

Enquist, B. J., Norberg, J., Bonser, S. P., Violle, C., Webb, C. T., Henderson, A., Sloat, L. L., & Savage, V. M. (2015). Chapter Nine - Scaling from Traits to Ecosystems: Developing a General Trait Driver Theory via Integrating Trait-Based and Metabolic Scaling Theories. In S. Pawar, G. Woodward, & A. I. Dell (Eds.), *Advances in Ecological Research* (Vol. 52, pp. 249–318). Academic Press. https://doi.org/10.1016/bs.aecr.2015.02.001

Forzieri, G., Dakos, V., McDowell, N. G., Ramdane, A., & Cescatti, A. (2022). Emerging signals of declining forest resilience under climate change. *Nature*, *608*(7923), 534–539. https://doi.org/10.1038/s41586-022-04959-9

Freschet, G. T., Violle, C., Bourget, M. Y., Scherer-Lorenzen, M., & Fort, F. (2018). Allocation, morphology, physiology, architecture: The multiple facets of plant above- and below-ground responses to resource stress. *New Phytologist*, *219*(4), 1338–1352. https://doi.org/10.1111/nph.15225

Gagic, V., Bartomeus, I., Jonsson, T., Taylor, A., Winqvist, C., Fischer, C., Slade, E. M., Steffan-Dewenter, I., Emmerson, M., Potts, S. G., Tscharntke, T., Weisser, W., & Bommarco, R. (2015). Functional identity and diversity of animals predict ecosystem functioning better than species-based indices. *Proceedings of the Royal Society B: Biological Sciences*, *282*(1801), 20142620. https://doi.org/10.1098/rspb.2014.2620

Gaston, K. J. (2000). Global patterns in biodiversity. *Nature*, *405*(6783), 220–227. https://doi.org/10.1038/35012228

Gessler, A., Schaub, M., & McDowell, N. G. (2017). The role of nutrients in drought-induced tree mortality and recovery. *New Phytologist*, *214*(2), 513–520. https://doi.org/10.1111/nph.14340

Gladstone-Gallagher, R. V., Pilditch, C. A., Stephenson, F., & Thrush, S. F. (2019). Linking Traits across Ecological Scales Determines Functional Resilience. *Trends in Ecology & Evolution*, *34*(12), 1080–1091. https://doi.org/10.1016/j.tree.2019.07.010

Global Forest Resources Assessment 2020. (2020). FAO. https://doi.org/10.4060/ca9825en

Goodwin, N. R., Coops, N. C., & Culvenor, D. S. (2006). Assessment of forest structure with airborne LiDAR and the effects of platform altitude. *Remote Sensing of Environment*, *103*(2), 140–152. https://doi.org/10.1016/j.rse.2006.03.003

Guadarrama-Escobar, L. M., Hunt, J., Gurung, A., Zarco-Tejada, P. J., Shabala, S., Camino, C., Hernandez, P., & Pourkheirandish, M. (2024). Back to the future for drought tolerance. *New Phytologist*, *242*(2), 372–383. https://doi.org/10.1111/nph.19619

Guz, J., & and Kulakowski, D. (2020). Forests in the Anthropocene. *Annals of the American Association of Geographers*, *111*(3), 869–879. https://doi.org/10.1080/24694452.2020.1813013

Hanley, M. E., Lamont, B. B., Fairbanks, M. M., & Rafferty, C. M. (2007). Plant structural traits and their role in anti-herbivore defence. *Perspectives in Plant Ecology, Evolution and Systematics*, *8*(4), 157–178. https://doi.org/10.1016/j.ppees.2007.01.001

Helfenstein, I. S., Schneider, F. D., Schaepman, M. E., & Morsdorf, F. (2022). Assessing biodiversity from space: Impact of spatial and spectral resolution on trait-based functional diversity. *Remote Sensing of Environment*, *275*, 113024. https://doi.org/10.1016/j.rse.2022.113024

Hisano, M., Ghazoul, J., Chen, X., & Chen, H. Y. H. (2024). Functional diversity enhances dryland forest productivity under long-term climate change. *Science Advances*, *10*(17), eadn4152. https://doi.org/10.1126/sciadv.adn4152

Hubau, W., Lewis, S. L., Phillips, O. L., Affum-Baffoe, K., Beeckman, H., Cuní-Sanchez, A., Daniels, A. K., Ewango, C. E. N., Fauset, S., Mukinzi, J. M., Sheil, D., Sonké, B., Sullivan, M. J. P., Sunderland, T. C. H., Taedoumg, H., Thomas, S. C., White, L. J. T., Abernethy, K. A., Adu-Bredu, S., … Zemagho, L. (2020). Asynchronous carbon sink saturation in African and Amazonian tropical forests. *Nature*, *579*(7797), 80–87. https://doi.org/10.1038/s41586-020-2035-0

Inoue, Y., Sakaiya, E., & Wang, C. (2014). Capability of C-band backscattering coefficients from high-resolution satellite SAR sensors to assess biophysical variables in paddy rice. *Remote Sensing of Environment*, *140*, 257–266. https://doi.org/10.1016/j.rse.2013.09.001

Jetz, W., Cavender-Bares, J., Pavlick, R., Schimel, D., Davis, F. W., Asner, G. P., Guralnick, R., Kattge, J., Latimer, A. M., & Moorcroft, P. (2016). Monitoring plant functional diversity from space. *Nature Plants*, *2*(3), 1–5.

Kavzoglu, T., Tso, B., & Mather, P. M. (2024). *Classification Methods for Remotely Sensed Data* (3rd ed.). CRC Press. https://doi.org/10.1201/9781003439172

Knyazikhin, Y., Schull, M. A., Stenberg, P., Mõttus, M., Rautiainen, M., Yang, Y., Marshak, A., Latorre Carmona, P., Kaufmann, R. K., Lewis, P., Disney, M. I., Vanderbilt, V., Davis, A. B., Baret, F., Jacquemoud, S., Lyapustin, A., & Myneni, R. B. (2013). Hyperspectral remote sensing of foliar nitrogen content. *Proceedings of the National Academy of Sciences*, *110*(3). https://doi.org/10.1073/pnas.1210196109

Laliberté, E., & Legendre, P. (2010). A distance-based framework for measuring functional diversity from multiple traits. *Ecology*, *91*(1), 299–305. https://doi.org/10.1890/08-2244.1

Langat, D. K., Maranga, E. K., Aboud, A. A., & Cheboiwo, J. K. (2016). Role of Forest Resources to Local Livelihoods: The Case of East Mau Forest Ecosystem, Kenya. *International Journal of Forestry Research*, *2016*(1), 4537354. https://doi.org/10.1155/2016/4537354

Laughlin, D. C. (2014). Applying trait-based models to achieve functional targets for theory-driven ecological restoration. *Ecology Letters*, *17*(7), 771–784. https://doi.org/10.1111/ele.12288

Lavorel, S., & Garnier, E. (2002). Predicting changes in community composition and ecosystem functioning from plant traits: Revisiting the Holy Grail. *Functional Ecology*, *16*(5), 545–556. https://doi.org/10.1046/j.1365-2435.2002.00664.x

Lõhmus, A., Lõhmus, P., & Runnel, K. (2018). A simple survey protocol for assessing terrestrial biodiversity in a broad range of ecosystems. *PLOS ONE*, *13*(12), e0208535. https://doi.org/10.1371/journal.pone.0208535

Maia, V. A., Santos, A. B. M., de Aguiar-Campos, N., de Souza, C. R., de Oliveira, M. C. F., Coelho, P. A., Morel, J. D., da Costa, L. S., Farrapo, C. L., Fagundes, N. C. A., de Paula, G. G. P., Santos, P. F., Gianasi, F. M., da Silva, W. B., de Oliveira, F., Girardelli, D. T., de Carvalho Araújo, F., Vilela, T. A., Pereira, R. T., … dos Santos, R. M. (2020). The carbon sink of tropical seasonal forests in southeastern Brazil can be under threat. *Science Advances*, *6*(51), eabd4548. https://doi.org/10.1126/sciadv.abd4548

Malhi, Y., Doughty, C., & Galbraith, D. (2011). The allocation of ecosystem net primary productivity in tropical forests. *Philosophical Transactions of the Royal Society B: Biological Sciences*, *366*(1582), 3225–3245. https://doi.org/10.1098/rstb.2011.0062

Malhi, Y., Franklin, J., Seddon, N., Solan, M., Turner, M. G., Field, C. B., & Knowlton, N. (2020). Climate change and ecosystems: Threats, opportunities and solutions. *Philosophical Transactions of the Royal Society B: Biological Sciences*, *375*(1794), 20190104. https://doi.org/10.1098/rstb.2019.0104

Malhi, Y., Girardin, C., Metcalfe, D. B., Doughty, C. E., Aragão, L. E. O. C., Rifai, S. W., Oliveras, I., Shenkin, A., Aguirre-Gutiérrez, J., Dahlsjö, C. A. L., Riutta, T., Berenguer, E., Moore, S., Huasco, W. H., Salinas, N., da Costa, A. C. L., Bentley, L. P., Adu-Bredu, S., Marthews, T. R., … Phillips, O. L. (2021). The Global Ecosystems Monitoring network: Monitoring ecosystem productivity and carbon cycling across the tropics. *Biological Conservation*, *253*, 108889. https://doi.org/10.1016/j.biocon.2020.108889

McGill, B. J., Enquist, B. J., Weiher, E., & Westoby, M. (2006). Rebuilding community ecology from functional traits. *Trends in Ecology & Evolution*, *21*(4), 178–185. https://doi.org/10.1016/j.tree.2006.02.002

Mermoz, S., Réjou-Méchain, M., Villard, L., Le Toan, T., Rossi, V., & Gourlet-Fleury, S. (2015). Decrease of L-band SAR backscatter with biomass of dense forests. *Remote Sensing of Environment*, *159*, 307–317. https://doi.org/10.1016/j.rse.2014.12.019

Mohammadpour, P., & Viegas, C. (2022). Applications of Multi-Source and Multi-Sensor Data Fusion of Remote Sensing for Forest Species Mapping. In *Advances in Remote Sensing for Forest Monitoring* (pp. 255–287). John Wiley & Sons, Ltd. https://doi.org/10.1002/9781119788157.ch12

Muscarella, R., & Uriarte, M. (2016). Do community-weighted mean functional traits reflect optimal strategies? *Proceedings of the Royal Society B: Biological Sciences*, *283*(1827), 20152434. https://doi.org/10.1098/rspb.2015.2434

Oldekop, J. A., Rasmussen, L. V., Agrawal, A., Bebbington, A. J., Meyfroidt, P., Bengston, D. N., Blackman, A., Brooks, S., Davidson-Hunt, I., Davies, P., Dinsi, S. C., Fontana, L. B., Gumucio, T., Kumar, C., Kumar, K., Moran, D., Mwampamba, T. H., Nasi, R., Nilsson, M., … Wilson, S. J. (2020). Forest-linked livelihoods in a globalized world. *Nature Plants*, *6*(12), 1400–1407. https://doi.org/10.1038/s41477-020-00814-9

Oliver, T. H., Heard, M. S., Isaac, N. J. B., Roy, D. B., Procter, D., Eigenbrod, F., Freckleton, R., Hector, A., Orme, C. D. L., Petchey, O. L., Proença, V., Raffaelli, D., Suttle, K. B., Mace, G. M., Martín-López, B., Woodcock, B. A., & Bullock, J. M. (2015). Biodiversity and Resilience of Ecosystem Functions. *Trends in Ecology & Evolution*, *30*(11), 673–684. https://doi.org/10.1016/j.tree.2015.08.009

Ollinger, S. V. (2011). Sources of variability in canopy reflectance and the convergent properties of plants. *New Phytologist*, *189*(2), 375–394. https://doi.org/10.1111/j.1469-8137.2010.03536.x

Palmer, M. W., Earls, P. G., Hoagland, B. W., White, P. S., & Wohlgemuth, T. (2002). Quantitative tools for perfecting species lists. *Environmetrics*, *13*(2), 121–137. https://doi.org/10.1002/env.516

Pan, Y., Birdsey, R. A., Fang, J., Houghton, R., Kauppi, P. E., Kurz, W. A., Phillips, O. L., Shvidenko, A., Lewis, S. L., Canadell, J. G., Ciais, P., Jackson, R. B., Pacala, S. W., McGuire, A. D., Piao, S., Rautiainen, A., Sitch, S., & Hayes, D. (2011). A Large and Persistent Carbon Sink in the World's Forests. *Science*, *333*(6045), 988–993. https://doi.org/10.1126/science.1201609

Pandey, P., Ge, Y., Stoerger, V., & Schnable, J. C. (2017). High Throughput In vivo Analysis of Plant Leaf Chemical Properties Using Hyperspectral Imaging. *Frontiers in Plant Science*, *8*. https://doi.org/10.3389/fpls.2017.01348

Pillay, R., Venter, M., Aragon-Osejo, J., González-del-Pliego, P., Hansen, A. J., Watson, J. E., & Venter, O. (2022). Tropical forests are home to over half of the world's vertebrate species. *Frontiers in Ecology and the Environment*, *20*(1), 10–15. https://doi.org/10.1002/fee.2420

Post, E. S., Pedersen, C., Wilmers, C. C., & Forchhammer, M. C. (2008). Phenological Sequences Reveal Aggregate Life History Response to Climatic Warming. *Ecology*, *89*(2), 363–370. https://doi.org/10.1890/06-2138.1

Pourshamsi, M., Xia, J., Yokoya, N., Garcia, M., Lavalle, M., Pottier, E., & Balzter, H. (2021). Tropical forest canopy height estimation from combined polarimetric SAR and LiDAR using machine-learning. *ISPRS Journal of Photogrammetry and Remote Sensing*, *172*, 79–94. https://doi.org/10.1016/j.isprsjprs.2020.11.008

Rosenfeld, J. S. (2002). Functional redundancy in ecology and conservation. *Oikos*, *98*(1), 156–162. https://doi.org/10.1034/j.1600-0706.2002.980116.x

Sakschewski, B., Von Bloh, W., Boit, A., Poorter, L., Peña-Claros, M., Heinke, J., Joshi, J., & Thonicke, K. (2016). Resilience of Amazon forests emerges from plant trait diversity. *Nature Climate Change*, *6*(11), 1032–1036. https://doi.org/10.1038/nclimate3109

Schneider, F. D., Morsdorf, F., Schmid, B., Petchey, O. L., Hueni, A., Schimel, D. S., & Schaepman, M. E. (2017). Mapping functional diversity from remotely sensed morphological and physiological forest traits. *Nature Communications*, *8*(1), 1441. https://doi.org/10.1038/s41467-017-01530-3

Seidl, R., Albrich, K., Erb, K., Formayer, H., Leidinger, D., Leitinger, G., Tappeiner, U., Tasser, E., & Rammer, W. (2019). What drives the future supply of regulating ecosystem services in a mountain forest landscape? *Forest Ecology and Management*, *445*, 37–47. https://doi.org/10.1016/j.foreco.2019.03.047

Sterck, F., Markesteijn, L., Schieving, F., & Poorter, L. (2011). Functional traits determine trade-offs and niches in a tropical forest community. *Proceedings of the National Academy of Sciences*, *108*(51), 20627–20632. https://doi.org/10.1073/pnas.1106950108

Suding, K. N., Lavorel, S., Chapin Iii, F. S., Cornelissen, J. H. C., Díaz, S., Garnier, E., Goldberg, D., Hooper, D. U., Jackson, S. T., & Navas, M.-L. (2008). Scaling environmental change through the community-level: A trait-based response-and-effect framework for plants. *Global Change Biology*, *14*(5), 1125–1140. https://doi.org/10.1111/j.1365-2486.2008.01557.x

Sullivan, M. J. P., Lewis, S. L., Affum-Baffoe, K., Castilho, C., Costa, F., Sanchez, A. C., Ewango, C. E. N., Hubau, W., Marimon, B., Monteagudo-Mendoza, A., Qie, L., Sonké, B., Martinez, R. V., Baker, T. R., Brienen, R. J. W., Feldpausch, T. R., Galbraith, D., Gloor, M., Malhi, Y., … Phillips, O. L. (2020). Long-term thermal sensitivity of Earth's tropical forests. *Science*, *368*(6493), 869–874. https://doi.org/10.1126/science.aaw7578

Swenson, N. G., & Rubio, V. E. (2025). The functional underpinnings of tropical forest dynamics—Functional traits, groups, and unmeasured diversity. *Biotropica*, *57*(1), e13360. https://doi.org/10.1111/btp.13360

Tavares, J. V., Oliveira, R. S., Mencuccini, M., Signori-Müller, C., Pereira, L., Diniz, F. C., Gilpin, M., Marca Zevallos, M. J., Salas Yupayccana, C. A., Acosta, M., Pérez Mullisaca, F. M., Barros, F. de V., Bittencourt, P., Jancoski, H., Scalon, M. C., Marimon, B. S., Oliveras Menor, I., Marimon, B. H., Fancourt, M., … Galbraith, D. R. (2023). Basin-wide variation in tree hydraulic safety margins predicts the carbon balance of Amazon forests. *Nature*, *617*(7959), 111–117. https://doi.org/10.1038/s41586-023-05971-3

Tedesco, M. (2015). Remote sensing and the cryosphere. In *Remote Sensing of the Cryosphere* (pp. 1–16). John Wiley & Sons, Ltd. https://doi.org/10.1002/9781118368909.ch1

Thomson, E. R., Spiegel, M. P., Althuizen, I. H. J., Bass, P., Chen, S., Chmurzynski, A., Halbritter, A. H., Henn, J. J., Jónsdóttir, I. S., Klanderud, K., Li, Y., Maitner, B. S., Michaletz, S. T., Niittynen, P., Roos, R. E., Telford, R. J., Enquist, B. J., Vandvik, V., Macias-Fauria, M., & Malhi, Y. (2021). Trait tundra. *Environmental Research Letters*, *16*(5), 055006. https://doi.org/10.1088/1748-9326/abf464

Tilman, D., Isbell, F., & Cowles, J. M. (2014). Biodiversity and Ecosystem Functioning. *Annual Review of Ecology, Evolution, and Systematics*, *45*(Volume 45, 2014), 471–493. https://doi.org/10.1146/annurev-ecolsys-120213-091917

Torabzadeh, H., Morsdorf, F., & Schaepman, M. E. (2014). Fusion of imaging spectroscopy and airborne laser scanning data for characterization of forest ecosystems – A review. *ISPRS Journal of Photogrammetry and Remote Sensing*, *97*, 25–35. https://doi.org/10.1016/j.isprsjprs.2014.08.001

Trew, B. T., & Maclean, I. M. D. (2021). Vulnerability of global biodiversity hotspots to climate change. *Global Ecology and Biogeography*, *30*(4), 768–783. https://doi.org/10.1111/geb.13272

Violle, C., Navas, M.-L., Vile, D., Kazakou, E., Fortunel, C., Hummel, I., & Garnier, E. (2007). Let the concept of trait be functional! *Oikos*, *116*(5), 882–892. https://doi.org/10.1111/j.0030-1299.2007.15559.x

Wang, R., & Gamon, J. A. (2019). Remote sensing of terrestrial plant biodiversity. *Remote Sensing of Environment*, *231*, 111218. https://doi.org/10.1016/j.rse.2019.111218

Zakharova, L., Meyer, K. M., & Seifan, M. (2019). Trait-based modelling in ecology: A review of two decades of research. *Ecological Modelling*, *407*, 108703. https://doi.org/10.1016/j.ecolmodel.2019.05.008

Zheng, Z., Zeng, Y., Schuman, M. C., Jiang, H., Schmid, B., Schaepman, M. E., & Morsdorf, F. (2022). Individual tree-based vs pixel-based approaches to mapping forest functional traits and diversity by remote sensing. *International Journal of Applied Earth Observation and Geoinformation*, *114*, 103074. https://doi.org/10.1016/j.jag.2022.103074

Chapter 2 Literature review

2.1. Temperate and tropical forests

Forest are essential terrestrial ecosystems, they provide critical ecosystem services such as climate regulation, carbon storage, and biodiversity conservation (Trumbore et al., 2015). Among the Earth's diverse forest biomes, temperate and tropical forests are the most widely distributed and ecologically significant biomes for their large extent, high productivity, and rich biological diversity (Malhi et al., 1999, 2024; Pan et al., 2011). Tropical forests, for instance, are estimated to harbour most Earth's terrestrial species (Brown, 2014). They also exhibit the highest mean net primary productivity of any terrestrial ecosystem (Malhi et al., 2011), making them critical carbon sinks. Temperate forests, while typically less diverse in terms of species richness, are often dominated by a few key tree species and play significant roles in regional climates and carbon storage, particularly in the mid-latitudes (Malhi et al., 1999; Moon et al., 2017). In addition, these two forest types differ remarkedly in climate, species composition, structural complexity, and ecological functioning. Temperate forests experience more pronounced seasonality, including cold winters and warm summers (Box & Fujiwara, 2015). In contrast, tropical forests, primarily located in a belt around the Equator, between the Tropics of Cancer (23.5°N) and Capricorn (23.5°S), are characterised by high annual rainfall (mean=1487 mm), minimal temperature variation (mean maximum daily temperature ranged from 28.33 °C to 30.12 °C) (Bunyavejchewin et al., 2009; Schippers et al., 2015), and unparalleled biodiversity (Ferreira et al., 2018). Both forest types are facing unprecedented pressures from anthropogenic activities and climate change (Malhi et al., 2004; S. J. Wright, 2005), necessitating a deeper understanding of their ecology and resilience.

2.1.1. Temperate forests of Chile: A biodiversity hotspot under pressure

Temperate forests of Chile, particularly the Valdivian temperate rainforests (~35°S to ~42°S), are a globally significant biodiversity hotspot (Myers et al., 2000), renowned for their unique ecosystems and high levels of endemism (NAHUELHUAL et al., 2007). Located in a narrow coastal strip between the Pacific Ocean and the Andes Mountains, Chilean temperate forests are characterised by dense understories of bamboos (e.g., *Chusquea quila* and *Chusquea culeou*) and ferns, and are dominated by evergreen angiosperm trees, with some deciduous species and conifers also present (Kitzberger et al., 2016; Pfadenhauer & Klötzli, 2020; Veblen, 2007). The climate is heavily influenced by the westerlies and the Humboldt Current (Gibson et al., 2007),

resulting in high precipitation and foggy, humid conditions, particularly along the coast (Smith-Ramírez, 2004). Approximately 50% of the woody plants in this ecoregion are endemic (Armesto et al., 2001).

Despite being recognised as a global biodiversity hotspot, Chilean temperate forests are under persistent threat. First, forest clearing for timber, fuelwood, and agriculture (Armesto et al., 2001) and the establishment of large-scale pine (*Pinus radiata*) and *Eucalyptus* (*Eucalyptus globulus* and *Eucalyptus nitens*) plantations has led to the decreasing of vast areas of native vegetation, particularly in the Coast Range since the 1970s (Neira et al., 2002; Salas et al., 2016). These plantations, while offering some soil stabilisation benefits, contribute to the fragmentation and degradation of native plant communities, reducing their continuity and altering natural vegetation dynamics (Heinrichs et al., 2018).

In addition, the Chilean Mediterranean region has been experiencing a "megadrought" for over a decade, leading to vegetation browning and increased aridity (Garreaud et al., 2017; Miranda et al., 2023). A decrease in precipitation has been observed in nearly half of the Sclerophyllous Forest Type patches, alongside increases in land surface temperature (Cueto et al., 2025). These climate-induced stresses are accelerating forest degradation and placing the Chilean Mediterranean forest on the verge of collapse (Smith-Ramírez et al., 2023).

Finally, accidental and intentional forest fires pose another major threat (Cordero et al., 2024; De la Barrera et al., 2018). Unlike other Mediterranean climate zones, fire is not a major natural component of these ecosystems, and native species are not well-adapted to its effects (Delpiano et al., 2024). The presence of fire-adapted and non-native plantation species like *Pinus radiata* can exacerbate the spread of fires into vulnerable native forests (Escobedo et al., 2024; Leal-Medina et al., 2024).

These multifaceted threats highlight the urgent need for effective conservation and management strategies to protect the unique biodiversity of Chilean temperate forests.

2.1.2. Forests of Mexico under intensifying warming and drought

Mexico, a megadiverse country and a key centre of species for genera like *Pinus* and *Quercus* (Gómez-Mendoza & Arriaga, 2007), hosts a variety of forest ecosystems, including extensive temperate forests (e.g., conifer and pine-oak forests in the Sierra Madre Occidental, Sierra Madre Oriental, and Trans-Mexican Volcanic Belt) in northern and central Mexico (Ávila-Akerberg et al., 2023; Galicia et al., 2015) and tropical forests (e.g., rainforests on the Atlantic

side and tropical deciduous forests on the Pacific side) in southern Mexico (Quigley & Platt, 2003). These forests are rich in biodiversity but increasingly vulnerable to the impacts of climate change and exacerbated by local anthropogenic pressures (Moreno-Sanchez et al., 2012), particularly intensifying warming and drought (López-Teloxa & Monterroso-Rivas, 2024; Ulises & Lucia, 2024).

Regional climate models for Mexico project significant temperature increases (1.5 °C by 2030, 2.3 °C by 2060, and 3.7 °C by 2090) alongside decreasing precipitation patterns (annual precipitation is expected to decline by 6.7% by 2030, 9.0% by 2060, and 18.2% by 2090) (Sáenz-Romero et al., 2010). This combination of rising temperatures and decreasing precipitation is anticipated to intensify aridity across much of the country, leading to severe soil moisture deficits and heightened water stress for vegetation, particularly in the North, West, and Bajío regions (Diaz et al., 2019; Magaña et al., 2012; Ulises & Lucia, 2024). In the coming decades, moderate to extreme drought conditions are projected to become more frequent and widespread, pushing ecosystems closer to their physiological limits (Méndez & Magaña, 2010; Murray-Tortarolo, 2021; Wehner et al., 2011).

Mexico's forests are already being impacted by the effects of climate change. Temperate forests are among the most affected. Drought-related stress has led to reduced tree vigour, defoliation, and increased vulnerability to pests and diseases (Sáenz-Romero et al., 2020). These impacts are expected to reduce the extent of climatically suitable habitat for major biomes such as pine-oak and conifer forests, and for key species like *Pinus hartwegii*, *Abies religiosa*, and *Pinus pseudostrobus* (Gómez-Pineda et al., 2020; Sáenz-Romero et al., 2020).

Tropical forests across Mexico and the broader Americas are also under threat, as species attempt to cope with shifting environmental baselines (Ortega et al., 2024). While certain tree species with adaptive traits such as drought tolerance, high wood density, or deciduousness may persist or even expand, many others are declining (Alvarado & Terrazas, 2023; Hordijk et al., 2025). The drying and warming of tropical soils pose an additional threat, accelerating the decomposition of long-stored soil carbon (McFarlane et al., 2024; Nottingham et al., 2020) and potentially transforming these forests from carbon sinks into carbon sources. Combined with the intensifying risks of fire, heatwaves, and prolonged droughts, the resilience of tropical forest ecosystems is being severely tested (Stan & Sanchez-Azofeifa, 2019).

Altogether, these climatic shifts have significant impacts on biodiversity, carbon storage, and the essential ecosystem services provided by Mexico's forests. Ongoing

deforestation, land cover transitions like agricultural expansion, and compounded by climate pressures, further increases carbon emissions and biodiversity loss (Bonilla-Moheno & Aide, 2020). Addressing these challenges requires practical strategies, including adaptive forest management and climate adaptation measures to protect Mexico's forest ecosystems and the key functions they perform.

2.2. Functional ecology and ecosystem functioning

Understanding how forest ecosystems respond to the environmental pressures requires moving beyond species inventories to consider the functional characteristics of the organisms within them (de Bello et al., 2021; Díaz et al., 2007; Messier et al., 2019). Trait-based ecology provides a powerful framework for this, focusing on the morpho-physio-phenological attributes of organisms that influence their performance and interactions with the environment (de Bello et al., 2021; Green et al., 2022; Westoby, 2025).

2.2.1. Defining functional traits

Functional traits are broadly defined as those characteristics measurable at the individual level that impact an organism's fitness-its growth, survival, and reproduction (Volaire et al., 2020). Violle et al. (2007) specified that a trait is "any morphological, physiological or phenological feature measurable at the individual level, from the cell to the whole organism" and becomes truly functional when it "impacts fitness (of an individual) indirectly via its effects on growth, reproduction and survival". These traits reflect evolutionary trade-offs in resource acquisition, utilisation, and conservation strategies developed in response to environmental pressures (Agrawal, 2020; Volaire et al., 2020). From an evolutionary viewpoint, it can be argued that all traits are potentially functional as any trait could be linked to fitness in at least one potential environmental context (Kearney et al., 2021; Sobral, 2021), highlighting the importance of considering the spatiotemporal variation of environmental pressures (Aubin et al., 2016).

Key plant functional trait categories include:

(1) Morphological traits: Those relate directly to physical and structural attributes of plants that define their form, architecture, and resource acquisition strategies (Freschet et al., 2018), such as specific leaf area (SLA, leaf area per unit dry mass, in $cm^2\ g^{-1}$), leaf size (in cm^2), and wood density (WD, in $g\ cm^{-3}$). SLA is a key component of the "leaf economics

spectrum" that reflects a trade-off between rapid resource capture (high SLA) and resource conservation (low SLA) (Reich, 2014a; I. J. Wright et al., 2004). WD relates to construction costs, mechanical support, and resistance to damage or embolism (Chave et al., 2009).

(2) Physiological traits: Those relate to the internal functioning and processes of plants, such as how plants acquire, use, and conserve resources (Reich et al., 2003). Specifically, they include **Leaf nutrients**: Concentrations of essential elements like nitrogen (N, in %), phosphorus (P, in %), and potassium (K, in %) in leaf tissues. These are critical for litter decomposition and nutrient cycling (Pietsch et al., 2014; Reich & Oleksyn, 2004). **Photosynthetic traits**: Parameters such as the maximum rate of photosynthesis under light- and CO_2-saturated conditions (A_{max}, in μmol m^{-2} s^{-1}) and light-saturated photosynthetic rate at ambient CO_2 concentrations (A_{sat}, in μmol m^{-2} s^{-1}), which determine a plant's photosynthetic capacity and are essential for understanding species' growth rates, carbon assimilation, and overall productivity under varying environmental conditions (Kositsup et al., 2010; Walker et al., 2017). **Hydraulic traits**: Characteristics associated with water transport efficiency and drought tolerance, influencing how plants manage water stress (Anderegg et al., 2018; Santiago et al., 2018), such as water potential at which 50% of hydraulic conductivity is lost (P50, in MPa) and the hydraulic safety margin (SM50, in MPa).

(3) Phenological traits: Those relate to the seasonal timing of life cycle events (Post et al., 2008) including timing of leaf emergence, leaf lifespan, and time of flowering and fruit development.

Traits that determine how organisms respond to environmental conditions are termed "response traits", while those that affect ecosystem processes (e.g., nutrient cycling, primary productivity) are "effect traits" (Nock et al., 2016). A single trait can often be both a response and an effect trait, particularly in plants (Nock et al., 2016).

2.2.2. Quantifying community functional structure

The functional structure of communities, representing the distribution and variation of these traits, is commonly characterised using a set of quantitative metrics. In mathematical terms, the "shape" of a community's trait density distribution can be characterised by various indices known as "moments" (de Bello et al., 2021), with the first to the fourth moment corresponding to the mean of the distribution, the variance, the skewness, and the kurtosis (de Bello et al., 2021). Similarly, in functional ecology, these four moments can be used to

characterise the distribution of traits within a community or across broader scales (de Bello et al., 2021; Le Bagousse-Pinguet et al., 2017). While all four moments offer unique insights, the first two provide a considerable amount of information and are central to many ecological analyses (de Bello et al., 2021). The community-weighted mean (CWM) of trait values is the most fundamental of these, which represents the first moment. For a given trait, the CWM is calculated as the average trait values weighted by their relative abundances (Laliberté & Legendre, 2010) or basal area (Aguirre-Gutiérrez et al., 2025; Pla et al., 2012) within the community. The CWM represents the expected trait value of a randomly selected individual from the community and reflects the dominant trait strategy (Muscarella & Uriarte, 2016). Complementing the CWM, the community-weighted variance (CWV), or trait variance at the community level, quantifies the spread of trait values around the CWM and corresponds to the second moment of the trait distribution. It is often calculated as the sum of the squared deviations of species' trait values from the CWM, weighted by their relative abundances or basal area. This metric indicates the degree of trait variability within the community (Bruelheide et al., 2018; Enquist et al., 2015). Higher moments like community-weighted skewness (third) and community-weighted kurtosis (fourth) can provide further detail but are less commonly used than CWM and CWV (de Bello et al., 2021).

Beyond these moments, functional diversity (FD) captures the value, range, and relative abundance of functional traits within a community (Díaz & Cabido, 2001). FD is multifaceted and can be decomposed into several components including functional richness, functional divergence, and functional evenness (de Bello et al., 2021; Mason et al., 2005; Villéger et al., 2008). Functional richness describes the amount of functional trait space occupied by the species in a community, often quantified as the convex hull volume encompassing all species in multivariate trait space (Villéger et al., 2008). Functional divergence quantifies how species' traits are spread out within the community, with a particular emphasis on the occupation of the extremes of the functional trait space (Villéger et al., 2008). Functional evenness measures the regularity of the distribution of species' abundances within this occupied trait space (Villéger et al., 2008). It is important to note that the framework for functional richness, functional divergence, and functional evenness is primarily developed for quantitative traits without missing values and for situations where there are more species than traits, although extensions to other trait types are suggested (Laliberté & Legendre, 2010). Furthermore, functional richness is well established that the range is not a robust measure of dispersion due to its high sensitivity to outliers, and it does not incorporate information on species' relative abundances.

As a result, rare species with extreme trait values can disproportionately inflate functional richness, which may or may not be desirable depending on the context of the analysis. In contrast, the functional evenness and functional divergence indices proposed by Villéger et al. (2008) do account for species abundances, but they do not quantify the overall dispersion of species in trait space (Laliberté & Legendre, 2010). Laliberté & Legendre (2010) proposed a multidimensional FD metric called functional dispersion (FDis), which measures the spread of species in trait space relative to the community centroid (the CWM in multivariate space) and is typically calculated as the abundance-weighted mean distance of individual species to this centroid (Laliberté & Legendre, 2010).

Finally, functional redundancy (FRed) refers to the degree to which multiple species within a community possess similar trait values and thus perform similar ecological roles (Rosenfeld, 2002). High FRed suggests that the loss of one species can be compensated by others with similar traits, potentially enhancing ecosystem stability and resilience (Biggs et al., 2020). It arises when multiple species share similar effect traits but may differ in their response traits, providing an "insurance" effect (Céréghino et al., 2022; Fischer & de Bello, 2023). FRed can be quantified by related formulations (Ricotta et al., 2016) (see **Section 3.3. Calculating functional trait composition, diversity, and redundancy, and carbon resilience** for details).

2.2.3. Biodiversity-ecosystem function relationships

At the centre of functional ecology is the biodiversity-ecosystem function (BEF) relationship, which states that biodiversity influences both the magnitude and stability of ecosystem processes (Gonzalez et al., 2020; Thompson et al., 2018). Numerous studies, including long-term experiments like those at Cedar Creek Ecosystem Science Reserve (Isbell et al., 2015, 2017), have shown that higher plant diversity (whether taxonomic, phylogenetic, or functional) often leads to increased ecosystem functioning (Le Bagousse-Pinguet et al., 2019; Schuldt et al., 2019), such as primary productivity (Isbell et al., 2015; Li et al., 2023; Powell & Rillig, 2018; Schweiger et al., 2018). The mechanisms underlying positive BEF relationships include but not limit to:

(1) Biological insurance: Functional redundancy and species asynchrony buffer ecosystems against fluctuations (Bello et al., 2021; Eisenhauer et al., 2024; Loreau et al., 2021). Functional redundancy plays a stabilising role by ensuring that species with overlapping roles can maintain ecosystem functions if others decline (Eisenhauer et al., 2010).

(2) Niche complementarity: Diverse species with differing traits may utilise resources more completely or efficiently, leading to greater overall productivity than any single species in monoculture (Eisenhauer et al., 2024; A. J. Wright et al., 2017, 2021).

(3) Selection effect: More diverse communities have a higher probability of containing highly productive or functionally important species (Eisenhauer et al., 2024; A. J. Wright et al., 2017, 2021).

(4) Performance-enhancing effect: A type of selection effect applies as environmental conditions shift, biodiversity increases the odds that some species will thrive and sustain key functions (Eisenhauer et al., 2024; Loreau et al., 2021).

(5) Resilience and resistance: Diverse communities tend to be more resistant to change (i.e., they maintain structure and function during disturbance) and more resilient, recovering more quickly afterward (Eisenhauer et al., 2024; Isbell et al., 2015; Van Meerbeek et al., 2021).

(6) Climate extremes: Increasing frequency and intensity of climate extremes including droughts, heatwaves, and storms pose significant challenges to ecosystem functioning. Biodiversity can buffer ecosystems against these events through enhanced resistance and recovery capacities (De Boeck et al., 2018). Climate extremes are defined by values of climate variables near the tails (e.g., 5% or 10%) of historical distributions and may act as pulse (short-term) or press (longer-term) disturbances (Field, 2012). Diverse ecosystems tend to be more stable under such stressors due to their compositional complexity and functional diversity (Craven et al., 2018; Polazzo & Rico, 2021).

(7) Trait-based trade-offs (fast-slow trade-off and growth-defence trade-off): Communities dominated by slow-growing species are more resistant but slower to recover, whereas fast-growing species confer rapid recovery but lower resistance (Bello et al., 2021; Eisenhauer et al., 2024; Reich, 2014b). Species investing more in defence may perform better under stress, particularly in species-rich communities where pathogen suppression is enhanced (Dietrich et al., 2021; Eisenhauer et al., 2024).

Together, these mechanisms highlight the critical role of biodiversity in maintaining and stabilising ecosystem functions, particularly under conditions of environmental stress and change. The nature and strength of BEF relationships can, however, be context-dependent and vary with spatial scale and the specific ecosystem function being considered (Eisenhauer et al., 2022). Functional traits, by providing a mechanistic link, are crucial for understanding and predicting these relationships (Gonzalez et al., 2020).

2.2.4. Ecosystem resilience and functional traits

Ecosystem resilience refers to the capacity of an ecosystem to withstand or recover from disturbances while maintaining its essential functions and structure (Folke, 2016; Holling, 1973). Biodiversity, particularly functional diversity and redundancy is thought to be a key determinant of resilience (Biggs et al., 2020; Dendoncker et al., 2023; Gladstone-Gallagher et al., 2019). Communities with greater functional diversity and/or greater functional redundancy may be more resilient because they possess a wider range of potential responses to environmental change or a greater capacity for compensatory dynamics if some species are lost (Gladstone-Gallagher et al., 2019; Oliver et al., 2015; Thomsen et al., 2019; Tilman et al., 2014). For instance, in the face of drought, a community with diverse rooting depths or water-use strategies (high functional diversity in hydraulic traits) might maintain overall function better than a community with uniform traits (Lourenço Jr. et al., 2022). Similarly, if multiple species perform the same key function (i.e., high functional redundancy), the loss of one such species may have minimal impact on the overall process (Fetzer et al., 2015; Mulder et al., 2001; Rosenfeld, 2002).

It is important to note, however, that functional diversity and redundancy are not direct measures of resilience. Rather, they represent underlying mechanisms that can promote the stability of ecosystem processes (e.g., lower variability in productivity, biomass, or carbon fluxes) and, by extension, contribute to resilience under disturbance and environmental change. Understanding these links is critical for managing ecosystems in an era of accelerating global change.

2.3. Remote sensing in ecological research

The study of functional ecology and biodiversity across meaningful spatial and temporal scales is often hampered by the limitations of traditional field-based methods (Lausch et al., 2016). Field surveys, while providing detailed data, are typically labour-intensive, costly, restricted in spatial coverage (R. Wang & Gamon, 2019), and can be context-dependent or influenced by observer bias (Asner, Martin, et al., 2015; Lõhmus et al., 2018; Thomson et al., 2021). Remote sensing offers a transformative approach to overcome many of these challenges by providing consistent, objective, and spatially contiguous data over large areas and with regular temporal repetition (Asner et al., 2017; Asner, Martin, et al., 2015; Cavender-Bares et al., 2020; Helfenstein et al., 2022).

2.3.1. Fundamental principles and development of ecological remote sensing

Remote sensing is the technique of gathering information about objects or phenomena from a distance, typically by detecting and measuring electromagnetic radiation reflected or emitted from the Earth's surface (Cavender-Bares et al., 2020). The interaction of electromagnetic radiation with vegetation is complex, influenced by leaf biochemistry (pigments, water, dry matter), canopy structure (leaf angle, leaf area index, and vertical stratification), and background components like soil and shadow (Abu-Elsaoud et al., 2022; Asner, 1998; Panferov et al., 2001; Yang, 2022). These interactions form the physical basis for deriving information about vegetation characteristics, including functional traits and biodiversity, from remotely sensed data.

The application of remote sensing in ecology has evolved significantly from early uses in habitat mapping (Kerr & Ostrovsky, 2003; Miller & Rogan, 2007) to more sophisticated estimations of biophysical and biochemical parameters (Stagakis et al., 2010), forest structure (Lechner et al., 2020; Zellweger et al., 2013), species distributions (He et al., 2015a; Randin et al., 2020), and, recently and increasingly, direct mapping of plant functional traits and diversity (Aguirre-Gutiérrez et al., 2025; Asner et al., 2017; Bae et al., 2019; Cherif et al., 2023a; Hauser et al., 2021; Helfenstein et al., 2022; Jetz et al., 2016; Ma et al., 2019; Schneider et al., 2017; R. Wang & Gamon, 2019). This evolution has been driven by advancements in sensor technology, the availability of diverse remote sensing platforms, and the development of progressive analytical techniques.

2.3.2. Types of remotely sensed data

Remote sensing systems can be broadly classified based on their source of illumination:

(1) Passive remote sensing: These sensors detect naturally available radiation, primarily solar radiation reflected by the Earth's surface, or thermal radiation emitted by it (Smith et al., 2014). Dominant passive remote sensing sensors include:

Multispectral sensors: They capture data in a few, relatively broad spectral bands (e.g., visible, near-infrared, shortwave infrared) (Zhu et al., 2018). Instruments such as those aboard Landsat, a joint programme between the National Aeronautics and Space Administration (NASA) and the United States Geological Survey (USGS) since 1972 (Wulder et al., 2008), Sentinel-2 launched by the European Space Agency (ESA) in 2015 (Drusch et al., 2012), and

the Moderate Resolution Imaging Spectroradiometer (MODIS) launched by NASA in 1999 (Salomonson et al., 1989), capture data in several discrete and broad spectral bands from the visible to the shortwave infrared regions. The reflectance and absorption patterns in these bands are sensitive to leaf pigments (e.g., chlorophylls and carotenoids), leaf water content, and canopy structure (Sims & Gamon, 2002). Spectral vegetation indices, such as the normalised difference vegetation index (NDVI) (Rouse et al., 1974) and the enhanced vegetation index (EVI) (H. Q. Liu & Huete, 1995), are derived from these bands and are widely used to assess vegetation greenness (Taddeo et al., 2019), vigour (Xue & Su, 2017), and phenology (Gong et al., 2024), and have been empirically linked to traits like leaf morphological traits and leaf nutrients (Aguirre-Gutiérrez et al., 2025; Wallis et al., 2019). Pros: Wide availability, long historical archives (e.g., Landsat data are available from 1972 to the present), good spatial coverage, and often free data access. Cons: Limited spectral detail restricts the direct retrieval of vegetation properties (Pang et al., 2024); susceptible to atmospheric interference and cloud cover (Okin & Gu, 2015).

Hyperspectral sensors (Imaging spectroscopy): These advanced sensors collect data in hundreds of narrow, contiguous spectral bands, providing a detailed spectral signature for each pixel (van der Meer et al., 2012). This rich spectral information allows for the detection of subtle absorption features related to specific leaf biochemical constituents (e.g., nitrogen, lignin, cellulose, and water content) (Pandey et al., 2017; Serrano et al., 2002) and more precise quantification of pigment concentrations (Blackburn, 2007). Consequently, imaging spectroscopy is considered a powerful tool for the direct estimation of a range of leaf functional traits and is revolutionising our ability to characterise forest functions remotely (Knyazikhin et al., 2013; Watt et al., 2020). Examples include the Airborne Visible/Infrared Imaging Spectrometer (AVIRIS) (Vane et al., 1993) and the forthcoming Surface Biology and Geology satellite mission (Cawse-Nicholson et al., 2021). Pros: High spectral resolution enables detailed biochemical and biophysical characterisation. Cons: Data are often more expensive and less frequently available than multispectral data (Biehl & Landgrebe, 2002), particularly from spaceborne platforms until recently; larger data volumes require more processing power (Burger & Gowen, 2011); also susceptible to atmospheric and cloud effects.

(2) Active remote sensing: These sensors provide their own source of illumination and measure the backscattered signal (Tedesco, 2015). Two frequently used active sensors are:

Radio detection and ranging (Radar), including **synthetic aperture radar (SAR)**: SAR systems, such as C-band Sentinel-1 (Torres et al., 2012), L-band PALSAR (Rosenqvist

et al., 2004), and X-band COSMO-SkyMed (F.Covello et al., 2010), are active sensors that emit microwave pulses and record the backscattered signal (Woodhouse, 2017). Longer wavelengths (e.g., L-band and P-band) can penetrate forest canopies and interact with woody components (stems and branches) (Monteith & Ulander, 2018), while shorter wavelengths (e.g., C-band and X-band) are more sensitive to the upper canopy and leaves (McNairn & and Brisco, 2004). SAR data are valuable for estimating forest structural parameters such as aboveground biomass (Englhart et al., 2011), stem volume (Abdullahi et al., 2016), and canopy height (Pourshamsi et al., 2021), particularly in regions with persistent cloud cover, as microwaves can penetrate clouds (Mermoz et al., 2015). SAR backscatter intensity and phase information can also be sensitive to vegetation water content and surface roughness (Zhu et al., 2019), providing indirect links to traits related to plant water status and canopy architecture (Inoue et al., 2014). Pros: All-weather capability (cloud penetration); sensitivity to structural attributes and moisture (S. K. Singh et al., 2023). Cons: Signal interpretation can be complex due to interactions with multiple canopy and ground features (Neumann et al., 2010); geometric distortions in rugged terrain (Loew & Mauser, 2007).

Light detection and ranging (LiDAR): LiDAR systems emit laser pulses and measures the time taken for reflections to return (Behroozpour et al., 2017), airborne LiDAR systems and spaceborne missions (e.g., Global Ecosystem Dynamics Investigation (GEDI) and Ice, Cloud, and land Elevation Satellite 2 (ICESat-2), both were launched by NASA in 2018) provide direct and three-dimensional measurements of forest canopy structure, including canopy height, vertical foliage profiles, gap distributions, and underlying topography (Calders et al., 2014; Goodwin et al., 2006). These structural metrics are crucial for characterising habitat heterogeneity, light environments within the canopy (Coops et al., 2016; Müller et al., 2018), and can be linked to traits related to nutrient cycling and plant resource acquisition strategies (Asner, Anderson, et al., 2015). Pros: Direct measurement of 3D structure; high accuracy. Cons: Typically acquired from airborne platforms, which can be costly for large areas (Wulder et al., 2012); spaceborne LiDAR (e.g., GEDI) offers global coverage but with sparser sampling (Hancock et al., 2021).

2.3.3. Remote sensing platforms

The choice of platform influences the spatial resolution, coverage, revisit time, and cost of remotely sensed data:

(1) Satellite platforms: Satellites provide consistent and repetitive coverage at a global scale (e.g., Sentinel-1 SAR satellite, Sentinel-2 multispectral satellite, and GEDI LiDAR satellite). Moreover, the P-band BIOMASS SAR satellite (Scipal et al., 2010) that was launched recently on 29 April 2025 by ESA and forthcoming missions such as the Surface Biology and Geology (visible to shortwave infrared hyperspectral and multispectral midwave and thermal infrared) satellite that will potentially be launched by NASA in 2027 (Cawse-Nicholson et al., 2021), promise unprecedented satellite remotely sensed data globally. Satellite data are ideal for long-term monitoring and large-scale studies, though often with coarser spatial resolution than airborne systems (Dash & Ogutu, 2016). Primary satellite platforms frequently used in ecology are summarised in Table 2.1.

Table 2.1. Primary satellite platforms frequently used in ecology.

Satellite	Year of launch	Sensor(s)	Spatial resolution (m)	Temporal resolution (day)	Temporal coverage	Sensor characteristics
Multispectral						Spectral range (μm)
Landsat 1	1972	MSS	60	18	1972-1978	0.5-1.1
Landsat 2	1975	MSS	60	18	1975-1983	0.5-1.1
Landsat 3	1978	MSS	60	18	1978-1983	0.5-1.1
Landsat 4	1982	MSS and TM	30, 120	16	1982-1993	0.45-12.5
Landsat 5	1984	MSS and TM	30, 120	16	1984-2013	0.45-12.5
Landsat 7	1999	ETM+	15-60	16	1999-2024	0.45-12.5
Terra	1999	MODIS	250-1000	1	2000-now	0.459-14.385
Aqua	2002	MODIS	250-1000	1	2002-now	0.459-14.385
WorldView-1	2007	WV-1	0.5	1.7	2007-now	0.4-0.9
WorldView-2	2009	WV-110, WV-60	0.46	1.1	2009-now	0.45-1.04
Gaofen-1	2013	PMS, WFV	2-16	4	2013-now	0.45-0.89
Landsat 8	2013	OLI, TIRS	15-30	16	2013-now	0.43-12.51
SkySat-1	2013	Skybox Image Sensor	0.9-2	1.8 per day	2013-now	0.45-0.9
Gaofen-2	2014	PMS	0.8-3.2	5	2014-now	0.4-0.9
SkySat-2	2014	Skybox Image Sensor	0.9-2	1.8 per day	2014-now	0.45-0.9
WorldView-3	2014	WV-3	~0.3	1-4.5	2014-now	0.45-2.245
Sentinel-2	2015, 2016	MSI	10-60	5	2015-now	0.443-2.19
Gaofen-6	2018	PMS, WFV	2-16	2	2018-now	0.45-0.9
Landsat 9	2021	OLI, TIRS	15-100	16	2021-now	0.43-2.29
Hyperspectral						Spectral range (μm)
Earth Observing-1	2000	ALI, Hyperrion, LEISA, LAC	30	16	2000-2017	0.357-2.576
Gaofen-5	2018	AHSI, VIMS, GMI, EMI, DPC, AIUS	30	51	2018-now	0.24-12.5
EnMap	2022	HSI	30	27	2022-now	0.42-2.45
SAR						Wavelength (cm)
PALSAR-1	2006	L-band SAR	10-100	46	2006-2011	23.62

RADARSAT-2	2007	C-band SAR	3-100	7	2007-now	5.6
TerraSAR-X	2007	X-band SAR	1-16	11	2007-now	3.1
COSMO-SkyMed	2007	X-band SAR	1-100	16	2007-now	3.1
TanDEM-X	2010	X-band SAR	1-16	11	2010-now	3.1
Sentinel-1	2014, 2016	C-band SAR	10	6	2014-now	5.6
PALSAR-2	2014	L-band SAR	3-10	14	2014-now	~24
Gaofen-3	2016	C-band SAR	1-25	29	2016-now	5.55
LiDAR						Wavelength (nm)
GEDI	2018	Multiple laser beams	30	Variable	2018-now	1064
ICESAT-2	2018	ATLAS	0.7-280	91	2018-now	532

MSS: Multispectral Scanner, TM: Thematic Mapper, ETM+: Enhanced Thematic Mapper Plus, MODIS: Moderate Resolution Imaging Spectroradiometer, WV: WorldView, PMS: Panchromatic Multispectral, WFC: Wide Field View, OLI: Operational Land Imager, TIRS: Thermal Infrared Sensor, MSI: Multispectral Instrument, ALI: Advanced Land Imager, LEISA: Linear Etalon Imaging Spectrometer Array, LAC: LEISA Atmospheric Corrector, AHSI: Advanced Hyperspectral Imager, VIMS: Visible and Infrared Multispectral Sensor, GMI: Greenhouse-gases Monitoring Instrument, EMI: Environment Monitoring Instrument, DPC: Directional Polarisation Camera, AIUS: Atmospheric Infrared Ultraspectral, HSI: Hyperspectral Imager, ATLAS: Advanced Topographic Laser Altimeter System

(2) Airborne platforms: Airborne platforms provide flexibility in sensor deployment (including high-resolution hyperspectral and LiDAR), timing of acquisition, and achieving very high spatial resolution (Meerdink et al., 2019; Yan et al., 2015). Suitable for regional to landscape-scale studies but can be expensive and with less frequent coverage than satellites (Meerdink et al., 2019).

(3) Unmanned aerial vehicles (UAVs or drones): Drones have become increasingly important for ecological research for local-scale and on-demand data acquisition at very- or even ultra-high spatial resolution (often sub-centimetre) (Ventura et al., 2023). They can carry smaller and lighter multispectral, hyperspectral, thermal, or LiDAR sensors, but limited by payload, flight endurance, and regulatory constraints (Townsend et al., 2020).

(4) Close-range/proximal sensing: Instruments including towers like FLUXNET (Baldocchi et al., 2001), tripods (Moreno Párrizas & Andújar, 2023), and handheld spectrometers and LiDAR (Ramezani et al., 2020; Sorak et al., 2012). These are essential for detailed field measurements, calibration/validation of airborne and spaceborne data, and understanding fine-scale ecological processes (Alexopoulos et al., 2023). However, close-range sensing has limited spatial coverage, and they are often labour- and time-intensive, and there are temporal constraints.

2.3.4. Applications in forest ecology, trait, and biodiversity monitoring

Remote sensing technologies are transforming forest ecology by enabling comprehensive and multi-scale observations of forest ecosystems. They provide crucial tools for monitoring forest cover and dynamics, which allows researchers and policymakers to detect and quantify deforestation, afforestation, and forest degradation across large spatial and temporal scales (Gao et al., 2020; Mitchell et al., 2017). These observations form the foundation for global forest change assessments (Hansen et al., 2010, 2013) and carbon accounting efforts (Lagomasino et al., 2019; Malerba et al., 2023). Moreover, advances in active remote sensing technologies such as LiDAR and SAR have made it possible to estimate key structural attributes of forests including canopy height (Pourshamsi et al., 2021; Simard et al., 2011), vertical layering (Ehbrecht et al., 2016; Neumann et al., 2010), leaf area index (Hosseini et al., 2015; Y. Wang & Fang, 2020), and aboveground biomass (Cao et al., 2016; Yu & Saatchi, 2016), thus enhancing our understanding of forest architecture and its ecological functions.

Remote sensing is also revolutionising the way trait-based ecology is studied, not only by enabling the large-scale estimation of plant functional traits, but also by facilitating assessments of functional trait diversity and redundancy. Because many of these traits influence plant optical and structural properties, they can be inferred from remotely sensed data (Asner & Martin, 2016; Ustin & Gamon, 2010). Airborne imaging spectroscopy has played a foundational role in mapping plant functional traits. Platforms such as NASA's AVIRIS, the Global Airborne Observatory, HyMap, and HySpex have enabled detailed retrievals of leaf chemical and physiological traits across diverse ecosystems (Ali et al., 2016; Kattenborn et al., 2017; Ordway et al., 2022; A. Singh et al., 2015). These studies, often using techniques like partial least squares regression and radiative transfer models, have shown that hyperspectral data can reliably estimate traits like leaf nitrogen, leaf mass per area, and water content. However, airborne campaigns remain limited by high operational costs, data availability, sparse geographic and temporal coverage, and a lack of repeated coverage, restricting their utility for long-term or continental-scale monitoring.

Combining hyperspectral imaging with LiDAR has proven particularly valuable for characterising both biochemical and structural traits (Fu et al., 2024). For instance, hyperspectral data provide detailed spectral signatures of leaf chemistry, while LiDAR captures vertical forest structure (Ewald et al., 2018), enabling a fuller picture of trait distributions and ecosystem complexity (Asner et al., 2007; Asner, Martin, et al., 2015; Shi et al., 2018). Studies demonstrate that such integration enhances estimates of biodiversity and enables trait-based

measures of ecosystem heterogeneity (Kamoske et al., 2022; Ming et al., 2024; Zheng et al., 2022).

Satellite multispectral remote sensing, though lower in spectral resolution than hyperspectral systems, offers global, frequent, and consistent coverage. Missions such as Sentinel-2, Landsat, and MODIS have been applied to map key traits (e.g., chlorophyll content, SLA, and leaf water content) (Aguirre-Gutiérrez et al., 2021, 2025; An et al., 2024; S. Liu et al., 2024; Švik et al., 2023; Wan et al., 2024). While limited in trait specificity, multispectral data contribute significantly to long-term monitoring and allow derivation of spectral diversity metrics and phenology-based proxies of functional composition and turnover (Rocchini et al., 2022). The integration of satellite multispectral and LiDAR can enhance assessments of functional trait distributions and vertical complexity over broad spatial and temporal scales. However, satellite-based LiDAR coverage remains sparse and temporally constrained compared to spectral sensors (Bhardwaj et al., 2016).

Despite its underuse in trait-based ecology, SAR holds immense promise for assessing functional traits and trait-based diversity. Unlike spectral sensors, SAR operates independently of sunlight and cloud cover and can penetrate canopy layers (Tsai et al., 2019). Its sensitivity to vegetation structure and moisture enables the estimation of traits related to biomass, wood density, and canopy water content (Lucas et al., 2010; Saatchi & Moghaddam, 2000; Sinha et al., 2015). SAR also captures vegetation heterogeneity across multiple spatial and vertical scales (Tsyganskaya et al., 2018), making it a powerful tool for analysing functional traits and biodiversity (Cavender-Bares et al., 2020), especially in tropical forests and cloudy regions where spectral data are often limited (Hayes & Cohen, 2007; Ningthoujam et al., 2018). Yet, the application of SAR-either alone or fused with spectral or LiDAR data-for ecology remains underexplored (Betbeder et al., 2015; Grattepanche et al., 2018). Integrating SAR data offers an innovative path forward in capturing plant functional trait variation and biodiversity patterns across diverse ecosystems.

In addition, functional diversity metrics (e.g., functional richness, evenness, divergence, and dispersion) and redundancy indices derived from functional traits are essential for understanding ecosystem stability, productivity, and resilience. Remote sensing enables spatially explicit quantification of these indices, bridging the gap between species-level biodiversity and ecosystem functioning (Cavender-Bares et al., 2022; Lausch et al., 2016; Reddy, 2021). For instance, spectral diversity (i.e., variability in spectral signals) is increasingly used as a proxy for trait diversity and ecological heterogeneity, often

outperforming taxonomic diversity in predicting ecosystem processes (Schweiger et al., 2018). Furthermore, by first estimating functional traits at fine scales, indices including functional richness, functional evenness, functional divergence (Aguirre-Gutiérrez et al., 2025; Durán et al., 2019; Helfenstein et al., 2022; Schneider et al., 2017), and functional dispersion (Ma et al., 2019, 2020) can be computed across landscapes. These approaches are particularly promising for linking biodiversity patterns to ecosystem services and disturbances (Abelleira Martínez et al., 2016; Cavender-Bares et al., 2022).

Nevertheless, several challenges remain. Trait detection is challenged by factors like canopy structure, background noise (e.g., soil), phenological variation, and sensor limitations (Bian et al., 2022; Tang et al., 2016). Merging datasets across sensors, campaigns, and ecosystems is also difficult due to inconsistencies in resolution, protocols, and calibration (Pasetto et al., 2018). Despite these hinders, recent and ongoing satellite missions (e.g., BIOMASS and Surface Biology and Geology) and methodological advances in modelling and machine learning are poised to deliver more consistent and global-scale trait and diversity maps.

In summary, the combination of remote sensing technologies including hyperspectral, multispectral, LiDAR, and SAR provides an increasingly robust framework for mapping not only plant functional traits but also the spatial patterns of functional trait diversity and redundancy. This integration is essential for advancing our understanding of ecosystem structure, function, and resilience in the face of rapid environmental change (Cavender-Bares et al., 2020).

2.3.5. Data fusion and advanced analytical techniques

The most comprehensive characterisation of forest ecosystems and their functional traits often arises from the synergistic use of multiple remotely sensed data types (data fusion) (Mohammadpour & Viegas, 2022; Torabzadeh et al., 2014) and the application of advanced analytical techniques. Integrating data from multiple sensor types enables a more complete characterisation of vegetation. This is because each sensor type captures different, yet complementary aspects of plant systems: passive sensors are sensitive to foliar biochemical properties, while active sensors provide critical structural information. For example, combining spectral data (sensitive to biochemistry) with LiDAR (sensitive to structure) and SAR (sensitive to structure and moisture) can provide a more holistic view of forest composition and function than any single sensor alone (Alonzo et al., 2014; Cavender-Bares et al., 2020).

By bringing these data sources together, researchers can generate richer and multidimensional representations of forest composition, structure, and function (Guimarães et al., 2020; Lausch et al., 2018).

Furthermore, extracting ecologically meaningful information from these complex and high-dimensional datasets necessitate the use of advanced analytical techniques (Asner, Martin, et al., 2015; Himeur et al., 2022). Machine learning algorithms such as Random forests (RF) (Breiman, 2001) and Partial Least Squares Regression (Wold et al., 2001) are frequently used to model complex and non-linear relationships between spectral or structural signals and ecological variables such as plant traits (Aguirre-Gutiérrez et al., 2021, 2025; Féret et al., 2019), species distributions (Anand et al., 2021; He et al., 2015b), and biodiversity indices (Aguirre-Gutiérrez et al., 2025; Zheng et al., 2021, 2023). More recently, deep learning approaches (LeCun et al., 2015), including Convolutional Neural Networks (LeCun & Bengio, 1998) and Multilayer Perceptron (MLP) (Rosenblatt, 1958), are being explored for their capacity to automatically learn hierarchical features from imagery, potentially improving classification and prediction tasks in ecological studies (Borowiec et al., 2022; Park & Lek, 2016; Pichler & Hartig, 2023) including mapping plant functional traits (Cherif et al., 2023b).

Together, the integration of diverse sensor systems with cutting-edge analytical tools is rapidly advancing the ability to monitor forest functional diversity at broad scales (Ma et al., 2020). These developments are laying the foundation for operational systems that can track biodiversity patterns and ecological resilience over time (Cavender-Bares et al., 2022), helping to address critical questions about ecosystem responses to climate change and other global pressures (Pettorelli et al., 2018; Zhao et al., 2023).

2.4. Bridging the gaps: research imperatives and thesis contributions

Despite rapid advances in remote sensing and trait-based ecology, key challenges remain in accurately and consistently mapping a broad set of functional traits across complex forested landscapes. While imaging spectroscopy and LiDAR have proven valuable for capturing some traits, scaling these methods to pan-tropical forests remain difficult due to sensor limitations, forest heterogeneity, and logistical constraints (Aguirre-Gutiérrez et al., 2025; Durán et al., 2019; Ordway et al., 2022). This thesis addresses the need for integrative approaches by evaluating the complementary strengths of spectral, LiDAR, and SAR data, and by comparing

advanced modelling techniques including machine learning and deep learning for robust and scalable trait estimation (**Chapter 4**).

Equally important is the empirical application of functional diversity theory across ecologically significant but understudied regions. In South American temperate forests, functional trait composition, diversity, and redundancy remain poorly characterised (Gutiérrez et al., 2014), despite their relevance for understanding ecosystem responses to environmental gradients. This thesis fills this gap by examining how different facets (morphology, nutrients, photosynthesis, and hydraulics) of functional diversity and redundancy are driven by multiple environmental variables, offering new insights into the resilience and vulnerability of these unique ecosystems, and informing conservation and land management efforts in a changing climate (**Chapter 5**).

The role of functional diversity and redundancy in modulating forest resilience, particularly with respect to carbon cycling, is also not fully understood (Hisano et al., 2024). While biodiversity is widely recognised as a stabilising force, the mechanisms linking trait variation to carbon stocks and carbon dynamics under climate stress remain unclear. This research investigates how initial levels of functional diversity and redundancy influence carbon stocks and dynamics in both temperate and tropical forests, which aims to clarify how different trait dimensions contribute to ecosystem stability under disturbance, particularly in terms of intensifying warming and drought conditions (**Chapter 6**).

2.5. References

Abdullahi, S., Kugler, F., & Pretzsch, H. (2016). Prediction of stem volume in complex temperate forest stands using TanDEM-X SAR data. *Remote Sensing of Environment*, *174*, 197–211. https://doi.org/10.1016/j.rse.2015.12.012

Abelleira Martínez, O. J., Fremier, A. K., Günter, S., Ramos Bendaña, Z., Vierling, L., Galbraith, S. M., Bosque-Pérez, N. A., & Ordoñez, J. C. (2016). Scaling up functional traits for ecosystem services with remote sensing: Concepts and methods. *Ecology and Evolution*, *6*(13), 4359–4371. https://doi.org/10.1002/ece3.2201

Abu-Elsaoud, A. M., Abdulmajeed, A. M., Alhaithloul, H. A. S., & Soliman, M. H. (2022). Role of Electromagnetic Radiation in Abiotic Stress Tolerance. In *Plant Abiotic Stress Physiology*. Apple Academic Press.

Agrawal, A. A. (2020). A scale-dependent framework for trade-offs, syndromes, and specialization in organismal biology. *Ecology*, *101*(2), e02924. https://doi.org/10.1002/ecy.2924

Aguirre-Gutiérrez, J., Rifai, S., Shenkin, A., Oliveras, I., Bentley, L. P., Svátek, M., Girardin, C. A. J., Both, S., Riutta, T., Berenguer, E., Kissling, W. D., Bauman, D., Raab, N., Moore, S., Farfan-Rios, W., Figueiredo, A. E. S., Reis, S. M., Ndong, J. E., Ondo, F. E., … Malhi, Y. (2021). Pantropical modelling of canopy functional traits using Sentinel-2 remote sensing data. *Remote Sensing of Environment*, *252*, 112122. https://doi.org/10.1016/j.rse.2020.112122

Aguirre-Gutiérrez, J., Rifai, S. W., Deng, X., ter Steege, H., Thomson, E., Corral-Rivas, J. J., Guimaraes, A. F., Muller, S., Klipel, J., Fauset, S., Resende, A. F., Wallin, G., Joly, C. A., Abernethy, K., Adu-Bredu, S., Alexandre Silva, C., de Oliveira, E. A., Almeida, D. R. A., Alvarez-Davila, E., … Malhi, Y. (2025). Canopy functional trait variation across Earth's tropical forests. *Nature*, 1–8. https://doi.org/10.1038/s41586-025-08663-2

Alexopoulos, A., Koutras, K., Ali, S. B., Puccio, S., Carella, A., Ottaviano, R., & Kalogeras, A. (2023). Complementary Use of Ground-Based Proximal Sensing and Airborne/Spaceborne Remote Sensing Techniques in Precision Agriculture: A Systematic Review. *Agronomy*, *13*(7), Article 7. https://doi.org/10.3390/agronomy13071942

Ali, A. M., Skidmore, A. K., Darvishzadeh, R., van Duren, I., Holzwarth, S., & Mueller, J. (2016). Retrieval of forest leaf functional traits from HySpex imagery using radiative transfer models and continuous wavelet analysis. *ISPRS Journal of Photogrammetry and Remote Sensing*, *122*, 68–80. https://doi.org/10.1016/j.isprsjprs.2016.09.015

Alonzo, M., Bookhagen, B., & Roberts, D. A. (2014). Urban tree species mapping using hyperspectral and lidar data fusion. *Remote Sensing of Environment*, *148*, 70–83. https://doi.org/10.1016/j.rse.2014.03.018

Alvarado, M. V., & Terrazas, T. (2023). Tree species differ in plant economic spectrum traits in the tropical dry forest of Mexico. *PLOS ONE*, *18*(11), e0293430. https://doi.org/10.1371/journal.pone.0293430

An, N., Lu, N., Chen, W., Chen, Y., Shi, H., Wu, F., & Fu, B. (2024). Spatial mapping of key plant functional traits in terrestrial ecosystems across China. *Earth System Science Data*, *16*(4), 1771–1810. https://doi.org/10.5194/essd-16-1771-2024

Anand, A., Pandey, M. K., Srivastava, P. K., Gupta, A., & Khan, M. L. (2021). Integrating Multi-Sensors Data for Species Distribution Mapping Using Deep Learning and Envelope Models. *Remote Sensing*, *13*(16), Article 16. https://doi.org/10.3390/rs13163284

Anderegg, W. R. L., Konings, A. G., Trugman, A. T., Yu, K., Bowling, D. R., Gabbitas, R., Karp, D. S., Pacala, S., Sperry, J. S., Sulman, B. N., & Zenes, N. (2018). Hydraulic

diversity of forests regulates ecosystem resilience during drought. *Nature*, *561*(7724), 538–541. https://doi.org/10.1038/s41586-018-0539-7

Armesto, J. J., Rozzi, R., & Caspersen, J. (2001). Temperate Forests of North and South America. In F. S. Chapin, O. E. Sala, & E. Huber-Sannwald (Eds.), *Global Biodiversity in a Changing Environment: Scenarios for the 21st Century* (pp. 223–249). Springer. https://doi.org/10.1007/978-1-4613-0157-8_11

Asner, G. P. (1998). Biophysical and Biochemical Sources of Variability in Canopy Reflectance. *Remote Sensing of Environment*, *64*(3), 234–253. https://doi.org/10.1016/S0034-4257(98)00014-5

Asner, G. P., Anderson, C. B., Martin, R. E., Tupayachi, R., Knapp, D. E., & Sinca, F. (2015). Landscape biogeochemistry reflected in shifting distributions of chemical traits in the Amazon forest canopy. *Nature Geoscience*, *8*(7), 567–573. https://doi.org/10.1038/ngeo2443

Asner, G. P., Knapp, D. E., Kennedy-Bowdoin, T., Jones, M. O., Martin, R. E., Boardman, J. W., & Field, C. B. (2007). Carnegie Airborne Observatory: In-flight fusion of hyperspectral imaging and waveform light detection and ranging for three-dimensional studies of ecosystems. *Journal of Applied Remote Sensing*, *1*(1), 013536. https://doi.org/10.1117/1.2794018

Asner, G. P., & Martin, R. E. (2016). Spectranomics: Emerging science and conservation opportunities at the interface of biodiversity and remote sensing. *Global Ecology and Conservation*, *8*, 212–219. https://doi.org/10.1016/j.gecco.2016.09.010

Asner, G. P., Martin, R. E., Anderson, C. B., & Knapp, D. E. (2015). Quantifying forest canopy traits: Imaging spectroscopy versus field survey. *Remote Sensing of Environment*, *158*, 15–27. https://doi.org/10.1016/j.rse.2014.11.011

Asner, G. P., Martin, R. E., Knapp, D. E., Tupayachi, R., Anderson, C. B., Sinca, F., Vaughn, N. R., & Llactayo, W. (2017). Airborne laser-guided imaging spectroscopy to map forest trait diversity and guide conservation. *Science*, *355*(6323), 385–389. https://doi.org/10.1126/science.aaj1987

Aubin, I., Munson, A. D., Cardou, F., Burton, P. J., Isabel, N., Pedlar, J. H., Paquette, A., Taylor, A. R., Delagrange, S., Kebli, H., Messier, C., Shipley, B., Valladares, F., Kattge, J., Boisvert-Marsh, L., & McKenney, D. (2016). Traits to stay, traits to move: A review of functional traits to assess sensitivity and adaptive capacity of temperate and boreal trees to climate change. *Environmental Reviews*, *24*(2), 164–186. https://doi.org/10.1139/er-2015-0072

Ávila-Akerberg, V., Rosaliano-Evaristo, R., González-Martínez, T., Pichardo-García, B., & Serrano-González, D. (2023). Classification and nomenclature of temperate forest types in Mexico. *Vegetation Classification and Survey*, *4*, 329–341. https://doi.org/10.3897/VCS.100796

Bae, S., Levick, S. R., Heidrich, L., Magdon, P., Leutner, B. F., Wöllauer, S., Serebryanyk, A., Nauss, T., Krzystek, P., Gossner, M. M., Schall, P., Heibl, C., Bässler, C., Doerfler, I., Schulze, E.-D., Krah, F.-S., Culmsee, H., Jung, K., Heurich, M., … Müller, J. (2019). Radar vision in the mapping of forest biodiversity from space. *Nature Communications*, *10*(1), 4757. https://doi.org/10.1038/s41467-019-12737-x

Baldocchi, D., Falge, E., Gu, L., Olson, R., Hollinger, D., Running, S., Anthoni, P., Bernhofer, C., Davis, K., Evans, R., Fuentes, J., Goldstein, A., Katul, G., Law, B., Lee, X., Malhi, Y., Meyers, T., Munger, W., Oechel, W., … Wofsy, S. (2001). *FLUXNET: A New Tool to Study the Temporal and Spatial Variability of Ecosystem-Scale Carbon Dioxide, Water Vapor, and Energy Flux Densities*.

https://journals.ametsoc.org/view/journals/bams/82/11/1520-0477_2001_082_2415_fantts_2_3_co_2.xml

Behroozpour, B., Sandborn, P. A. M., Wu, M. C., & Boser, B. E. (2017). Lidar System Architectures and Circuits. *IEEE Communications Magazine*, *55*(10), 135–142. https://doi.org/10.1109/MCOM.2017.1700030

Bello, F. de, Lavorel, S., Hallett, L. M., Valencia, E., Garnier, E., Roscher, C., Conti, L., Galland, T., Goberna, M., Májeková, M., Montesinos-Navarro, A., Pausas, J. G., Verdú, M., E-Vojtkó, A., Götzenberger, L., & Lepš, J. (2021). Functional trait effects on ecosystem stability: Assembling the jigsaw puzzle. *Trends in Ecology & Evolution*, *36*(9), 822–836. https://doi.org/10.1016/j.tree.2021.05.001

Betbeder, J., Hubert-Moy, L., Burel, F., Corgne, S., & Baudry, J. (2015). Assessing ecological habitat structure from local to landscape scales using synthetic aperture radar. *Ecological Indicators*, *52*, 545–557. https://doi.org/10.1016/j.ecolind.2014.11.009

Bhardwaj, A., Sam, L., Bhardwaj, A., & Martín-Torres, F. J. (2016). LiDAR remote sensing of the cryosphere: Present applications and future prospects. *Remote Sensing of Environment*, *177*, 125–143. https://doi.org/10.1016/j.rse.2016.02.031

Bian, L., Zhang, H., Ge, Y., Čepl, J., Stejskal, J., & EL-Kassaby, Y. A. (2022). Closing the gap between phenotyping and genotyping: Review of advanced, image-based phenotyping technologies in forestry. *Annals of Forest Science*, *79*(1), 22. https://doi.org/10.1186/s13595-022-01143-x

Biehl, L., & Landgrebe, D. (2002). MultiSpec—A tool for multispectral–hyperspectral image data analysis. *Computers & Geosciences*, *28*(10), 1153–1159. https://doi.org/10.1016/S0098-3004(02)00033-X

Biggs, C. R., Yeager, L. A., Bolser, D. G., Bonsell, C., Dichiera, A. M., Hou, Z., Keyser, S. R., Khursigara, A. J., Lu, K., & Muth, A. F. (2020). Does functional redundancy affect

ecological stability and resilience? A review and meta-analysis. *Ecosphere*, *11*(7), e03184.

Blackburn, G. A. (2007). Hyperspectral remote sensing of plant pigments. *Journal of Experimental Botany*, *58*(4), 855–867. https://doi.org/10.1093/jxb/erl123

Bonilla-Moheno, M., & Aide, T. M. (2020). Beyond deforestation: Land cover transitions in Mexico. *Agricultural Systems*, *178*, 102734. https://doi.org/10.1016/j.agsy.2019.102734

Borowiec, M. L., Dikow, R. B., Frandsen, P. B., McKeeken, A., Valentini, G., & White, A. E. (2022). Deep learning as a tool for ecology and evolution. *Methods in Ecology and Evolution*, *13*(8), 1640–1660. https://doi.org/10.1111/2041-210X.13901

Box, E. O., & Fujiwara, K. (2015). Warm-Temperate Deciduous Forests: Concept and Global Overview. In E. O. Box & K. Fujiwara (Eds.), *Warm-Temperate Deciduous Forests around the Northern Hemisphere* (pp. 7–26). Springer International Publishing. https://doi.org/10.1007/978-3-319-01261-2_2

Breiman, L. (2001). Random forests. *Machine Learning*, *45*, 5–32.

Brown, J. H. (2014). Why are there so many species in the tropics? *Journal of Biogeography*, *41*(1), 8–22. https://doi.org/10.1111/jbi.12228

Bruelheide, H., Dengler, J., Purschke, O., Lenoir, J., Jiménez-Alfaro, B., Hennekens, S. M., Botta-Dukát, Z., Chytrý, M., Field, R., Jansen, F., Kattge, J., Pillar, V. D., Schrodt, F., Mahecha, M. D., Peet, R. K., Sandel, B., van Bodegom, P., Altman, J., Alvarez-Dávila, E., … Jandt, U. (2018). Global trait–environment relationships of plant communities. *Nature Ecology & Evolution*, *2*(12), 1906–1917. https://doi.org/10.1038/s41559-018-0699-8

Bunyavejchewin, S., LaFrankie, J. V., Baker, P. J., Davies, S. J., & Ashton, P. J. (2009). *Forest Trees of Huai Kha Khaeng Wildlife Sanctuary, Thailand: Data from the 50-Hectare*

Forest Dynamics Plot. National Parks, Wildlife & Plant Conservation Department. https://research.monash.edu/en/publications/forest-trees-of-huai-kha-khaeng-wildlife-sanctuary-thailand-data-

Burger, J., & Gowen, A. (2011). Data handling in hyperspectral image analysis. *Chemometrics and Intelligent Laboratory Systems*, *108*(1), 13–22. https://doi.org/10.1016/j.chemolab.2011.04.001

Calders, K., Armston, J., Newnham, G., Herold, M., & Goodwin, N. (2014). Implications of sensor configuration and topography on vertical plant profiles derived from terrestrial LiDAR. *Agricultural and Forest Meteorology*, *194*, 104–117. https://doi.org/10.1016/j.agrformet.2014.03.022

Cao, L., Coops, N. C., Innes, J. L., Sheppard, S. R. J., Fu, L., Ruan, H., & She, G. (2016). Estimation of forest biomass dynamics in subtropical forests using multi-temporal airborne LiDAR data. *Remote Sensing of Environment*, *178*, 158–171. https://doi.org/10.1016/j.rse.2016.03.012

Cavender-Bares, J., Gamon, J. A., & Townsend, P. A. (Eds.). (2020). *Remote Sensing of Plant Biodiversity*. Springer International Publishing. https://doi.org/10.1007/978-3-030-33157-3

Cavender-Bares, J., Schneider, F. D., Santos, M. J., Armstrong, A., Carnaval, A., Dahlin, K. M., Fatoyinbo, L., Hurtt, G. C., Schimel, D., Townsend, P. A., Ustin, S. L., Wang, Z., & Wilson, A. M. (2022). Integrating remote sensing with ecology and evolution to advance biodiversity conservation. *Nature Ecology & Evolution*, *6*(5), 506–519. https://doi.org/10.1038/s41559-022-01702-5

Cawse-Nicholson, K., Townsend, P. A., Schimel, D., Assiri, A. M., Blake, P. L., Buongiorno, M. F., Campbell, P., Carmon, N., Casey, K. A., Correa-Pabón, R. E., Dahlin, K. M., Dashti, H., Dennison, P. E., Dierssen, H., Erickson, A., Fisher, J. B., Frouin, R., Gatebe,

C. K., Gholizadeh, H., … Zhang, Q. (2021). NASA's surface biology and geology designated observable: A perspective on surface imaging algorithms. *Remote Sensing of Environment*, *257*, 112349. https://doi.org/10.1016/j.rse.2021.112349

Céréghino, R., Trzcinski, M. K., MacDonald, A. A. M., Marino, N. A. C., Acosta Mercado, D., Leroy, C., Corbara, B., Romero, G. Q., Farjalla, V. F., Barberis, I. M., Dézerald, O., Hammill, E., Atwood, T. B., Piccoli, G. C. O., Ospina Bautista, F., Carrias, J.-F., Leal, J. S., Montero, G., Antiqueira, P. A. P., … Srivastava, D. S. (2022). Functional redundancy dampens precipitation change impacts on species-rich invertebrate communities across the Neotropics. *Functional Ecology*, *36*(7), 1559–1572. https://doi.org/10.1111/1365-2435.14048

Chave, J., Coomes, D., Jansen, S., Lewis, S. L., Swenson, N. G., & Zanne, A. E. (2009). Towards a worldwide wood economics spectrum. *Ecology Letters*, *12*(4), 351–366. https://doi.org/10.1111/j.1461-0248.2009.01285.x

Cherif, E., Feilhauer, H., Berger, K., Dao, P. D., Ewald, M., Hank, T. B., He, Y., Kovach, K. R., Lu, B., Townsend, P. A., & Kattenborn, T. (2023a). From spectra to plant functional traits: Transferable multi-trait models from heterogeneous and sparse data. *Remote Sensing of Environment*, *292*, 113580. https://doi.org/10.1016/j.rse.2023.113580

Cherif, E., Feilhauer, H., Berger, K., Dao, P. D., Ewald, M., Hank, T. B., He, Y., Kovach, K. R., Lu, B., Townsend, P. A., & Kattenborn, T. (2023b). From spectra to plant functional traits: Transferable multi-trait models from heterogeneous and sparse data. *Remote Sensing of Environment*, *292*, 113580. https://doi.org/10.1016/j.rse.2023.113580

Coops, N. C., Tompaski, P., Nijland, W., Rickbeil, G. J. M., Nielsen, S. E., Bater, C. W., & Stadt, J. J. (2016). A forest structure habitat index based on airborne laser scanning data. *Ecological Indicators*, *67*, 346–357. https://doi.org/10.1016/j.ecolind.2016.02.057

Cordero, R. R., Feron, S., Damiani, A., Carrasco, J., Karas, C., Wang, C., Kraamwinkel, C. T., & Beaulieu, A. (2024). Extreme fire weather in Chile driven by climate change and El Niño–Southern Oscillation (ENSO). *Scientific Reports*, *14*(1), 1974.

Craven, D., Eisenhauer, N., Pearse, W. D., Hautier, Y., Isbell, F., Roscher, C., Bahn, M., Beierkuhnlein, C., Bönisch, G., Buchmann, N., Byun, C., Catford, J. A., Cerabolini, B. E. L., Cornelissen, J. H. C., Craine, J. M., De Luca, E., Ebeling, A., Griffin, J. N., Hector, A., … Manning, P. (2018). Multiple facets of biodiversity drive the diversity–stability relationship. *Nature Ecology & Evolution*, *2*(10), 1579–1587. https://doi.org/10.1038/s41559-018-0647-7

Dash, J., & Ogutu, B. O. (2016). Recent advances in space-borne optical remote sensing systems for monitoring global terrestrial ecosystems. *Progress in Physical Geography: Earth and Environment*, *40*(2), 322–351. https://doi.org/10.1177/0309133316639403

de Bello, F., Carmona, C. P., Dias, A. T. C., Götzenberger, L., Moretti, M., & Berg, M. P. (2021). *Handbook of Trait-Based Ecology: From Theory to R Tools* (1st ed.). Cambridge University Press. https://doi.org/10.1017/9781108628426

De Boeck, H. J., Bloor, J. M. G., Kreyling, J., Ransijn, J. C. G., Nijs, I., Jentsch, A., & Zeiter, M. (2018). Patterns and drivers of biodiversity–stability relationships under climate extremes. *Journal of Ecology*, *106*(3), 890–902. https://doi.org/10.1111/1365-2745.12897

De la Barrera, F., Barraza, F., Favier, P., Ruiz, V., & Quense, J. (2018). Megafires in Chile 2017: Monitoring multiscale environmental impacts of burned ecosystems. *Science of the Total Environment*, *637*, 1526–1536.

Delpiano, C. A., Vargas, S., Ovalle, J. F., Cáceres, C., Zorondo-Rodríguez, F., Miranda, A., Pohl, N., Rojas, C., & Squeo, F. A. (2024). Unveiling emerging interdisciplinary research challenges in the highly threatened sclerophyllous forests of central Chile.

Revista Chilena de Historia Natural, *97*(1), 7. https://doi.org/10.1186/s40693-024-00130-y

Dendoncker, M., Taugourdeau, S., Messier, C., & Vincke, C. (2023). A Functional Trait-Based Approach to Evaluate the Resilience of Key Ecosystem Functions of Tropical Savannas. *Forests*, *14*(2), Article 2. https://doi.org/10.3390/f14020291

Diaz, J. D. G., Monterroso, A. I., Ruiz, P., Lechuga, L. M., Álvarez, A. C. C., & Asensio, C. (2019). Soil moisture regimes in Mexico in a global 1.5°C warming scenario. *International Journal of Climate Change Strategies and Management*, *11*(4), 465–482. https://doi.org/10.1108/IJCCSM-08-2018-0062

Díaz, S., Lavorel, S., McINTYRE, S., Falczuk, V., Casanoves, F., Milchunas, D. G., Skarpe, C., Rusch, G., Sternberg, M., Noy-Meir, I., Landsberg, J., Zhang, W., Clark, H., & Campbell, B. D. (2007). Plant trait responses to grazing – a global synthesis. *Global Change Biology*, *13*(2), 313–341. https://doi.org/10.1111/j.1365-2486.2006.01288.x

Dietrich, P., Eisenhauer, N., Otto, P., & Roscher, C. (2021). Plant history and soil history jointly influence the selection environment for plant species in a long-term grassland biodiversity experiment. *Ecology and Evolution*, *11*(12), 8156–8169. https://doi.org/10.1002/ece3.7647

Díaz, S., & Cabido, M. (2001). Vive la différence: Plant functional diversity matters to ecosystem processes. *Trends in Ecology & Evolution*, *16*(11), 646–655.

Drusch, M., Del Bello, U., Carlier, S., Colin, O., Fernandez, V., Gascon, F., Hoersch, B., Isola, C., Laberinti, P., Martimort, P., Meygret, A., Spoto, F., Sy, O., Marchese, F., & Bargellini, P. (2012). Sentinel-2: ESA's Optical High-Resolution Mission for GMES Operational Services. *Remote Sensing of Environment*, *120*, 25–36. https://doi.org/10.1016/j.rse.2011.11.026

Durán, S. M., Martin, R. E., Díaz, S., Maitner, B. S., Malhi, Y., Salinas, N., Shenkin, A., Silman, M. R., Wieczynski, D. J., Asner, G. P., Bentley, L. P., Savage, V. M., & Enquist, B. J. (2019). Informing trait-based ecology by assessing remotely sensed functional diversity across a broad tropical temperature gradient. *Science Advances*, *5*(12), eaaw8114. https://doi.org/10.1126/sciadv.aaw8114

Ehbrecht, M., Schall, P., Juchheim, J., Ammer, C., & Seidel, D. (2016). Effective number of layers: A new measure for quantifying three-dimensional stand structure based on sampling with terrestrial LiDAR. *Forest Ecology and Management*, *380*, 212–223. https://doi.org/10.1016/j.foreco.2016.09.003

Eisenhauer, N., Beßler, H., Engels, C., Gleixner, G., Habekost, M., Milcu, A., Partsch, S., Sabais, A. C. W., Scherber, C., Steinbeiss, S., Weigelt, A., Weisser, W. W., & Scheu, S. (2010). Plant diversity effects on soil microorganisms support the singular hypothesis. *Ecology*, *91*(2), 485–496. https://doi.org/10.1890/08-2338.1

Eisenhauer, N., Bonfante, P., Buscot, F., Cesarz, S., Guerra, C., Heintz-Buschart, A., Hines, J., Patoine, G., Rillig, M., Schmid, B., Verheyen, K., Wirth, C., & Ferlian, O. (2022). Biotic Interactions as Mediators of Context-Dependent Biodiversity-Ecosystem Functioning Relationships. *Research Ideas and Outcomes*, *8*, e85873. https://doi.org/10.3897/rio.8.e85873

Eisenhauer, N., Mueller, K., Ebeling, A., Gleixner, G., Huang, Y., Madaj, A.-M., Roscher, C., Weigelt, A., Bahn, M., Bonkowski, M., Brose, U., Cesarz, S., Feilhauer, H., Guimaraes-Steinicke, C., Heintz-Buschart, A., Hines, J., Lange, M., Meyer, S. T., Mohanbabu, N., … Isbell, F. (2024). The multiple-mechanisms hypothesis of biodiversity–stability relationships. *Basic and Applied Ecology*, *79*, 153–166. https://doi.org/10.1016/j.baae.2024.07.004

Englhart, S., Keuck, V., & Siegert, F. (2011). Aboveground biomass retrieval in tropical forests—The potential of combined X- and L-band SAR data use. *Remote Sensing of Environment*, *115*(5), 1260–1271. https://doi.org/10.1016/j.rse.2011.01.008

Enquist, B. J., Norberg, J., Bonser, S. P., Violle, C., Webb, C. T., Henderson, A., Sloat, L. L., & Savage, V. M. (2015). Chapter Nine - Scaling from Traits to Ecosystems: Developing a General Trait Driver Theory via Integrating Trait-Based and Metabolic Scaling Theories. In S. Pawar, G. Woodward, & A. I. Dell (Eds.), *Advances in Ecological Research* (Vol. 52, pp. 249–318). Academic Press. https://doi.org/10.1016/bs.aecr.2015.02.001

Escobedo, V. M., Gómez, P., Molina-Montenegro, M. A., & Acuña-Rodríguez, I. S. (2024). Post-fire negative relationship between a native tree and an invasive pine at the Coastal Maulino Forest in Central Chile. *Frontiers in Ecology and Evolution*, *12*. https://doi.org/10.3389/fevo.2024.1494548

Ewald, M., Aerts, R., Lenoir, J., Fassnacht, F. E., Nicolas, M., Skowronek, S., Piat, J., Honnay, O., Garzón-López, C. X., Feilhauer, H., Van De Kerchove, R., Somers, B., Hattab, T., Rocchini, D., & Schmidtlein, S. (2018). LiDAR derived forest structure data improves predictions of canopy N and P concentrations from imaging spectroscopy. *Remote Sensing of Environment*, *211*, 13–25. https://doi.org/10.1016/j.rse.2018.03.038

F.Covello, Battazza, F., Coletta, A., Lopinto, E., Fiorentino, C., Pietranera, L., Valentini, G., & Zoffoli, S. (2010). COSMO-SkyMed an existing opportunity for observing the Earth. *Journal of Geodynamics*, *49*(3), 171–180. https://doi.org/10.1016/j.jog.2010.01.001

Féret, J.-B., le Maire, G., Jay, S., Berveiller, D., Bendoula, R., Hmimina, G., Cheraiet, A., Oliveira, J. C., Ponzoni, F. J., Solanki, T., de Boissieu, F., Chave, J., Nouvellon, Y., Porcar-Castell, A., Proisy, C., Soudani, K., Gastellu-Etchegorry, J.-P., & Lefèvre-Fonollosa, M.-J. (2019). Estimating leaf mass per area and equivalent water thickness

based on leaf optical properties: Potential and limitations of physical modeling and machine learning. *Remote Sensing of Environment*, *231*, 110959. https://doi.org/10.1016/j.rse.2018.11.002

Ferreira, J., Lennox, G. D., Gardner, T. A., Thomson, J. R., Berenguer, E., Lees, A. C., Mac Nally, R., Aragão, L. E. O. C., Ferraz, S. F. B., Louzada, J., Moura, N. G., Oliveira, V. H. F., Pardini, R., Solar, R. R. C., Vieira, I. C. G., & Barlow, J. (2018). Carbon-focused conservation may fail to protect the most biodiverse tropical forests. *Nature Climate Change*, *8*(8), 744–749. https://doi.org/10.1038/s41558-018-0225-7

Fetzer, I., Johst, K., Schäwe, R., Banitz, T., Harms, H., & Chatzinotas, A. (2015). The extent of functional redundancy changes as species' roles shift in different environments. *Proceedings of the National Academy of Sciences*, *112*(48), 14888–14893. https://doi.org/10.1073/pnas.1505587112

Field, C. B. (2012). *Managing the risks of extreme events and disasters to advance climate change adaptation: Special report of the intergovernmental panel on climate change*. Cambridge University Press.

Fischer, F. M., & de Bello, F. (2023). On the uniqueness of functional redundancy. *Npj Biodiversity*, *2*(1), 1–3. https://doi.org/10.1038/s44185-023-00029-z

Folke, C. (2016). Resilience (Republished). *Ecology and Society*, *21*(4). https://www.jstor.org/stable/26269991

Freschet, G. T., Violle, C., Bourget, M. Y., Scherer-Lorenzen, M., & Fort, F. (2018). Allocation, morphology, physiology, architecture: The multiple facets of plant above- and below-ground responses to resource stress. *New Phytologist*, *219*(4), 1338–1352. https://doi.org/10.1111/nph.15225

Fu, B., Deng, L., Sun, W., He, H., Li, H., Wang, Y., & Wang, Y. (2024). Quantifying vegetation species functional traits along hydrologic gradients in karst wetland based on 3D

mapping with UAV hyperspectral point cloud. *Remote Sensing of Environment*, *307*, 114160. https://doi.org/10.1016/j.rse.2024.114160

Galicia, L., Potvin, C., & Messier, C. (2015). Maintaining the high diversity of pine and oak species in Mexican temperate forests: A new management approach combining functional zoning and ecosystem adaptability. *Canadian Journal of Forest Research*, *45*(10), 1358–1368. https://doi.org/10.1139/cjfr-2014-0561

Gao, Y., Skutsch, M., Paneque-Gálvez, J., & Ghilardi, A. (2020). Remote sensing of forest degradation: A review. *Environmental Research Letters*, *15*(10), 103001. https://doi.org/10.1088/1748-9326/abaad7

Garreaud, R. D., Alvarez-Garreton, C., Barichivich, J., Boisier, J. P., Christie, D., Galleguillos, M., LeQuesne, C., McPhee, J., & Zambrano-Bigiarini, M. (2017). The 2010–2015 megadrought in central Chile: Impacts on regional hydroclimate and vegetation. *Hydrology and Earth System Sciences*, *21*(12), 6307–6327. https://doi.org/10.5194/hess-21-6307-2017

Gibson, R. N., Atkinson, R. J. A., & Gordon, J. D. M. (Eds.). (2007). THE HUMBOLDT CURRENT SYSTEM OF NORTHERN AND CENTRAL CHILE. In *Oceanography and Marine Biology*. CRC Press.

Gladstone-Gallagher, R. V., Pilditch, C. A., Stephenson, F., & Thrush, S. F. (2019). Linking Traits across Ecological Scales Determines Functional Resilience. *Trends in Ecology & Evolution*, *34*(12), 1080–1091. https://doi.org/10.1016/j.tree.2019.07.010

Gómez-Mendoza, L., & Arriaga, L. (2007). Modeling the Effect of Climate Change on the Distribution of Oak and Pine Species of Mexico. *Conservation Biology*, *21*(6), 1545–1555. https://doi.org/10.1111/j.1523-1739.2007.00814.x

Gómez-Pineda, E., Sáenz-Romero, C., Ortega-Rodríguez, J. M., Blanco-García, A., Madrigal-Sánchez, X., Lindig-Cisneros, R., Lopez-Toledo, L., Pedraza-Santos, M. E., & Rehfeldt,

G. E. (2020). Suitable climatic habitat changes for Mexican conifers along altitudinal gradients under climatic change scenarios. *Ecological Applications*, *30*(2), e02041. https://doi.org/10.1002/eap.2041

Gong, Z., Ge, W., Guo, J., & Liu, J. (2024). Satellite remote sensing of vegetation phenology: Progress, challenges, and opportunities. *ISPRS Journal of Photogrammetry and Remote Sensing*, *217*, 149–164. https://doi.org/10.1016/j.isprsjprs.2024.08.011

Gonzalez, A., Germain, R. M., Srivastava, D. S., Filotas, E., Dee, L. E., Gravel, D., Thompson, P. L., Isbell, F., Wang, S., Kéfi, S., Montoya, J., Zelnik, Y. R., & Loreau, M. (2020). Scaling-up biodiversity-ecosystem functioning research. *Ecology Letters*, *23*(4), 757–776. https://doi.org/10.1111/ele.13456

Goodwin, N. R., Coops, N. C., & Culvenor, D. S. (2006). Assessment of forest structure with airborne LiDAR and the effects of platform altitude. *Remote Sensing of Environment*, *103*(2), 140–152. https://doi.org/10.1016/j.rse.2006.03.003

Grattepanche, J.-D., Walker, L. M., Ott, B. M., Paim Pinto, D. L., Delwiche, C. F., Lane, C. E., & Katz, L. A. (2018). Microbial Diversity in the Eukaryotic SAR Clade: Illuminating the Darkness Between Morphology and Molecular Data. *BioEssays*, *40*(4), 1700198. https://doi.org/10.1002/bies.201700198

Green, S. J., Brookson, C. B., Hardy, N. A., & Crowder, L. B. (2022). Trait-based approaches to global change ecology: Moving from description to prediction. *Proceedings of the Royal Society B: Biological Sciences*, *289*(1971), 20220071. https://doi.org/10.1098/rspb.2022.0071

Guimarães, N., Pádua, L., Marques, P., Silva, N., Peres, E., & Sousa, J. J. (2020). Forestry Remote Sensing from Unmanned Aerial Vehicles: A Review Focusing on the Data, Processing and Potentialities. *Remote Sensing*, *12*(6), Article 6. https://doi.org/10.3390/rs12061046

Gutiérrez, A. G., Armesto, J. J., Díaz, M. F., & Huth, A. (2014). Increased Drought Impacts on Temperate Rainforests from Southern South America: Results of a Process-Based, Dynamic Forest Model. *PLOS ONE*, *9*(7), e103226. https://doi.org/10.1371/journal.pone.0103226

Hancock, S., McGrath, C., Lowe, C., Davenport, I., & Woodhouse, I. (2021). Requirements for a global lidar system: Spaceborne lidar with wall-to-wall coverage. *Royal Society Open Science*, *8*(12), 211166. https://doi.org/10.1098/rsos.211166

Hansen, M. C., Potapov, P. V., Moore, R., Hancher, M., Turubanova, S. A., Tyukavina, A., Thau, D., Stehman, S. V., Goetz, S. J., Loveland, T. R., Kommareddy, A., Egorov, A., Chini, L., Justice, C. O., & Townshend, J. R. G. (2013). High-Resolution Global Maps of 21st-Century Forest Cover Change. *Science*, *342*(6160), 850–853. https://doi.org/10.1126/science.1244693

Hansen, M. C., Stehman, S. V., & Potapov, P. V. (2010). Quantification of global gross forest cover loss. *Proceedings of the National Academy of Sciences*, *107*(19), 8650–8655. https://doi.org/10.1073/pnas.0912668107

Hauser, L. T., Féret, J.-B., An Binh, N., van der Windt, N., Sil, Â. F., Timmermans, J., Soudzilovskaia, N. A., & van Bodegom, P. M. (2021). Towards scalable estimation of plant functional diversity from Sentinel-2: In-situ validation in a heterogeneous (semi-)natural landscape. *Remote Sensing of Environment*, *262*, 112505. https://doi.org/10.1016/j.rse.2021.112505

Hayes, D. J., & Cohen, W. B. (2007). Spatial, spectral and temporal patterns of tropical forest cover change as observed with multiple scales of optical satellite data. *Remote Sensing of Environment*, *106*(1), 1–16. https://doi.org/10.1016/j.rse.2006.07.002

He, K. S., Bradley, B. A., Cord, A. F., Rocchini, D., Tuanmu, M.-N., Schmidtlein, S., Turner, W., Wegmann, M., & Pettorelli, N. (2015a). Will remote sensing shape the next

generation of species distribution models? *Remote Sensing in Ecology and Conservation*, *1*(1), 4–18. https://doi.org/10.1002/rse2.7

He, K. S., Bradley, B. A., Cord, A. F., Rocchini, D., Tuanmu, M.-N., Schmidtlein, S., Turner, W., Wegmann, M., & Pettorelli, N. (2015b). Will remote sensing shape the next generation of species distribution models? *Remote Sensing in Ecology and Conservation*, *1*(1), 4–18. https://doi.org/10.1002/rse2.7

Heinrichs, S., Pauchard, A., & Schall, P. (2018). Native Plant Diversity and Composition Across a Pinus radiata D.Don Plantation Landscape in South-Central Chile—The Impact of Plantation Age, Logging Roads and Alien Species. *Forests*, *9*(9), Article 9. https://doi.org/10.3390/f9090567

Helfenstein, I. S., Schneider, F. D., Schaepman, M. E., & Morsdorf, F. (2022). Assessing biodiversity from space: Impact of spatial and spectral resolution on trait-based functional diversity. *Remote Sensing of Environment*, *275*, 113024. https://doi.org/10.1016/j.rse.2022.113024

Himeur, Y., Rimal, B., Tiwary, A., & Amira, A. (2022). Using artificial intelligence and data fusion for environmental monitoring: A review and future perspectives. *Information Fusion*, *86–87*, 44–75. https://doi.org/10.1016/j.inffus.2022.06.003

Hisano, M., Ghazoul, J., Chen, X., & Chen, H. Y. H. (2024). Functional diversity enhances dryland forest productivity under long-term climate change. *Science Advances*, *10*(17), eadn4152. https://doi.org/10.1126/sciadv.adn4152

Holling, C. S. (1973). Resilience and Stability of Ecological Systems. *Annual Review of Ecology and Systematics*, *4*, 1–23.

Hordijk, I., Poorter, L., Liang, J., Reich, P. B., de-Miguel, S., Nabuurs, G.-J., Gamarra, J. G. P., Chen, H. Y. H., Zhou, M., Wiser, S. K., Pretzsch, H., Paquette, A., Picard, N., Hérault, B., Bastin, J.-F., Alberti, G., Abegg, M., Adou Yao, Y. C., Almeyda Zambrano, A. M., …

Crowther, T. W. (2025). Effect of climate on traits of dominant and rare tree species in the world's forests. *Nature Communications*, *16*(1), 4773. https://doi.org/10.1038/s41467-025-59754-7

Hosseini, M., McNairn, H., Merzouki, A., & Pacheco, A. (2015). Estimation of Leaf Area Index (LAI) in corn and soybeans using multi-polarization C- and L-band radar data. *Remote Sensing of Environment*, *170*, 77–89. https://doi.org/10.1016/j.rse.2015.09.002

Inoue, Y., Sakaiya, E., & Wang, C. (2014). Capability of C-band backscattering coefficients from high-resolution satellite SAR sensors to assess biophysical variables in paddy rice. *Remote Sensing of Environment*, *140*, 257–266. https://doi.org/10.1016/j.rse.2013.09.001

Isbell, F., Adler, P. R., Eisenhauer, N., Fornara, D., Kimmel, K., Kremen, C., Letourneau, D. K., Liebman, M., Polley, H. W., Quijas, S., & Scherer-Lorenzen, M. (2017). Benefits of increasing plant diversity in sustainable agroecosystems. *Journal of Ecology*, *105*(4), 871–879. https://doi.org/10.1111/1365-2745.12789

Isbell, F., Craven, D., Connolly, J., Loreau, M., Schmid, B., Beierkuhnlein, C., Bezemer, T. M., Bonin, C., Bruelheide, H., & De Luca, E. (2015). Biodiversity increases the resistance of ecosystem productivity to climate extremes. *Nature*, *526*(7574), 574–577.

Jetz, W., Cavender-Bares, J., Pavlick, R., Schimel, D., Davis, F. W., Asner, G. P., Guralnick, R., Kattge, J., Latimer, A. M., & Moorcroft, P. (2016). Monitoring plant functional diversity from space. *Nature Plants*, *2*(3), 1–5.

Kamoske, A. G., Dahlin, K. M., Read, Q. D., Record, S., Stark, S. C., Serbin, S. P., Zarnetske, P. L., & Dornelas, M. (2022). Towards mapping biodiversity from above: Can fusing lidar and hyperspectral remote sensing predict taxonomic, functional, and phylogenetic tree diversity in temperate forests? *Global Ecology and Biogeography*, *31*(7), 1440–1460. https://doi.org/10.1111/geb.13516

Kattenborn, T., Fassnacht, F. E., Pierce, S., Lopatin, J., Grime, J. P., & Schmidtlein, S. (2017). Linking plant strategies and plant traits derived by radiative transfer modelling. *Journal of Vegetation Science*, *28*(4), 717–727. https://doi.org/10.1111/jvs.12525

Kearney, M. R., Jusup, M., McGeoch, M. A., Kooijman, S. A. L. M., & Chown, S. L. (2021). Where do functional traits come from? The role of theory and models. *Functional Ecology*, *35*(7), 1385–1396. https://doi.org/10.1111/1365-2435.13829

Kerr, J. T., & Ostrovsky, M. (2003). From space to species: Ecological applications for remote sensing. *Trends in Ecology & Evolution*, *18*(6), 299–305. https://doi.org/10.1016/S0169-5347(03)00071-5

Kitzberger, T., Perry ,GLW, Paritsis ,J, Gowda ,JH, Tepley ,AJ, Holz ,A, & and Veblen, T. (2016). Fire–vegetation feedbacks and alternative states: Common mechanisms of temperate forest vulnerability to fire in southern South America and New Zealand. *New Zealand Journal of Botany*, *54*(2), 247–272. https://doi.org/10.1080/0028825X.2016.1151903

Knyazikhin, Y., Schull, M. A., Stenberg, P., Mõttus, M., Rautiainen, M., Yang, Y., Marshak, A., Latorre Carmona, P., Kaufmann, R. K., Lewis, P., Disney, M. I., Vanderbilt, V., Davis, A. B., Baret, F., Jacquemoud, S., Lyapustin, A., & Myneni, R. B. (2013). Hyperspectral remote sensing of foliar nitrogen content. *Proceedings of the National Academy of Sciences*, *110*(3). https://doi.org/10.1073/pnas.1210196109

Kositsup, B., Kasemsap, P., Thanisawanyangkura, S., Chairungsee, N., Satakhun, D., Teerawatanasuk, K., Ameglio, T., & Thaler, P. (2010). Effect of leaf age and position on light-saturated CO2 assimilation rate, photosynthetic capacity, and stomatal conductance in rubber trees. *Photosynthetica*, *48*(1), 67–78. https://doi.org/10.1007/s11099-010-0010-y

Lagomasino, D., Fatoyinbo, T., Lee, S., Feliciano, E., Trettin, C., Shapiro, A., & Mangora, M. M. (2019). Measuring mangrove carbon loss and gain in deltas. *Environmental Research Letters*, *14*(2), 025002. https://doi.org/10.1088/1748-9326/aaf0de

Laliberté, E., & Legendre, P. (2010). A distance-based framework for measuring functional diversity from multiple traits. *Ecology*, *91*(1), 299–305. https://doi.org/10.1890/08-2244.1

Lausch, A., Bannehr, L., Beckmann, M., Boehm, C., Feilhauer, H., Hacker, J. M., Heurich, M., Jung, A., Klenke, R., Neumann, C., Pause, M., Rocchini, D., Schaepman, M. E., Schmidtlein, S., Schulz, K., Selsam, P., Settele, J., Skidmore, A. K., & Cord, A. F. (2016). Linking Earth Observation and taxonomic, structural and functional biodiversity: Local to ecosystem perspectives. *Ecological Indicators*, *70*, 317–339. https://doi.org/10.1016/j.ecolind.2016.06.022

Lausch, A., Borg, E., Bumberger, J., Dietrich, P., Heurich, M., Huth, A., Jung, A., Klenke, R., Knapp, S., Mollenhauer, H., Paasche, H., Paulheim, H., Pause, M., Schweitzer, C., Schmulius, C., Settele, J., Skidmore, A. K., Wegmann, M., Zacharias, S., … Schaepman, M. E. (2018). Understanding Forest Health with Remote Sensing, Part III: Requirements for a Scalable Multi-Source Forest Health Monitoring Network Based on Data Science Approaches. *Remote Sensing*, *10*(7), Article 7. https://doi.org/10.3390/rs10071120

Le Bagousse-Pinguet, Y., Gross, N., Maestre, F. T., Maire, V., de Bello, F., Fonseca, C. R., Kattge, J., Valencia, E., Leps, J., & Liancourt, P. (2017). Testing the environmental filtering concept in global drylands. *Journal of Ecology*, *105*(4), 1058–1069. https://doi.org/10.1111/1365-2745.12735

Le Bagousse-Pinguet, Y., Soliveres, S., Gross, N., Torices, R., Berdugo, M., & Maestre, F. T. (2019). Phylogenetic, functional, and taxonomic richness have both positive and

negative effects on ecosystem multifunctionality. *Proceedings of the National Academy of Sciences*, *116*(17), 8419–8424. https://doi.org/10.1073/pnas.1815727116

Leal-Medina, C., Lopatin, J., Contreras, A., González, M. E., & Galleguillos, M. (2024). Post-fire *Pinus radiata* invasion in a threatened biodiversity hotspot forest: A multi-scale remote sensing assessment. *Forest Ecology and Management*, *561*, 121861. https://doi.org/10.1016/j.foreco.2024.121861

Lechner, A. M., Foody, G. M., & Boyd, D. S. (2020). Applications in Remote Sensing to Forest Ecology and Management. *One Earth*, *2*(5), 405–412. https://doi.org/10.1016/j.oneear.2020.05.001

LeCun, Y., & Bengio, Y. (1998). Convolutional networks for images, speech, and time series. In *The handbook of brain theory and neural networks* (pp. 255–258). MIT Press.

LeCun, Y., Bengio, Y., & Hinton, G. (2015). Deep learning. *Nature*, *521*(7553), 436–444. https://doi.org/10.1038/nature14539

Li, Y., Schmid, B., Schuldt, A., Li, S., Wang, M.-Q., Fornoff, F., Staab, M., Guo, P.-F., Anttonen, P., Chesters, D., Bruelheide, H., Zhu, C.-D., Ma, K., & Liu, X. (2023). Multitrophic arthropod diversity mediates tree diversity effects on primary productivity. *Nature Ecology & Evolution*, *7*(6), 832–840. https://doi.org/10.1038/s41559-023-02049-1

Liu, H. Q., & Huete, A. (1995). A feedback based modification of the NDVI to minimize canopy background and atmospheric noise. *IEEE Transactions on Geoscience and Remote Sensing*, *33*(2), 457–465. https://doi.org/10.1109/TGRS.1995.8746027

Liu, S., Wang, Z., Lin, Z., Zhao, Y., Yan, Z., Zhang, K., Visser, M., Townsend, P. A., & Wu, J. (2024). Spectra-phenology integration for high-resolution, accurate, and scalable mapping of foliar functional traits using time-series Sentinel-2 data. *Remote Sensing of Environment*, *305*, 114082. https://doi.org/10.1016/j.rse.2024.114082

Loew, A., & Mauser, W. (2007). Generation of geometrically and radiometrically terrain corrected SAR image products. *Remote Sensing of Environment*, *106*(3), 337–349. https://doi.org/10.1016/j.rse.2006.09.002

Lõhmus, A., Lõhmus, P., & Runnel, K. (2018). A simple survey protocol for assessing terrestrial biodiversity in a broad range of ecosystems. *PLOS ONE*, *13*(12), e0208535. https://doi.org/10.1371/journal.pone.0208535

López-Teloxa, L. C., & Monterroso-Rivas, A. I. (2024). A Spatio-Temporal Analysis of the Frequency of Droughts in Mexico's Forest Ecosystems. *Forests*, *15*(7), Article 7. https://doi.org/10.3390/f15071241

Loreau, M., Barbier, M., Filotas, E., Gravel, D., Isbell, F., Miller, S. J., Montoya, J. M., Wang, S., Aussenac, R., Germain, R., Thompson, P. L., Gonzalez, A., & Dee, L. E. (2021). Biodiversity as insurance: From concept to measurement and application. *Biological Reviews*, *96*(5), 2333–2354. https://doi.org/10.1111/brv.12756

Lourenço Jr., J., Enquist, B. J., von Arx, G., Sonsin-Oliveira, J., Morino, K., Thomaz, L. D., & Milanez, C. R. D. (2022). Hydraulic tradeoffs underlie local variation in tropical forest functional diversity and sensitivity to drought. *New Phytologist*, *234*(1), 50–63. https://doi.org/10.1111/nph.17944

Lucas, R., Armston, J., Fairfax, R., Fensham, R., Accad, A., Carreiras, J., Kelley, J., Bunting, P., Clewley, D., Bray, S., Metcalfe, D., Dwyer, J., Bowen, M., Eyre, T., Laidlaw, M., & Shimada, M. (2010). An Evaluation of the ALOS PALSAR L-Band Backscatter—Above Ground Biomass Relationship Queensland, Australia: Impacts of Surface Moisture Condition and Vegetation Structure. *IEEE Journal of Selected Topics in Applied Earth Observations and Remote Sensing*, *3*(4), 576–593. https://doi.org/10.1109/JSTARS.2010.2086436

Ma, X., Mahecha, M. D., Migliavacca, M., van der Plas, F., Benavides, R., Ratcliffe, S., Kattge, J., Richter, R., Musavi, T., Baeten, L., Barnoaiea, I., Bohn, F. J., Bouriaud, O., Bussotti, F., Coppi, A., Domisch, T., Huth, A., Jaroszewicz, B., Joswig, J., … Wirth, C. (2019). Inferring plant functional diversity from space: The potential of Sentinel-2. *Remote Sensing of Environment*, *233*, 111368. https://doi.org/10.1016/j.rse.2019.111368

Ma, X., Migliavacca, M., Wirth, C., Bohn, F. J., Huth, A., Richter, R., & Mahecha, M. D. (2020). Monitoring Plant Functional Diversity Using the Reflectance and Echo from Space. *Remote Sensing*, *12*(8), Article 8. https://doi.org/10.3390/rs12081248

Magaña, V., Zermeño, D., & Neri, C. (2012). Climate change scenarios and potential impacts on water availability in northern Mexico. *Climate Research*, *51*(2), 171–184.

Malerba, M. E., Duarte de Paula Costa, M., Friess, D. A., Schuster, L., Young, M. A., Lagomasino, D., Serrano, O., Hickey, S. M., York, P. H., Rasheed, M., Lefcheck, J. S., Radford, B., Atwood, T. B., Ierodiaconou, D., & Macreadie, P. (2023). Remote sensing for cost-effective blue carbon accounting. *Earth-Science Reviews*, *238*, 104337. https://doi.org/10.1016/j.earscirev.2023.104337

Malhi, Y., Baldocchi, D., & Jarvis, P. (1999). The carbon balance of tropical, temperate and boreal forests. *Plant, Cell & Environment*, *22*(6), 715–740.

Malhi, Y., Christmann, T., Deng, X., Zhang-Zheng, H., Moore, S., & Riutta, T. (2024). Forest carbon budgets and climate change. In *Routledge Handbook of Forest Ecology* (2nd ed.). Routledge.

Malhi, Y., Doughty, C., & Galbraith, D. (2011). The allocation of ecosystem net primary productivity in tropical forests. *Philosophical Transactions of the Royal Society B: Biological Sciences*, *366*(1582), 3225–3245. https://doi.org/10.1098/rstb.2011.0062

Malhi, Y., Phillips, O. L., Malhi, Y., & Phillips, O. L. (2004). Tropical forests and global atmospheric change: A synthesis. *Philosophical Transactions of the Royal Society of*

London. Series B: Biological Sciences, *359*(1443), 549–555. https://doi.org/10.1098/rstb.2003.1449

Mason, N. W. H., Mouillot, D., Lee, W. G., & Wilson, J. B. (2005). Functional richness, functional evenness and functional divergence: The primary components of functional diversity. *Oikos*, *111*(1), 112–118. https://doi.org/10.1111/j.0030-1299.2005.13886.x

McFarlane, K. J., Cusack, D. F., Dietterich, L. H., Hedgpeth, A. L., Finstad, K. M., & Nottingham, A. T. (2024). Experimental warming and drying increase older carbon contributions to soil respiration in lowland tropical forests. *Nature Communications*, *15*(1), 7084. https://doi.org/10.1038/s41467-024-51422-6

McNairn, H., & and Brisco, B. (2004). The application of C-band polarimetric SAR for agriculture: A review. *Canadian Journal of Remote Sensing*, *30*(3), 525–542. https://doi.org/10.5589/m03-069

Meerdink, S. K., Roberts, D. A., Roth, K. L., King, J. Y., Gader, P. D., & Koltunov, A. (2019). Classifying California plant species temporally using airborne hyperspectral imagery. *Remote Sensing of Environment*, *232*, 111308. https://doi.org/10.1016/j.rse.2019.111308

Méndez, M., & Magaña, V. (2010). *Regional Aspects of Prolonged Meteorological Droughts over Mexico and Central America*. https://doi.org/10.1175/2009JCLI3080.1

Mermoz, S., Réjou-Méchain, M., Villard, L., Le Toan, T., Rossi, V., & Gourlet-Fleury, S. (2015). Decrease of L-band SAR backscatter with biomass of dense forests. *Remote Sensing of Environment*, *159*, 307–317. https://doi.org/10.1016/j.rse.2014.12.019

Messier, C., Bauhus, J., Doyon, F., Maure, F., Sousa-Silva, R., Nolet, P., Mina, M., Aquilué, N., Fortin, M.-J., & Puettmann, K. (2019). The functional complex network approach to foster forest resilience to global changes. *Forest Ecosystems*, *6*(1), 21. https://doi.org/10.1186/s40663-019-0166-2

Miller, J., & Rogan, J. (2007). Using GIS and remote sensing for ecological mapping and monitoring. *Integration of GIS and Remote Sensing*, *3*, 233.

Ming, L., Liu, J., Quan, Y., Li, M., Wang, B., & Wei, G. (2024). Mapping tree species diversity in a typical natural secondary forest by combining multispectral and LiDAR data. *Ecological Indicators*, *159*, 111711. https://doi.org/10.1016/j.ecolind.2024.111711

Miranda, A., Syphard, A. D., Berdugo, M., Carrasco, J., Gómez-González, S., Ovalle, J. F., Delpiano, C. A., Vargas, S., Squeo, F. A., Miranda, M. D., Dobbs, C., Mentler, R., Lara, A., & Garreaud, R. (2023). Widespread synchronous decline of Mediterranean-type forest driven by accelerated aridity. *Nature Plants*, *9*(11), 1810–1817. https://doi.org/10.1038/s41477-023-01541-7

Mitchell, A. L., Rosenqvist, A., & Mora, B. (2017). Current remote sensing approaches to monitoring forest degradation in support of countries measurement, reporting and verification (MRV) systems for REDD+. *Carbon Balance and Management*, *12*(1), 9. https://doi.org/10.1186/s13021-017-0078-9

Mohammadpour, P., & Viegas, C. (2022). Applications of Multi-Source and Multi-Sensor Data Fusion of Remote Sensing for Forest Species Mapping. In *Advances in Remote Sensing for Forest Monitoring* (pp. 255–287). John Wiley & Sons, Ltd. https://doi.org/10.1002/9781119788157.ch12

Monteith, A. R., & Ulander, L. M. H. (2018). Temporal Survey of P- and L-Band Polarimetric Backscatter in Boreal Forests. *IEEE Journal of Selected Topics in Applied Earth Observations and Remote Sensing*, *11*(10), 3564–3577. https://doi.org/10.1109/JSTARS.2018.2814825

Moon, J., Lee, W. K., Song, C., Lee, S. G., Heo, S. B., Shvidenko, A., Kraxner, F., Lamchin, M., Lee, E. J., Zhu, Y., Kim, D., & Cui, G. (2017). An introduction to mid-latitude

ecotone: Sustainability and environmental challenges. *Siberian Journal of Forest Science*, *6*, 41–51. https://doi.org/10.15372/SJFS20170603

Moreno Párrizas, H., & Andújar, D. (2023). *Proximal sensing for geometric characterization of vines: A review of the latest advances*. https://digital.csic.es/handle/10261/330589

Moreno-Sanchez, R., Torres-Rojo, J. M., Moreno-Sanchez, F., Hawkins, S., Little, J., & McPartland, S. (2012). National assessment of the fragmentation, accessibility and anthropogenic pressure on the forests in Mexico. *Journal of Forestry Research*, *23*(4), 529–541. https://doi.org/10.1007/s11676-012-0293-x

Mulder, C. P. H., Uliassi, D. D., & Doak, D. F. (2001). Physical stress and diversity-productivity relationships: The role of positive interactions. *Proceedings of the National Academy of Sciences*, *98*(12), 6704–6708. https://doi.org/10.1073/pnas.111055298

Müller, J., Brandl, R., Brändle, M., Förster, B., de Araujo, B. C., Gossner, M. M., Ladas, A., Wagner, M., Maraun, M., Schall, P., Schmidt, S., Heurich, M., Thorn, S., & Seibold, S. (2018). LiDAR-derived canopy structure supports the more-individuals hypothesis for arthropod diversity in temperate forests. *Oikos*, *127*(6), 814–824. https://doi.org/10.1111/oik.04972

Murray-Tortarolo, G. N. (2021). Seven decades of climate change across Mexico. *Atmósfera*, *34*(2), 217–226. https://doi.org/10.20937/atm.52803

Muscarella, R., & Uriarte, M. (2016). Do community-weighted mean functional traits reflect optimal strategies? *Proceedings of the Royal Society B: Biological Sciences*, *283*(1827), 20152434. https://doi.org/10.1098/rspb.2015.2434

Myers, N., Mittermeier, R. A., Mittermeier, C. G., da Fonseca, G. A. B., & Kent, J. (2000). Biodiversity hotspots for conservation priorities. *Nature*, *403*(6772), 853–858. https://doi.org/10.1038/35002501

NAHUELHUAL, L., DONOSO, P., LARA, A., NÚÑEZ, D., OYARZÚN, C., & NEIRA, E. (2007). VALUING ECOSYSTEM SERVICES OF CHILEAN TEMPERATE RAINFORESTS. *Environment, Development and Sustainability*, *9*(4), 481–499. https://doi.org/10.1007/s10668-006-9033-8

Neira, E., Verscheure, H., & Revenga, C. (2002). *Chile's frontier forests: Conserving a global treasure*. Global Forest Watch, World Resources Institute Washington DC.

Neumann, M., Ferro-Famil, L., & Reigber, A. (2010). Estimation of Forest Structure, Ground, and Canopy Layer Characteristics From Multibaseline Polarimetric Interferometric SAR Data. *IEEE Transactions on Geoscience and Remote Sensing*, *48*(3), 1086–1104. https://doi.org/10.1109/TGRS.2009.2031101

Ningthoujam, R. K., Joshi, P. K., & Roy, P. S. (2018). Retrieval of forest biomass for tropical deciduous mixed forest using ALOS PALSAR mosaic imagery and field plot data. *International Journal of Applied Earth Observation and Geoinformation*, *69*, 206–216. https://doi.org/10.1016/j.jag.2018.03.007

Nock, C. A., Vogt, R. J., & Beisner, B. E. (2016). Functional Traits. In Wiley, *Encyclopedia of Life Sciences* (1st ed., pp. 1–8). Wiley. https://doi.org/10.1002/9780470015902.a0026282

Nottingham, A. T., Meir, P., Velasquez, E., & Turner, B. L. (2020). Soil carbon loss by experimental warming in a tropical forest. *Nature*, *584*(7820), 234–237. https://doi.org/10.1038/s41586-020-2566-4

Okin, G. S., & Gu, J. (2015). The impact of atmospheric conditions and instrument noise on atmospheric correction and spectral mixture analysis of multispectral imagery. *Remote Sensing of Environment*, *164*, 130–141. https://doi.org/10.1016/j.rse.2015.03.032

Oliver, T. H., Heard, M. S., Isaac, N. J. B., Roy, D. B., Procter, D., Eigenbrod, F., Freckleton, R., Hector, A., Orme, C. D. L., Petchey, O. L., Proença, V., Raffaelli, D., Suttle, K. B.,

Mace, G. M., Martín-López, B., Woodcock, B. A., & Bullock, J. M. (2015). Biodiversity and Resilience of Ecosystem Functions. *Trends in Ecology & Evolution*, *30*(11), 673–684. https://doi.org/10.1016/j.tree.2015.08.009

Ordway, E. M., Asner, G. P., Burslem, D. F. R. P., Lewis, S. L., Nilus, R., Martin, R. E., O'Brien, M. J., Phillips, O. L., Qie, L., Vaughn, N. R., & Moorcroft, P. R. (2022). Mapping tropical forest functional variation at satellite remote sensing resolutions depends on key traits. *Communications Earth & Environment*, *3*(1), 247. https://doi.org/10.1038/s43247-022-00564-w

Ortega, M. A., Cayuela, L., Griffith, D. M., Camacho, A., Coronado, I. M., Castillo, R. F. del, Figueroa-Rangel, B. L., Fonseca, W., Garibaldi, C., Kelly, D. L., Letcher, S. G., Meave, J. A., Merino-Martín, L., Meza, V. H., Ochoa-Gaona, S., Olvera-Vargas, M., Ramírez-Marcial, N., Tun-Dzul, F. J., Valdez-Hernández, M., … Muñoz, J. (2024). Climate change increases threat to plant diversity in tropical forests of Central America and southern Mexico. *PLOS ONE*, *19*(2), e0297840. https://doi.org/10.1371/journal.pone.0297840

Pan, Y., Birdsey, R. A., Fang, J., Houghton, R., Kauppi, P. E., Kurz, W. A., Phillips, O. L., Shvidenko, A., Lewis, S. L., Canadell, J. G., Ciais, P., Jackson, R. B., Pacala, S. W., McGuire, A. D., Piao, S., Rautiainen, A., Sitch, S., & Hayes, D. (2011). A Large and Persistent Carbon Sink in the World's Forests. *Science*, *333*(6045), 988–993. https://doi.org/10.1126/science.1201609

Pandey, P., Ge, Y., Stoerger, V., & Schnable, J. C. (2017). High Throughput In vivo Analysis of Plant Leaf Chemical Properties Using Hyperspectral Imaging. *Frontiers in Plant Science*, *8*. https://doi.org/10.3389/fpls.2017.01348

Panferov, O., Knyazikhin, Y., Myneni, R. B., Szarzynski, J., Engwald, S., Schnitzler, K. G., & Gravenhorst, G. (2001). The role of canopy structure in the spectral variation of

transmission and absorption of solar radiation in vegetation canopies. *IEEE Transactions on Geoscience and Remote Sensing*, *39*(2), 241–253. https://doi.org/10.1109/36.905232

Pang, Y., Räsänen, A., Wolff, F., Tahvanainen, T., Männikkö, M., Aurela, M., Korpelainen, P., Kumpula, T., & Virtanen, T. (2024). Comparing multispectral and hyperspectral UAV data for detecting peatland vegetation patterns. *International Journal of Applied Earth Observation and Geoinformation*, *132*, 104043. https://doi.org/10.1016/j.jag.2024.104043

Park, Y.-S., & Lek, S. (2016). Chapter 7 - Artificial Neural Networks: Multilayer Perceptron for Ecological Modeling. In S. E. Jørgensen (Ed.), *Developments in Environmental Modelling* (Vol. 28, pp. 123–140). Elsevier. https://doi.org/10.1016/B978-0-444-63623-2.00007-4

Pasetto, D., Arenas-Castro, S., Bustamante, J., Casagrandi, R., Chrysoulakis, N., Cord, A. F., Dittrich, A., Domingo-Marimon, C., El Serafy, G., Karnieli, A., Kordelas, G. A., Manakos, I., Mari, L., Monteiro, A., Palazzi, E., Poursanidis, D., Rinaldo, A., Terzago, S., Ziemba, A., & Ziv, G. (2018). Integration of satellite remote sensing data in ecosystem modelling at local scales: Practices and trends. *Methods in Ecology and Evolution*, *9*(8), 1810–1821. https://doi.org/10.1111/2041-210X.13018

Pettorelli, N., Schulte to Bühne, H., Tulloch, A., Dubois, G., Macinnis-Ng, C., Queirós, A. M., Keith, D. A., Wegmann, M., Schrodt, F., Stellmes, M., Sonnenschein, R., Geller, G. N., Roy, S., Somers, B., Murray, N., Bland, L., Geijzendorffer, I., Kerr, J. T., Broszeit, S., … Nicholson, E. (2018). Satellite remote sensing of ecosystem functions: Opportunities, challenges and way forward. *Remote Sensing in Ecology and Conservation*, *4*(2), 71–93. https://doi.org/10.1002/rse2.59

Pfadenhauer, J. S., & Klötzli, F. A. (2020). Zonal Vegetation of the Humid Nemoral (Cool–Temperate) Zone. In J. S. Pfadenhauer & F. A. Klötzli (Eds.), *Global Vegetation: Fundamentals, Ecology and Distribution* (pp. 599–693). Springer International Publishing. https://doi.org/10.1007/978-3-030-49860-3_11

Pichler, M., & Hartig, F. (2023). Machine learning and deep learning—A review for ecologists. *Methods in Ecology and Evolution*, *14*(4), 994–1016. https://doi.org/10.1111/2041-210X.14061

Pietsch, K. A., Ogle, K., Cornelissen, J. H. C., Cornwell, W. K., Bönisch, G., Craine, J. M., Jackson, B. G., Kattge, J., Peltzer, D. A., Penuelas, J., Reich, P. B., Wardle, D. A., Weedon, J. T., Wright, I. J., Zanne, A. E., & Wirth, C. (2014). Global relationship of wood and leaf litter decomposability: The role of functional traits within and across plant organs. *Global Ecology and Biogeography*, *23*(9), 1046–1057. https://doi.org/10.1111/geb.12172

Pla, L., Casanoves, F., & Di Rienzo, J. (2012). *Quantifying Functional Biodiversity*. Springer Netherlands. https://doi.org/10.1007/978-94-007-2648-2

Polazzo, F., & Rico, A. (2021). Effects of multiple stressors on the dimensionality of ecological stability. *Ecology Letters*, *24*(8), 1594–1606. https://doi.org/10.1111/ele.13770

Post, E. S., Pedersen, C., Wilmers, C. C., & Forchhammer, M. C. (2008). Phenological Sequences Reveal Aggregate Life History Response to Climatic Warming. *Ecology*, *89*(2), 363–370. https://doi.org/10.1890/06-2138.1

Pourshamsi, M., Xia, J., Yokoya, N., Garcia, M., Lavalle, M., Pottier, E., & Balzter, H. (2021). Tropical forest canopy height estimation from combined polarimetric SAR and LiDAR using machine-learning. *ISPRS Journal of Photogrammetry and Remote Sensing*, *172*, 79–94. https://doi.org/10.1016/j.isprsjprs.2020.11.008

Powell, J. R., & Rillig, M. C. (2018). Biodiversity of arbuscular mycorrhizal fungi and ecosystem function. *New Phytologist*, *220*(4), 1059–1075. https://doi.org/10.1111/nph.15119

Quigley, M. F., & Platt, W. J. (2003). Composition and Structure of Seasonally Deciduous Forests in the Americas. *Ecological Monographs*, *73*(1), 87–106. https://doi.org/10.1890/0012-9615(2003)073[0087:CASOSD]2.0.CO;2

Ramezani, M., Wang, Y., Camurri, M., Wisth, D., Mattamala, M., & Fallon, M. (2020). The Newer College Dataset: Handheld LiDAR, Inertial and Vision with Ground Truth. *2020 IEEE/RSJ International Conference on Intelligent Robots and Systems (IROS)*, 4353–4360. https://doi.org/10.1109/IROS45743.2020.9340849

Randin, C. F., Ashcroft, M. B., Bolliger, J., Cavender-Bares, J., Coops, N. C., Dullinger, S., Dirnböck, T., Eckert, S., Ellis, E., Fernández, N., Giuliani, G., Guisan, A., Jetz, W., Joost, S., Karger, D., Lembrechts, J., Lenoir, J., Luoto, M., Morin, X., … Payne, D. (2020). Monitoring biodiversity in the Anthropocene using remote sensing in species distribution models. *Remote Sensing of Environment*, *239*, 111626. https://doi.org/10.1016/j.rse.2019.111626

Reddy, C. S. (2021). Remote sensing of biodiversity: What to measure and monitor from space to species? *Biodiversity and Conservation*, *30*(10), 2617–2631. https://doi.org/10.1007/s10531-021-02216-5

Reich, P. B. (2014a). The world-wide 'fast–slow' plant economics spectrum: A traits manifesto. *Journal of Ecology*, *102*(2), 275–301. https://doi.org/10.1111/1365-2745.12211

Reich, P. B. (2014b). The world-wide 'fast–slow' plant economics spectrum: A traits manifesto. *Journal of Ecology*, *102*(2), 275–301. https://doi.org/10.1111/1365-2745.12211

Reich, P. B., & Oleksyn, J. (2004). Global patterns of plant leaf N and P in relation to temperature and latitude. *Proceedings of the National Academy of Sciences*, *101*(30), 11001–11006. https://doi.org/10.1073/pnas.0403588101

Reich, P. B., Wright, I. J., Cavender-Bares, J., Craine, J. M., Oleksyn, J., Westoby, M., & Walters, M. B. (2003). The Evolution of Plant Functional Variation: Traits, Spectra, and Strategies. *International Journal of Plant Sciences*, *164*(S3), S143–S164. https://doi.org/10.1086/374368

Ricotta, C., De Bello, F., Moretti, M., Caccianiga, M., Cerabolini, B. E. L., & Pavoine, S. (2016). Measuring the functional redundancy of biological communities: A quantitative guide. *Methods in Ecology and Evolution*, *7*(11), 1386–1395. https://doi.org/10.1111/2041-210X.12604

Rocchini, D., Santos, M. J., Ustin, S. L., Féret, J.-B., Asner, G. P., Beierkuhnlein, C., Dalponte, M., Feilhauer, H., Foody, G. M., Geller, G. N., Gillespie, T. W., He, K. S., Kleijn, D., Leitão, P. J., Malavasi, M., Moudrý, V., Müllerová, J., Nagendra, H., Normand, S., … Lenoir, J. (2022). The Spectral Species Concept in Living Color. *Journal of Geophysical Research: Biogeosciences*, *127*(9), e2022JG007026. https://doi.org/10.1029/2022JG007026

Rosenblatt, F. (1958). The perceptron: A probabilistic model for information storage and organization in the brain. *Psychological Review*, *65*(6), 386–408. https://doi.org/10.1037/h0042519

Rosenfeld, J. S. (2002). Functional redundancy in ecology and conservation. *Oikos*, *98*(1), 156–162. https://doi.org/10.1034/j.1600-0706.2002.980116.x

Rosenqvist, A., Shimada, M., & Watanabe, M. (2004). *ALOS PALSAR: Technical outline and mission concepts*. 1–7.

Rouse, J. W., Haas, R. H., Schell, J. A., & Deering, D. W. (1974, January 1). *Monitoring vegetation systems in the Great Plains with ERTS*. https://ntrs.nasa.gov/citations/19740022614

Saatchi, S. S., & Moghaddam, M. (2000). Estimation of crown and stem water content and biomass of boreal forest using polarimetric SAR imagery. *IEEE Transactions on Geoscience and Remote Sensing*, *38*(2), 697–709. https://doi.org/10.1109/36.841999

Sáenz-Romero, C., Mendoza-Maya, E., Gómez-Pineda, E., Blanco-García, A., Endara-Agramont, A. R., Lindig-Cisneros, R., López-Upton, J., Trejo-Ramírez, O., Wehenkel, C., Cibrián-Tovar, D., Flores-López, C., Plascencia-González, A., & Vargas-Hernández, J. J. (2020). Recent evidence of Mexican temperate forest decline and the need for ex situ conservation, assisted migration, and translocation of species ensembles as adaptive management to face projected climatic change impacts in a megadiverse country. *Canadian Journal of Forest Research*, *50*(9), 843–854. https://doi.org/10.1139/cjfr-2019-0329

Sáenz-Romero, C., Rehfeldt, G. E., Crookston, N. L., Duval, P., St-Amant, R., Beaulieu, J., & Richardson, B. A. (2010). Spline models of contemporary, 2030, 2060 and 2090 climates for Mexico and their use in understanding climate-change impacts on the vegetation. *Climatic Change*, *102*(3), 595–623. https://doi.org/10.1007/s10584-009-9753-5

Salas, C., Donoso, P. J., Vargas, R., Arriagada, C. A., Pedraza, R., & Soto, D. P. (2016). The Forest Sector in Chile: An Overview and Current Challenges. *Journal of Forestry*, *114*(5), 562–571. https://doi.org/10.5849/jof.14-062

Salomonson, V. V., Barnes, W. L., Maymon, P. W., Montgomery, H. E., & Ostrow, H. (1989). MODIS: Advanced facility instrument for studies of the Earth as a system. *IEEE*

Transactions on Geoscience and Remote Sensing, *27*(2), 145–153. https://doi.org/10.1109/36.20292

Santiago, L. S., De Guzman, M. E., Baraloto, C., Vogenberg, J. E., Brodie, M., Hérault, B., Fortunel, C., & Bonal, D. (2018). Coordination and trade-offs among hydraulic safety, efficiency and drought avoidance traits in Amazonian rainforest canopy tree species. *New Phytologist*, *218*(3), 1015–1024. https://doi.org/10.1111/nph.15058

Schippers, P., Sterck, F., Vlam, M., & Zuidema, P. A. (2015). Tree growth variation in the tropical forest: Understanding effects of temperature, rainfall and CO2. *Global Change Biology*, *21*(7), 2749–2761. https://doi.org/10.1111/gcb.12877

Schneider, F. D., Morsdorf, F., Schmid, B., Petchey, O. L., Hueni, A., Schimel, D. S., & Schaepman, M. E. (2017). Mapping functional diversity from remotely sensed morphological and physiological forest traits. *Nature Communications*, *8*(1), 1441. https://doi.org/10.1038/s41467-017-01530-3

Schuldt, A., Ebeling, A., Kunz, M., Staab, M., Guimarães-Steinicke, C., Bachmann, D., Buchmann, N., Durka, W., Fichtner, A., Fornoff, F., Härdtle, W., Hertzog, L. R., Klein, A.-M., Roscher, C., Schaller, J., von Oheimb, G., Weigelt, A., Weisser, W., Wirth, C., … Eisenhauer, N. (2019). Multiple plant diversity components drive consumer communities across ecosystems. *Nature Communications*, *10*(1), 1460. https://doi.org/10.1038/s41467-019-09448-8

Schweiger, A. K., Cavender-Bares, J., Townsend, P. A., Hobbie, S. E., Madritch, M. D., Wang, R., Tilman, D., & Gamon, J. A. (2018). Plant spectral diversity integrates functional and phylogenetic components of biodiversity and predicts ecosystem function. *Nature Ecology & Evolution*, *2*(6), 976–982. https://doi.org/10.1038/s41559-018-0551-1

Scipal, K., Arcioni, M., Chave, J., Dall, J., Fois, F., LeToan, T., Lin, C.-C., Papathanassiou, K., Quegan, S., Rocca, F., Saatchi, S., Shugart, H., Ulander, L., & Williams, M. (2010).

The BIOMASS mission—An ESA Earth Explorer candidate to measure the BIOMASS of the earth's forests. *2010 IEEE International Geoscience and Remote Sensing Symposium*, 52–55. https://doi.org/10.1109/IGARSS.2010.5648979

Serrano, L., Peñuelas, J., & Ustin, S. L. (2002). Remote sensing of nitrogen and lignin in Mediterranean vegetation from AVIRIS data: Decomposing biochemical from structural signals. *Remote Sensing of Environment*, *81*(2), 355–364. https://doi.org/10.1016/S0034-4257(02)00011-1

Shi, Y., Skidmore, A. K., Wang, T., Holzwarth, S., Heiden, U., Pinnel, N., Zhu, X., & Heurich, M. (2018). Tree species classification using plant functional traits from LiDAR and hyperspectral data. *International Journal of Applied Earth Observation and Geoinformation*, *73*, 207–219. https://doi.org/10.1016/j.jag.2018.06.018

Simard, M., Pinto, N., Fisher, J. B., & Baccini, A. (2011). Mapping forest canopy height globally with spaceborne lidar. *Journal of Geophysical Research: Biogeosciences*, *116*(G4). https://doi.org/10.1029/2011JG001708

Sims, D. A., & Gamon, J. A. (2002). Relationships between leaf pigment content and spectral reflectance across a wide range of species, leaf structures and developmental stages. *Remote Sensing of Environment*, *81*(2), 337–354. https://doi.org/10.1016/S0034-4257(02)00010-X

Singh, A., Serbin, S. P., McNeil, B. E., Kingdon, C. C., & Townsend, P. A. (2015). Imaging spectroscopy algorithms for mapping canopy foliar chemical and morphological traits and their uncertainties. *Ecological Applications*, *25*(8), 2180–2197. https://doi.org/10.1890/14-2098.1

Singh, S. K., Prasad, R., Srivastava, P. K., Yadav, S. A., Yadav, V. P., & Sharma, J. (2023). Incorporation of first-order backscattered power in Water Cloud Model for improving the Leaf Area Index and Soil Moisture retrieval using dual-polarized Sentinel-1 SAR

data. *Remote Sensing of Environment*, *296*, 113756. https://doi.org/10.1016/j.rse.2023.113756

Sinha, S., Jeganathan, C., Sharma, L. K., & Nathawat, M. S. (2015). A review of radar remote sensing for biomass estimation. *International Journal of Environmental Science and Technology*, *12*(5), 1779–1792. https://doi.org/10.1007/s13762-015-0750-0

Smith, A. M. S., Kolden, C. A., Tinkham, W. T., Talhelm, A. F., Marshall, J. D., Hudak, A. T., Boschetti, L., Falkowski, M. J., Greenberg, J. A., Anderson, J. W., Kliskey, A., Alessa, L., Keefe, R. F., & Gosz, J. R. (2014). Remote sensing the vulnerability of vegetation in natural terrestrial ecosystems. *Remote Sensing of Environment*, *154*, 322–337. https://doi.org/10.1016/j.rse.2014.03.038

Smith-Ramírez, C. (2004). The Chilean coastal range: A vanishing center of biodiversity and endemism in South American temperate rainforests. *Biodiversity & Conservation*, *13*(2), 373–393. https://doi.org/10.1023/B:BIOC.0000006505.67560.9f

Smith-Ramírez, C., Grez, A., Galleguillos, M., Cerda, C., Ocampo-Melgar, A., Miranda, M. D., Muñoz, A. A., Rendón-Funes, A., Díaz, I., Cifuentes, C., Alaniz, A., Seguel, O., Ovalle, J., Montenegro, G., Saldes-Cortés, A., Martínez-Harms, M. J., Armesto, J. J., & Vita, A. (2023). Ecosystem services of Chilean sclerophyllous forests and shrublands on the verge of collapse: A review. *Journal of Arid Environments*, *211*, 104927. https://doi.org/10.1016/j.jaridenv.2022.104927

Sobral, M. (2021). All Traits Are Functional: An Evolutionary Viewpoint. *Trends in Plant Science*, *26*(7), 674–676. https://doi.org/10.1016/j.tplants.2021.04.004

Sorak, D., Herberholz ,Lars, Iwascek ,Sylvia, Altinpinar ,Sedakat, Pfeifer ,Frank, & and Siesler, H. W. (2012). New Developments and Applications of Handheld Raman, Mid-Infrared, and Near-Infrared Spectrometers. *Applied Spectroscopy Reviews*, *47*(2), 83–115. https://doi.org/10.1080/05704928.2011.625748

Stagakis, S., Markos, N., Sykioti, O., & Kyparissis, A. (2010). Monitoring canopy biophysical and biochemical parameters in ecosystem scale using satellite hyperspectral imagery: An application on a *Phlomis fruticosa* Mediterranean ecosystem using multiangular CHRIS/PROBA observations. *Remote Sensing of Environment*, *114*(5), 977–994. https://doi.org/10.1016/j.rse.2009.12.006

Stan, K., & Sanchez-Azofeifa, A. (2019). Tropical Dry Forest Diversity, Climatic Response, and Resilience in a Changing Climate. *Forests*, *10*(5), Article 5. https://doi.org/10.3390/f10050443

Švik, M., Lukeš ,Petr, Lhotáková ,Zuzana, Neuwirthová ,Eva, Albrechtová ,Jana, Campbell ,Petya E., & and Homolová, L. (2023). Retrieving plant functional traits through time series analysis of satellite observations using machine learning methods. *International Journal of Remote Sensing*, *44*(10), 3083–3105. https://doi.org/10.1080/01431161.2023.2216847

Taddeo, S., Dronova, I., & Depsky, N. (2019). Spectral vegetation indices of wetland greenness: Responses to vegetation structure, composition, and spatial distribution. *Remote Sensing of Environment*, *234*, 111467. https://doi.org/10.1016/j.rse.2019.111467

Tang, J., Körner, C., Muraoka, H., Piao, S., Shen, M., Thackeray, S. J., & Yang, X. (2016). Emerging opportunities and challenges in phenology: A review. *Ecosphere*, *7*(8), e01436. https://doi.org/10.1002/ecs2.1436

Tedesco, M. (2015). Remote sensing and the cryosphere. In *Remote Sensing of the Cryosphere* (pp. 1–16). John Wiley & Sons, Ltd. https://doi.org/10.1002/9781118368909.ch1

Thompson, P. L., Isbell, F., Loreau, M., O'Connor, M. I., & Gonzalez, A. (2018). The strength of the biodiversity–ecosystem function relationship depends on spatial scale. *Proceedings of the Royal Society B: Biological Sciences*, *285*(1880), 20180038. https://doi.org/10.1098/rspb.2018.0038

Thomsen, M. S., Godbold, J. A., Garcia, C., Bolam, S. G., Parker, R., & Solan, M. (2019). Compensatory responses can alter the form of the biodiversity–function relation curve. *Proceedings of the Royal Society B: Biological Sciences*, *286*(1901), 20190287. https://doi.org/10.1098/rspb.2019.0287

Thomson, E. R., Spiegel, M. P., Althuizen, I. H. J., Bass, P., Chen, S., Chmurzynski, A., Halbritter, A. H., Henn, J. J., Jónsdóttir, I. S., Klanderud, K., Li, Y., Maitner, B. S., Michaletz, S. T., Niittynen, P., Roos, R. E., Telford, R. J., Enquist, B. J., Vandvik, V., Macias-Fauria, M., & Malhi, Y. (2021). Trait tundra. *Environmental Research Letters*, *16*(5), 055006. https://doi.org/10.1088/1748-9326/abf464

Tilman, D., Isbell, F., & Cowles, J. M. (2014). Biodiversity and Ecosystem Functioning. *Annual Review of Ecology, Evolution, and Systematics*, *45*(Volume 45, 2014), 471–493. https://doi.org/10.1146/annurev-ecolsys-120213-091917

Torabzadeh, H., Morsdorf, F., & Schaepman, M. E. (2014). Fusion of imaging spectroscopy and airborne laser scanning data for characterization of forest ecosystems – A review. *ISPRS Journal of Photogrammetry and Remote Sensing*, *97*, 25–35. https://doi.org/10.1016/j.isprsjprs.2014.08.001

Torres, R., Snoeij, P., Geudtner, D., Bibby, D., Davidson, M., Attema, E., Potin, P., Rommen, B., Floury, N., Brown, M., Traver, I. N., Deghaye, P., Duesmann, B., Rosich, B., Miranda, N., Bruno, C., L'Abbate, M., Croci, R., Pietropaolo, A., … Rostan, F. (2012). GMES Sentinel-1 mission. *Remote Sensing of Environment*, *120*, 9–24. https://doi.org/10.1016/j.rse.2011.05.028

Townsend, A., Jiya, I. N., Martinson, C., Bessarabov, D., & Gouws, R. (2020). A comprehensive review of energy sources for unmanned aerial vehicles, their shortfalls and opportunities for improvements. *Heliyon*, *6*(11). https://doi.org/10.1016/j.heliyon.2020.e05285

Trumbore, S., Brando, P., & Hartmann, H. (2015). Forest health and global change. *Science*, *349*(6250), 814–818. https://doi.org/10.1126/science.aac6759

Tsai, Y.-L. S., Dietz, A., Oppelt, N., & Kuenzer, C. (2019). Remote Sensing of Snow Cover Using Spaceborne SAR: A Review. *Remote Sensing*, *11*(12), Article 12. https://doi.org/10.3390/rs11121456

Tsyganskaya, V., Martinis ,Sandro, Marzahn ,Philip, & and Ludwig, R. (2018). SAR-based detection of flooded vegetation – a review of characteristics and approaches. *International Journal of Remote Sensing*, *39*(8), 2255–2293. https://doi.org/10.1080/01431161.2017.1420938

Ulises, R.-S. H., & Lucia, F.-M. A. (2024). Impacts of Climate Change on Forest Resources in Mexico: Regional Projections and Vulnerabilities. *Journal of Geography, Environment and Earth Science International*, *28*(12), 67–93. https://doi.org/10.9734/jgeesi/2024/v28i12849

Ustin, S. L., & Gamon, J. A. (2010). Remote sensing of plant functional types. *New Phytologist*, *186*(4), 795–816. https://doi.org/10.1111/j.1469-8137.2010.03284.x

van der Meer, F. D., van der Werff, H. M. A., van Ruitenbeek, F. J. A., Hecker, C. A., Bakker, W. H., Noomen, M. F., van der Meijde, M., Carranza, E. J. M., Smeth, J. B. de, & Woldai, T. (2012). Multi- and hyperspectral geologic remote sensing: A review. *International Journal of Applied Earth Observation and Geoinformation*, *14*(1), 112–128. https://doi.org/10.1016/j.jag.2011.08.002

Van Meerbeek, K., Jucker, T., & Svenning, J.-C. (2021). Unifying the concepts of stability and resilience in ecology. *Journal of Ecology*, *109*(9), 3114–3132. https://doi.org/10.1111/1365-2745.13651

Vane, G., Green, R. O., Chrien, T. G., Enmark, H. T., Hansen, E. G., & Porter, W. M. (1993). The airborne visible/infrared imaging spectrometer (AVIRIS). *Remote Sensing of Environment*, *44*(2), 127–143. https://doi.org/10.1016/0034-4257(93)90012-M

Veblen, T. T. (2007). Temperate Forests of the Southern Andean Region. In T. Veblen, K. Young, & A. Orme (Eds.), *The Physical Geography of South America* (p. 0). Oxford University Press. https://doi.org/10.1093/oso/9780195313413.003.0021

Ventura, D., Grosso, L., Pensa, D., Casoli, E., Mancini, G., Valente, T., Scardi, M., & Rakaj, A. (2023). Coastal benthic habitat mapping and monitoring by integrating aerial and water surface low-cost drones. *Frontiers in Marine Science*, *9*. https://doi.org/10.3389/fmars.2022.1096594

Villéger, S., Mason, N. W. H., & Mouillot, D. (2008). New Multidimensional Functional Diversity Indices for a Multifaceted Framework in Functional Ecology. *Ecology*, *89*(8), 2290–2301. https://doi.org/10.1890/07-1206.1

Violle, C., Navas, M.-L., Vile, D., Kazakou, E., Fortunel, C., Hummel, I., & Garnier, E. (2007). Let the concept of trait be functional! *Oikos*, *116*(5), 882–892. https://doi.org/10.1111/j.0030-1299.2007.15559.x

Volaire, F., Gleason, S. M., & Delzon, S. (2020). What do you mean "functional" in ecology? Patterns versus processes. *Ecology and Evolution*, *10*(21), 11875–11885. https://doi.org/10.1002/ece3.6781

Walker, A. P., Quaife, T., van Bodegom, P. M., De Kauwe, M. G., Keenan, T. F., Joiner, J., Lomas, M. R., MacBean, N., Xu, C., Yang, X., & Woodward, F. I. (2017). The impact of alternative trait-scaling hypotheses for the maximum photosynthetic carboxylation rate (Vcmax) on global gross primary production. *New Phytologist*, *215*(4), 1370–1386. https://doi.org/10.1111/nph.14623

Wallis, C. I. B., Homeier, J., Peña, J., Brandl, R., Farwig, N., & Bendix, J. (2019). Modeling tropical montane forest biomass, productivity and canopy traits with multispectral remote sensing data. *Remote Sensing of Environment*, *225*, 77–92. https://doi.org/10.1016/j.rse.2019.02.021

Wan, L., Ryu, Y., Dechant, B., Lee, J., Zhong, Z., & Feng, H. (2024). Improving retrieval of leaf chlorophyll content from Sentinel-2 and Landsat-7/8 imagery by correcting for canopy structural effects. *Remote Sensing of Environment*, *304*, 114048. https://doi.org/10.1016/j.rse.2024.114048

Wang, R., & Gamon, J. A. (2019). Remote sensing of terrestrial plant biodiversity. *Remote Sensing of Environment*, *231*, 111218. https://doi.org/10.1016/j.rse.2019.111218

Wang, Y., & Fang, H. (2020). Estimation of LAI with the LiDAR Technology: A Review. *Remote Sensing*, *12*(20), Article 20. https://doi.org/10.3390/rs12203457

Watt, M. S., Buddenbaum, H., Leonardo, E. M. C., Estarija, H. J. C., Bown, H. E., Gomez-Gallego, M., Hartley, R., Massam, P., Wright, L., & Zarco-Tejada, P. J. (2020). Using hyperspectral plant traits linked to photosynthetic efficiency to assess N and P partition. *ISPRS Journal of Photogrammetry and Remote Sensing*, *169*, 406–420. https://doi.org/10.1016/j.isprsjprs.2020.09.006

Wehner, M., Easterling, D. R., Lawrimore, J. H., Heim, R. R., Vose, R. S., & Santer, B. D. (2011). *Projections of Future Drought in the Continental United States and Mexico*. https://doi.org/10.1175/2011JHM1351.1

Westoby, M. (2025). Trait-based ecology, trait-free ecology, and in between. *New Phytologist*, *245*(1), 33–39. https://doi.org/10.1111/nph.20197

Wold, S., Sjöström, M., & Eriksson, L. (2001). PLS-regression: A basic tool of chemometrics. *Chemometrics and Intelligent Laboratory Systems*, *58*(2), 109–130. https://doi.org/10.1016/S0169-7439(01)00155-1

Woodhouse, I. H. (2017). *Introduction to Microwave Remote Sensing*. CRC Press. https://doi.org/10.1201/9781315272573

Wright, A. J., Barry, K. E., Lortie, C. J., & Callaway, R. M. (2021). Biodiversity and ecosystem functioning: Have our experiments and indices been underestimating the role of facilitation? *Journal of Ecology*, *109*(5), 1962–1968. https://doi.org/10.1111/1365-2745.13665

Wright, A. J., Wardle, D. A., Callaway, R., & Gaxiola, A. (2017). The Overlooked Role of Facilitation in Biodiversity Experiments. *Trends in Ecology & Evolution*, *32*(5), 383–390. https://doi.org/10.1016/j.tree.2017.02.011

Wright, I. J., Reich, P. B., Westoby, M., Ackerly, D. D., Baruch, Z., Bongers, F., Cavender-Bares, J., Chapin, T., Cornelissen, J. H. C., Diemer, M., Flexas, J., Garnier, E., Groom, P. K., Gulias, J., Hikosaka, K., Lamont, B. B., Lee, T., Lee, W., Lusk, C., … Villar, R. (2004). The worldwide leaf economics spectrum. *Nature*, *428*(6985), 821–827. https://doi.org/10.1038/nature02403

Wright, S. J. (2005). Tropical forests in a changing environment. *Trends in Ecology & Evolution*, *20*(10), 553–560. https://doi.org/10.1016/j.tree.2005.07.009

Wulder, M. A., White, J. C., Goward, S. N., Masek, J. G., Irons, J. R., Herold, M., Cohen, W. B., Loveland, T. R., & Woodcock, C. E. (2008). Landsat continuity: Issues and opportunities for land cover monitoring. *Remote Sensing of Environment*, *112*(3), 955–969. https://doi.org/10.1016/j.rse.2007.07.004

Wulder, M. A., White, J. C., Nelson, R. F., Næsset, E., Ørka, H. O., Coops, N. C., Hilker, T., Bater, C. W., & Gobakken, T. (2012). Lidar sampling for large-area forest characterization: A review. *Remote Sensing of Environment*, *121*, 196–209. https://doi.org/10.1016/j.rse.2012.02.001

Xue, J., & Su, B. (2017). Significant Remote Sensing Vegetation Indices: A Review of Developments and Applications. *Journal of Sensors*, *2017*(1), 1353691. https://doi.org/10.1155/2017/1353691

Yan, W. Y., Shaker, A., & El-Ashmawy, N. (2015). Urban land cover classification using airborne LiDAR data: A review. *Remote Sensing of Environment*, *158*, 295–310. https://doi.org/10.1016/j.rse.2014.11.001

Yang, P. (2022). Exploring the interrelated effects of soil background, canopy structure and sun-observer geometry on canopy photochemical reflectance index. *Remote Sensing of Environment*, *279*, 113133. https://doi.org/10.1016/j.rse.2022.113133

Yu, Y., & Saatchi, S. (2016). Sensitivity of L-Band SAR Backscatter to Aboveground Biomass of Global Forests. *Remote Sensing*, *8*(6), Article 6. https://doi.org/10.3390/rs8060522

Zellweger, F., Braunisch, V., Baltensweiler, A., & Bollmann, K. (2013). Remotely sensed forest structural complexity predicts multi species occurrence at the landscape scale. *Forest Ecology and Management*, *307*, 303–312. https://doi.org/10.1016/j.foreco.2013.07.023

Zhao, S., Liu, M., Tao, M., Zhou, W., Lu, X., Xiong, Y., Li, F., & Wang, Q. (2023). The role of satellite remote sensing in mitigating and adapting to global climate change. *Science of The Total Environment*, *904*, 166820. https://doi.org/10.1016/j.scitotenv.2023.166820

Zheng, Z., Schmid, B., Zeng, Y., Schuman, M. C., Zhao, D., Schaepman, M. E., & Morsdorf, F. (2023). Remotely sensed functional diversity and its association with productivity in a subtropical forest. *Remote Sensing of Environment*, *290*, 113530. https://doi.org/10.1016/j.rse.2023.113530

Zheng, Z., Zeng, Y., Schneider, F. D., Zhao, Y., Zhao, D., Schmid, B., Schaepman, M. E., & Morsdorf, F. (2021). Mapping functional diversity using individual tree-based morphological and physiological traits in a subtropical forest. *Remote Sensing of Environment*, *252*, 112170. https://doi.org/10.1016/j.rse.2020.112170

Zheng, Z., Zeng, Y., Schuman, M. C., Jiang, H., Schmid, B., Schaepman, M. E., & Morsdorf, F. (2022). Individual tree-based vs pixel-based approaches to mapping forest functional traits and diversity by remote sensing. *International Journal of Applied Earth Observation and Geoinformation*, *114*, 103074. https://doi.org/10.1016/j.jag.2022.103074

Zhu, L., Suomalainen, J., Liu, J., Hyyppä, J., Kaartinen, H., & Haggren, H. (2018). A review: Remote sensing sensors. *Multi-Purposeful Application of Geospatial Data*, *19*, 19–42.

Zhu, L., Walker, J. P., Ye, N., & Rüdiger, C. (2019). Roughness and vegetation change detection: A pre-processing for soil moisture retrieval from multi-temporal SAR imagery. *Remote Sensing of Environment*, *225*, 93–106. https://doi.org/10.1016/j.rse.2019.02.027

Chapter 3 Overview of methods

This thesis employs a multi-faceted methodological approach, integrating data from various sources and utilising advanced analytical tools. The research combines field-based ecological data, remotely sensed observations from multiple platforms, and environmental datasets across multiple forest sites. Key methodological components include the characterisation of study areas and sampling design, compilation and processing of vegetation census data and remotely sensed data, calculation of functional trait composition, diversity, redundancy, and carbon resilience metrics, and the development of predictive models to explore trait-environment relationships and assess ecosystem resilience. Each step in the workflow is designed to support robust and spatially explicit analyses of functional traits and forest dynamics. Fig. 1.2 presents a general workflow diagram that summarises the methodological framework applied across the thesis.

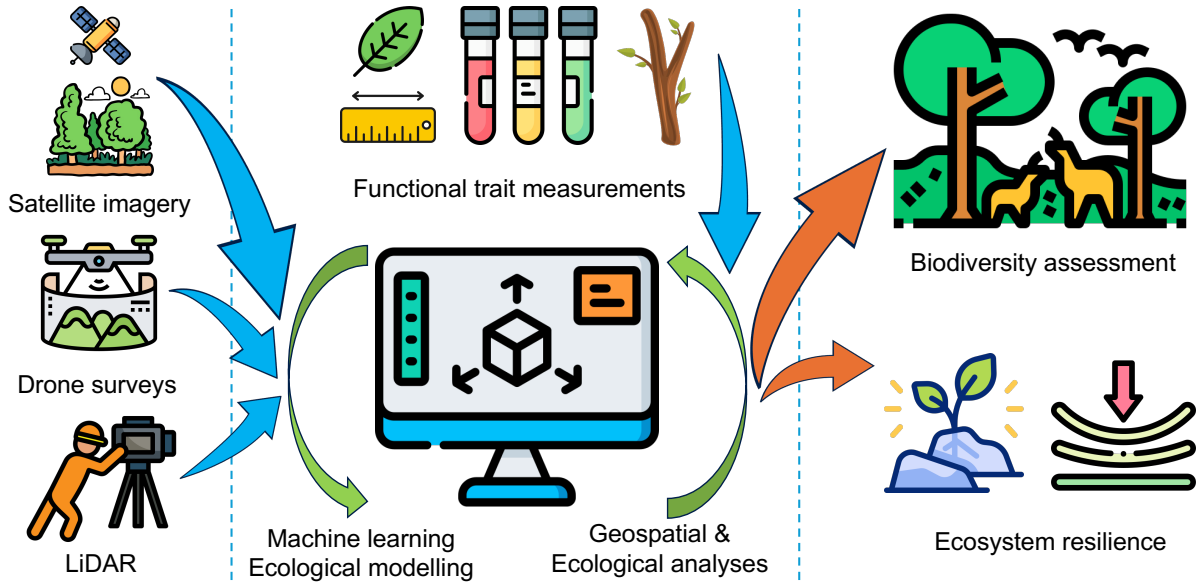

Fig. 3.1. Overview of thesis workflow. The workflow progresses from data collection to trait modelling and analysis, and finally to applications in biodiversity and resilience assessment.

3.1. Study sites

For **Research question 1**, **Chapter 4**, we used data from 1814 georeferenced vegetation plots compiled from the Global Ecosystems Monitoring network (GEM, http://gem.tropicalforests.ox.ac.uk/), (Malhi et al., 2021), the Monitoreo Nacional Forestal network (MONAFOR, http://fcfposgrado.ujed.mx/monafor/inicio/), and associated

contributors to ForestPlots network (https://forestplots.net/) (Lopez-Gonzalez et al., 2011). These plots span a wide range of environmental conditions across tropical forests and together represent a sampled area of 799.5 ha. Each plot includes detailed census data on individual trees, including species identification (standardised using the Taxonomic Name Resolution Service [TNRS, https://tnrs.biendata.org]), spatial location within the plot, and structural measurements such as diameter at beast height (DBH), tree height, and basal area (see **Section 4.6. Methods** for details).

For **Research question 2**, **Chapter 5**, the study area spans temperate forests along a broad latitudinal gradient (approximately 30°S to 53°S) in Chile. Climate across this range varies substantially, from hot, dry summers in the north to cool, wet conditions in the south, with annual precipitation ranging from 450 to 4500 mm and mean annual temperatures from 5.7°C to 13°C. At each site, we established two or three permanent plots, totalling 16 vegetation plots and 8104 individual trees (≥10 cm DBH) identified to species level. Specifically, we established three 0.36-ha plots in Las Cabras, three 0.36-ha plots in Radal Siete Tazas, two 1-ha plots in San Pablo de Tregua, two 0.6-ha plots in Alerce Costero National Park, two 1-ha plots in Correntoso, two 1-ha plots in Trapananda National Reserve, and two 1-ha plots in Magallanes National Reserve. While most plots represent temperate forest types, the Las Cabras plots are also characteristic of drier, shrubbier vegetation; for simplicity, we refer to all sites as "forests". Dominant tree species (by basal area) varied by site and included *Lithraea caustica*, *Peumus boldus*, *Austrocedrus chilensis*, *Nothofagus dombeyi*, *Nothofagus obliqua*, *Laureliopsis philippiana*, *Saxegothaea conspicua*, *Drimys winteri*, *Fitzroya cupressoides*, *Nothofagus betuloides*, *Nothofagus pumilio*, and *Nothofagus antarctica*.

For **Research question 3**, **Chapter 6**, repeated forest census data were compiled from 293 structurally intact plots across Mexico, spanning latitudes 16.02° to 30.33°N and longitudes 87.77° to 108.68°W (Gadow, 2023). These plots are part of the MONAFOR network (http://fcfposgrado.ujed.mx/monafor/inicio/), established by the Mexican National Forestry Commission to support sustainable forest management and long-term ecological monitoring. Each plot (0.25 ha, totalling 73.25 ha) was free from fire and anthropogenic disturbance (Brienen et al., 2015; Hubau et al., 2020), and was censused two to three times between 2007 and 2021, yielding 690 census intervals with a mean interval of 6.77 years. The dataset includes 13056 trees with DBH≥5 cm, representing 194 species, with plot-level species richness ranging from 1 to 45 (mean=9.65). Most plots are in temperate forests (278 plots), with the remainder in tropical forests (15 plots). Tree measurements followed the protocol of

Corral-Rivas et al. (2009). Trees were permanently tagged at breast height to enable remeasurement. The MONAFOR platform provides infrastructure for data entry, visualisation, and analysis.

3.2. Data

3.2.1. Functional trait data

For **Research question 1**, **Chapter 4**, we applied the pixel-level CWM trait method from Aguirre-Gutiérrez et al. (2025), calculating CWM values of 15 traits for each 10×10 m Sentinel-2 pixel based on the canopy area occupied by individual tree crowns within that pixel. Our analysis included 79955 pixels across 1814 permanent forest plots in 18 countries spanning the all tropical continents. For each plot, we geolocated individual trees and, where crown maps were unavailable, estimated crown polygons using regional allometric equations. CWM values were computed using crown area as a weighting factor, and only pixels with ≥70% basal area coverage from trees with trait data were retained. A full methodological description is provided in Aguirre-Gutiérrez et al. (2025).

For **Research question 2**, **Chapter 5**, we collected data from 8104 individuals across 16 vegetation plots mentioned in **Section 3.1. Study sites** spanning a wide latitudinal and elevational gradient (from 327.34 to 1251.71 m). While most plots represent temperate forests, plots in Las Cabras also include drier and shrubby vegetation-hereafter all referred to as "forests". Fieldwork took place between February 2020 and January 2022. To assess functional trait composition (CWM and CWV), functional diversity (FDis), and functional redundancy (FRed), we measured and calculated 24 plant functional traits (see Supplementary Sample design and Trait measurement in **Chapter 5** for details) across four categories: morphological, chemical (leaf nutrients), hydraulic, and photosynthetic traits. These traits capture key aspects of plant structure, physiology, and ecological strategies. Data were collected for the most abundant species in each plot, ensuring at least 80% basal area coverage with trait values.

For **Research question 3**, **Chapter 6**, we used individual-level census data that were measured and calculated by local researchers in Mexico and species-level trait data from existing global trait databases including the TRY (Kattge et al., 2011, 2020) and the Botanical Information and Ecology Network (BIEN) (Maitner et al., 2018) to calculate FDis and FRed.

3.2.2. Remotely sensed data

This study integrated and processed multi-source remotely sensed data from satellites, drones, and handheld sensors, including multispectral, SAR, and LiDAR datasets. Specifically, multispectral images were sourced from Sentinel-2 (**Research questions 1** and **2**, **Chapters 4** and **5**), PlanetScope (https://www.planet.com, **Research question 2**, **Chapter 5**), and the MicaSense Altum multispectral camera (**Research question 2**, **Chapter 5**). SAR data were obtained from Sentinel-1 (**Research question 1**, **Chapter 4**), while LiDAR measurements were derived from GEDI (**Research question 1**, **Chapter 4**) and the Global Forest Canopy Height (GFCH) product that integrated GEDI and Landsat data (Potapov et al., 2021) (**Research question 2**, **Chapter 5**). All satellite images and derived products (Sentinel-1, Sentinel-2, GEDI, and GFCH) were accessed and processed through the Google Earth Engine (GEE) (Gorelick et al., 2017), a cloud-based geospatial platform offering free access to petabytes of remotely sensed data and ready-to-use products, high-performance parallel processing, and integrated machine learning algorithms (Tamiminia et al., 2020).

3.2.3. Environmental variables

A range of environmental datasets were integrated to model trait-environment relationships and identify key drivers of functional diversity and redundancy and carbon resilience. Climate variables, such as temperature (in °C), vapour pressure deficit (VPD, in kPa), and maximum climatological water deficit (MCWD, in mm) (Malhi et al., 2009), were sourced from the TerraClimate dataset (Abatzoglou et al., 2018), which provides monthly climate data at ~ 4 km (**Research questions 1**, **2**, and **3**, **Chapters 4**, **5**, and **6**). Soil properties, including texture, organic carbon, and pH, were obtained from SoilGrids at 250 m (Hengl et al., 2017) (**Research questions 1** and **2**, **Chapters 4** and **5**), while topographic variables (slope and aspect) were derived from the Shuttle Radar Topography Mission (SRTM) digital elevation data at 30 m (Farr et al., 2007) (**Research questions 1** and **2**, **Chapters 4** and **5**). Hydrological stress including evapotranspiration (ET, in mm), evaporative stress index (ESI, unitless), and water use efficiency (WUE, in g C kg^{-1} H_2O) was characterised using data from the ECOsystem Spaceborne Thermal Radiometer Experiment on Space Station (ECOSTRESS), which provides high-resolution (70 m) thermal imagery for estimating evapotranspiration and water stress patterns (Fisher et al., 2020) (**Research question 2**, **Chapter 5**). These environmental

variables were harmonised with remotely sensed data to assess environmental filtering, trait variation, and ecosystem function across spatial gradients.

3.3. Calculating functional trait composition, diversity, and redundancy, and carbon resilience

CWM (**Research questions 1** and **2**, **Chapters 4** and **5**) and CWV (**Research question 2**, **Chapter 5**) for each functional trait is calculated as follows:

$$\mathrm{CWM}=\frac{\sum_{i=1}^{N} \mathrm{BA}_i \times \mathrm{t}_i}{\sum_{i=1}^{N} \mathrm{BA}_i} \quad (1)$$

$$\mathrm{CWV}=\frac{\sum_{i=1}^{N} \mathrm{BA}_i \times (\mathrm{t}_i-\mathrm{CWM})^2}{\sum_{i=1}^{N} \mathrm{BA}_i} \quad (2)$$

where N is the total number of tree individuals in a community, which, in this thesis, a plot, BA_i and t_i denote the basal area and trait value of the ith individual.

FDis of each trait category (morphology, nutrients, hydraulics, and photosynthesis for **Research question 2**, **Chapter 5**, and morphology and nutrients for **Research question 3**, **Chapter 6**) is calculated using the "dbFD" function of the R "FD" package (Lalibert et al., 2014):

$$\mathrm{FDis}=\frac{\sum_{i=1}^{N} \mathrm{BA}_i \times z_i}{\sum_{i=1}^{N} \mathrm{BA}_i} \quad (3)$$

where BA_i is the basal area of species i in a plot, and z_i stands for the distance of species i in a plot to the weighted centroid of the N individual species in the trait space.

In addition, FRed of each trait category (morphology, nutrients, hydraulics, and photosynthesis for **Research question 2**, **Chapter 5**, and morphology and nutrients for **Research question 3**, **Chapter 6**) is derived from the "uniqueness" function of the R "adiv" package:

$$\mathrm{FUni}=\frac{\sum_{i=1}^{N} p_i \times \sum_{j=1}^{N} p_j \delta_{ij}}{\sum_{j=1}^{N} p_j (1-p_i)} \quad (4)$$

$$\mathrm{FRed}=1-\mathrm{FUni} \quad (5)$$

where N is the total number of tree individuals in a plot, FUni is functional uniqueness that refers to the distinctiveness of species with similar traits measured at community level, p_i with

$0<p_i\leq 1$ and $\sum_{i=1}^{N} p_i = 1$ represents the relative abundance of a given species i, and δ_{ij} denotes the pairwise functional dissimilarity between species i and j ($\delta_{ij}=\delta_{ji}$ and $\delta_{ii}=0$).

For **Research question 3**, **Chapter 6**, I used repeated forest inventory plot data between 2007 and 2021 in Mexico to calculate carbon stocks (in Mg C ha^{-1}) and carbon dynamics including carbon gains (in Mg C ha^{-1} yr^{-1}), carbon losses (in Mg C ha^{-1} yr^{-1}), and net carbon sink (in Mg C ha^{-1} yr^{-1}). Specifically, I applied allometric equations to calculate aboveground carbon (AGC) for temperate and tropical forests in Mexico, then plot-level carbon stocks in each census were estimated as the sum of the AGC of all living trees, scaled by plot area (0.25 ha). Carbon gains were calculated as the AGC accumulated by surviving trees plus that of recruits, divided by the census interval and scaled per hectare. Carbon losses were estimated as the AGC of trees that died during the interval, also scaled by census length and area. Net carbon sink was calculated as gains minus losses (see **Section 6.6. Methods** for details). Finally, I quantified temporal change rate in carbon stocks (in Mg C ha^{-1} yr^{-1}) and carbon dynamics (in Mg C ha^{-1} yr^{-2}).

3.4. Modelling

The RF machine learning algorithm was applied to model relationships between remotely sensed predictors, environmental variables, and trait CWM (**Research questions 1** and **2**, **Chapters 4** and **5**), CWV (**Research question 2**, **Chapter 5**), FDis (**Research question 2**, **Chapter 5**), and FRed (**Research question 2**, **Chapter 5**). The deep learning algorithm MLP was also employed to map and predict trait CWMs across the tropics using remotely sensed data and environmental variables for **Research question 1**, **Chapter 4**. I selected the coefficient of determination (R^2) and the root mean square error (RMSE) metrics to evaluate the model performance of both RF and MLP algorithms. Furthermore, I extracted the variable importance score for each predictor to determine the contribution of different predictors (**Research questions 1** and **2**, **Chapters 4** and **5**).

For **Research question 3**, **Chapter 6**, I fitted the linear mixed-effects models (LMMs) to estimate the rate of change in the carbon metrics over time, considering potential drivers including temporal trends (calendar year), FDis, FRed, and climatic variables (see **Section 6.6. Methods** for details).

3.5. References

Abatzoglou, J. T., Dobrowski, S. Z., Parks, S. A., & Hegewisch, K. C. (2018). TerraClimate, a high-resolution global dataset of monthly climate and climatic water balance from 1958–2015. *Scientific Data*, *5*(1), 170191. https://doi.org/10.1038/sdata.2017.191

Aguirre-Gutiérrez, J., Rifai, S. W., Deng, X., ter Steege, H., Thomson, E., Corral-Rivas, J. J., Guimaraes, A. F., Muller, S., Klipel, J., Fauset, S., Resende, A. F., Wallin, G., Joly, C. A., Abernethy, K., Adu-Bredu, S., Alexandre Silva, C., de Oliveira, E. A., Almeida, D. R. A., Alvarez-Davila, E., … Malhi, Y. (2025). Canopy functional trait variation across Earth's tropical forests. *Nature*, 1–8. https://doi.org/10.1038/s41586-025-08663-2

Brienen, R. J. W., Phillips, O. L., Feldpausch, T. R., Gloor, E., Baker, T. R., Lloyd, J., Lopez-Gonzalez, G., Monteagudo-Mendoza, A., Malhi, Y., Lewis, S. L., Vásquez Martinez, R., Alexiades, M., Álvarez Dávila, E., Alvarez-Loayza, P., Andrade, A., Aragão, L. E. O. C., Araujo-Murakami, A., Arets, E. J. M. M., Arroyo, L., … Zagt, R. J. (2015). Long-term decline of the Amazon carbon sink. *Nature*, *519*(7543), 344–348. https://doi.org/10.1038/nature14283

Corral-Rivas, J., Vargas, B., Wehenkel, C., Aguirre, C., Álvarez, G., & Rojo, A. (2009). Guía para el establecimiento de sitios de investigación forestal y de suelos en bosques del estado de Durango. *Editorial UJED. Durango, México*.

Farr, T. G., Rosen, P. A., Caro, E., Crippen, R., Duren, R., Hensley, S., Kobrick, M., Paller, M., Rodriguez, E., & Roth, L. (2007). The shuttle radar topography mission. *Reviews of Geophysics*, *45*(2).

Fisher, J. B., Lee, B., Purdy, A. J., Halverson, G. H., Dohlen, M. B., Cawse-Nicholson, K., Wang, A., Anderson, R. G., Aragon, B., Arain, M. A., Baldocchi, D. D., Baker, J. M., Barral, H., Bernacchi, C. J., Bernhofer, C., Biraud, S. C., Bohrer, G., Brunsell, N., Cappelaere, B., … Hook, S. (2020). ECOSTRESS: NASA's Next Generation Mission

to Measure Evapotranspiration From the International Space Station. *Water Resources Research*, *56*(4), e2019WR026058. https://doi.org/10.1029/2019WR026058

Gadow, K. v. (2023). Stabilizing forest productivity and resilience at multiple scales. *Forest Ecosystems*, *10*, 100136. https://doi.org/10.1016/j.fecs.2023.100136

Gorelick, N., Hancher, M., Dixon, M., Ilyushchenko, S., Thau, D., & Moore, R. (2017). Google Earth Engine: Planetary-scale geospatial analysis for everyone. *Remote Sensing of Environment*, *202*, 18–27. https://doi.org/10.1016/j.rse.2017.06.031

Hengl, T., Mendes de Jesus, J., Heuvelink, G. B., Ruiperez Gonzalez, M., Kilibarda, M., Blagotić, A., Shangguan, W., Wright, M. N., Geng, X., & Bauer-Marschallinger, B. (2017). SoilGrids250m: Global gridded soil information based on machine learning. *PLoS One*, *12*(2), e0169748.

Hubau, W., Lewis, S. L., Phillips, O. L., Affum-Baffoe, K., Beeckman, H., Cuní-Sanchez, A., Daniels, A. K., Ewango, C. E. N., Fauset, S., Mukinzi, J. M., Sheil, D., Sonké, B., Sullivan, M. J. P., Sunderland, T. C. H., Taedoumg, H., Thomas, S. C., White, L. J. T., Abernethy, K. A., Adu-Bredu, S., … Zemagho, L. (2020). Asynchronous carbon sink saturation in African and Amazonian tropical forests. *Nature*, *579*(7797), 80–87. https://doi.org/10.1038/s41586-020-2035-0

Kattge, J., Bönisch, G., Díaz, S., Lavorel, S., Prentice, I. C., Leadley, P., Tautenhahn, S., Werner, G. D. A., Aakala, T., Abedi, M., Acosta, A. T. R., Adamidis, G. C., Adamson, K., Aiba, M., Albert, C. H., Alcántara, J. M., Alcázar C, C., Aleixo, I., Ali, H., … Wirth, C. (2020). TRY plant trait database – enhanced coverage and open access. *Global Change Biology*, *26*(1), 119–188. https://doi.org/10.1111/gcb.14904

Kattge, J., Díaz, S., Lavorel, S., Prentice, I. C., Leadley, P., Bönisch, G., Garnier, E., Westoby, M., Reich, P. B., Wright, I. J., Cornelissen, J. H. C., Violle, C., Harrison, S. P., Van BODEGOM, P. M., Reichstein, M., Enquist, B. J., Soudzilovskaia, N. A., Ackerly, D.

D., Anand, M., … Wirth, C. (2011). TRY – a global database of plant traits. *Global Change Biology*, *17*(9), 2905–2935. https://doi.org/10.1111/j.1365-2486.2011.02451.x

Lalibert, E., Legendre, P., & Shipley, B. (2014). Measuring functional diversity from multiple traits, and other tools for functional ecology. *R-Package FD*.

Lopez-Gonzalez, G., Lewis, S. L., Burkitt, M., & Phillips, O. L. (2011). ForestPlots.net: A web application and research tool to manage and analyse tropical forest plot data. *Journal of Vegetation Science*, *22*(4), 610–613. https://doi.org/10.1111/j.1654-1103.2011.01312.x

Maitner, B. S., Boyle, B., Casler, N., Condit, R., Donoghue II, J., Durán, S. M., Guaderrama, D., Hinchliff, C. E., Jørgensen, P. M., Kraft, N. J. B., McGill, B., Merow, C., Morueta-Holme, N., Peet, R. K., Sandel, B., Schildhauer, M., Smith, S. A., Svenning, J.-C., Thiers, B., … Enquist, B. J. (2018). The bien r package: A tool to access the Botanical Information and Ecology Network (BIEN) database. *Methods in Ecology and Evolution*, *9*(2), 373–379. https://doi.org/10.1111/2041-210X.12861

Malhi, Y., Aragão, L. E., Galbraith, D., Huntingford, C., Fisher, R., Zelazowski, P., Sitch, S., McSweeney, C., & Meir, P. (2009). Exploring the likelihood and mechanism of a climate-change-induced dieback of the Amazon rainforest. *Proceedings of the National Academy of Sciences*, *106*(49), 20610–20615.

Malhi, Y., Girardin, C., Metcalfe, D. B., Doughty, C. E., Aragão, L. E. O. C., Rifai, S. W., Oliveras, I., Shenkin, A., Aguirre-Gutiérrez, J., Dahlsjö, C. A. L., Riutta, T., Berenguer, E., Moore, S., Huasco, W. H., Salinas, N., da Costa, A. C. L., Bentley, L. P., Adu-Bredu, S., Marthews, T. R., … Phillips, O. L. (2021). The Global Ecosystems Monitoring network: Monitoring ecosystem productivity and carbon cycling across the tropics. *Biological Conservation*, *253*, 108889. https://doi.org/10.1016/j.biocon.2020.108889

Potapov, P., Li, X., Hernandez-Serna, A., Tyukavina, A., Hansen, M. C., Kommareddy, A., Pickens, A., Turubanova, S., Tang, H., Silva, C. E., Armston, J., Dubayah, R., Blair, J. B., & Hofton, M. (2021). Mapping global forest canopy height through integration of GEDI and Landsat data. *Remote Sensing of Environment*, *253*, 112165. https://doi.org/10.1016/j.rse.2020.112165

Tamiminia, H., Salehi, B., Mahdianpari, M., Quackenbush, L., Adeli, S., & Brisco, B. (2020). Google Earth Engine for geo-big data applications: A meta-analysis and systematic review. *ISPRS Journal of Photogrammetry and Remote Sensing*, *164*, 152–170. https://doi.org/10.1016/j.isprsjprs.2020.04.001

Chapter 4 Multimodal remote sensing fusion for functional trait estimation across tropical forests: comparing machine learning and deep learning approaches (Paper 1)

4.1. Preface

As the technical foundation of this thesis, this chapter (**Paper 1**) focuses on identifying the most effective and robust fusion of remotely sensed data and modelling approaches for mapping plant functional traits, considering community-weighted means (CWMs), across tropical forests. By systematically comparing traditional machine learning and deep learning algorithms using multi-source remotely sensed and trait CWM data, this chapter establishes the methodological framework for trait estimation applied in subsequent chapters. The approaches developed here are further used in **Paper 2** to map trait variance, functional diversity, and redundancy across temperate forests and to identify areas of potential ecological resilience. **Paper 3** then builds upon these results to explore how functional diversity and redundancy relate to carbon resilience under intensifying warming and drought across temperate and tropical forests in Mexico.

4.1.1. Highlights

This chapter developed and evaluated a methodological framework for mapping plant functional traits across tropical forests by integrating multi-source remotely sensed data with advance algorithms. By comparing Random forests and Multilayer Perceptron, we predicted 15 key functional traits at 10-m resolution, achieving the highest accuracy for nutrient traits, with multispectral data contributing most consistently.

This paper is prepared for submission to *Nature Communications*, which requires the Method section to be placed at the end of the manuscript in accordance with the journal's author guidelines.

4.1.2. Author information and contribution statement

Xiongjie Deng[1*], David Coomes[2], Imma Oliveras Menor[1,3,4], Zhenfeng Shao[5], Huanyuan Zhang-Zheng[1,6], Yuankun Wang[5], Jarcilene Almeida Silva[7], Resende F Angelica[8], Gregory P. Asner[9], Tim Baker[10], Jos Barlow[11], Maíra Benchimol[12], Erika Berenguera[1,11], Rodrigo S.

Bergamin[13], Lilian Blanc[14,15], Damien Bonal[16], Robson Borges de Lima[17], David F.R.P. Burslem[18], Jaime A. Cabezas Duarte[19], Domingos Cardoso[20], Samuel Carvalho de Padua Chaves e[21], Larissa Cavalheiro[22], Lucas A. Cernusak[23], Antonio Carlos da Silva Zanzini[24], Marie Ruth Dago[25], Domingos de Jesus Rodrigues[22], Tony C. de Sousa Oliveira[26,27], Géraldine Derroire[28,29,30], Mário Marcos do Espírito Santo[31], Brian Enquist[32], Letícia Fernandes da Silva[33], Tomas Ferreira Domingues[34,35], Angelo Gilberto Manzatto[36], Aretha Franklin Guimaraes[37], Marina Guimarães Freitas[38], Bruno Hérault[14,15], Zo-Bi Irié Casimir[25], Sreejith Kalpuzha Ashtamoorthy[39], Joice Klipel[40,41], William F. Laurance[23], Maurício Lima Dan[42], William E. Magnusson[43], Eduardo Malta Campos-Filho[44], Roberta Martin[9], Thiago Metzker[45], Peter Moonlight[46], Robert Muscarella[47], Maria Guadalupe Nava-Miranda[48,49], Jhonathan Oliveira Silva[50], Marco Patacca[51,52], Pablo Pena Rodrigues[20], Lucas Pereira Zanzini[24], Cinthia Pereira de Oliveira[17], Carlos A. Peres[53], Sami W. Rifai[54], Gonzalo Rivas-Torres[55], Clarissa Rosa[43], Norma Salinas[56], Alexander Shenkin[57], Priscyla Maria Silva Rodrigues[50], Marcos Silveira[58], Axa Emanuelle Simões Figueiredo[59], Tereza Sposito[45], Danielle Storck-Tonon[60], Martin J.P. Sullivan[61], Martin Svátek[62], Wagner Tadeu Vieira Santiago[63], Yit Arn Teh[64], Hans ter Steege[65,66], Elmar Veenendaal[67], Badouard Vincyane[25], Göran Wallin[68], Etienne Zibera[68,69], Joeri A. Zwerts[70], Oliver L. Phillips[10], Yadvinder Malhi[1,6], Jesús Aguirre-Gutiérrez[1,6]

[1]Environmental Change Institute, School of Geography and the Environment, University of Oxford, Oxford, OX1 3QY, UK

[2]Department of Plant Sciences and Conservation Research Institute, University of Cambridge, CB2 3EA, UK

[3]Programa de Pós-Graduação em Ciências Ambientais – PPGCA, Universidade do Estado de Mato Grosso – UNEMAT, Avenida Santos Dumont, s/nº, Cidade Universitária (Bloco II), CEP 78200-000, Cáceres, Mato Grosso, Brazil

[4]AMAP – botAnique et Modélisation de l'Architecture des Plantes et des Végétations, Université de Montpellier, CIRAD, CNRS, INRAE, IRD, Montpellier CEDEX 5, France

[5]The State Key Laboratory of Information Engineering in Surveying, Mapping and Remote Sensing, Wuhan University, 430079, Wuhan, China

[6]Leverhulme Centre for Nature Recovery, University of Oxford, Oxford OX1 3QY, UK

[7]Departamento de Botânica, Centro de Biociências, Universidade Federal de Pernambuco, Recife-PE. Brazil

[8]Department of Forest Sciences, Luiz de Queiroz College of Agriculture, University of São Paulo
(USP/ESALQ), Piracicaba, Brazil

[9]Center for Global Discovery and Conservation Science, Arizona State University

[10]School of Geography, University of Leeds, UK

[11]Lancaster Environment Centre, Lancaster University, UK

[12]Applied Ecology and Conservation Lab, Universidade Estadual de Santa Cruz – UESC, Ilhéus, Bahia, Brazil

[13]School of Geography, Earth and Environmental Sciences. University of Birmingham, UK

[14]CIRAD, Forêts et Sociétés, F-34398 Montpellier, France

[15]Forêts et Sociétés, Univ Montpellier, CIRAD, Montpellier, France

[16]INRAE

[17]Laboratório de Manejo Florestal, Universidade do Estado do Amapá, Macapá, Amapá, Brazil

[18]Interdisciplinary Institute and School of Biological Sciences, University of Aberdeen, Aberdeen AB24 3UU, Scotland, UK

[19]Universidad de los Andes, Laboratorio de Ecología de Bosques Tropicales y Primatología - LEBTYP

[20]Jardim Botânico do Rio de Janeiro, Brazil

[21]Institute of Forestry, Rural University of Rio de Janeiro, Seropedica, Brazil

[22]Universidade Federal de Mato Grosso, Campus Universitário de Sinop,Sinop, MT, Brazil

[23]Centre for Tropical Environmental and Sustainability Science, and College of Science and Engineering, James Cook University, Cairns, Queensland 4878, Australia

[24]Universidade Federal de Lavras, Departamento de Ciências Florestais, Lavras, Brazil

[25]UMRI Sciences Agronomiques et Procédés de Transformation, Institut National Polytechnique Félix Houphouët-Boigny (UMRI SAPT / INP-HB), Yamoussoukro, Côte d'Ivoire

[26]Institute of Biogeosciences, IBG2: Plant Sciences, Forschungszentrum Jülich GmbH, Jülich, Germany

[27]Faculty of Communication and Environment, Hochschule Rhein-Waal, Kamp-Lintfort, Germany

[28]Cirad, UMR EcoFoG (AgroParistech, CNRS, INRAE, Université des Antilles, Université de la Guyane), Campus Agronomique, Kourou, French Guiana

[29]Cirad, UPR Forêts et Sociétés, University of Montpellier, Montpellier, France

[30]University of Brasilia, Department of Forestry, Campus Darcy Ribeiro, Brasília 70.900-910, Brazil

[31]Departamento de Biologia Geral, Universidade Estadual de Montes Claros, Montes Claros-MG, Brazil

[32]Department of Ecology and Evolutionary Biology, University of Arizona, Arizona, AZ 85721, USA

[33]Universidade Federal do Acre, Rio Branco, Acre, Brazil

[34]Faculdade de Filosofia, Ciências e Letras de Ribeirão Preto

[35]Universidade de São Pualo (FFCLRP-USP)

[36]Universidade Federal de Rondônia, Porto Velho, Rondônia, Brazil

[37]Instituto Nacional de Pesquisas da Amazonia, Manaus, Brazil

[38]Programa de Pós-Graduação Profissional Biodiversidade em Unidades de Conservação, Escola Nacional de Botânica Tropical,Instituto de Pesquisas Jardim Botânico do Rio de Janeiro, Brasil

[39]Forest Ecology Department, KSCSTE-Kerala Forest Research Institute, Peechi, India

[40]Leuphana University of Lüneburg, Germany

[41]Universidade Federal do Rio Grande do Sul, Brazil

[42]Centro de Pesquisa, Desenvolvimento e Inovação Sul, Instituto Capixaba de Pesquisa, Assistência Técnica e Extensão Rural, Cachoeiro de Itapemirim, Brazil

[43]Instituto Nacional de Pesquisas da Amazônia, Manaus, Brazil

[44]Instituto Socioambiental - ISA, Brazil

[45]IBAM - Instituto Bem Ambiental

[46]Botany, School of Natural Sciences, Trinity College Dublin, Ireland

[47]Department of Ecology and Genetics, Uppsala University, Sweden

[48]Colegio de Ciencias y Humanidades, Universidad Juárez del Estado de Durango, Durango, Mexico

[49]Escuela Politécnica Superior de Ingeniería, Universidad de Santiago de Compostela, Campus Terra, Lugo, España

[50]Universidade Federal do Vale do São Francisco, Brazil

[51]Sustainable Forest Management group, Wageningen Environmental Research, Wageningen, The Netherlands

[52]Forest Ecology & Forest Management group, Wageningen University & Research, Wageningen, The Netherlands

[53]School of Environmental Sciences, University of East Anglia, Norwich, UK

[54]School of Biological Sciences, The University of Adelaide

[55]Estación de Biodiversidad Tiputini, Universidad San Francisco de Quito, Quito, Ecuador

[56]Institute for the Sciences of Nature, Earth and Energy (INTE-PUCP), Pontifical Catholic University of Peru. Av. Universitaria 1801, Lima 15088, Peru

[57]School of Informatics, Computing, and Cyber Systems, Northern Arizona University, Flagstaff, AZ, USA

[58]Centro de Ciências Biológicas e da Natureza, Universidade Federal do Acre, Acre, Brazil

[59]Universidade Federal do Oeste do Pará. Departamento de Agronomia. Campi Juruti, Pará, Brazil

[60]Universidade do Estado de Mato Grosso, Tangará da Serra, Brazil

[61]Department of Natural Sciences, Manchester Metropolitan University, Manchester, UK

[62]Department of Forest Botany, Dendrology and Geobiocoenology, Faculty of Forestry and Wood Technology, Mendel University in Brno, Brno, Czech Republic

[63]CESAM - Centro de Estudos do Ambiente e do Mar, Departamento de Biologia. Pesquisador Colaborador, Universidade de Aveiro, Aveiro, Portugal

[64]School of Natural and Environmental Sciences, Newcastle University, Newcastle upon Tyne, NE1 7RU, UK

[65]Naturalis Biodiversity Center, Leiden, The Netherlands

[66]Quantitative Biodiversity Dynamics, Dept. Biology, Utrecht University, The Netherlands

[67]Plant Ecology and Nature Conservation Group, Wageningen University. Wageningen, The Netherlands

[68]Department of Biological and Environmental Sciences, University of Gothenburg, Sweden

[69]College of Agriculture, Forestry and food sciences, University of Rwanda, Rwanda

[70]Wildlife Ecology & Nature Restoration, Utrecht University, Utrecht, The Netherlands

Xiongjie Deng: Writing – original draft, Writing – review & editing, Methodology, Spatial analyses, Investigation, Software, Formal analysis, Conceptualisation. **Zhenfeng Shao:** Writing – review & editing, Methodology, Spatial analyses. **Huanyuan Zhang-Zheng:** Writing – review & editing, Methodology, Spatial analyses. **Yuankun Wang:** Writing – review & editing, Methodology, Spatial analyses. **Yadvinder Malhi:** Writing – review & editing, Supervision. **Jesús Aguirre-Gutiérrez:** Writing – review & editing, Methodology, Conceptualisation, Supervision. **All authors:** Writing – review & editing.

4.2. Abstract

Tropical forests play a vital role in adjusting the global climate and atmosphere. Accurately monitoring their functional composition and structure is of high priority for mitigating biodiversity loss. The main goal of this study is to evaluate to what extent remotely sensed data and environmental variables can be useful to map and predict functional traits including morphology, nutrients, and photosynthesis across the tropics with artificial intelligence methods. We integrated multi-source remotely sensed data with *in-situ* plant trait measurements from 1814 plots to map and predict 15 functional traits at 10 m resolution. Two approaches were compared: a machine learning algorithm (Random forests, RF) and a deep learning algorithm (Multilayer Perceptron, MLP). Across pan-tropical forests, RF generally outperformed MLP, and it yielded higher predictive accuracies with mean R^2 scores of 0.42, 0.41, and 0.62 for predicting photosynthetic, morphological, and nutrient traits, respectively.

We further explored trait distribution and variation across multiple spatial scales and identified main factors in driving the distribution and variation of each trait, with multispectral images contributing most strongly to predictions. Our results demonstrate that multimodal remote sensing, particularly when coupled with machine learning, provides an effective approach for mapping functional traits and offers valuable insights into biodiversity-ecosystem function relationships under global environmental change in the most biodiverse terrestrial ecosystem.

Keywords: **Functional traits; Tropical forests; Traits distribution and variation; Sentinel-1; Sentinel-2; GEDI; Environmental drivers; Random forests; Multilayer Perceptron**

4.3. Main

As the most biodiverse ecosystems on Earth (Cooper et al., 2024) and home to over half of global biodiversity (Malhi et al., 2021) and about 80% of tree species (Beech et al., 2017; ter Steege et al., 2016), tropical forests play a critical role in stabilising the global carbon cycle (Cuni-Sanchez et al., 2021; Pan et al., 2011; Zhang-Zheng et al., 2024) and sustaining global biodiversity (Malhi et al., 2022) from both ecological and biological points of view. However, tropical forests are suffering from unprecedented negative impacts from deforestation and forest degradation due to a combination of ongoing climate change and direct human-induced disturbances (França et al., 2020). To quantify the potential of tropical forests for mitigating climate change and maintaining Earth's biodiversity and offering an empirical reference for policymakers and decision-making progress (Aguirre-Gutiérrez et al., 2025; Gurdak et al., 2014), there is an urgent need to adequately understand and track the ecological dynamics across tropical forests.

Building on the recognition of the critical role that tropical forests play in global biodiversity and climate regulation, accurately mapping and predicting plant functional traits across these ecosystems emerges as a vital approach to deepening and strengthening our understanding of their ecological dynamics. Functional traits are defined as any morphological, physiological or phenological property measurable at the individual level (Reiss et al., 2009), they affect overall plant fitness through their influence on survival, growth, and reproduction (Brussel & Brewer, 2021; Violle et al., 2007), and they are key indicators of how species interact with their environment, influence ecosystem processes, and respond to environmental

changes (Suding et al., 2008; Violle et al., 2007). In addition, trait-based approaches enable the identification of functional diversity patterns and the underlying ecological processes that drive biodiversity distribution, and offer a more comprehensive understanding of ecosystem functioning than species diversity alone (Díaz et al., 2016; Lavorel & Garnier, 2002; Thomson et al., 2021). This knowledge is crucial for predicting how tropical forests will respond to future environmental changes and for developing strategies that enhance their role in mitigating climate change and preserving biodiversity. However, traditional field surveys of traits are time-consuming and labour-intensive, making it not possible to carry out large-scale trait field collections, resulting in spatially biassed (e.g. towards accessible locations) and discontinuous trait collections in space and time (Thomson et al., 2021). Therefore, it is still rather challenging yet imperative to map and predict functional traits across the tropics.

Remote sensing has proved to be a robust tool for mapping key forest variables (Chen et al., 2023; Lechner et al., 2020) and assessing plant and ecosystem diversity at relatively high spatial- and temporal- resolutions over a broad area (Nagendra, 2001; Skidmore et al., 2015; R. Wang & Gamon, 2019). In recent decades, studies have been carried out to estimate functional diversity through functional traits with passive remotely sensed imagery including multispectral images (Aguirre-Gutiérrez et al., 2025; Ali et al., 2017; Hauser et al., 2021; Helfenstein et al., 2022; Thomson et al., 2021) and hyperspectral images (Asner et al., 2017; Ollinger et al., 2008; Z. Wang, 2019), active remotely sensed data like light detection and ranging (LiDAR) (Greaves et al., 2015), or combinations of multiple platforms (Abelleira Martínez et al., 2016; Zheng et al., 2021). In general, passive remotely sensed data, which are captured by passive sensors that measure reflected sunlight emitted from the sun (Moya et al., 2004), have been widely applied to traits mapping and estimation as they directly measure biophysical and biochemical properties of vegetation (Jetz et al., 2016; Ustin & Gamon, 2010). As for active remotely sensed data of which sensors emit electromagnetic radiation to scan objects and areas whereupon a sensor then detects and measures the radiation reflected or backscattered from the target (Byrd et al., 2005), LiDAR data have also been utilised to retrieval functional traits alone (Greaves et al., 2015) or with passive remotely sensed images (Abelleira Martínez et al., 2016). However, as the other frequently used active remotely sensed data source, although studies have been exploring the potential of radio detection and ranging (radar) data in biodiversity monitoring and ecological research, such as forest above-ground biomass estimation (Bouvet et al., 2018), forest area mapping (dos Santos et al., 2021; Martone et al., 2018), and forest biodiversity monitoring (Bae et al., 2019; Wollersheim et al., 2011),

traits mapping related research is rarely developed. Additionally, in comparison with optical remotely sensed data, whose imaging quality is dominantly influenced and limited by atmospheric conditions and cloud cover that typically happens in humid tropical regions (Asner, 2001; dos Santos et al., 2021), synthetic aperture radar (SAR) sensors are able to penetrate thick clouds and are an ideal way for traits mapping and monitoring by offering all-sky and high temporal resolution observations regardless of unfavourable illumination and weather conditions (Mason et al., 2014). The rationale behind SAR's applications in ecology and vegetation research is that SAR backscatter signals demonstrate unique sensitivity and intensity to different land cover types (e.g. forest, water, grassland, and bare soil) and different components of a certain kind of object (e.g. leaves, branches, and stems of trees) due to their physical and electromagnetic characteristics, and thus can extract ecologically meaningful structural information from terrain and vegetation (Bae et al., 2019). When combined with environmental variables such as climatic data, terrain characteristics, and soil properties, these remotely sensed data can enhance our ability to predict functional traits and produce a more complete understanding of traits (Aguirre-Gutiérrez et al., 2025).

The integration of the diverse remotely sensed data sources and environmental variables necessitates the use of advanced machine learning and deep learning algorithms capable of handling high-dimensional data and capturing complex relationships between environmental predictors and functional traits at large spatial scales. Machine learning and deep learning are two prominent approaches that can manage complex datasets. Machine learning algorithms, such as Random forests (RF), are typically more interpretable, faster to train, require less computational power, and well-suited for structured data with clear patterns (Breiman, 2001; Domingos, 2012). In contrast, deep learning algorithms, such as Multilayer Perceptron (MLP), are highly effective at learning hierarchical features from large datasets and excel in capturing complex, non-linear relationships, especially in high-dimensional and unstructured data, which makes it particularly advantageous for ecological modelling like deforestation and fragmentation dynamics modelling (Singh et al., 2017) and landscape monitoring (Sardar & Samadder, 2021), where they can automatically learn spatial hierarchies and patterns directly from the input data. Given these differences, comparing the performance of machine learning and deep learning algorithms in the context of tropical forest trait mapping is essential. By comparing these two approaches, we aim to determine which method offers the best trade-off between interpretability, accuracy, and computational efficiency for predicting functional traits across tropical regions.

Here we mapped and predicted 15 functional traits (Table 4.1) including morphology, nutrients, and photosynthesis across the tropics by integrating three different satellite remotely sensed platforms: Sentinel-1 SAR observations, Sentinel-2 optical images, and Global Ecosystem Dynamics Investigation (GEDI) LiDAR data, and environmental variables including climatic characteristics, terrain, and soil properties with *in-situ* plant trait measurements across 1814 permanent plots in 18 tropical countries that cover all tropical continents (Fig. 4.1). We compared the performance of two widely used models: RF and MLP, representing machine learning and deep learning approaches, respectively, and we examined the effect of spatial autocorrelation on model's performance by applying multiple cross-validation methods at different spatial scales. We also investigated patterns of trait distribution and variation across different regions. Additionally, we conducted variable importance evaluation to find the foremost factors in driving trait distribution and variation.

Table 4.1. Description of all functional traits in this study.

Trait	Abbreviation	Unit	Description
Photosynthetic	A_{max}	μmol m^{-2} s^{-1}	Light-saturated maximum rates of net photosynthesis at saturated CO_2 (2000 ppm CO_2)
	A_{sat}	μmol m^{-2} s^{-1}	Light-saturated rates of net photosynthesis at ambient CO_2 concentration (400 ppm CO_2)
Morphological	Leaf dry mass	g	Mass of a dry leaf
	Leaf fresh mass	g	Mass of a fresh leaf
	Leaf area	cm^2	One-sided area of the leaf
	Leaf water content	%	Water content per unit dry leaf mass
	Specific leaf area (SLA)	cm^2 g^{-1}	A ratio indicating how much leaf area a plant builds with a given amount of leaf biomass
	Leaf thickness	mm	Thickness of a fresh leaf

	Wood density	G cm^{-3}	The dry weight per unit volume of wood, the amount of wood in a unit
Nutrient	Leaf carbon (C) content	%	Carbon content per unit dry leaf mass
	Leaf calcium (Ca) content	%	Calcium content per unit dry leaf mass
	Leaf potassium (K) content	%	Potassium content per unit dry leaf mass
	Leaf magnesium (Mg) content	%	Magnesium content per unit dry leaf mass
	Leaf nitrogen (N) content	%	Nitrogen content per unit dry leaf mass
	Leaf phosphorus (P) content	%	Phosphorus content per unit dry leaf mass

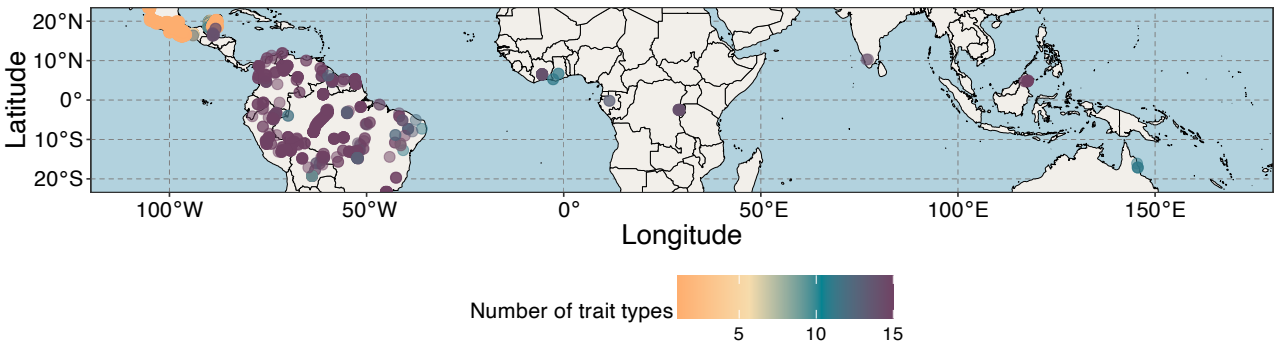

Fig. 4.1. Spatial distribution of all plots across the tropics. A total of 1814 forest inventory plots (displayed as circles) were employed for geospatial modelling of functional traits mapping and prediction. Different filling colours of the circles indicated the number of trait types in each plot. Note that all the circles were magnified for visualisation purposes.

4.4. Results

4.4.1. Model performance

The results of our models showed varying levels of predictive accuracy across the 15 functional traits (Table 4.2). RF generally achieved higher coefficient of determination (R^2) values and lower root mean square error (RMSE) across most traits. For instance, RF outperformed MLP

for predicting leaf P (R^2=0.79 versus R^2=0.63) and Mg (R^2=0.63 versus R^2=0.26) contents. Similarly, RF achieved higher accuracy for morphological traits such as leaf thickness (R^2=0.41 versus R^2=0.08) and wood density (R^2=0.61 versus R^2=0.49). At the same time, performance differences between the two algorithms were modest for several traits, such as leaf dry mass (R^2=0.48 versus R^2=0.45), SLA (R^2=0.42 versus R^2=0.40), and leaf K content (R^2=0.48 versus R^2=0.47). For some traits, MLP performed equally well or slightly better than RF: leaf Ca content was predicted with identical accuracy (R^2=0.67 versus R^2=0.67), and MLP outperformed RF for A_{max} (R^2=0.48 versus R^2=0.43). For subsequent trait mapping, we adopted RF because of its more consistent performance across trait groups.

In addition, we noticed distinct predictive patterns across the three groups of functional traits from both RF and MLP algorithms. Nutrient traits were predicted with the highest accuracy, especially by the RF algorithm (mean R^2=0.62). The MLP algorithm, while generally less accurate, also performed best on nutrient traits. Photosynthetic traits (A_{max} and A_{sat}) were moderately predicted by both algorithms, with the only exception that MLP slightly outperformed RF (R^2=0.43 and 0.48 for predicting A_{max} from RF and MLP, respectively). Eventually, morphological traits were more challenging to predict, especially leaf fresh mass and leaf area, which had lower R^2 values in both algorithms . RF achieved moderate accuracy for leaf thickness (R^2=0.41), whereas MLP struggled more with this trait as it achieved the lowest R^2 of 0.08. Furthermore, we conducted four cross-validation approaches (see Methods) to explore the reliability of the RF regression algorithm used to predict traits at multiple spatial scales. For the leave-one-cluster-out approach, we applied the Moran's *I* test on model residuals to quantify spatial autocorrelation, and we consistently found strong spatial correlation (*P*-values<0.05) for each trait (Supplementary Table S4.1). We then grouped trait observations into clusters based on the distance threshold (ranging from ~0.15 to ~3.06 km, Supplementary Table S4.1) from empirical variogram analysis. We noticed R^2 remained relatively high using leave-one-cluster-out (Supplementary Table S4.2) and leave-one-plot-out (Supplementary Table S4.3) cross-validation, it dropped more in the leave-one-country-out (Supplementary Table S4.4) method, and this trend became clearer in the leave-one-continent-out approach, where R^2 values decreased to the lowest for most traits (Supplementary Table S4.5), especially when we left the Americas out, in which most trait *in-situ* data were available.

Table 4.2. Evaluation results of prediction accuracy for functional traits.

Type	Trait	R^2		RMSE	
		RF	MLP	RF	MLP
Photosynthetic	A_{max}	0.43	0.48	3.79	0.08
	A_{sat}	0.40	0.27	1.40	1.70
		mean=0.42	mean=0.38		
Morphological	Leaf dry mass	0.48	0.45	2.58	3.79
	Leaf fresh mass	0.24	0.17	5.80	7.28
	Leaf area	0.33	0.23	170.11	161.24
	Leaf water content	0.38	0.29	4.22	4.69
	SLA	0.42	0.40	22.73	22.79
	Thickness	0.41	0.08	4.56	7.21
	Wood density	0.61	0.49	0.07	0.08
		mean=0.41	mean=0.30		
Nutrient	C	0.52	0.43	1.19	1.59
	Ca	0.67	0.67	0.20	0.30
	K	0.48	0.47	0.19	0.21
	Mg	0.63	0.26	0.06	0.09
	N	0.61	0.52	0.26	0.31
	P	0.79	0.63	0.02	0.03
		mean=0.62	mean=0.50		

4.4.2. Functional trait distribution and variation at continental scale

The variation in functional traits was substantial across all tropical continents (Figs. 4.2, 4.3, Supplementary Table S4.6). Both photosynthetic traits showed notable differences, with A_{max}

highest in Africa (median: 14.43 μmol m^{-2} s^{-1}) compared to Asia (13.45 μmol m^{-2} s^{-1}) and the Americas (12.24 μmol m^{-2} s^{-1}). A_{sat} followed the similar pattern, being higher in Africa (median: 6.04 μmol m^{-2} s^{-1}) than in Asia (5.17 μmol m^{-2} s^{-1}) and the Americas (5.10 μmol m^{-2} s^{-1}). Moreover, morphological traits showed wide ranges, with leaf area having a median of 167.18 cm^2 in Africa, compared to 90.64 cm^2 in the Americas and 89.18 cm^2 in Asia, but with much larger variation (standard deviation>200 cm^2) in the Americas and Asia. Median values of leaf dry mass, fresh mass, SLA, and wood density were all generally the highest in Africa, yet median leaf thickness was the lowest in Africa. While the highest median leaf thickness was found in the Americas, the corresponding median leaf dry mass and fresh mass in the Americas were the lowest. Nutrient traits revealed relatively moderate variation compared to photosynthetic and morphological traits. And like photosynthetic and morphological traits, most median nutrients' lowest values were frequently found in the Americas (0.60%, 0.61%, 0.24%, and 0.09% for leaf contents of Ca, K, Mg, and P, respectively), leaf C content was relatively stable across continents, around 45-48%. In addition, we consistently noticed that all *P*-values from the one-way analysis of variance test were smaller than 0.05, thus significant differences in the 15 functional traits across continents were suggested. Then the post-hoc Tukey honestly significant difference analysis (Supplementary Table S4.7) further demonstrated specific differences between continents pairwise. Both photosynthetic traits exhibited significant differences between all continent pairs, with Africa showing significantly higher A_{max} than both the Americas and Asia (*P*-values<0.05), and Asia having higher A_{max} than the Americas (*P*-values<0.05). For A_{sat}, Africa had higher values compared to both the Americas and Asia, while Asia exceeded the Americas. Morphological traits like leaf area, dry mass, and fresh mass showed substantial differences between Africa and the Americas/Asia, with Africa having clearly larger and heavier leaves. However, no significant difference was found between Asia and the Americas for these three leaf morphological traits. SLA was also significantly higher in Africa compared to both the Americas and Asia, with Asia having the lowest SLA. The numerical differences in wood density observed between continent pairs were minor compared to other morphological traits that exhibited greater variability. At last, nutrients tended to show nonsignificant differences as mean trait differences larger than 1% were only found in leaf contents of C. In specific, Africa had the highest leaf contents of Ca, N, and P compared to the Americas and Asia. Leaf C content was relatively higher in the Americas.

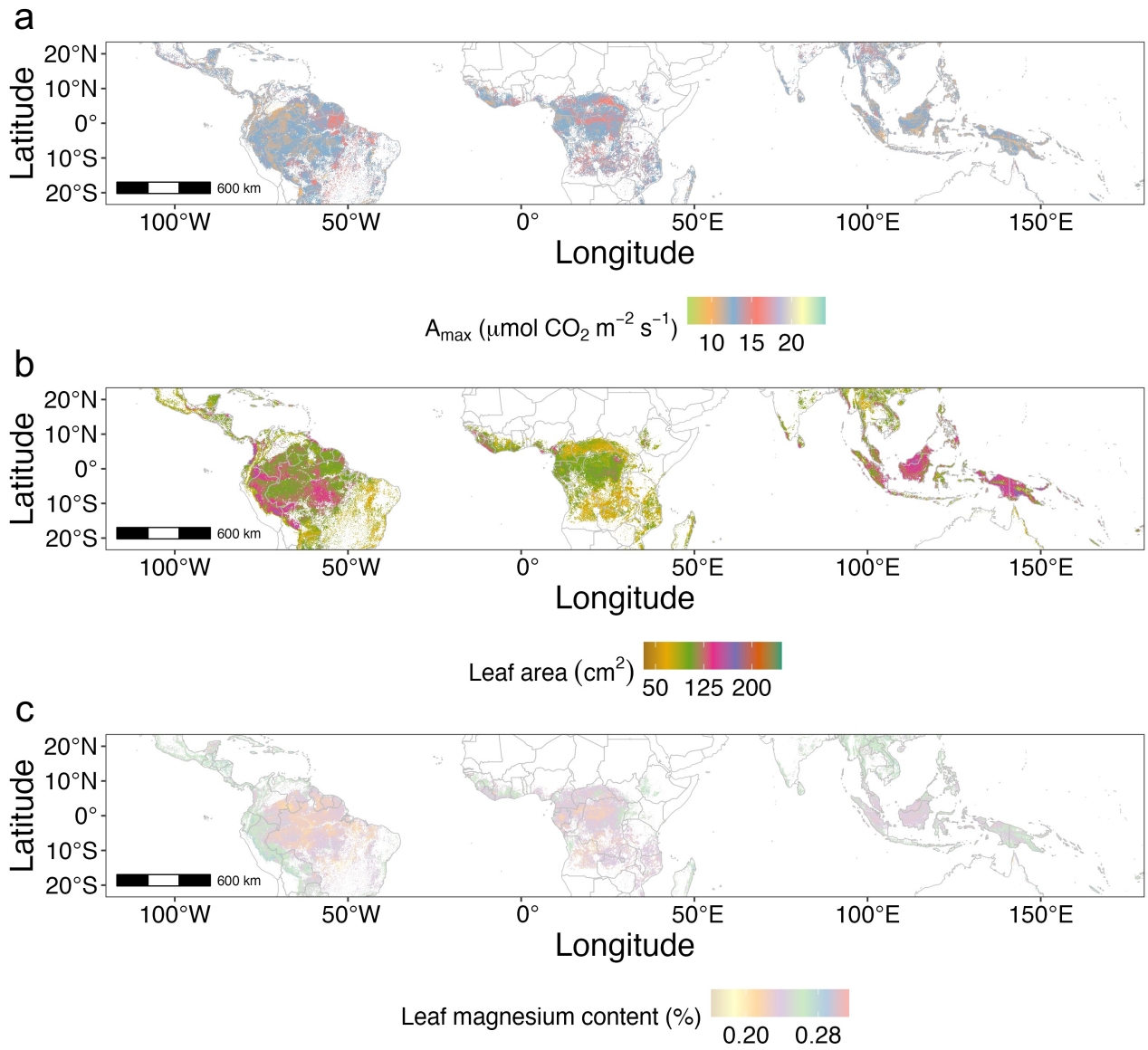

Fig. 4.2. Spatial distribution of plant functional traits. a-c, trait maps of A_{max}, leaf area, and Mg content, respectively, representing photosynthetic, morphological, and nutrient traits. All trait maps see Supplementary Figs. S4.1 to S4.12.

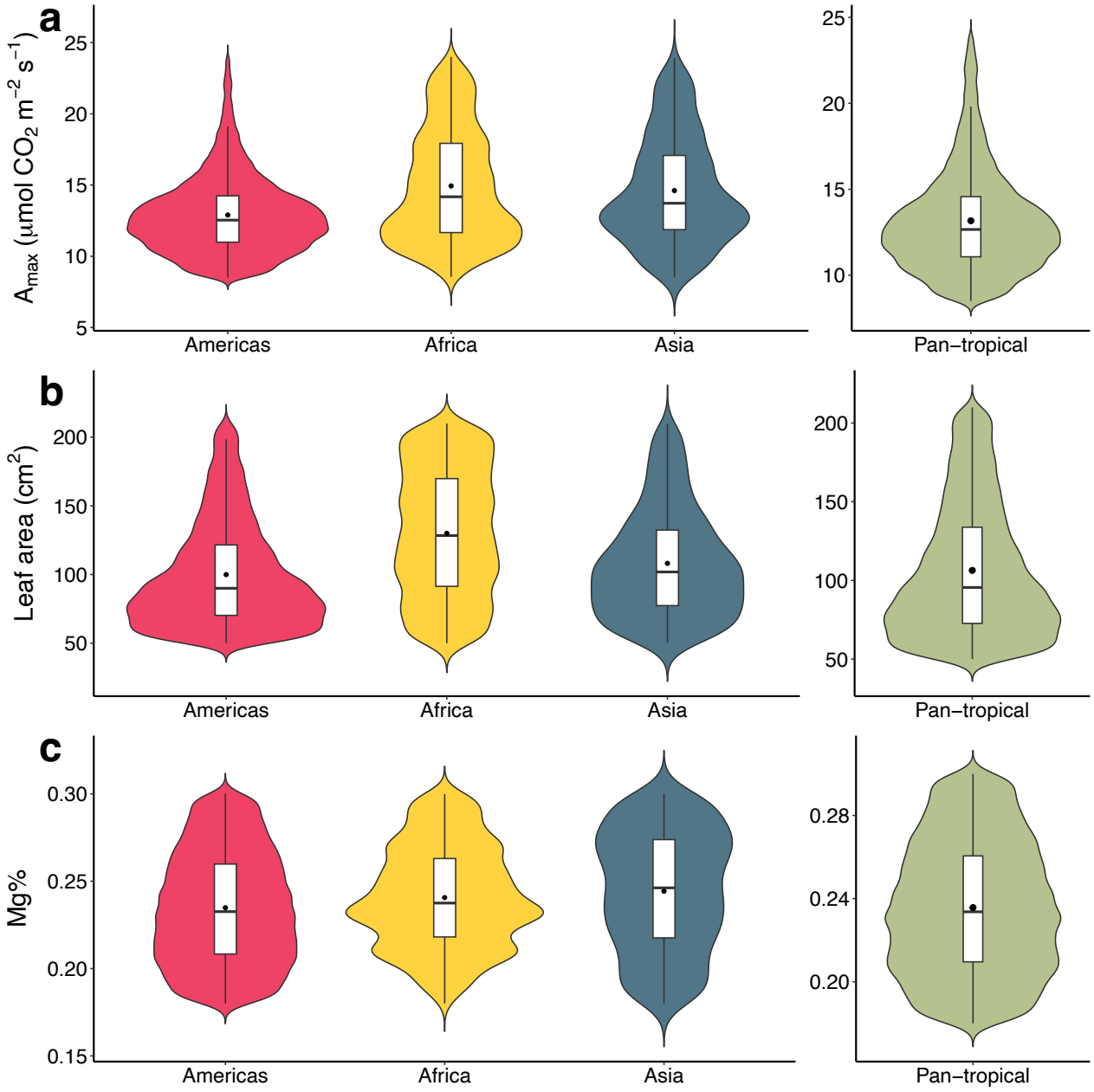

Fig. 4.3. Functional trait distributions and variations at continental and pan-tropical scales. a-c, violin plots for distributions and variations of A_{max}, leaf area, and Mg content, respectively. Inside each violin plot is a box plot demonstrating the median value, mean value, interquartile range, and 1.5 times interquartile range of a trait. The wider sections of the violin plot indicate a higher probability that multiple trait variables distribute around this given value, while the thinner sections represent a lower probability. All trait distribution and variation plots see Supplementary Figs. S4.13 to S4.24.

4.4.3. The most relevant variables to map and predict functional traits

Based on the importance measurement of every input variable from the RF regression algorithm for predicting functional traits (Supplementary Fig. S4.25), we calculated mean and median importance scores for the six input variable groups (Fig. 4.4): SAR data, spectral images, LiDAR metrics, and properties of climate, soil, and terrain (selection of specific variables and generated metrics see Methods). The results highlighted the critical role of spectral remotely sensed data in predicting all trait groups. Spectral bands and related indices consistently emerged as the top predictor for all seven morphological traits and the majority of nutrients including leaf Ca, K, N, and P contents. For the rest traits, spectral data were also important variables by ranking the second for A_{sat}, leaf C, and Mg contents and the third for A_{max}. SAR data were particularly important for both photosynthetic traits and leaf Mg content, and SAR data and terrain property (slope in this study) ranked moderately across most traits. Soil and climate variables generally ranked lower, and LiDAR metrics consistently ranked the last for most traits (all morphological traits and nutrients except for SLA and leaf N content).

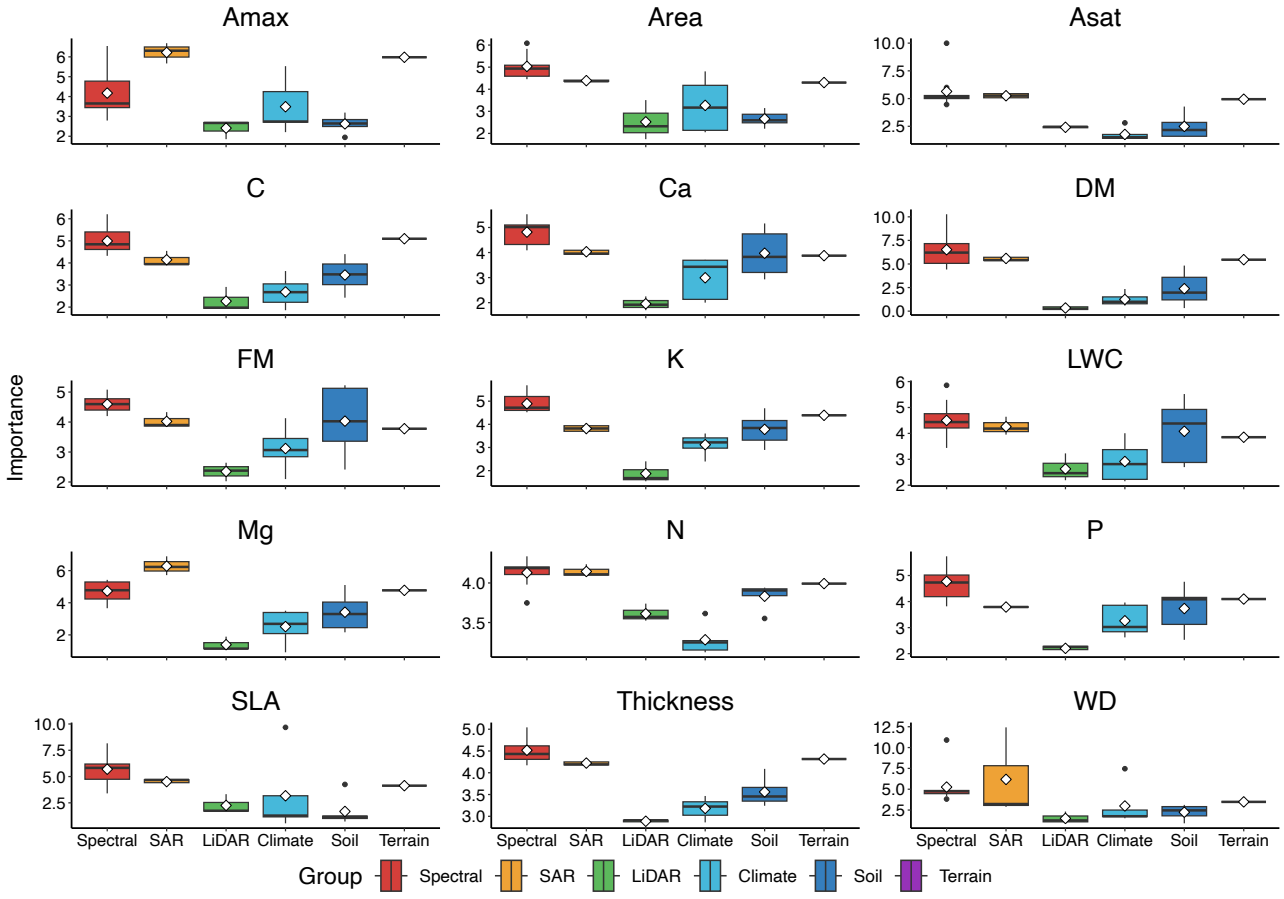

Fig. 4.4. Variable importance assessment results. In each box, the white diamond is the mean variable importance score, the three black horizontal lines from the bottom to the top denote the first (25%) quartile, median (50%), and the third (75%) quartile of a variable's importance

score. The two black vertical lines are whiskers that extend to maximum (upward) and minimum (downward) of a variable's importance score. Area: leaf area, DM: leaf dry mass, FM: leaf fresh mass, LWC: leaf water content, Thickness: leaf thickness, WD: wood density.

4.5. Discussion

We structure the discussion around three main findings of this study: the comparative performance of RF and MLP algorithms, differences in trait predictability across functional groups, and the relative contributions of multispectral, SAR, and LiDAR data, which is summarised in Table 4.3, with further details provided in the following subsections.

Table 4.3. Summary of model performance, trait predictability, and relative sensor importance in predicting functional traits across the tropics.

Key finding	Evidence	Interpretation	Implications
RF outperforms MLP	RF shows higher R^2 and lower RMSE across most traits compared to MLP	RF can handle heterogeneous ecological datasets and smaller sample sizes better than MLP	Ensemble methods are highly suitable for trait mapping
Trait predictability varies across groups	Nutrients and photosynthetic traits have higher predictive accuracy; morphological traits show weaker performance	Nutrients are more directly linked to spectral properties; morphological traits less visible to current RS data	Future hyperspectral missions and data integration are needed to improve trait predictions
Relative sensor importance	Multispectral data consistently top predictors; SAR contributes indirectly to photosynthesis; LiDAR adds value for SLA and N	Multispectral is robust across traits; SAR provides indirect info; LiDAR captures 3D canopy structure	Multi-sensor integration enhances trait mapping

4.5.1. Model performance in pan-tropical trait mapping

As far as we are aware, this study is the first to map and predict a wide range of plant functional traits by leveraging the three common types of remotely sensed data: optical, SAR, and LiDAR, combined with environmental variables including climate, soil, and terrain across the tropics using the largest known tropical trait dataset. When compared to other research efforts that used only spectral and environmental data, our integrated approach shows comparable or even improved accuracy for some traits like leaf dry mass, leaf water content, and leaf contents of Ca, Mg, N, P (Aguirre-Gutiérrez et al., 2025).

The use of the traditional machine learning algorithm RF regression provides reliable results, outperforming a deep learning method MLP algorithm. RF's ensemble approach is

particularly well-suited to heterogeneous ecological datasets because it can flexibly capture nonlinear relationships, handle missing values (Cutler et al., 2007), and reduce the risk of overfitting through bootstrapped aggregation (Breiman, 2001). In contrast, the MLP algorithm requires very large and well-balanced training datasets to generalise effectively, and although around 40000 pixels per trait represents a substantial sample size for ecological applications, it is still modest for deep learning, which typically relies on orders of magnitude more data (Vabalas et al., 2019). Furthermore, we opt for MLP as a baseline deep learning approach due to its widespread use and interpretability, while recognising that more advanced architectures (e.g. recurrent neural networks) may be better suited to capturing spatial patterns or sequential dependencies in remotely sensed data. Future research can test such algorithms, especially with the availability of larger training datasets from harmonised trait databases.

In terms of model evaluation, we apply leave-one-plot/cluster/country/continent-out cross-validation methods to assess the spatial robustness of RF algorithm, and it shows that trait predictions are highly accurate at local scales but decrease as the spatial scale of validation increased. And as model performance diminishes as the spatial scale increases, a presence of strong regional effects and spatial variation in trait-environment relationships is noticed. This indicates that while algorithms capture trait-environment relationships well within smaller regions, they may face challenges when applied across broader geographic areas, which indicates some heterogeneity in trait-environment dynamics, and previous studies have shown similar spatial autocorrelation challenges (Meyer et al., 2018).

Another limitation is the comparatively weak predictive performance for morphological traits such as SLA and leaf thickness. These traits are less directly expressed in spectral signals than biochemical traits (e.g. leaf N, P, or water content) and may therefore require higher spectral resolution (e.g. forthcoming hyperspectral sensors such as NASA's Surface Biology and Geology) or novel modelling frameworks to improve predictions. Similarly, SAR data, while not directly related to leaf-level traits, contributed indirectly to photosynthetic traits and Mg content by capturing canopy structure and moisture dynamics. This highlights the complementary value of integrating multiple sensor modalities, even when the mechanistic links to traits are indirect.

4.5.2. Trait distribution and variation patterns

The variation in functional traits observed at continental scale can largely be attributed to the influence of environmental gradients, including climate, soil properties, and terrain across regions. Photosynthetic traits, A_{max} in particular, are strongly influenced by climatic factors (Fig. 4.4). Recent studies have shown how water availability directly impacts plant photosynthetic activity, with higher A_{max} and A_{sat} values corresponding to regions with stable moisture levels (Anderegg et al., 2019; Grossiord et al., 2020). In regions where water stress is less pronounced, plants exhibit higher photosynthetic capacities (Supplementary Table S4.6) compared to more arid regions, where plants face higher water stress and soil limitations.

For most morphological traits, the observed differences likely reflect regional adaptations to terrain and soil conditions. Larger and heavier leaves observed (Supplementary Table S4.6) suggest that increased precipitation and soil fertility promote larger and heavier leaves that optimise photosynthesis (Wright et al., 2017). Conversely, smaller leaves may be an adaptation to water-limited conditions and steeper slopes, where smaller leaf surfaces reduce transpiration (Poorter et al., 2009). Furthermore, regions with nutrient-poor soils (characterised by high clay content and high pH in water) tend to exhibit higher dry mass in plant leaves, which reflects an adaptive strategy for resource conservation in challenging environments, while regions with lower leaf dry mass may have thinner leaves (with lower leaf thickness, Supplementary Table S4.6) adapted to rapid growth in more fertile or moisture-rich environments (Niinemets, 2010). Leaves with higher dry mass are denser and tougher (Meziane & Shipley, 1999), which makes them more durable and resistant to environmental stresses (Poorter et al., 2009; Wright et al., 2004), including nutrient scarcity and water limitations. These traits are associated with lower nutrient availability because thicker and tougher leaves require less frequent nutrient uptake (Onoda et al., 2008; Sophia et al., 2024) and provide greater protection against environmental damage.

Leaf nutrients, though less variable across regions, still reflect strong influences of soil and terrain properties. Regions with gentler slopes and high soil fertility demonstrate higher leaf nutrient content including Ca, K, Mg, N, and P, suggesting a direct relationship between soil nutrient availability and plant nutrient storage (Miatto et al., 2016). For instance, the relatively higher nutrient levels in Africa can be linked to richer soil quality (characterised by lower clay content), which results in plants with higher nutrient content and slower growth rates (Wigley et al., 2016). And landscapes with gentler slopes provide environments with slower water runoff, which leads to abundant water and nutrient availability (Yang et al., 2020).

4.5.3. Main drivers of distribution and variation of functional traits

The analysis of variable importance from RF regression proves the influence of remotely sensed data, particularly multispectral images with texture information of vegetation indices contributing the most to predicting traits among all the variables (Supplementary Fig. S4.25), on the spatial prediction of functional traits across tropical forests. This aligns with previous studies that have highlighted the ability of spectral data to capture subtle variations in plant physiology and biochemistry, such as chlorophyll content and leaf water status, which are closely linked to these traits (Aguirre-Gutiérrez et al., 2025; Asner et al., 2011; Serbin et al., 2015). The consistency of spectral data as a top predictor across multiple trait groups further emphasises its robustness and versatility in ecological modelling. Additionally, SAR data demonstrate significant importance for both photosynthetic traits (A_{max} and A_{sat}) and leaf Mg content, likely due to its sensitivity to structural properties and moisture of vegetation, such as canopy architecture and biomass, which influence photosynthetic capacity and nutrient distribution (Englhart et al., 2011; Inoue et al., 2014). Although LiDAR metrics are found to have the lowest importance scores for most traits, their contributions to SLA and leaf N content suggest that three-dimensional structural information, such as canopy height and complexity, may still be relevant in understanding trait variability in certain contexts (Chlus et al., 2020). These results highlight the advantages of integrating multiple remote sensing modalities to improve predictions of plant traits at large scales.

In contrast to remotely sensed data, environmental variables such as soil properties, climate conditions, and terrain features play a relatively minor role in predicting functional traits. Climate variables, including temperature and VPD, have been widely linked to species distributions and broad-scale trait patterns (Bruelheide et al., 2018; Reich, 2014); however, their lower importance in this study suggests that short-term trait variations may be more directly influenced by plant physiology rather than long-term climatic conditions. Soil properties, which are known to affect nutrient availability and plant growth, also exhibit lower predictive power, possibly due to their spatial heterogeneity, the difficulty of capturing their fine-scale variation, and failure of representing regional soil characteristics accurately using broad-scale datasets (Cramer et al., 2019). Interestingly, the terrain property (slope in this study) shows moderate importance for several traits, which indicates that topographical variations may exert localised influences on plant function through microclimatic effects or water and nutrient availability (Jucker et al., 2018). While environmental variables remain essential for understanding broader ecological patterns, their limited predictive power in this

study suggests that direct physiological and structural measurements through remote sensing are more effective for trait-level predictions.

4.5.4. Geographic representativeness, limitations, and future directions

This chapter demonstrates the feasibility of mapping functional traits at a pan-tropical scale, but it also highlights critical limitations and clear opportunities for advancing the field. The uneven geographic distribution of ground plots remains a central constraint, emphasising the need to expand trait inventories in Africa, Asia, and other underrepresented regions to improve model representativeness and global applicability. Although the application of multiple spatial validation approaches strengthen confidence in the models where data exist, they do not create independent ground observations in under-sampled regions. Consequently, predictions for underrepresented regions should be interpreted with caution, and future research should prioritise the expansion of functional trait inventories in these regions to improve the accuracy, representativeness, and generality of global-scale functional trait models.

Looking ahead, several developments are expected to transform global functional trait ecology. Forthcoming hyperspectral missions, such as NASA's Surface Biology and Geology and ESA's CHIME, will provide unprecedented spectral and spatial resolution for resolving plant traits across diverse forest ecosystems. At the same time, the ongoing harmonisation of trait datasets (e.g. TRY and ForestGEO) will improve the consistency and scope of trait information available for model training and validation. Methodological advances, particularly in artificial intelligence, offer further potential: deep learning architectures, transfer learning, and multimodal data fusion approaches can increase model scalability, flexibility, and predictive power across biomes.

By linking the present findings to these emerging opportunities, this study provides a foundation for next-generation global functional trait mapping. Future work should prioritise the integration of forthcoming hyperspectral data streams, harmonised trait inventories, and AI-based modelling frameworks to develop more accurate, representative, and generalisable models of forest functional ecology.

Key lessons from **Chapter 4**

- Methodological: Combining large-scale remote sensing with functional trait data demonstrates the feasibility of pan-tropical trait mapping, while highlighting the importance of validation strategies and data representativeness.
- Ecological: Trait-based approaches reveal the spatial heterogeneity of functional strategies across tropical forests, with implications for resilience to environmental change.
- Practical: Expanding trait inventories, harnessing new hyperspectral missions, and adopting advanced AI tools are critical next steps toward operational global functional ecology.

4.6. Methods

4.6.1. Field trait measurements

In this study, we collected 15 functional traits (Table 4.2) from 1814 vegetation plots distributed in 18 tropical countries: Australia, Belize, Bolivia, Brazil, Colombia, Cote d'Ivoire, Ecuador, French Guiana, Gabon, Ghana, Guyana, India, Malaysia, Mexico, Peru, Rwanda, Suriname, and Venezuela, which cover all tropical continents, from 2013 to 2021. The trait measurements are affiliated with the Global Ecosystems Monitoring (GEM) network (http://gem.tropicalforests.ox.ac.uk/) (Malhi et al., 2021), the Monitoreo Nacional Forestal network (MONAFOR, http://fcfposgrado.ujed.mx/monafor/inicio/), and associated contributors to ForestPlots network (https://forestplots.net/) (Lopez-Gonzalez et al., 2011). Specifically, we used leaf samples for trait measurements including photosynthesis (maximum photosynthetic rate: A_{max}, and light-saturated photosynthetic rate: A_{sat}), morphology (leaf dry mass, fresh mass, area, water content, specific leaf area: SLA, thickness, and wood density), and nutrients (leaf contents of carbon: C, calcium: Ca, potassium: K, magnesium: Mg, nitrogen: N, and phosphorus: P) (see Table 4.1 for detailed descriptions for these traits).

4.6.2. Pixel-level community-weighted mean of traits

We used community-weighted mean (CWM) of each trait at pixel level (10×10 m, matching the highest spatial resolution of all input remotely sensed data) from Aguirre-Gutiérrez et al. (2025). In summary, we derived the CWM trait values for each pixel at 10 m that overlapped with a plot. This involved geolocating the plot and mapping the distribution of individual trees within it. In cases where tree crowns were not mapped, we estimated crown areas using regional allometric equations to generate circular crown polygons. For each pixel, we then calculated

the trait CWM, weighting by the horizontal area of individual tree crowns. Only pixels with at least 70% basal area coverage containing trait values at species or genus level were included in the final CWM calculations.

4.6.3. Remotely sensed data

4.6.3.1. Sentinel-1 SAR images

Sentinel-1 provides high-resolution (10 m) C-band SAR imagery regardless of weather conditions, day or night. With a 12-day repeat cycle for each satellite, the two-satellite Sentinel-1 constellation provides a six-day repeat (Torres et al., 2012). Sentinel-1's ability to penetrate clouds and its frequent revisit times make it an indispensable tool for environmental monitoring and traits mapping across humid tropical regions. Sentinel-1's suitability for vegetation monitoring and mapping functional traits relies on its dual-polarisation capabilities, specifically the VV (vertical transmit, vertical receive) and VH (vertical transmit, horizontal receive) polarisation channels. We leveraged the freely available Google Earth Engine (GEE, https://code.earthengine.google.com/) cloud-based platform (Gorelick et al., 2017) to load Sentinel-1 images with dual-polarisation mode (VV-VH) from 2014 to 2021. Sentinel-1 ground range detected imagery in GEE is provided as radiometrically calibrated sigma-nought (σ^0) backscatter in decibels (dB), with preprocessing including orbit correction, radiometric calibration, border noise removal, and thermal noise removal applied by default. To account for local incidence angle and topographic effects, we applied radiometric terrain correction by converting σ^0 to gamma-nought (γ^0) in natural (linear) units using the standard calibration formula and the 30-m Shuttle Radar Topography Mission (SRTM) (Farr et al., 2007) digital elevation model (DEM). We also adopted a refined Lee filter (Lee, 1981) with a 7×7 kernel to eliminate the adverse effect of speckle noises in SAR data and to obtain smoother images.

$$\sigma^0_{linear} = 10^{\frac{\sigma^0_{dB}}{10}} \quad (1)$$

$$\gamma^0 = \frac{\sigma^0_{linear}}{\cos(\theta)} \quad (2)$$

where σ^0_{linear} and σ^0_{dB} are SAR image's backscattering coefficients in power and dB units, respectively, γ^0 is the radiometrically terrain-corrected backscatter coefficient, and θ is the local incidence angle derived using the SRTM DEM.

The VV and VH polarimetric values in power units enable the generation of SAR-derived metrics that are valuable for vegetation analysis. To enhance the mapping and prediction of functional traits, we calculated two key indices: the Radar Vegetation Index (Nasirzadehdizaji et al., 2019) and the Dual Polarisation SAR Vegetation Index (Periasamy, 2018). These indices leverage the unique sensitivity of SAR data to vegetation structure and biomass, which potentially can strengthen our understanding of traits. Details on producing these metrics see **Section 4.8.3. SAR metrics calculation**.

4.6.3.2. Sentinel-2 multispectral images

Sentinel-2 provides high spectral (13 bands spanning the visible, near-infrared [NIR], and shortwave infrared [SWIR] regions of the electromagnetic spectrum), spatial resolution (10 m for visible and NIR bands, 20 m for red-edge and SWIR bands, and 60 m for bands primarily used for atmospheric correction and cloud detection), and temporal (five-day revisit time at the equator) resolutions imagery for a wide range of environmental monitoring applications. The mission consists of two satellites as well, which operate together to obtain images with a revisit time of five days at the equator (Drusch et al., 2012). The multispectral instrument on Sentinel-2 includes specific bands designed for vegetation monitoring, such as the red-edge bands and NIR band that are crucial for assessing functional traits because they are sensitive to variations in chlorophyll content and vegetation structure, which is directly related to plant photosynthetic activity and leaf structure (Clevers & Gitelson, 2013, p. 3). Similarly, we loaded Sentinel-2 images with cloud coverage lower than 40% from 2015 to 2021 across the tropics on GEE, masked clouds and cloud shadows, and derived several vegetation indices including modified chlorophyll absorption in reflectance index (MCARI (Daughtry et al., 2000)), modified soil adjusted vegetation index 2 (MSAVI2 (Qi et al., 1994)), normalised difference red-edge index (NDRE (Fitzgerald et al., 2010)), and their corresponding texture information (correlation and entropy) from a 9×9 grey level co-occurrence matrix. Details on producing these metrics see Supplementary Tables S4.8 and S4.9.

4.6.3.3. GEDI LiDAR data

GEDI provides high-resolution (25 m) LiDAR data specifically designed for measuring the three-dimensional structure of Earth's forests, it captures detailed vertical profiles of vegetation, enabling the assessment of forest structure and its dynamics at a global scale. The

LiDAR system on GEDI transmits laser pulses to the Earth's surface and measures the time it takes for the pulses to return, thereby generating precise information on vegetation height, density, and structure. In this study, several key metrics derived from GEDI LiDAR data were utilised to map and predict functional traits. One of the primary metrics is canopy height, specifically the 98th percentile relative height (RH98), which represents the height below which 98% of the LiDAR returns are captured. Canopy cover, another essential metric, measures the proportion of ground covered by vegetation when viewed from above. Foliage height diversity, on the other hand, is a metric that captures the complexity and vertical stratification of the canopy, and it is calculated based on the distribution of foliage at different heights and is indicative of habitat diversity and ecological complexity within the forest (Clawges et al., 2008). Plant area volume density (PAVD) is another key metric that quantifies the vertical distribution of plant materials like leaves and branches within a forest canopy (Dhargay et al., 2022).

4.6.4. Environmental variables

We integrated a set of environmental variables from multiple sources to enhance the understanding of functional traits. Climatic data (Table 4.4, Supplementary Figs. S4.26 to S4.30), including soil moisture, downward surface shortwave radiation (SRAD), maximum temperature, vapour pressure deficit (VPD), and maximum climatological water deficit (MCWD, calculated as in Malhi et al. (2009)), were sourced from TerraClimate (Abatzoglou et al., 2018) (https://www.climatologylab.org/terraclimate.html), a dataset ideal for analysing monthly water availability and stress conditions in vegetation at ~4 km. A terrain indicator, specifically slope (30 m, Supplementary Fig. S31), was derived from the SRTM DEM (Farr et al., 2007) to assess the influence of topography on vegetation distribution. Additionally, soil characteristics (Supplementary Figs. S4.32 to S4.35), including physical properties (clay and sand contents) and chemical properties (cation exchange capacity (CEC), soil organic carbon (SOC), and soil pH in water (pHH_2O)), were obtained from SoilGrids (Hengl et al., 2017) (https://soilgrids.org/) at a spatial resolution of 250 m, which were critical for understanding soil fertility, texture, and their effects on plant health and productivity.

Table 4.4. Summary of environmental variables used in this study.

Category	Variables	Resolution	Source

Climate	Soil moisture, SRAD, maximum temperature, VPD, MCWD	~4 km	TerraClimate (Abatzoglou et al., 2018)
Topography	Slope	30 m	SRTM (Farr et al., 2007)
Soils	Sand, clay, SOC, CEC, pHH_2O	250 m	SoilGrids (Hengl et al., 2017)

4.6.5. Multi-scales mapping and prediction of plant functional traits

To map and predict functional traits across the tropics, we firstly calculated pairwise correlation between variables mentioned above (Supplementary Fig. S4.36), and we only kept variables with correlation $r<|0.80|$. Eventually we maintained variables below: VH, radar vegetation index, and dual polarisation SAR vegetation index from Sentinel-1, blue, NIR, SWIR 1, MCARI, MSAVI2, NDRE, correlation of MCARI and MSAVI2, and entropy of NDRE from Sentinel-2, canopy cover, PAVD, and RH98 from GEDI, soil moisture, SRAD, maximum temperature, VPD, and MCWD from TerraClimate, slope from SRTM, sand and clay contents, SOC, CEC, and pHH_2O from SoilGrids.

We compared the performance of a machine learning algorithm and a deep learning algorithm: Random forests (RF) regression and Multilayer Perceptron (MLP) regression. Both algorithms were trained using comprehensive datasets that included remotely sensed data and environmental variables. The input data were split into training (80%) and validation (20%) datasets to ensure the algorithms were trained on a representative sample and evaluated on a separate dataset. The predictive performance of both algorithms was evaluated using the coefficient of determination (R^2) and root mean square error (RMSE) to determine their accuracies.

$$R^2=1-\frac{\sum_{i=1}^{n}(y_i-\hat{y}_i)^2}{\sum_{i=1}^{n}(y_i-\bar{y})^2} \quad (3)$$

$$RMSE=\sqrt{\frac{1}{n}\sum_{i=1}^{n}(y_i-\hat{y}_i)^2} \quad (4)$$

where n is the total number of observations, y_i, $\hat{y}_i$, and $\bar{y}$ denote the observed value, predicted value for the ith observation, and the mean of the observed values, respectively.

4.6.5.1. Random forests regression

The RF regression algorithm was trained on the 80% training dataset using a 10-fold cross-validation approach to ensure robustness and avoid overfitting (Breiman, 2001). In 10-fold cross-validation, the training data were divided into 10 equal parts. The model was trained on 9 of these parts and validated on the remaining part. This process was repeated 10 times, with each part used once as the validation fold. The performance was then averaged across all 10 iterations. To tune the two key hyperparameters, the number of trees in the forest was tested from 50 to 1000 with a step size of 50 to identify the optimal complexity. Additionally, the number of variables considered at each split was tested across a range from 1 to 26 (the total number of input features), with a step size of 1 (see Supplementary Table S4.10 for detailed hyperparameter values for each trait). The model's performance was validated on the 20% validation dataset using R^2 and RMSE. Furthermore, the importance of each predictor variable was calculated to identify the most influential factors driving the distribution of traits.

4.6.5.2. Multilayer Perceptron regression

We implemented a fully connected feed-forward MLP to capture nonlinear trait-environment relationships. Input data were structured into spatial patches, enabling the model to learn both local and global patterns within the data (Zhang et al., 2018). Training was performed with the Adam optimiser to minimise mean-squared-error loss through standard forward and back-propagation. Hyperparameters, namely the number of hidden units, dropout rate, and learning rate, were tuned via random search. For each functional trait, the best model was selected based on R^2 and RMSE, in line with the criteria used for the Random forests model.

4.6.5.3. Cross-validation methods

Spatial autocorrelation in input data was sometimes ignored and thus resulted in overoptimistic evaluation of models' predictive power (Ploton et al., 2020). Taking spatial autocorrelation into consideration provided additional assessment of spatial validation and ensured that models' performance could generalise across different geographical scales, from local plots to entire continents, thus verified the models' robustness across multiple spatial hierarchies. In the spatial autocorrelation analysis, we used empirical variogram analysis to determine the distance threshold by examining how trait similarity decreased with increasing distance between trait record points. This provided a clear indication of spatial dependency and enabled the definition of a distance threshold, marking where spatial autocorrelation became insignificant. Following

this, we applied the Moran's *I* test to quantify spatial autocorrelation, then grouped trait observations into clusters based on their proximity (within the defined distance threshold). To mitigate the effects of spatial autocorrelation during model evaluation, we employed leave-one-cluster-out cross-validation, where clusters of data were systematically omitted during model training and testing. In addition to leave-one-cluster-out, we also performed leave-one-plot-, leave-one-country-, and leave-one-continent-out cross-validations. For each iteration of these cross-validation methods, data from one specific plot, cluster, country, or continent was excluded from model training and used solely for validation.

4.6.6. Statistical analysis

To assess continental variation in plant functional traits, we conducted a one-way analysis of variance (ANOVA), followed by post-hoc Tukey's honestly significant difference (HSD) test. The ANOVA was used to determine whether there were statistically significant differences in trait CWM values across continents, and we treated continent as the independent categorical variable and each plant functional trait as the dependent variable. To further explore pairwise differences between continents, Tukey's HSD test was applied as a post-hoc analysis. This test controls for Type I error rates by adjusting *P*-values for multiple comparisons and ensured robust identification of specific continental pairs that significantly differ in trait CWM values. Together, these statistical methods provided a comprehensive understanding of how plant functional traits vary across continents.

4.7. References

Abatzoglou, J. T., Dobrowski, S. Z., Parks, S. A., & Hegewisch, K. C. (2018). TerraClimate, a high-resolution global dataset of monthly climate and climatic water balance from 1958–2015. *Scientific Data*, *5*(1), 170191. https://doi.org/10.1038/sdata.2017.191

Abelleira Martínez, O. J., Fremier, A. K., Günter, S., Ramos Bendaña, Z., Vierling, L., Galbraith, S. M., Bosque-Pérez, N. A., & Ordoñez, J. C. (2016). Scaling up functional traits for ecosystem services with remote sensing: Concepts and methods. *Ecology and Evolution*, *6*(13), 4359–4371. https://doi.org/10.1002/ece3.2201

Aguirre-Gutiérrez, J., Rifai, S. W., Deng, X., ter Steege, H., Thomson, E., Corral-Rivas, J. J., Guimaraes, A. F., Muller, S., Klipel, J., Fauset, S., Resende, A. F., Wallin, G., Joly, C. A., Abernethy, K., Adu-Bredu, S., Alexandre Silva, C., de Oliveira, E. A., Almeida, D. R. A., Alvarez-Davila, E., … Malhi, Y. (2025). Canopy functional trait variation across Earth's tropical forests. *Nature*, *641*(8061), 129–136. https://doi.org/10.1038/s41586-025-08663-2

Ali, A. M., Darvishzadeh, R., & Skidmore, A. K. (2017). Retrieval of Specific Leaf Area From Landsat-8 Surface Reflectance Data Using Statistical and Physical Models. *IEEE Journal of Selected Topics in Applied Earth Observations and Remote Sensing*, *10*(8), 3529–3536. IEEE Journal of Selected Topics in Applied Earth Observations and Remote Sensing. https://doi.org/10.1109/JSTARS.2017.2690623

Anderegg, W. R. L., Trugman, A. T., Bowling, D. R., Salvucci, G., & Tuttle, S. E. (2019). Plant functional traits and climate influence drought intensification and land–atmosphere feedbacks. *Proceedings of the National Academy of Sciences*, *116*(28), 14071–14076. https://doi.org/10.1073/pnas.1904747116

Asner, G. P. (2001). Cloud cover in Landsat observations of the Brazilian Amazon. *International Journal of Remote Sensing*, *22*(18), 3855–3862. https://doi.org/10.1080/01431160010006926

Asner, G. P., Martin, R. E., Knapp, D. E., Tupayachi, R., Anderson, C. B., Sinca, F., Vaughn, N. R., & Llactayo, W. (2017). Airborne laser-guided imaging spectroscopy to map forest trait diversity and guide conservation. *Science*, *355*(6323), 385–389. https://doi.org/10.1126/science.aaj1987

Asner, G. P., Martin, R. E., Knapp, D. E., Tupayachi, R., Anderson, C., Carranza, L., Martinez, P., Houcheime, M., Sinca, F., & Weiss, P. (2011). Spectroscopy of canopy chemicals in humid tropical forests. *Remote Sensing of Environment*, *115*(12), 3587–3598. https://doi.org/10.1016/j.rse.2011.08.020

Bae, S., Levick, S. R., Heidrich, L., Magdon, P., Leutner, B. F., Wöllauer, S., Serebryanyk, A., Nauss, T., Krzystek, P., Gossner, M. M., Schall, P., Heibl, C., Bässler, C., Doerfler, I., Schulze, E.-D., Krah, F.-S., Culmsee, H., Jung, K., Heurich, M., … Müller, J. (2019). Radar vision in the mapping of forest biodiversity from space. *Nature Communications*, *10*(1), 4757. https://doi.org/10.1038/s41467-019-12737-x

Beech, E., Rivers, M., Oldfield, S., & Smith, P. P. (2017). GlobalTreeSearch: The first complete global database of tree species and country distributions. *Journal of Sustainable Forestry*, *36*(5), 454–489. https://doi.org/10.1080/10549811.2017.1310049

Bouvet, A., Mermoz, S., Le Toan, T., Villard, L., Mathieu, R., Naidoo, L., & Asner, G. P. (2018). An above-ground biomass map of African savannahs and woodlands at 25 m resolution derived from ALOS PALSAR. *Remote Sensing of Environment*, *206*, 156–173. https://doi.org/10.1016/j.rse.2017.12.030

Breiman, L. (2001). Random forests. *Machine Learning*, *45*, 5–32.

Bruelheide, H., Dengler, J., Purschke, O., Lenoir, J., Jiménez-Alfaro, B., Hennekens, S. M., Botta-Dukát, Z., Chytrý, M., Field, R., Jansen, F., Kattge, J., Pillar, V. D., Schrodt, F., Mahecha, M. D., Peet, R. K., Sandel, B., van Bodegom, P., Altman, J., Alvarez-Dávila, E., … Jandt, U. (2018). Global trait–environment relationships of plant communities. *Nature Ecology & Evolution*, *2*(12), 1906–1917. https://doi.org/10.1038/s41559-018-0699-8

Brussel, T., & Brewer, S. C. (2021). Functional Paleoecology and the Pollen-Plant Functional Trait Linkage. *Frontiers in Ecology and Evolution*, *8*. https://doi.org/10.3389/fevo.2020.564609

Byrd, R. C., Moss, J. M., Priedhorsky, W. C., Pura, C. A., Richter, G. W., Saeger, K. J., Scarlett, W. R., Scott, S. C., & Wagner, R. L. (2005). Nuclear detection to prevent or defeat clandestine nuclear attack. *IEEE Sensors Journal*, *5*(4), 593–609. IEEE Sensors Journal. https://doi.org/10.1109/JSEN.2005.846376

Chen, J., Shao, Z., Deng, X., Huang, X., & Dang, C. (2023). Vegetation as the catalyst for water circulation on global terrestrial ecosystem. *Science of The Total Environment*, *895*, 165071. https://doi.org/10.1016/j.scitotenv.2023.165071

Chlus, A., Kruger, E. L., & Townsend, P. A. (2020). Mapping three-dimensional variation in leaf mass per area with imaging spectroscopy and lidar in a temperate broadleaf forest. *Remote Sensing of Environment*, *250*, 112043. https://doi.org/10.1016/j.rse.2020.112043

Clawges, R., Vierling, K., Vierling, L., & Rowell, E. (2008). The use of airborne lidar to assess avian species diversity, density, and occurrence in a pine/aspen forest. *Remote Sensing of Environment*, *112*(5), 2064–2073. https://doi.org/10.1016/j.rse.2007.08.023

Clevers, J. G., & Gitelson, A. A. (2013). Remote estimation of crop and grass chlorophyll and nitrogen content using red-edge bands on Sentinel-2 and-3. *International Journal of Applied Earth Observation and Geoinformation*, *23*, 344–351.

Cooper, D. L. M., Lewis, S. L., Sullivan, M. J. P., Prado, P. I., ter Steege, H., Barbier, N., Slik, F., Sonké, B., Ewango, C. E. N., Adu-Bredu, S., Affum-Baffoe, K., de Aguiar, D. P. P., Ahuite Reategui, M. A., Aiba, S.-I., Albuquerque, B. W., de Almeida Matos, F. D., Alonso, A., Amani, C. A., do Amaral, D. D., … Zent, S. (2024). Consistent patterns of common species across tropical tree communities. *Nature*, *625*(7996), 728–734. https://doi.org/10.1038/s41586-023-06820-z

Cramer, M. D., Wootton, L. M., van Mazijk, R., & Verboom, G. A. (2019). New regionally modelled soil layers improve prediction of vegetation type relative to that based on global soil models. *Diversity and Distributions*, *25*(11), 1736–1750. https://doi.org/10.1111/ddi.12973

Cuni-Sanchez, A., Sullivan, M. J. P., Platts, P. J., Lewis, S. L., Marchant, R., Imani, G., Hubau, W., Abiem, I., Adhikari, H., Albrecht, T., Altman, J., Amani, C., Aneseyee, A. B., Avitabile, V., Banin, L., Batumike, R., Bauters, M., Beeckman, H., Begne, S. K., … Zibera, E. (2021). High aboveground carbon stock of African tropical montane forests. *Nature*, *596*(7873), 536–542. https://doi.org/10.1038/s41586-021-03728-4

Cutler, D. R., Edwards Jr., T. C., Beard, K. H., Cutler, A., Hess, K. T., Gibson, J., & Lawler, J. J. (2007). Random Forests for Classification in Ecology. *Ecology*, *88*(11), 2783–2792. https://doi.org/10.1890/07-0539.1

Daughtry, C. S. T., Walthall, C. L., Kim, M. S., de Colstoun, E. B., & McMurtrey, J. E. (2000). Estimating Corn Leaf Chlorophyll Concentration from Leaf and Canopy Reflectance. *Remote Sensing of Environment*, *74*(2), 229–239. https://doi.org/10.1016/S0034-4257(00)00113-9

Dhargay, S., Lyell, C. S., Brown, T. P., Inbar, A., Sheridan, G. J., & Lane, P. N. J. (2022). Performance of GEDI Space-Borne LiDAR for Quantifying Structural Variation in the Temperate Forests of South-Eastern Australia. *Remote Sensing*, *14*(15), Article 15. https://doi.org/10.3390/rs14153615

Díaz, S., Kattge, J., Cornelissen, J. H. C., Wright, I. J., Lavorel, S., Dray, S., Reu, B., Kleyer, M., Wirth, C., Colin Prentice, I., Garnier, E., Bönisch, G., Westoby, M., Poorter, H., Reich, P. B., Moles, A. T., Dickie, J., Gillison, A. N., Zanne, A. E., … Gorné, L. D. (2016). The global spectrum of plant form and function. *Nature*, *529*(7585), 167–171. https://doi.org/10.1038/nature16489

Domingos, P. (2012). A few useful things to know about machine learning. *Commun. ACM*, *55*(10), 78–87. https://doi.org/10.1145/2347736.2347755

dos Santos, E. P., Da Silva, D. D., & do Amaral, C. H. (2021). Vegetation cover monitoring in tropical regions using SAR-C dual-polarization index: Seasonal and spatial influences. *International Journal of Remote Sensing*, *42*(19), 7581–7609. https://doi.org/10.1080/01431161.2021.1959955

Drusch, M., Del Bello, U., Carlier, S., Colin, O., Fernandez, V., Gascon, F., Hoersch, B., Isola, C., Laberinti, P., & Martimort, P. (2012). Sentinel-2: ESA's optical high-resolution mission for GMES operational services. *Remote Sensing of Environment*, *120*, 25–36.

Englhart, S., Keuck, V., & Siegert, F. (2011). Aboveground biomass retrieval in tropical forests—The potential of combined X- and L-band SAR data use. *Remote Sensing of Environment*, *115*(5), 1260–1271. https://doi.org/10.1016/j.rse.2011.01.008

Farr, T. G., Rosen, P. A., Caro, E., Crippen, R., Duren, R., Hensley, S., Kobrick, M., Paller, M., Rodriguez, E., & Roth, L. (2007). The shuttle radar topography mission. *Reviews of Geophysics*, *45*(2).

Fitzgerald, G., Rodriguez, D., & O'Leary, G. (2010). Measuring and predicting canopy nitrogen nutrition in wheat using a spectral index—The canopy chlorophyll content index (CCCI). *Field Crops Research*, *116*(3), 318–324. https://doi.org/10.1016/j.fcr.2010.01.010

França, F. M., Benkwitt, C. E., Peralta, G., Robinson, J. P. W., Graham, N. A. J., Tylianakis, J. M., Berenguer, E., Lees, A. C., Ferreira, J., Louzada, J., & Barlow, J. (2020). Climatic and local stressor interactions threaten tropical forests and coral reefs. *Philosophical Transactions of the Royal Society B: Biological Sciences*, *375*(1794), 20190116. https://doi.org/10.1098/rstb.2019.0116

Gorelick, N., Hancher, M., Dixon, M., Ilyushchenko, S., Thau, D., & Moore, R. (2017). Google Earth Engine: Planetary-scale geospatial analysis for everyone. *Remote Sensing of Environment*, *202*, 18–27. https://doi.org/10.1016/j.rse.2017.06.031

Greaves, H. E., Vierling, L. A., Eitel, J. U. H., Boelman, N. T., Magney, T. S., Prager, C. M., & Griffin, K. L. (2015). Estimating aboveground biomass and leaf area of low-stature Arctic shrubs with terrestrial LiDAR. *Remote Sensing of Environment*, *164*, 26–35. https://doi.org/10.1016/j.rse.2015.02.023

Grossiord, C., Buckley, T. N., Cernusak, L. A., Novick, K. A., Poulter, B., Siegwolf, R. T. W., Sperry, J. S., & McDowell, N. G. (2020). Plant responses to rising vapor pressure deficit. *New Phytologist*, *226*(6), 1550–1566. https://doi.org/10.1111/nph.16485

Gurdak, D. J., Aragão, L. E. O. C., Rozas-Dávila, A., Huasco, W. H., Cabrera, K. G., Doughty, C. E., Farfan-Rios, W., Silva-Espejo, J. E., Metcalfe, D. B., Silman, M. R., & Malhi, Y. (2014). Assessing above-ground woody debris dynamics along a gradient of elevation in Amazonian cloud forests in Peru: Balancing above-ground inputs and respiration outputs. *Plant Ecology & Diversity*, *7*(1–2), 143–160. https://doi.org/10.1080/17550874.2013.818073

Hauser, L. T., Féret, J.-B., An Binh, N., Van Der Windt, N., Sil, Â. F., Timmermans, J., Soudzilovskaia, N. A., & Van Bodegom, P. M. (2021). Towards scalable estimation of plant functional diversity from Sentinel-2: In-situ validation in a heterogeneous (semi-)natural landscape. *Remote Sensing of Environment*, *262*, 112505. https://doi.org/10.1016/j.rse.2021.112505

Helfenstein, I. S., Schneider, F. D., Schaepman, M. E., & Morsdorf, F. (2022). Assessing biodiversity from space: Impact of spatial and spectral resolution on trait-based functional diversity. *Remote Sensing of Environment*, *275*, 113024. https://doi.org/10.1016/j.rse.2022.113024

Hengl, T., Mendes de Jesus, J., Heuvelink, G. B., Ruiperez Gonzalez, M., Kilibarda, M., Blagotić, A., Shangguan, W., Wright, M. N., Geng, X., & Bauer-Marschallinger, B. (2017). SoilGrids250m: Global gridded soil information based on machine learning. *PLoS One*, *12*(2), e0169748.

Inoue, Y., Sakaiya, E., & Wang, C. (2014). Capability of C-band backscattering coefficients from high-resolution satellite SAR sensors to assess biophysical variables in paddy rice. *Remote Sensing of Environment*, *140*, 257–266. https://doi.org/10.1016/j.rse.2013.09.001

Jetz, W., Cavender-Bares, J., Pavlick, R., Schimel, D., Davis, F. W., Asner, G. P., Guralnick, R., Kattge, J., Latimer, A. M., Moorcroft, P., Schaepman, M. E., Schildhauer, M. P., Schneider, F. D., Schrodt, F., Stahl, U., & Ustin, S. L. (2016). Monitoring plant functional diversity from space. *Nature Plants*, *2*(3), 16024. https://doi.org/10.1038/nplants.2016.24

Jucker, T., Bongalov, B., Burslem, D. F. R. P., Nilus, R., Dalponte, M., Lewis, S. L., Phillips, O. L., Qie, L., & Coomes, D. A. (2018). Topography shapes the structure, composition

and function of tropical forest landscapes. *Ecology Letters*, *21*(7), 989–1000. https://doi.org/10.1111/ele.12964

Lavorel, S., & Garnier, E. (2002). Predicting changes in community composition and ecosystem functioning from plant traits: Revisiting the Holy Grail. *Functional Ecology*, *16*(5), 545–556. https://doi.org/10.1046/j.1365-2435.2002.00664.x

Lechner, A. M., Foody, G. M., & Boyd, D. S. (2020). Applications in Remote Sensing to Forest Ecology and Management. *One Earth*, *2*(5), 405–412. https://doi.org/10.1016/j.oneear.2020.05.001

Lee, J.-S. (1981). Speckle analysis and smoothing of synthetic aperture radar images. *Computer Graphics and Image Processing*, *17*(1), 24–32. https://doi.org/10.1016/S0146-664X(81)80005-6

Lopez-Gonzalez, G., Lewis, S. L., Burkitt, M., & Phillips, O. L. (2011). ForestPlots.net: A web application and research tool to manage and analyse tropical forest plot data. *Journal of Vegetation Science*, *22*(4), 610–613. https://doi.org/10.1111/j.1654-1103.2011.01312.x

Malhi, Y., Aragão, L. E. O. C., Galbraith, D., Huntingford, C., Fisher, R., Zelazowski, P., Sitch, S., McSweeney, C., & Meir, P. (2009). Exploring the likelihood and mechanism of a climate-change-induced dieback of the Amazon rainforest. *Proceedings of the National Academy of Sciences*, *106*(49), 20610–20615. https://doi.org/10.1073/pnas.0804619106

Malhi, Y., Girardin, C., Metcalfe, D. B., Doughty, C. E., Aragão, L. E. O. C., Rifai, S. W., Oliveras, I., Shenkin, A., Aguirre-Gutiérrez, J., Dahlsjö, C. A. L., Riutta, T., Berenguer, E., Moore, S., Huasco, W. H., Salinas, N., da Costa, A. C. L., Bentley, L. P., Adu-Bredu, S., Marthews, T. R., … Phillips, O. L. (2021). The Global Ecosystems Monitoring

network: Monitoring ecosystem productivity and carbon cycling across the tropics. *Biological Conservation*, *253*, 108889. https://doi.org/10.1016/j.biocon.2020.108889

Malhi, Y., Riutta, T., Wearn, O. R., Deere, N. J., Mitchell, S. L., Bernard, H., Majalap, N., Nilus, R., Davies, Z. G., Ewers, R. M., & Struebig, M. J. (2022). Logged tropical forests have amplified and diverse ecosystem energetics. *Nature*, *612*(7941), 707–713. https://doi.org/10.1038/s41586-022-05523-1

Martone, M., Rizzoli, P., Wecklich, C., González, C., Bueso-Bello, J.-L., Valdo, P., Schulze, D., Zink, M., Krieger, G., & Moreira, A. (2018). The global forest/non-forest map from TanDEM-X interferometric SAR data. *Remote Sensing of Environment*, *205*, 352–373. https://doi.org/10.1016/j.rse.2017.12.002

Mason, D. C., Giustarini, L., Garcia-Pintado, J., & Cloke, H. L. (2014). Detection of flooded urban areas in high resolution Synthetic Aperture Radar images using double scattering. *International Journal of Applied Earth Observation and Geoinformation*, *28*, 150–159. https://doi.org/10.1016/j.jag.2013.12.002

Meyer, H., Reudenbach, C., Hengl, T., Katurji, M., & Nauss, T. (2018). Improving performance of spatio-temporal machine learning models using forward feature selection and target-oriented validation. *Environmental Modelling & Software*, *101*, 1–9. https://doi.org/10.1016/j.envsoft.2017.12.001

Meziane, D., & Shipley, B. (1999). Interacting determinants of specific leaf area in 22 herbaceous species: Effects of irradiance and nutrient availability. *Plant, Cell & Environment*, *22*(5), 447–459. https://doi.org/10.1046/j.1365-3040.1999.00423.x

Miatto, R. C., Wright, I. J., & Batalha, M. A. (2016). Relationships between soil nutrient status and nutrient-related leaf traits in Brazilian cerrado and seasonal forest communities. *Plant and Soil*, *404*(1), 13–33. https://doi.org/10.1007/s11104-016-2796-2

Moya, I., Camenen, L., Evain, S., Goulas, Y., Cerovic, Z. G., Latouche, G., Flexas, J., & Ounis, A. (2004). A new instrument for passive remote sensing: 1. Measurements of sunlight-induced chlorophyll fluorescence. *Remote Sensing of Environment*, *91*(2), 186–197. https://doi.org/10.1016/j.rse.2004.02.012

Nagendra, H. (2001). Using remote sensing to assess biodiversity. *International Journal of Remote Sensing*, *22*(12), 2377–2400. https://doi.org/10.1080/01431160117096

Nasirzadehdizaji, R., Balik Sanli, F., Abdikan, S., Cakir, Z., Sekertekin, A., & Ustuner, M. (2019). Sensitivity Analysis of Multi-Temporal Sentinel-1 SAR Parameters to Crop Height and Canopy Coverage. *Applied Sciences*, *9*(4), Article 4. https://doi.org/10.3390/app9040655

Niinemets, Ü. (2010). Responses of forest trees to single and multiple environmental stresses from seedlings to mature plants: Past stress history, stress interactions, tolerance and acclimation. *Forest Ecology and Management*, *260*(10), 1623–1639. https://doi.org/10.1016/j.foreco.2010.07.054

Ollinger, S. V., Richardson, A. D., Martin, M. E., Hollinger, D. Y., Frolking, S. E., Reich, P. B., Plourde, L. C., Katul, G. G., Munger, J. W., Oren, R., Smith, M.-L., Paw U, K. T., Bolstad, P. V., Cook, B. D., Day, M. C., Martin, T. A., Monson, R. K., & Schmid, H. P. (2008). Canopy nitrogen, carbon assimilation, and albedo in temperate and boreal forests: Functional relations and potential climate feedbacks. *Proceedings of the National Academy of Sciences*, *105*(49), 19336–19341. https://doi.org/10.1073/pnas.0810021105

Onoda, Y., Schieving, F., & Anten, N. P. R. (2008). Effects of Light and Nutrient Availability on Leaf Mechanical Properties of Plantago major: A Conceptual Approach. *Annals of Botany*, *101*(5), 727–736. https://doi.org/10.1093/aob/mcn013

Pan, Y., Birdsey, R. A., Fang, J., Houghton, R., Kauppi, P. E., Kurz, W. A., Phillips, O. L., Shvidenko, A., Lewis, S. L., Canadell, J. G., Ciais, P., Jackson, R. B., Pacala, S. W., McGuire, A. D., Piao, S., Rautiainen, A., Sitch, S., & Hayes, D. (2011). A Large and Persistent Carbon Sink in the World's Forests. *Science*, *333*(6045), 988–993. https://doi.org/10.1126/science.1201609

Periasamy, S. (2018). Significance of dual polarimetric synthetic aperture radar in biomass retrieval: An attempt on Sentinel-1. *Remote Sensing of Environment*, *217*, 537–549. https://doi.org/10.1016/j.rse.2018.09.003

Ploton, P., Mortier, F., Réjou-Méchain, M., Barbier, N., Picard, N., Rossi, V., Dormann, C., Cornu, G., Viennois, G., Bayol, N., Lyapustin, A., Gourlet-Fleury, S., & Pélissier, R. (2020). Spatial validation reveals poor predictive performance of large-scale ecological mapping models. *Nature Communications*, *11*(1), 4540. https://doi.org/10.1038/s41467-020-18321-y

Poorter, H., Niinemets, Ü., Poorter, L., Wright, I. J., & Villar, R. (2009). Causes and consequences of variation in leaf mass per area (LMA): A meta-analysis. *New Phytologist*, *182*(3), 565–588. https://doi.org/10.1111/j.1469-8137.2009.02830.x

Qi, J., Chehbouni, A., Huete, A. R., Kerr, Y. H., & Sorooshian, S. (1994). A modified soil adjusted vegetation index. *Remote Sensing of Environment*, *48*(2), 119–126. https://doi.org/10.1016/0034-4257(94)90134-1

Reich, P. B. (2014). The world-wide 'fast–slow' plant economics spectrum: A traits manifesto. *Journal of Ecology*, *102*(2), 275–301. https://doi.org/10.1111/1365-2745.12211

Reiss, J., Bridle, J. R., Montoya, J. M., & Woodward, G. (2009). Emerging horizons in biodiversity and ecosystem functioning research. *Trends in Ecology & Evolution*, *24*(9), 505–514. https://doi.org/10.1016/j.tree.2009.03.018

Sardar, P., & Samadder, S. R. (2021). Understanding the dynamics of landscape of greater Sundarban area using multi-layer perceptron Markov chain and landscape statistics approach. *Ecological Indicators*, *121*, 106914. https://doi.org/10.1016/j.ecolind.2020.106914

Serbin, S. P., Singh, A., Desai, A. R., Dubois, S. G., Jablonski, A. D., Kingdon, C. C., Kruger, E. L., & Townsend, P. A. (2015). Remotely estimating photosynthetic capacity, and its response to temperature, in vegetation canopies using imaging spectroscopy. *Remote Sensing of Environment*, *167*, 78–87. https://doi.org/10.1016/j.rse.2015.05.024

Singh, S., Reddy, C. S., Pasha, S. V., Dutta, K., Saranya, K. R. L., & Satish, K. V. (2017). Modeling the spatial dynamics of deforestation and fragmentation using Multi-Layer Perceptron neural network and landscape fragmentation tool. *Ecological Engineering*, *99*, 543–551. https://doi.org/10.1016/j.ecoleng.2016.11.047

Skidmore, A. K., Pettorelli, N., Coops, N. C., Geller, G. N., Hansen, M., Lucas, R., Mücher, C. A., O'Connor, B., Paganini, M., Pereira, H. M., Schaepman, M. E., Turner, W., Wang, T., & Wegmann, M. (2015). Environmental science: Agree on biodiversity metrics to track from space. *Nature*, *523*(7561), 403–405. https://doi.org/10.1038/523403a

Sophia, G., Caldararu, S., Stocker, B. D., & Zaehle, S. (2024). Leaf habit drives leaf nutrient resorption globally alongside nutrient availability and climate. *Biogeosciences*, *21*(18), 4169–4193. https://doi.org/10.5194/bg-21-4169-2024

Stysley, P. R., Coyle, D. B., Kay, R. B., Frederickson, R., Poulios, D., Cory, K., & Clarke, G. (2015). Long term performance of the High Output Maximum Efficiency Resonator (HOMER) laser for NASA′s Global Ecosystem Dynamics Investigation (GEDI) lidar. *Optics & Laser Technology*, *68*, 67–72. https://doi.org/10.1016/j.optlastec.2014.11.001

Suding, K. N., Lavorel, S., Chapin Iii, F. S., Cornelissen, J. H. C., Díaz, S., Garnier, E., Goldberg, D., Hooper, D. U., Jackson, S. T., & Navas, M.-L. (2008). Scaling

environmental change through the community-level: A trait-based response-and-effect framework for plants. *Global Change Biology*, *14*(5), 1125–1140. https://doi.org/10.1111/j.1365-2486.2008.01557.x

ter Steege, H., Vaessen, R. W., Cárdenas-López, D., Sabatier, D., Antonelli, A., de Oliveira, S. M., Pitman, N. C. A., Jørgensen, P. M., & Salomão, R. P. (2016). The discovery of the Amazonian tree flora with an updated checklist of all known tree taxa. *Scientific Reports*, *6*(1), 29549. https://doi.org/10.1038/srep29549

Thomson, E. R., Spiegel, M. P., Althuizen, I. H. J., Bass, P., Chen, S., Chmurzynski, A., Halbritter, A. H., Henn, J. J., Jónsdóttir, I. S., Klanderud, K., Li, Y., Maitner, B. S., Michaletz, S. T., Niittynen, P., Roos, R. E., Telford, R. J., Enquist, B. J., Vandvik, V., Macias-Fauria, M., & Malhi, Y. (2021). Trait tundra. *Environmental Research Letters*, *16*(5), 055006. https://doi.org/10.1088/1748-9326/abf464

Torres, R., Snoeij, P., Geudtner, D., Bibby, D., Davidson, M., Attema, E., Potin, P., Rommen, B., Floury, N., Brown, M., Traver, I. N., Deghaye, P., Duesmann, B., Rosich, B., Miranda, N., Bruno, C., L'Abbate, M., Croci, R., Pietropaolo, A., … Rostan, F. (2012). GMES Sentinel-1 mission. *Remote Sensing of Environment*, *120*, 9–24. https://doi.org/10.1016/j.rse.2011.05.028

Ustin, S. L., & Gamon, J. A. (2010). Remote sensing of plant functional types. *New Phytologist*, *186*(4), 795–816. https://doi.org/10.1111/j.1469-8137.2010.03284.x

Vabalas, A., Gowen, E., Poliakoff, E., & Casson, A. J. (2019). Machine learning algorithm validation with a limited sample size. *PLOS ONE*, *14*(11), e0224365. https://doi.org/10.1371/journal.pone.0224365

Violle, C., Navas, M.-L., Vile, D., Kazakou, E., Fortunel, C., Hummel, I., & Garnier, E. (2007). Let the concept of trait be functional! *Oikos*, *116*(5), 882–892. https://doi.org/10.1111/j.0030-1299.2007.15559.x

Wang, R., & Gamon, J. A. (2019). Remote sensing of terrestrial plant biodiversity. *Remote Sensing of Environment*, *231*, 111218. https://doi.org/10.1016/j.rse.2019.111218

Wang, Z. (2019). Mapping foliar functional traits and their uncertainties across three years in a grassland experiment. *Remote Sensing of Environment*, 12.

Wigley, B. J., Slingsby, J. A., Díaz, S., Bond, W. J., Fritz, H., & Coetsee, C. (2016). Leaf traits of African woody savanna species across climate and soil fertility gradients: Evidence for conservative versus acquisitive resource-use strategies. *Journal of Ecology*, *104*(5), 1357–1369. https://doi.org/10.1111/1365-2745.12598

Wollersheim, M., Collins, M. J., & Leckie, D. (2011). Estimating boreal forest species type with airborne polarimetric synthetic aperture radar. *International Journal of Remote Sensing*, *32*(9), 2481–2505. https://doi.org/10.1080/01431161003698377

Wright, I. J., Dong, N., Maire, V., Prentice, I. C., Westoby, M., Díaz, S., Gallagher, R. V., Jacobs, B. F., Kooyman, R., Law, E. A., Leishman, M. R., Niinemets, Ü., Reich, P. B., Sack, L., Villar, R., Wang, H., & Wilf, P. (2017). Global climatic drivers of leaf size. *Science*, *357*(6354), 917–921. https://doi.org/10.1126/science.aal4760

Wright, I. J., Reich, P. B., Westoby, M., Ackerly, D. D., Baruch, Z., Bongers, F., Cavender-Bares, J., Chapin, T., Cornelissen, J. H. C., Diemer, M., Flexas, J., Garnier, E., Groom, P. K., Gulias, J., Hikosaka, K., Lamont, B. B., Lee, T., Lee, W., Lusk, C., … Villar, R. (2004). The worldwide leaf economics spectrum. *Nature*, *428*(6985), 821–827. https://doi.org/10.1038/nature02403

Yang, J., El-Kassaby, Y. A., & Guan, W. (2020). The effect of slope aspect on vegetation attributes in a mountainous dry valley, Southwest China. *Scientific Reports*, *10*(1), 16465. https://doi.org/10.1038/s41598-020-73496-0

Zhang, C., Pan, X., Li, H., Gardiner, A., Sargent, I., Hare, J., & Atkinson, P. M. (2018). A hybrid MLP-CNN classifier for very fine resolution remotely sensed image classification.

ISPRS Journal of Photogrammetry and Remote Sensing, *140*, 133–144. https://doi.org/10.1016/j.isprsjprs.2017.07.014

Zhang-Zheng, H., Adu-Bredu, S., Duah-Gyamfi, A., Moore, S., Addo-Danso, S. D., Amissah, L., Valentini, R., Djagbletey, G., Anim-Adjei, K., Quansah, J., Sarpong, B., Owusu-Afriyie, K., Gvozdevaite, A., Tang, M., Ruiz-Jaen, M. C., Ibrahim, F., Girardin, C. A. J., Rifai, S., Dahlsjö, C. A. L., … Malhi, Y. (2024). Contrasting carbon cycle along tropical forest aridity gradients in West Africa and Amazonia. *Nature Communications*, *15*(1), 3158. https://doi.org/10.1038/s41467-024-47202-x

Zheng, Z., Zeng, Y., Schneider, F. D., Zhao, Y., Zhao, D., Schmid, B., Schaepman, M. E., & Morsdorf, F. (2021). Mapping functional diversity using individual tree-based morphological and physiological traits in a subtropical forest. *Remote Sensing of Environment*, *252*, 112170. https://doi.org/10.1016/j.rse.2020.112170

4.8. Supplementary materials

4.8.1. Figures

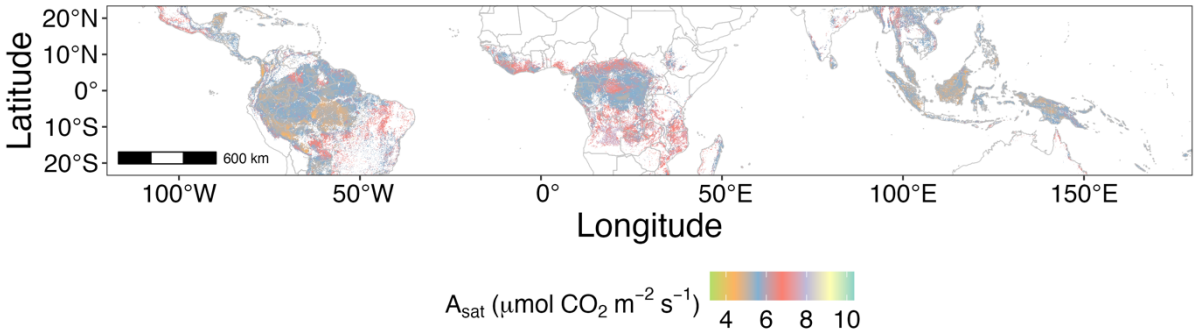

Fig. S4.1. Spatial distribution of A_{sat}.

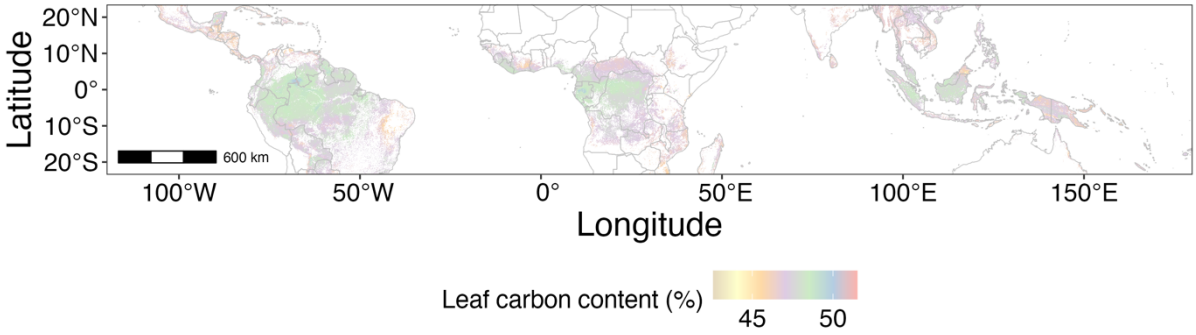

Fig. S4.2. Spatial distribution of leaf carbon content.

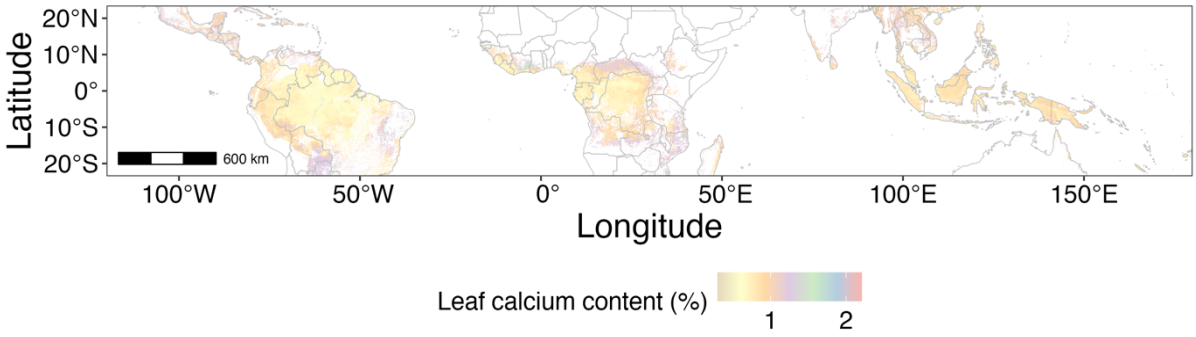

Fig. S4.3. Spatial distribution of leaf calcium content.

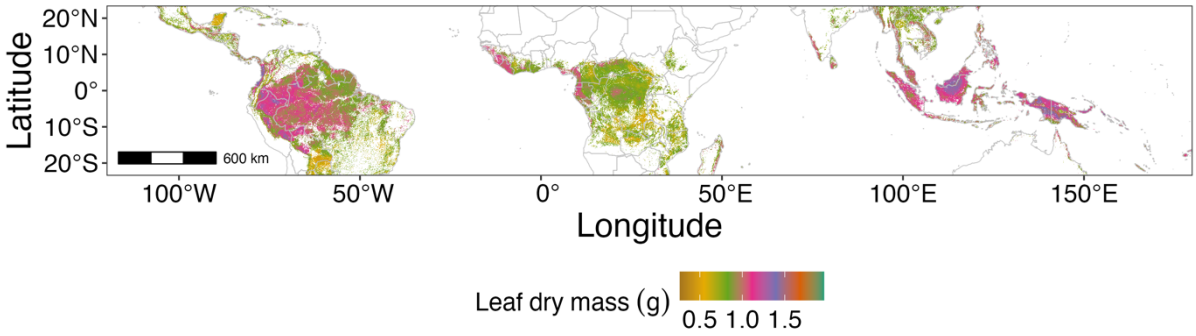

Fig. S4.4. Spatial distribution of leaf dry mass.

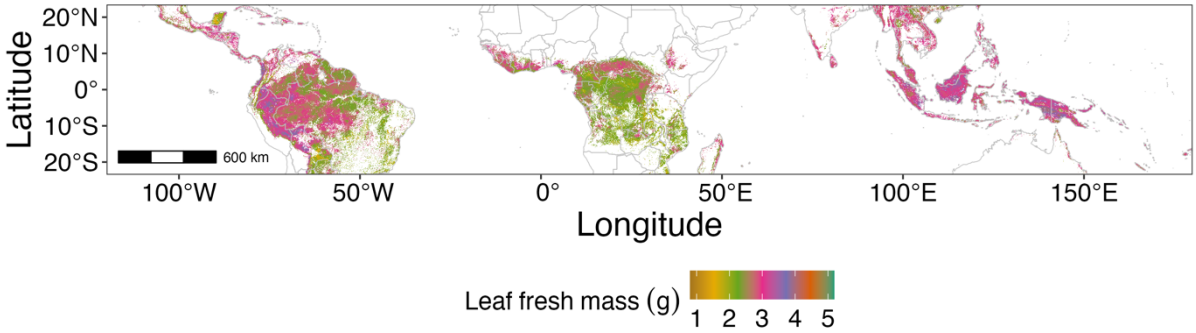

Fig. S4.5. Spatial distribution of leaf fresh mass.

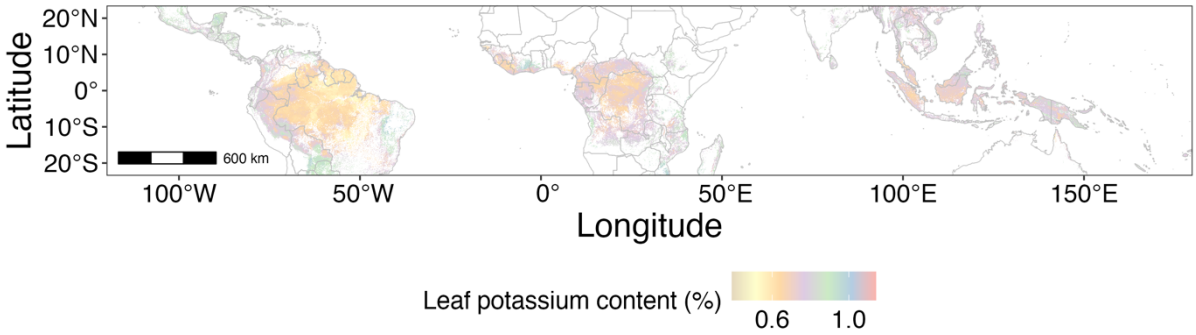

Fig. S4.6. Spatial distribution of leaf potassium content.

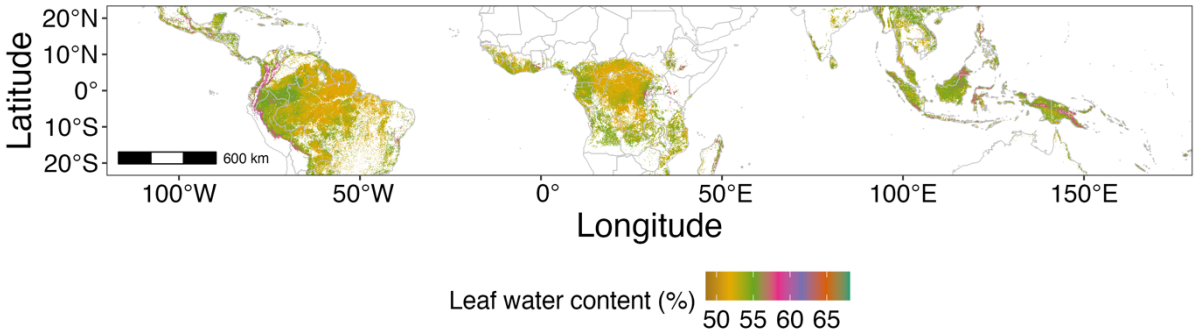

Fig. S4.7. Spatial distribution of leaf water content.

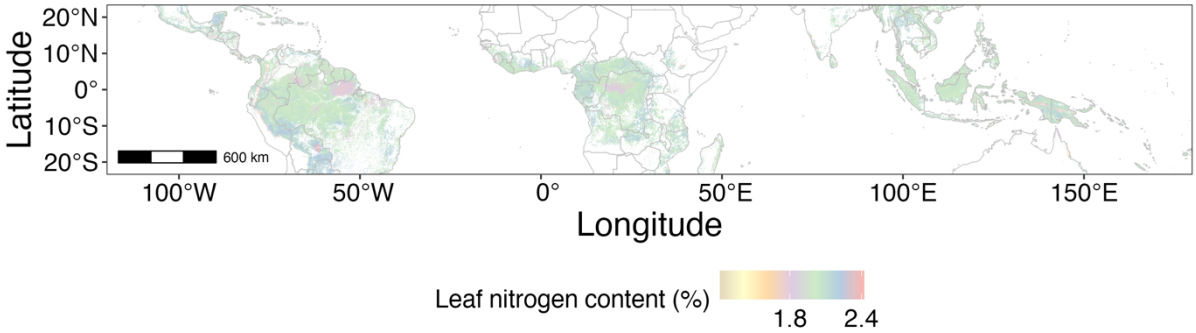

Fig. S4.8. Spatial distribution of leaf nitrogen content.

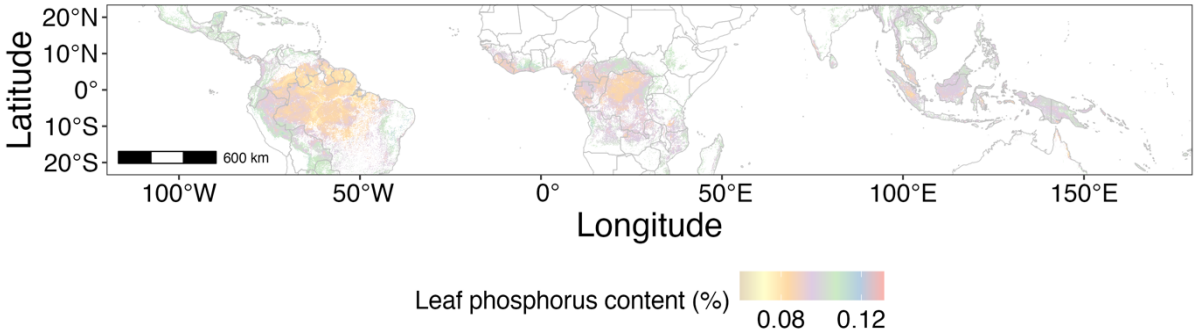

Fig. S4.9. Spatial distribution of leaf phosphorus content.

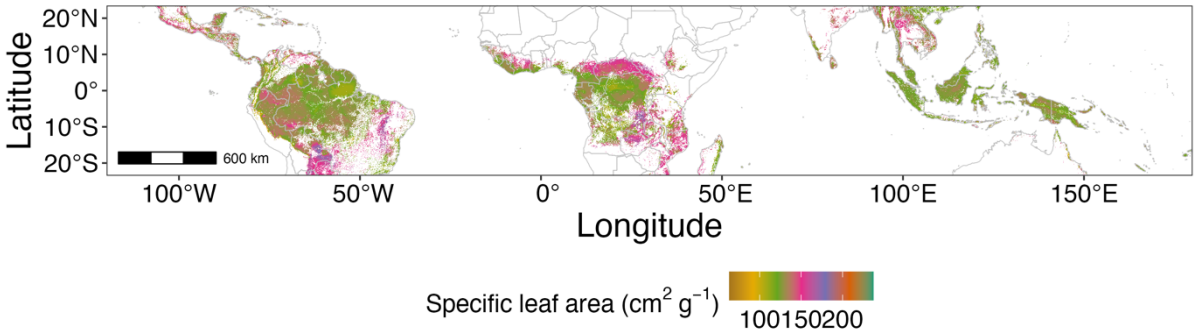

Fig. S4.10. Spatial distribution of specific leaf area.

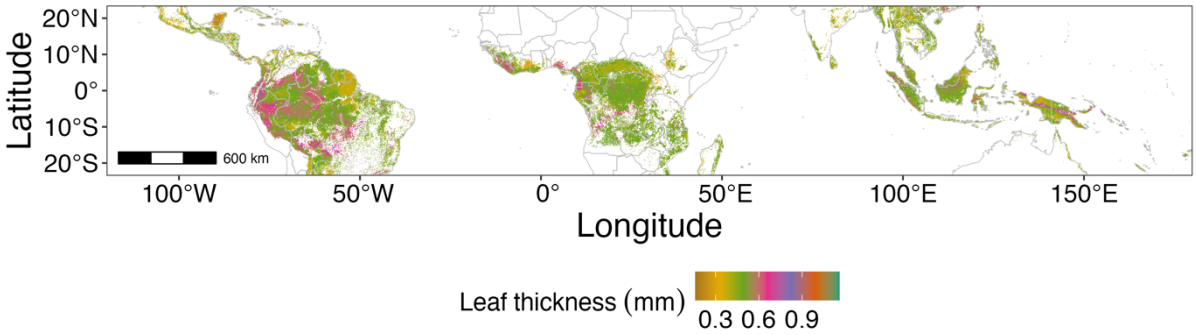

Fig. S4.11. Spatial distribution of leaf thickness.

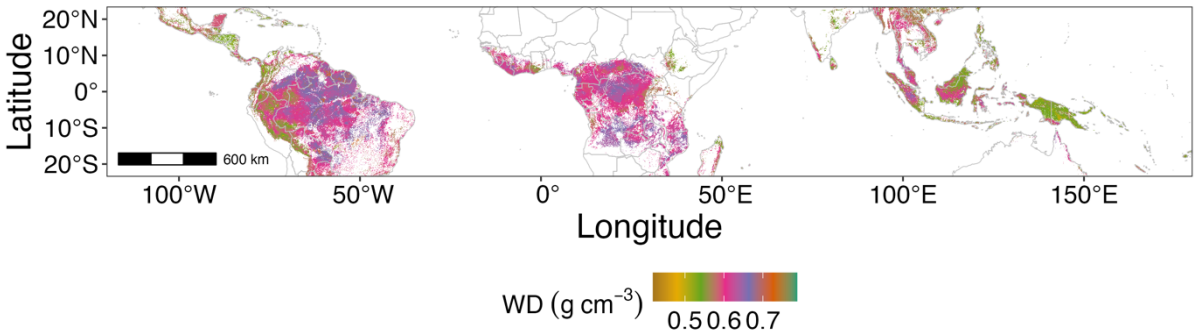

Fig. S4.12. Spatial distribution of wood density.

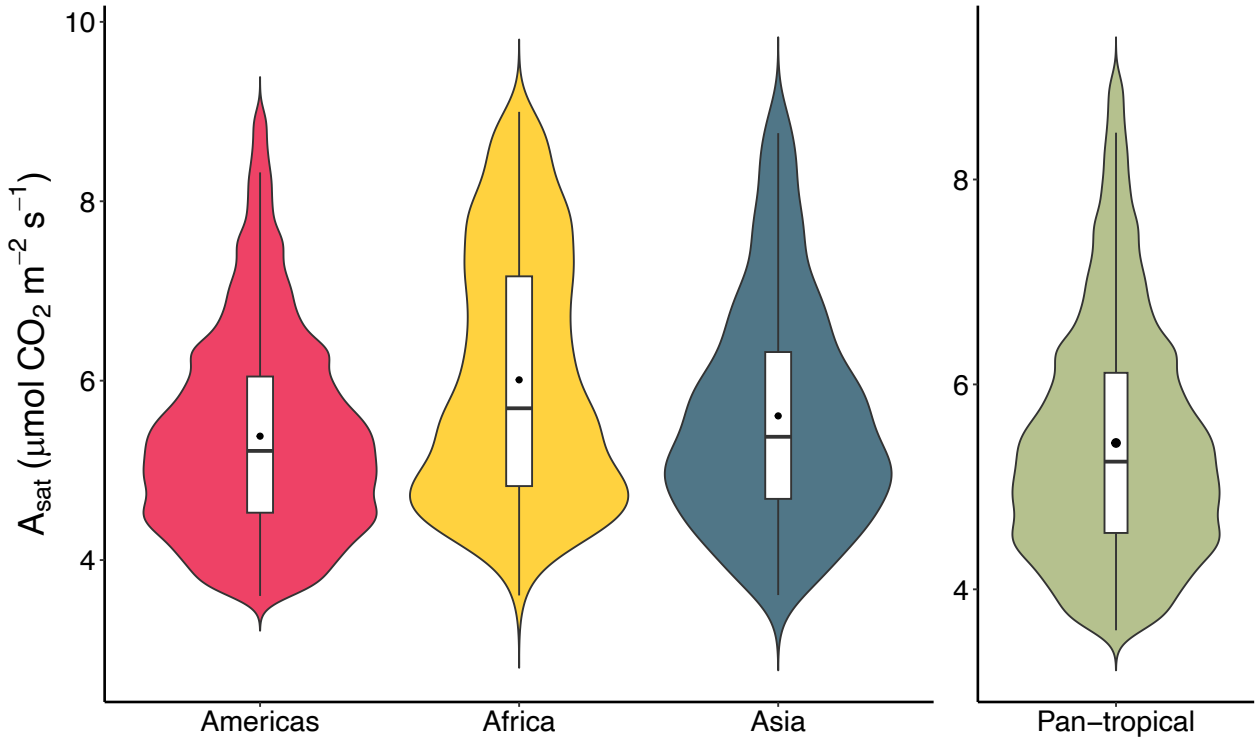

Fig. S4.13. Distribution and variation patterns of A_{sat} at continental and pan-tropical scales. Inside each violin plot is a box plot demonstrating the median value, mean value, interquartile range, and 1.5 times interquartile range of a trait. The wider sections of the violin plot indicate a higher probability that multiple trait variables distribute around this given value, while the thinner sections represent a lower probability.

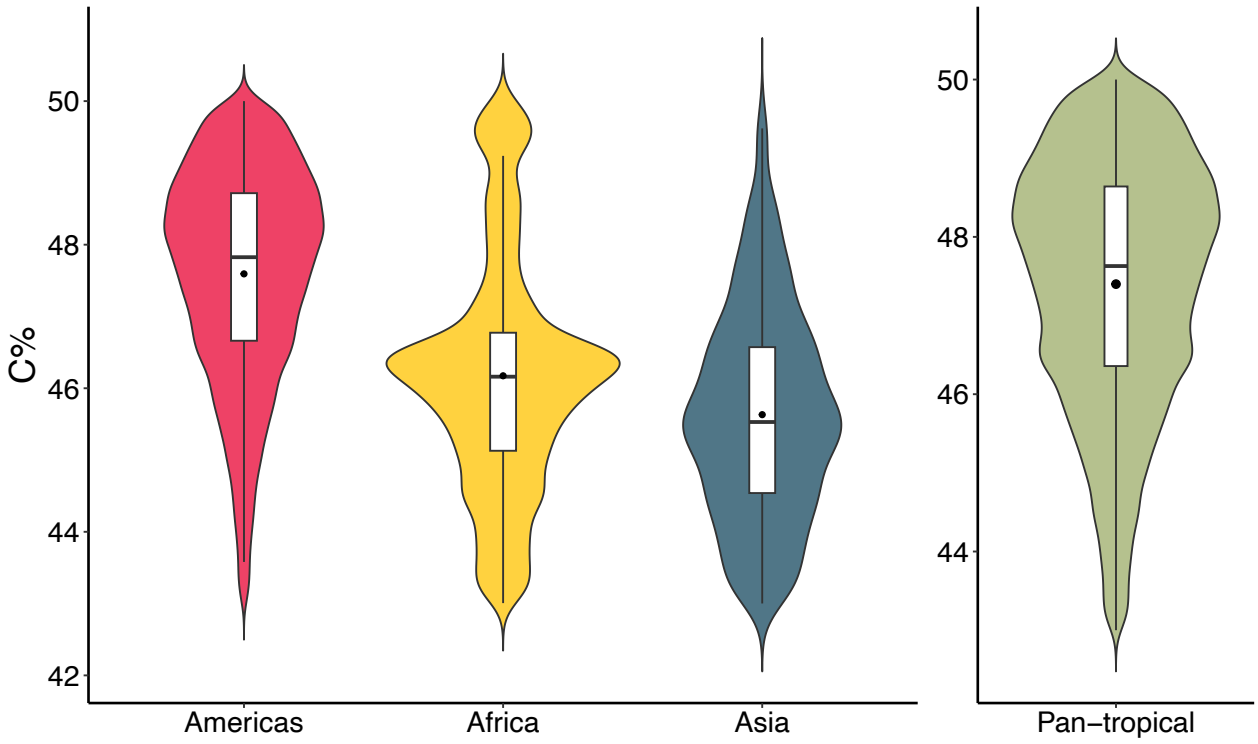

Fig. S4.14. Distribution and variation patterns of leaf carbon (C) content at continental and pan-tropical scales. Inside each violin plot is a box plot demonstrating the median value, mean value, interquartile range, and 1.5 times interquartile range of a trait. The wider sections of the violin plot indicate a higher probability that multiple trait variables distribute around this given value, while the thinner sections represent a lower probability.

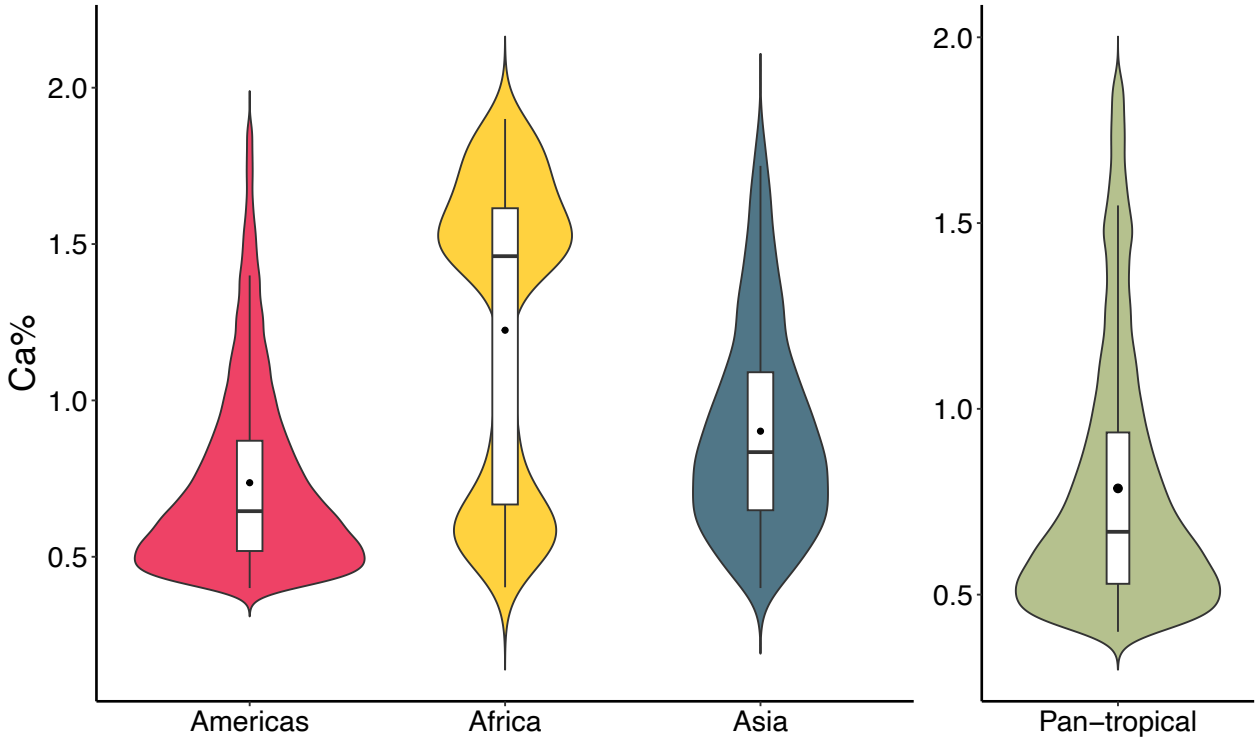

Fig. S4.15. Distribution and variation patterns of leaf calcium (Ca) content at continental and pan-tropical scales. Inside each violin plot is a box plot demonstrating the median value, mean value, interquartile range, and 1.5 times interquartile range of a trait. The wider sections of the violin plot indicate a higher probability that multiple trait variables distribute around this given value, while the thinner sections represent a lower probability.

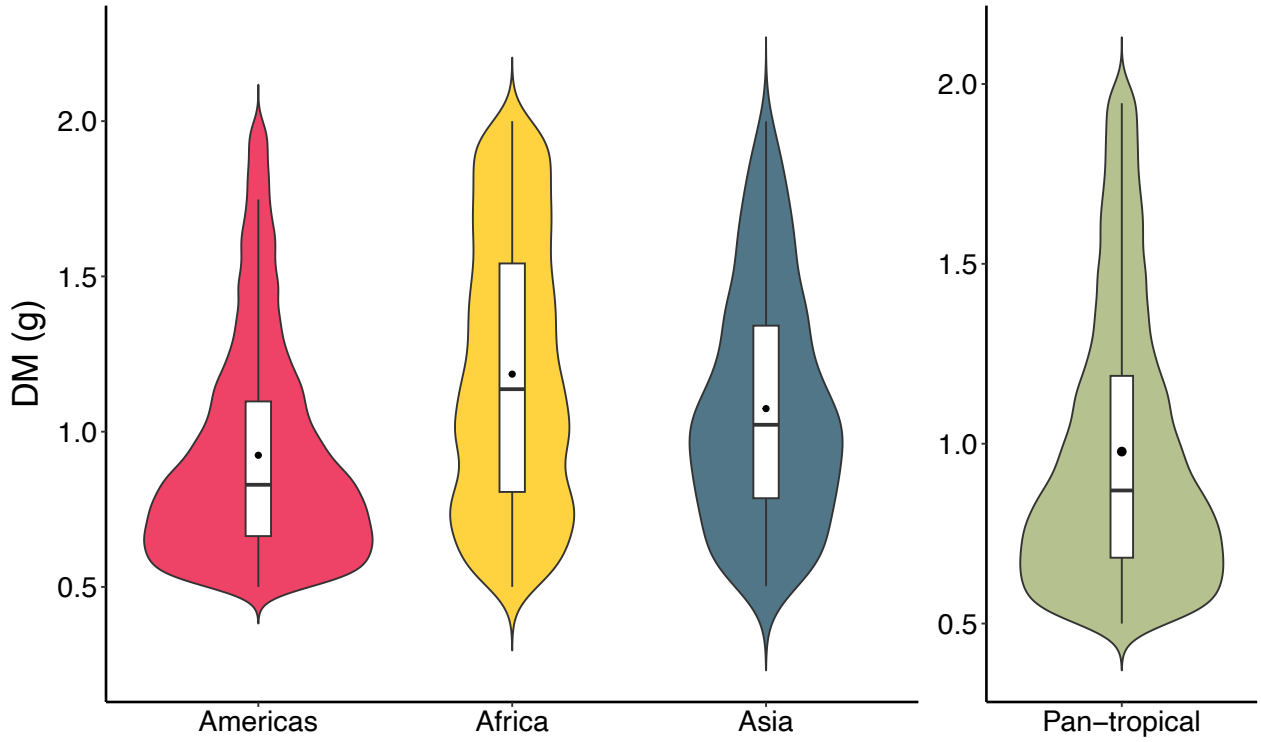

Fig. S4.16. Distribution and variation patterns of leaf dry mass (DM) at continental and pan-tropical scales. Inside each violin plot is a box plot demonstrating the median value, mean value, interquartile range, and 1.5 times interquartile range of a trait. The wider sections of the violin plot indicate a higher probability that multiple trait variables distribute around this given value, while the thinner sections represent a lower probability.

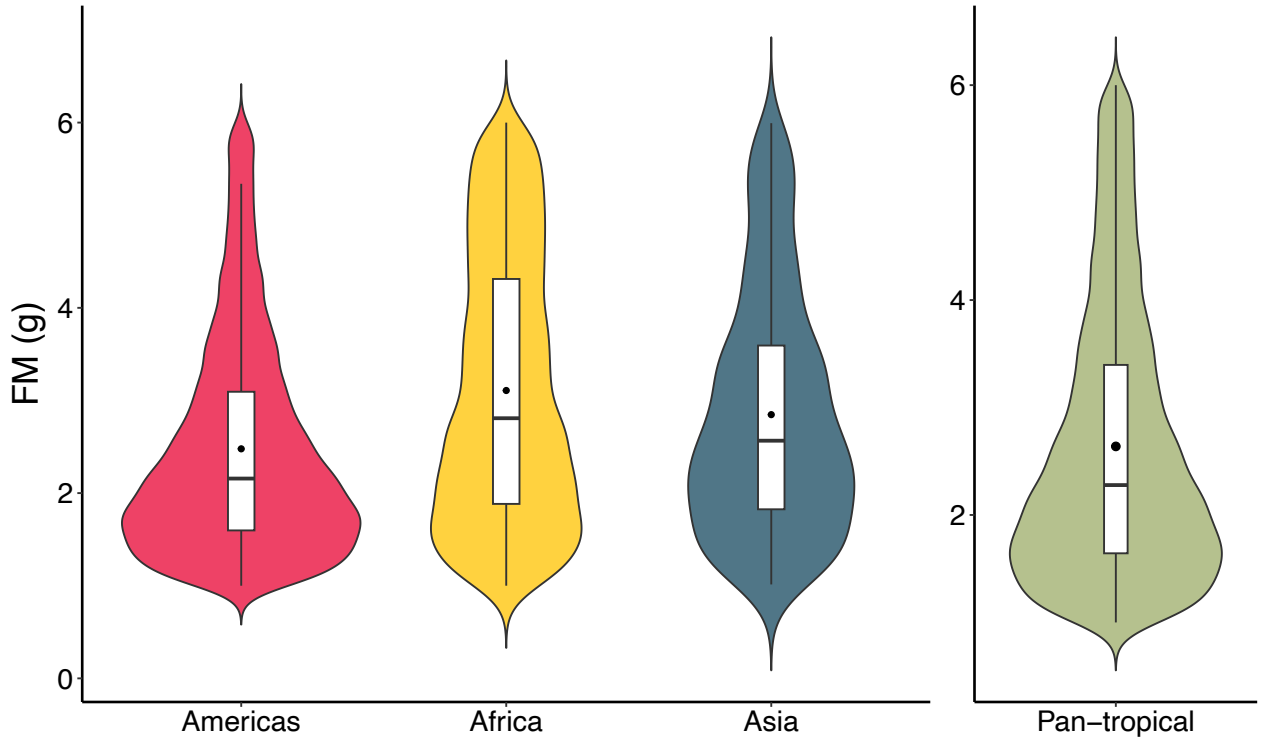

Fig. S4.17. Distribution and variation patterns of leaf fresh mass (FM) at continental and pan-tropical scales. Inside each violin plot is a box plot demonstrating the median value, mean value, interquartile range, and 1.5 times interquartile range of a trait. The wider sections of the violin plot indicate a higher probability that multiple trait variables distribute around this given value, while the thinner sections represent a lower probability.

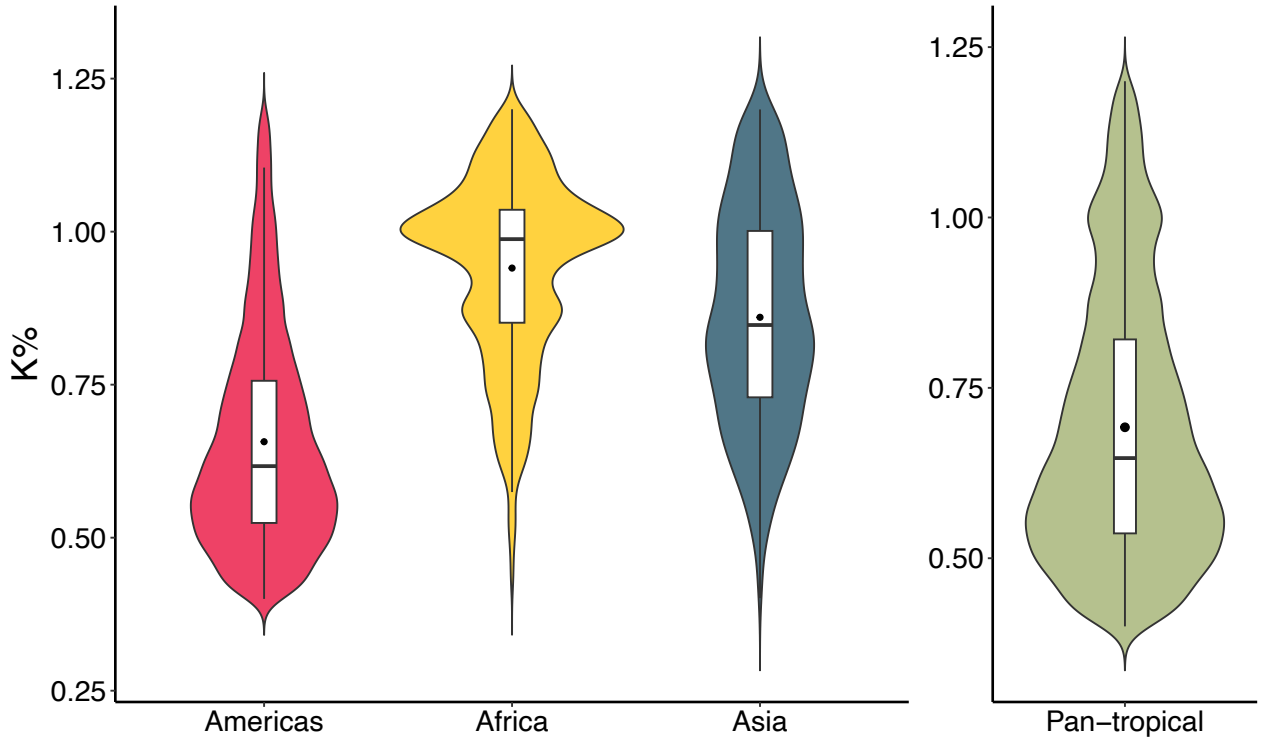

Fig. S4.18. Distribution and variation patterns of leaf potassium (K) content at continental and pan-tropical scales. Inside each violin plot is a box plot demonstrating the median value, mean value, interquartile range, and 1.5 times interquartile range of a trait. The wider sections of the violin plot indicate a higher probability that multiple trait variables distribute around this given value, while the thinner sections represent a lower probability.

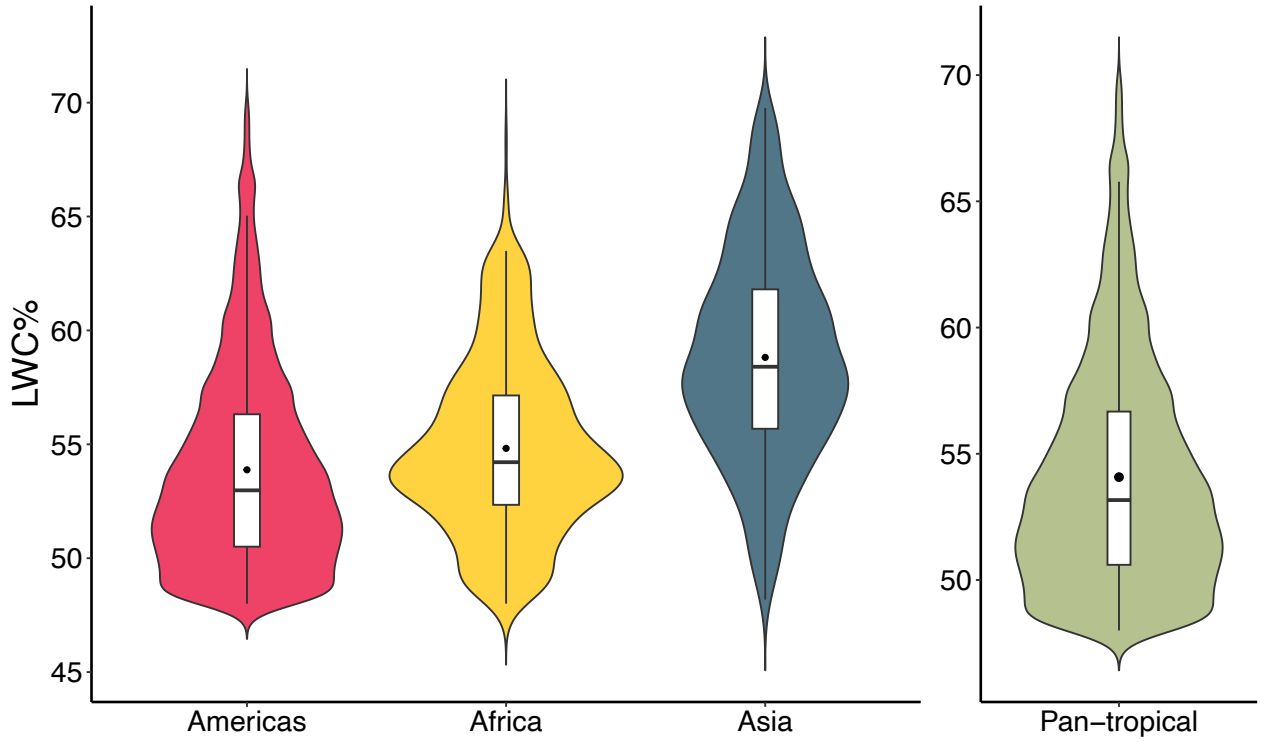

Fig. S4.19. Distribution and variation patterns of leaf water content (LWC) at continental and pan-tropical scales. Inside each violin plot is a box plot demonstrating the median value, mean value, interquartile range, and 1.5 times interquartile range of a trait. The wider sections of the violin plot indicate a higher probability that multiple trait variables distribute around this given value, while the thinner sections represent a lower probability.

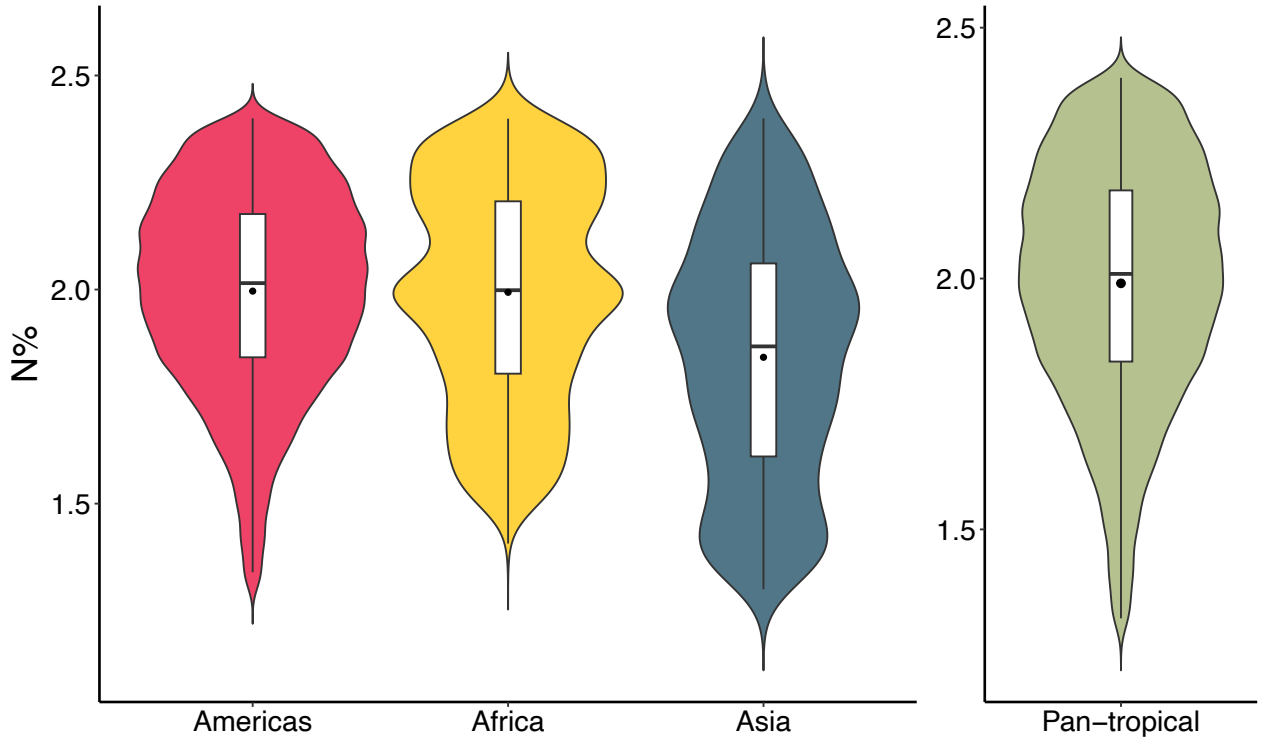

Fig. S4.20. Distribution and variation patterns of leaf nitrogen (N) content at continental and pan-tropical scales. Inside each violin plot is a box plot demonstrating the median value, mean value, interquartile range, and 1.5 times interquartile range of a trait. The wider sections of the violin plot indicate a higher probability that multiple trait variables distribute around this given value, while the thinner sections represent a lower probability.

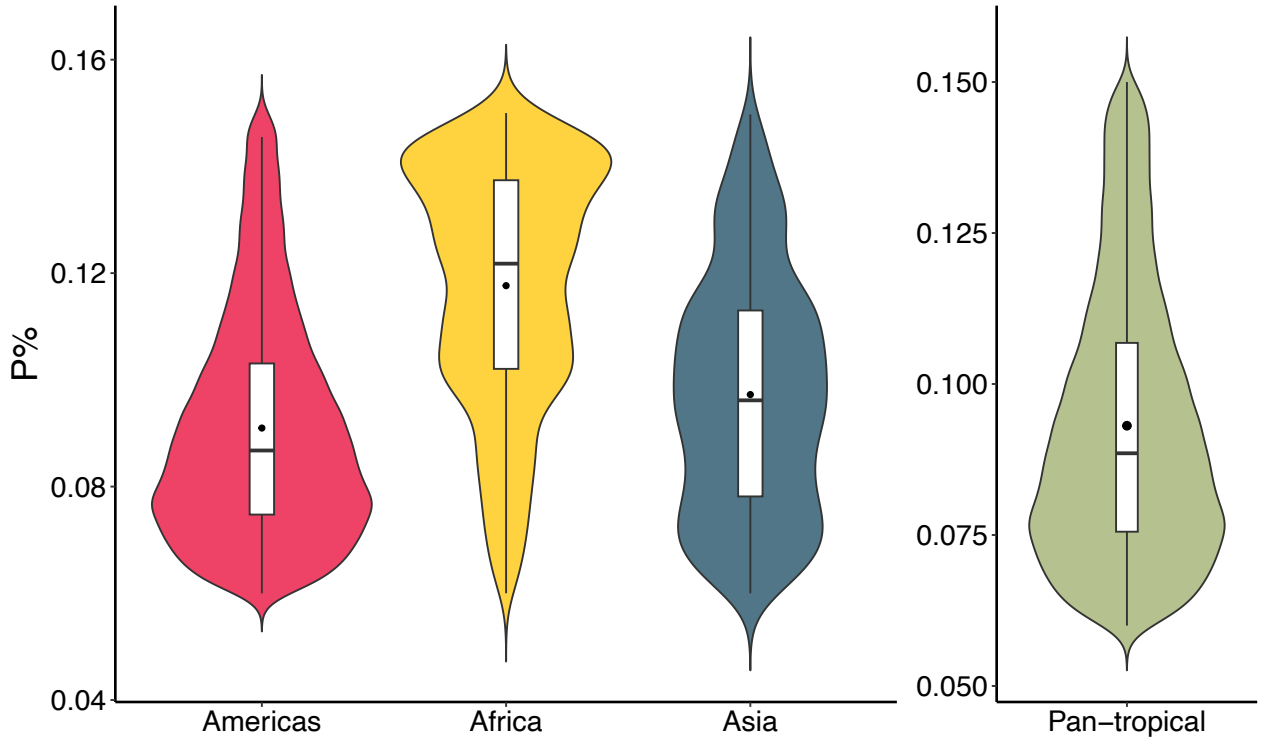

Fig. S4.21. Distribution and variation patterns of leaf phosphorus (P) content at continental and pan-tropical scales. Inside each violin plot is a box plot demonstrating the median value, mean value, interquartile range, and 1.5 times interquartile range of a trait. The wider sections of the violin plot indicate a higher probability that multiple trait variables distribute around this given value, while the thinner sections represent a lower probability.

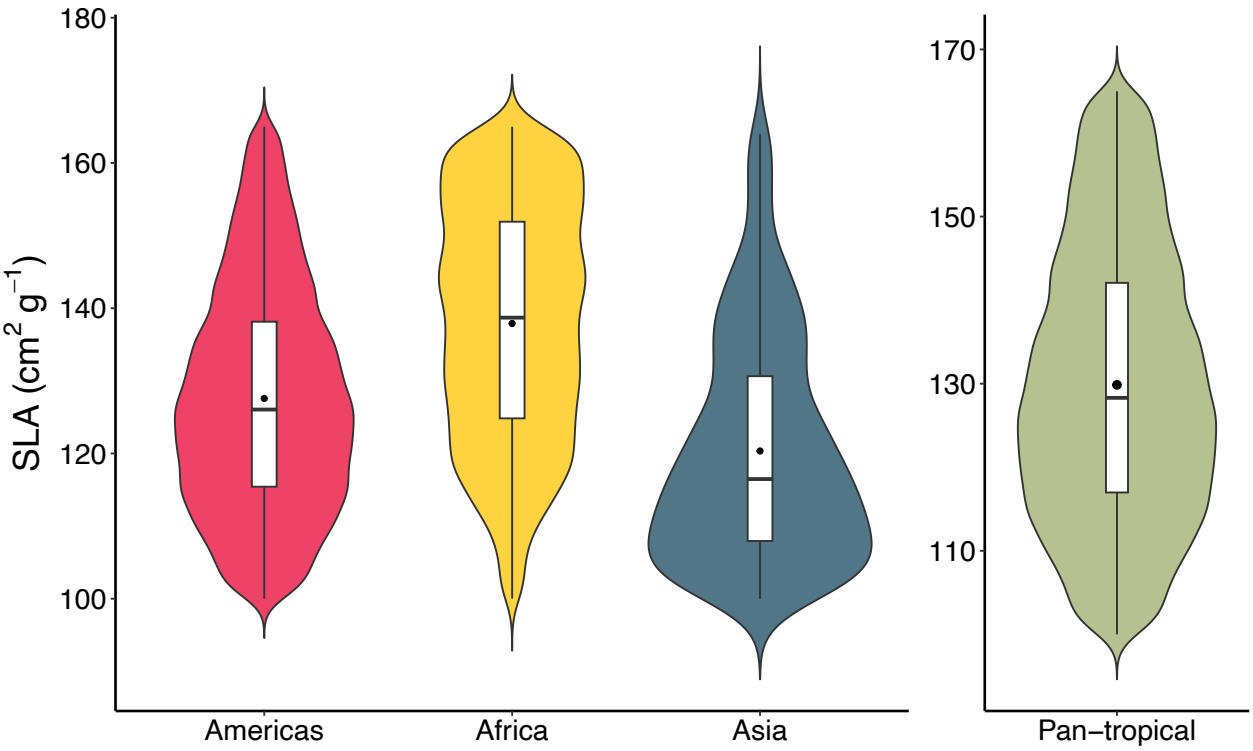

Fig. S4.22. Distribution and variation patterns of specific leaf area (SLA) at continental and pan-tropical scales. Inside each violin plot is a box plot demonstrating the median value, mean value, interquartile range, and 1.5 times interquartile range of a trait. The wider sections of the violin plot indicate a higher probability that multiple trait variables distribute around this given value, while the thinner sections represent a lower probability.

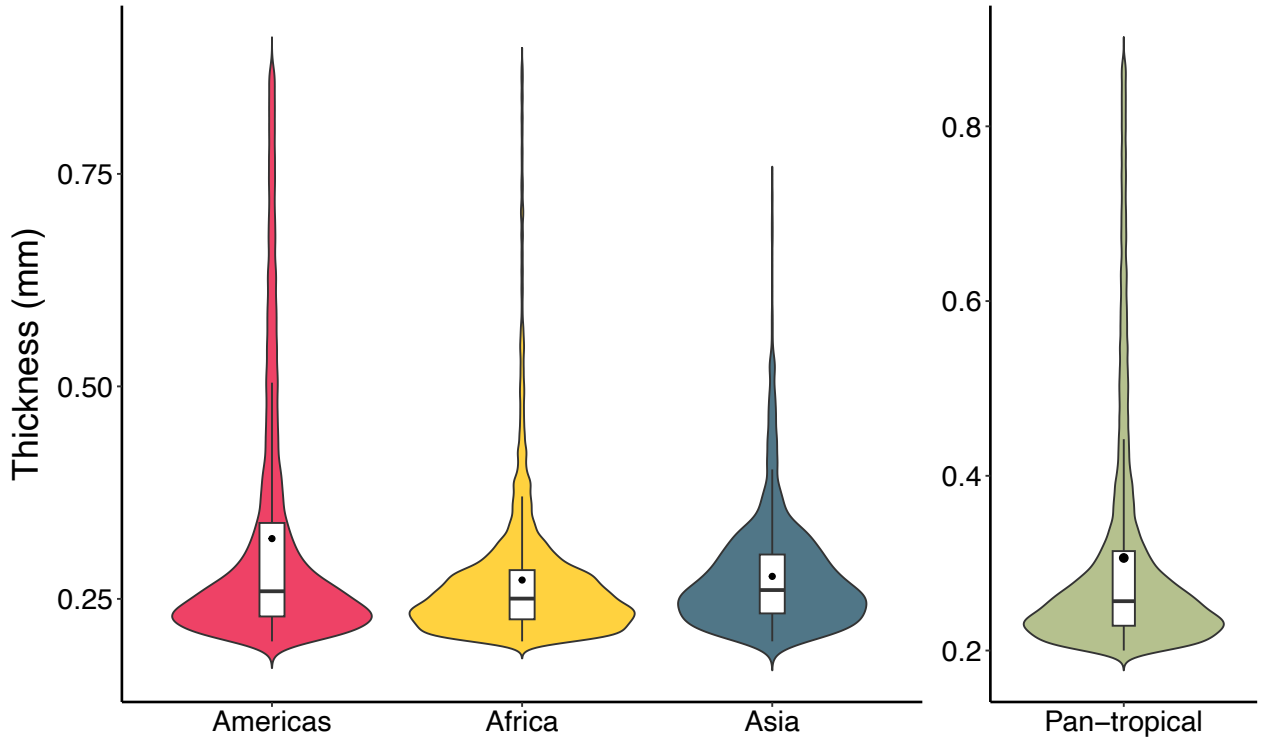

Fig. S4.23. Distribution and variation patterns of leaf thickness at continental and pan-tropical scales. Inside each violin plot is a box plot demonstrating the median value, mean value, interquartile range, and 1.5 times interquartile range of a trait. The wider sections of the violin plot indicate a higher probability that multiple trait variables distribute around this given value, while the thinner sections represent a lower probability.

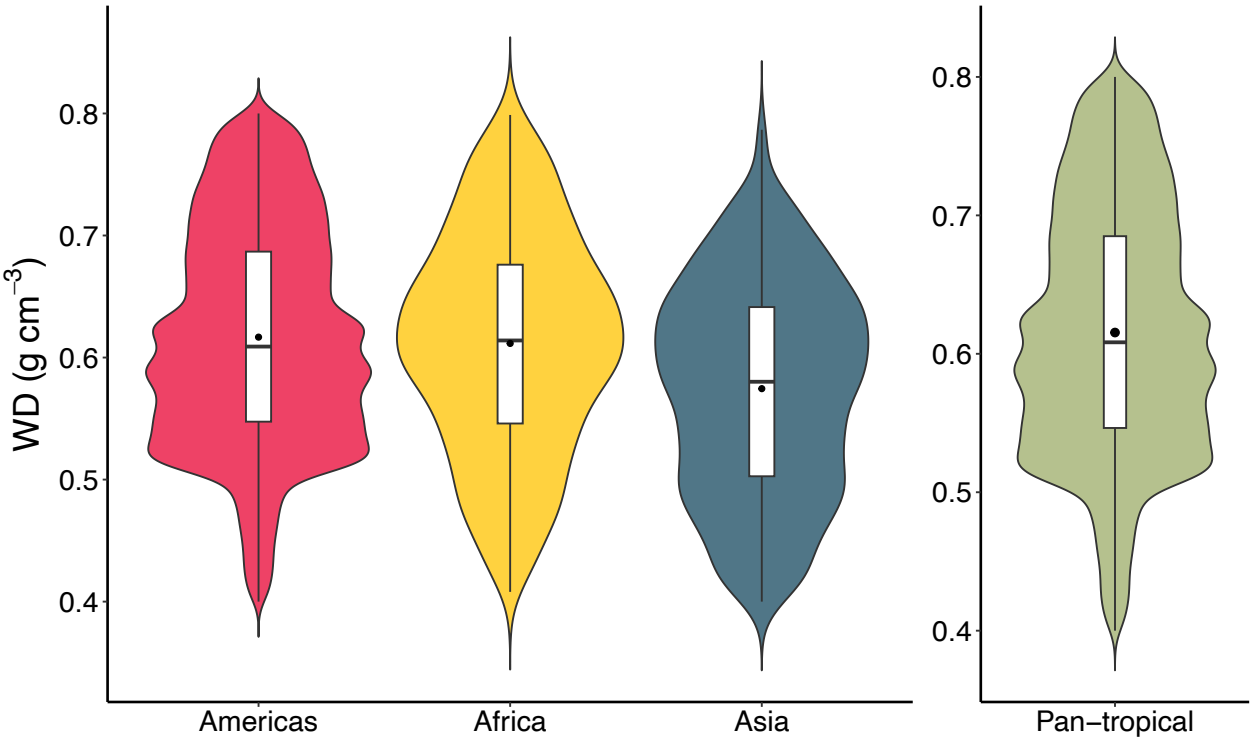

Fig. S4.24. Distribution and variation patterns of wood density (WD) at continental and pan-tropical scales. Inside each violin plot is a box plot demonstrating the median value, mean value, interquartile range, and 1.5 times interquartile range of a trait. The wider sections of the violin plot indicate a higher probability that multiple trait variables distribute around this given value, while the thinner sections represent a lower probability.

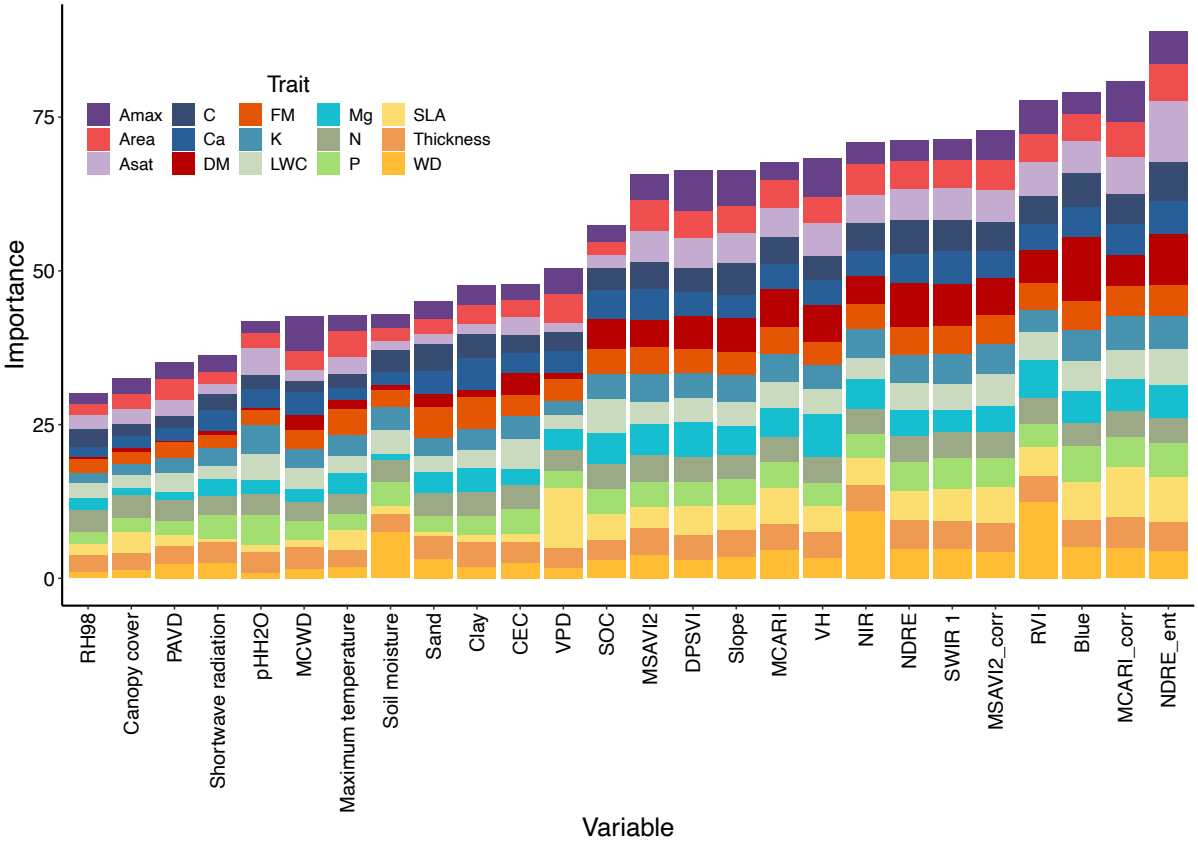

Fig. S4.25. Stacked bar plot for the importance of each variable for predicting each of the functional trait.

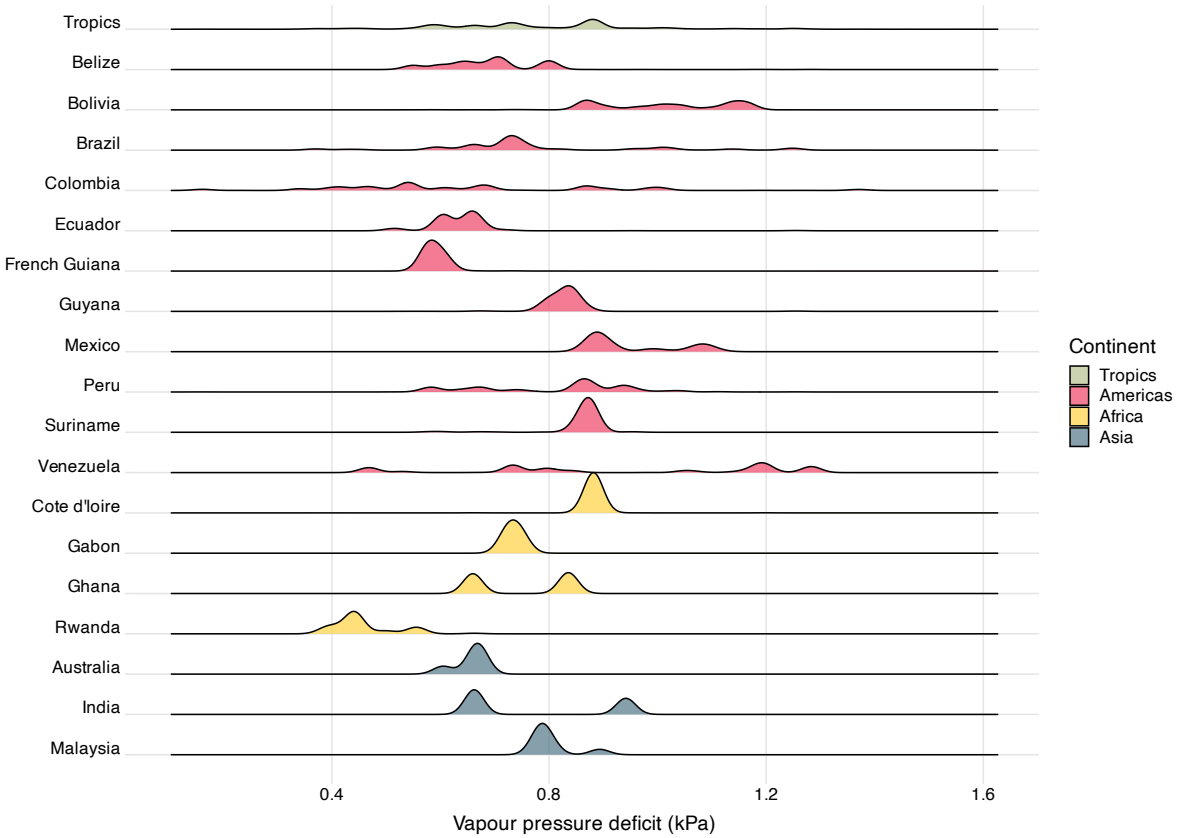

Fig. S4.26. Density distribution plot of vapour pressure deficit for each sampling country where plant functional traits were collected. The top ridgeline graph indicated vapour pressure deficit across tropical forests.

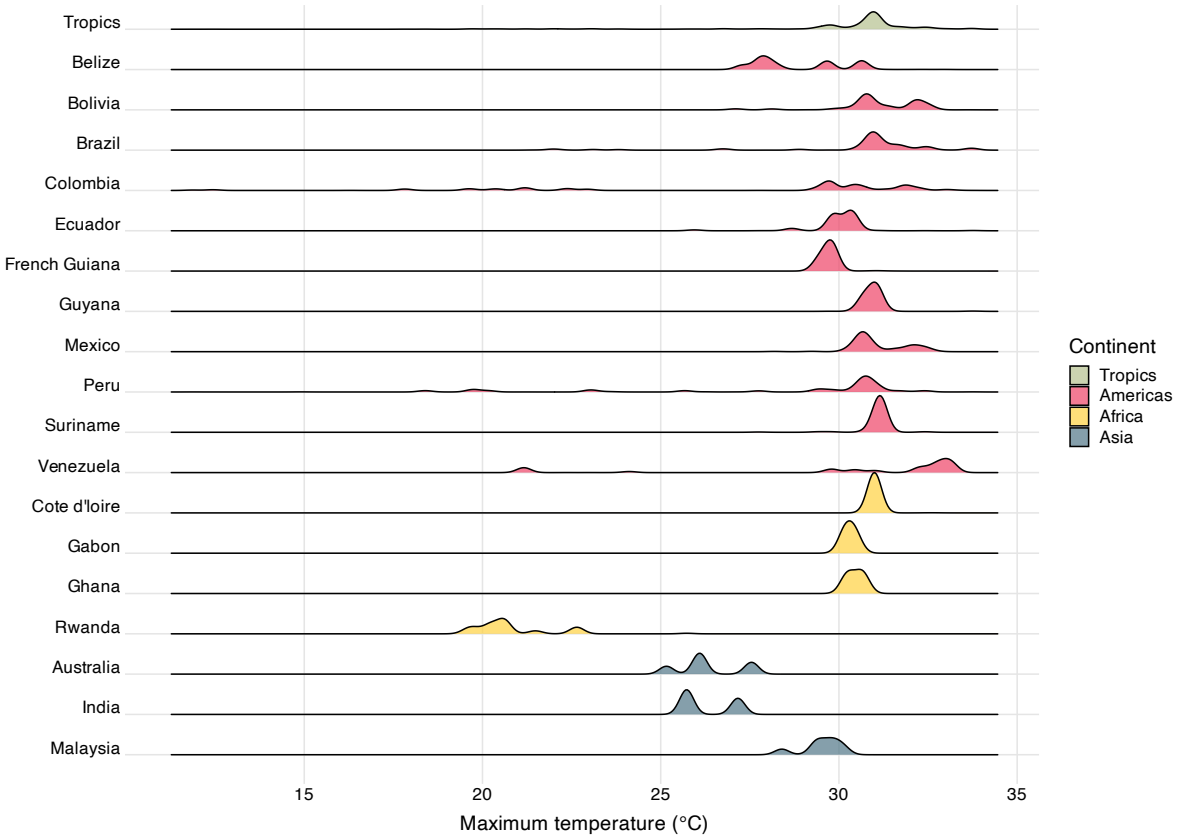

Fig. S4.27. Density distribution plot of maximum temperature for each sampling country where plant functional traits were collected. The top ridgeline graph indicated maximum temperature across tropical forests.

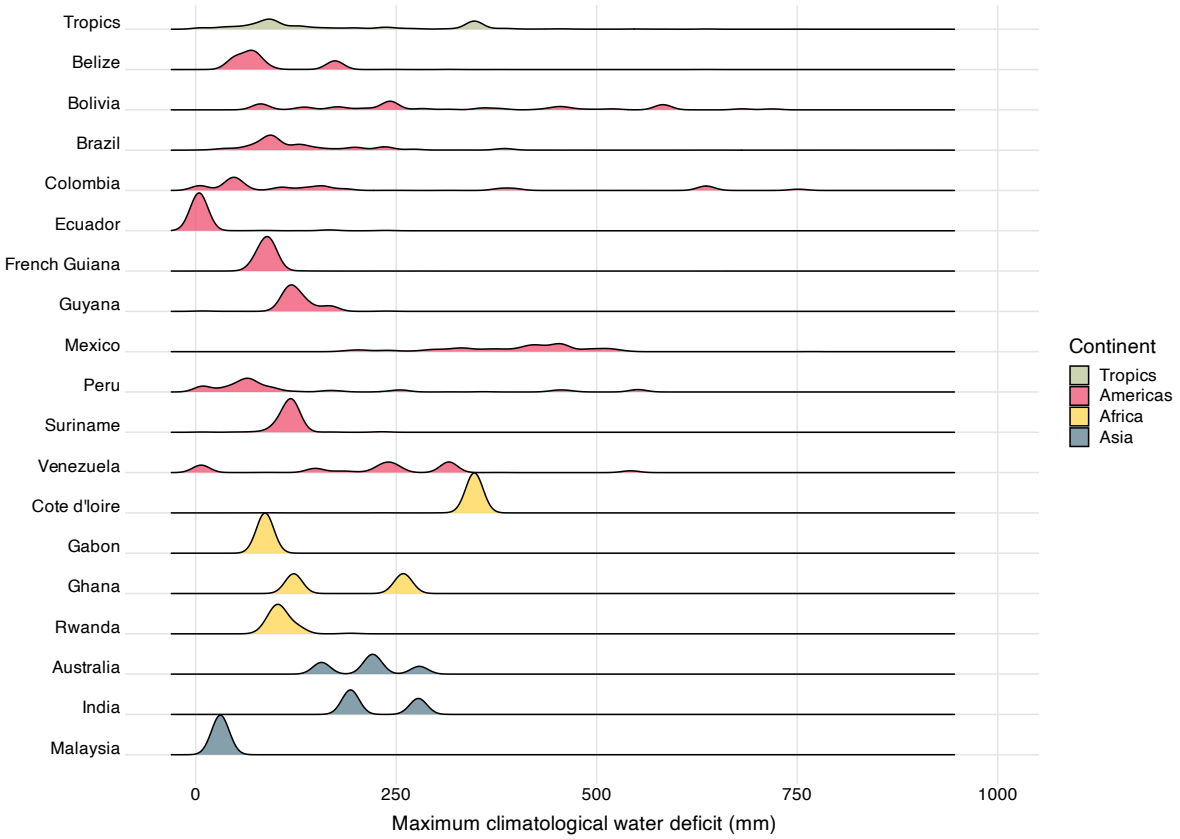

Fig. S4.28. Density distribution plot of maximum climatological water deficit for each sampling country where plant functional traits were collected. The top ridgeline graph indicated maximum climatological water deficit across tropical forests.

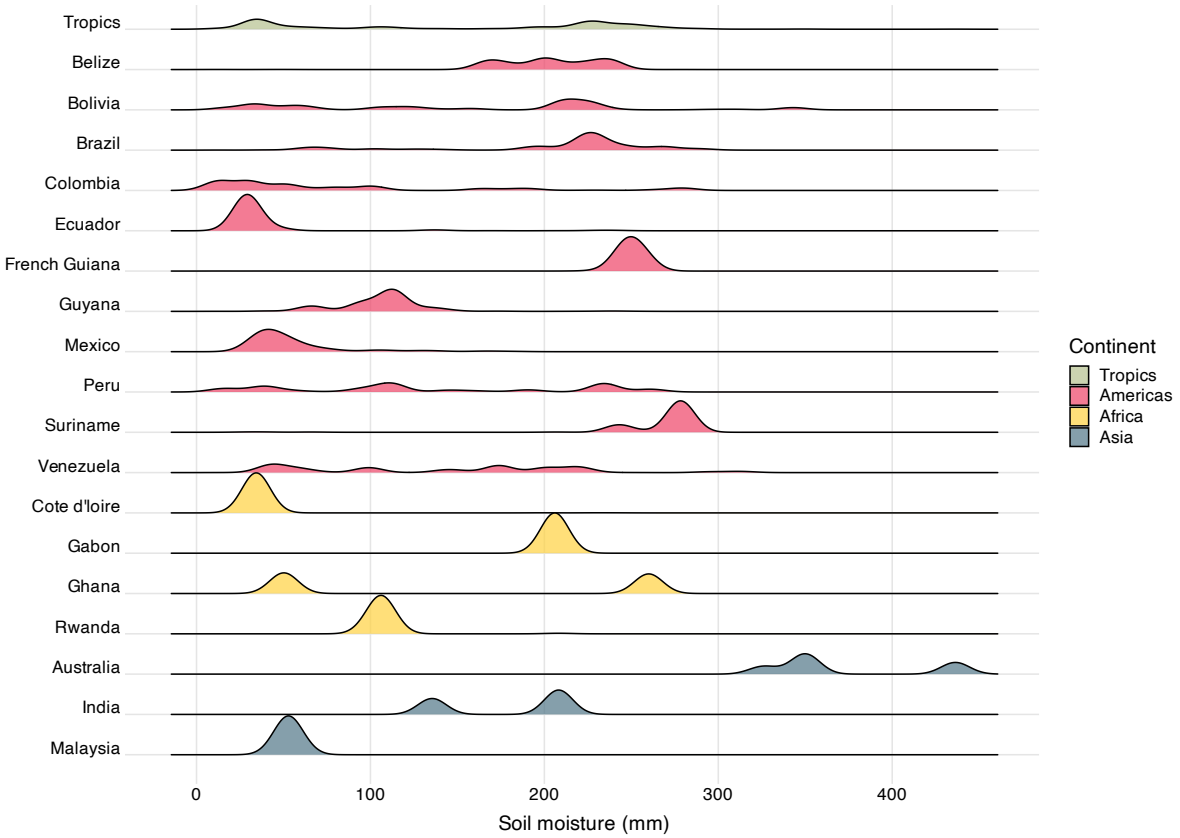

Fig. S4.29. Density distribution plot of soil moisture for each sampling country where plant functional traits were collected. The top ridgeline graph indicated soil moisture across tropical forests.

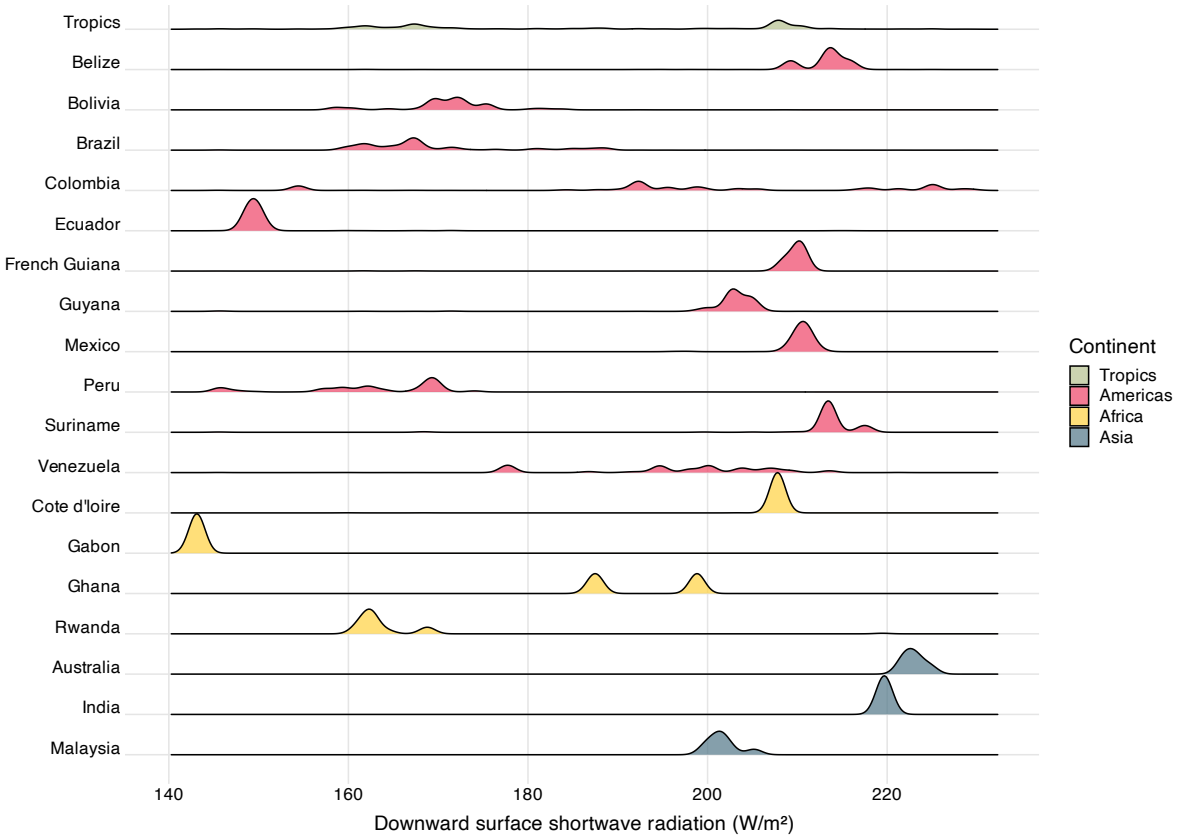

Fig. S4.30. Density distribution plot of downward surface shortwave radiation for each sampling country where plant functional traits were collected. The top ridgeline graph indicated downward surface shortwave radiation across tropical forests.

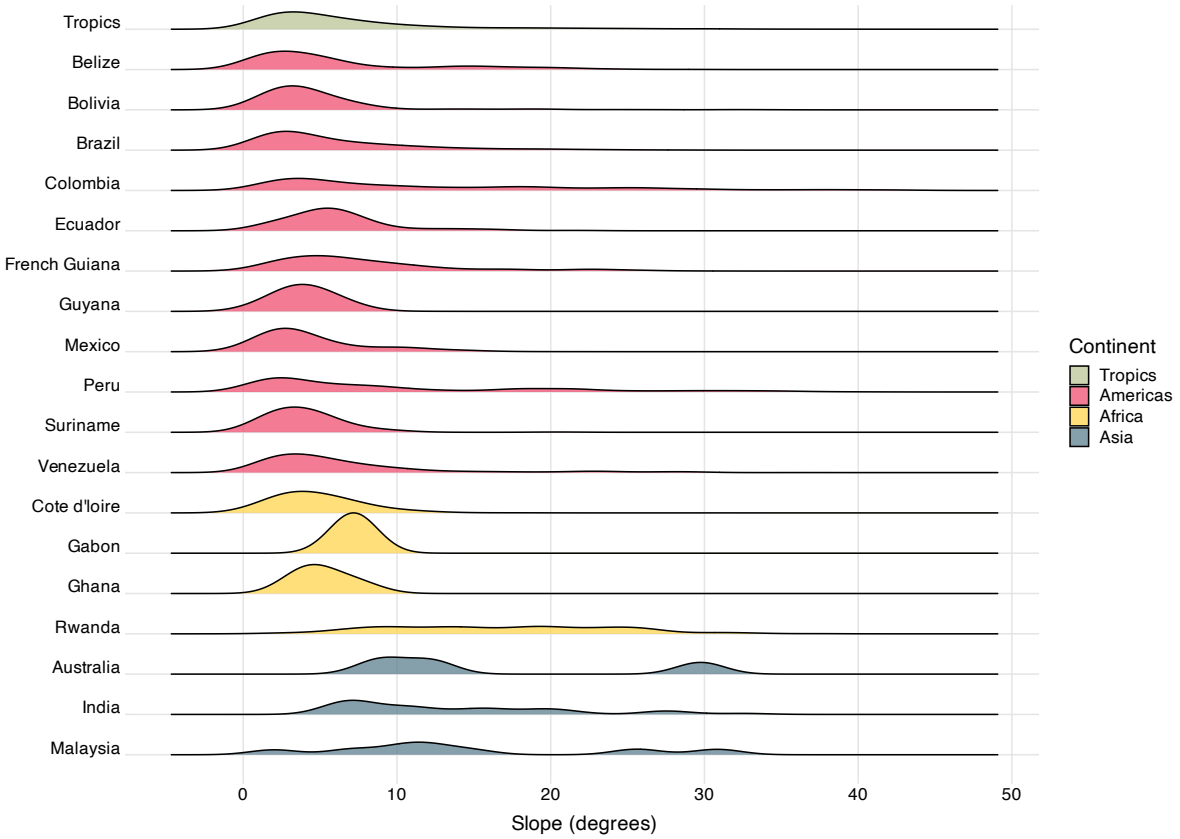

Fig. S4.31. Density distribution plot of slope for each sampling country where plant functional traits were collected. The top ridgeline graph indicated slope across tropical forests.

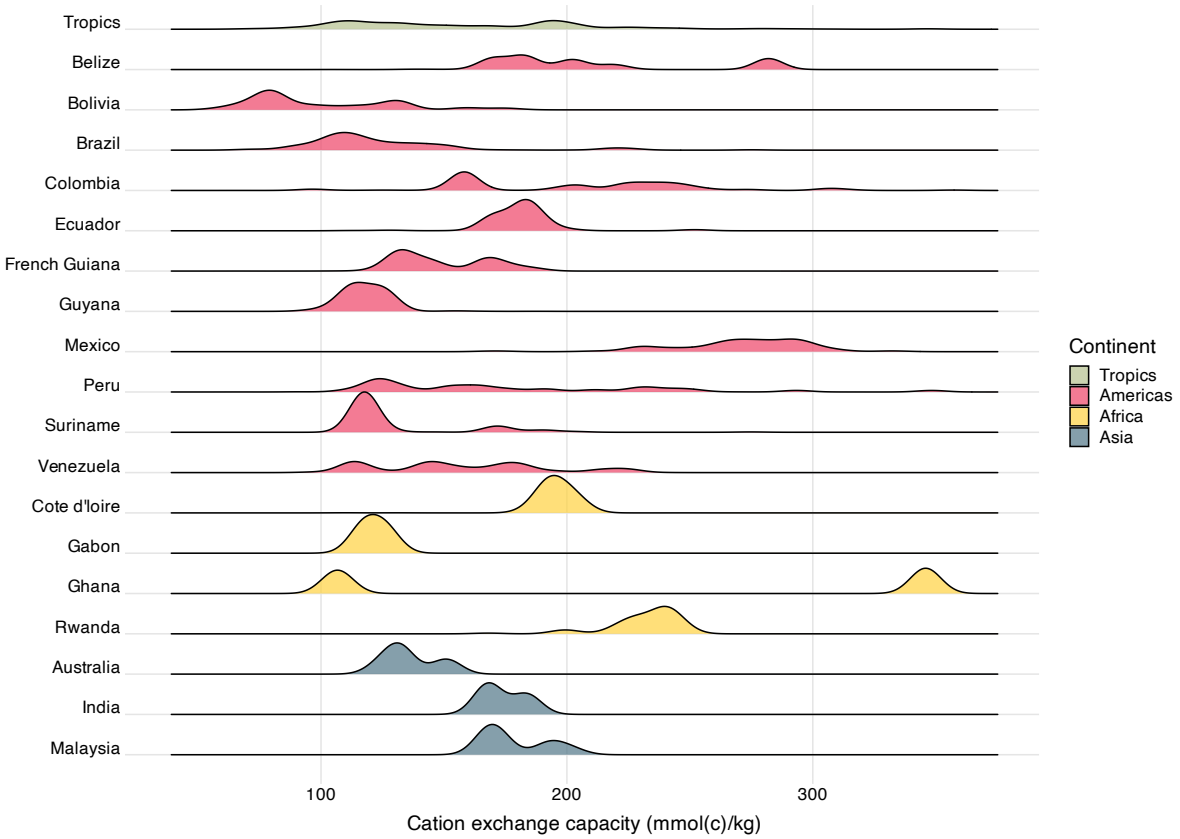

Fig. S4.32. Density distribution plot of cation exchange capacity for each sampling country where plant functional traits were collected. The top ridgeline graph indicated cation exchange capacity across tropical forests.

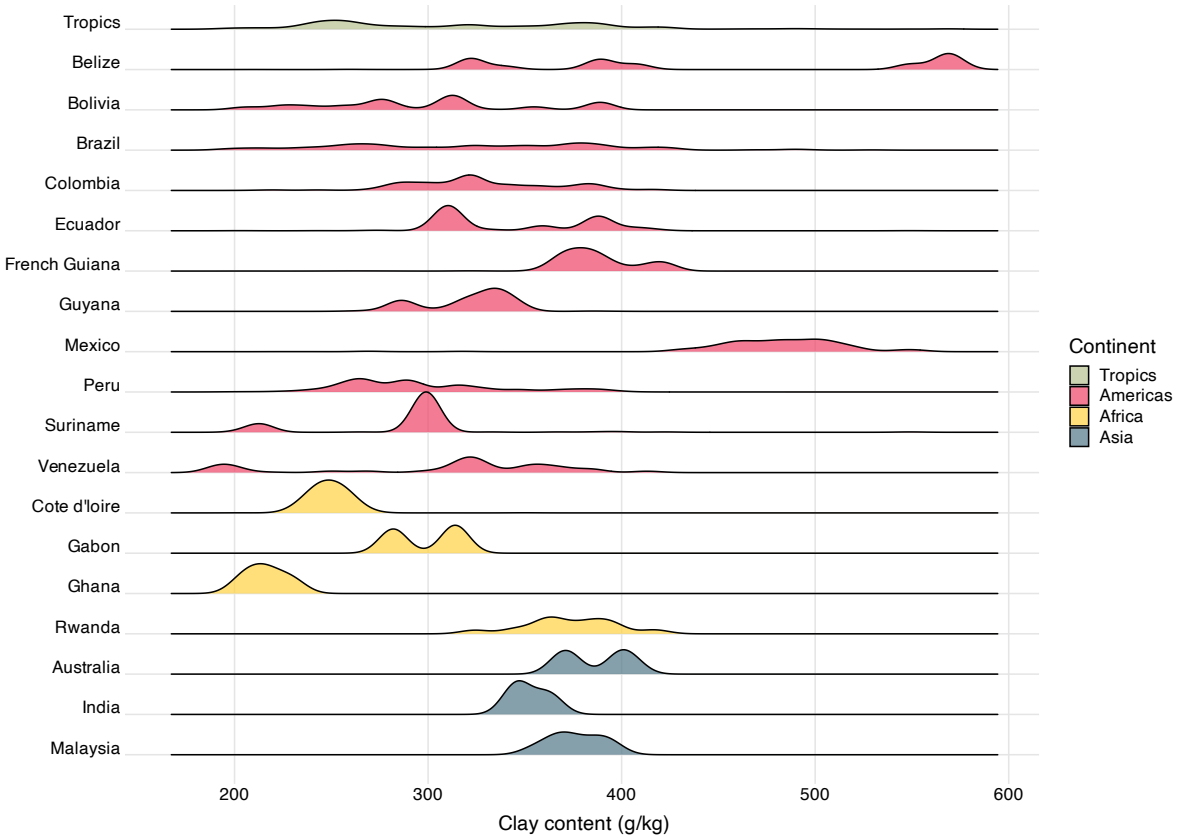

Fig. S4.33. Density distribution plot of clay content for each sampling country where plant functional traits were collected. The top ridgeline graph indicated clay content across tropical forests.

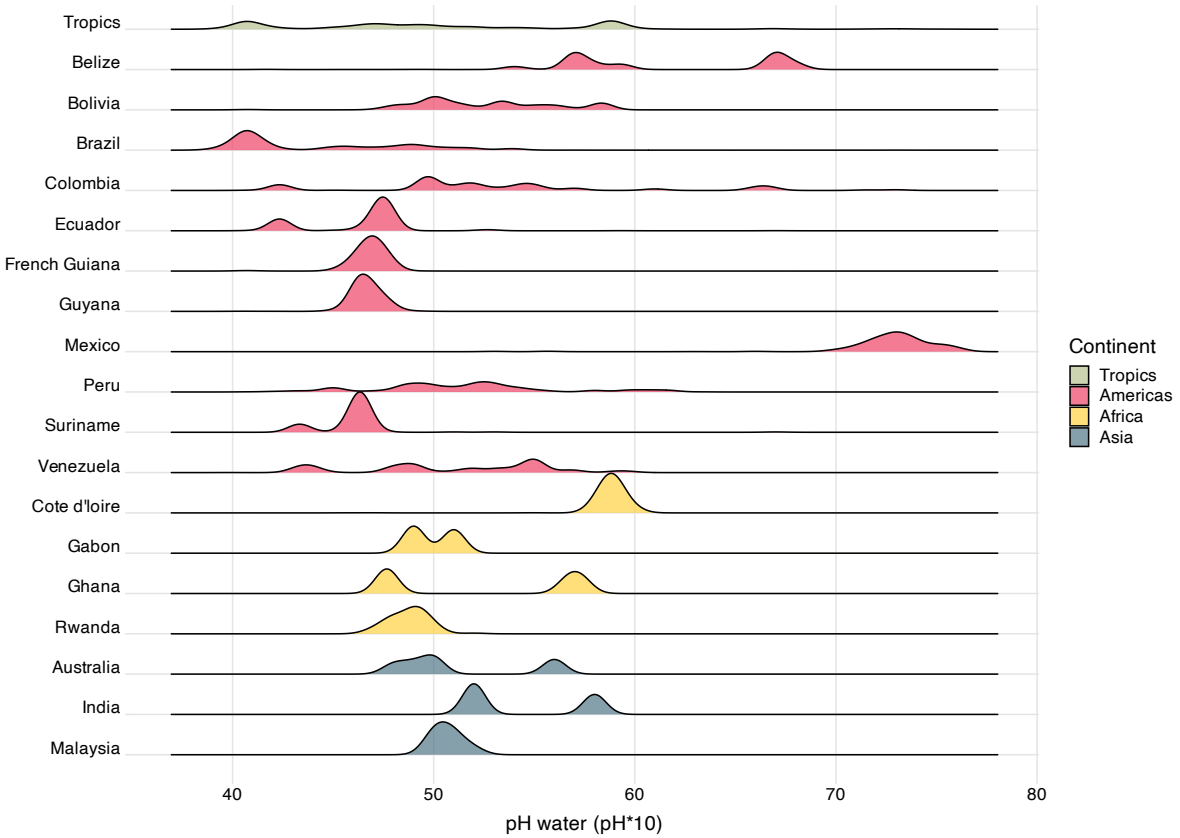

Fig. S4.34. Density distribution plot of soil pH in water for each sampling country where plant functional traits were collected. The top ridgeline graph indicated soil pH in water across tropical forests.

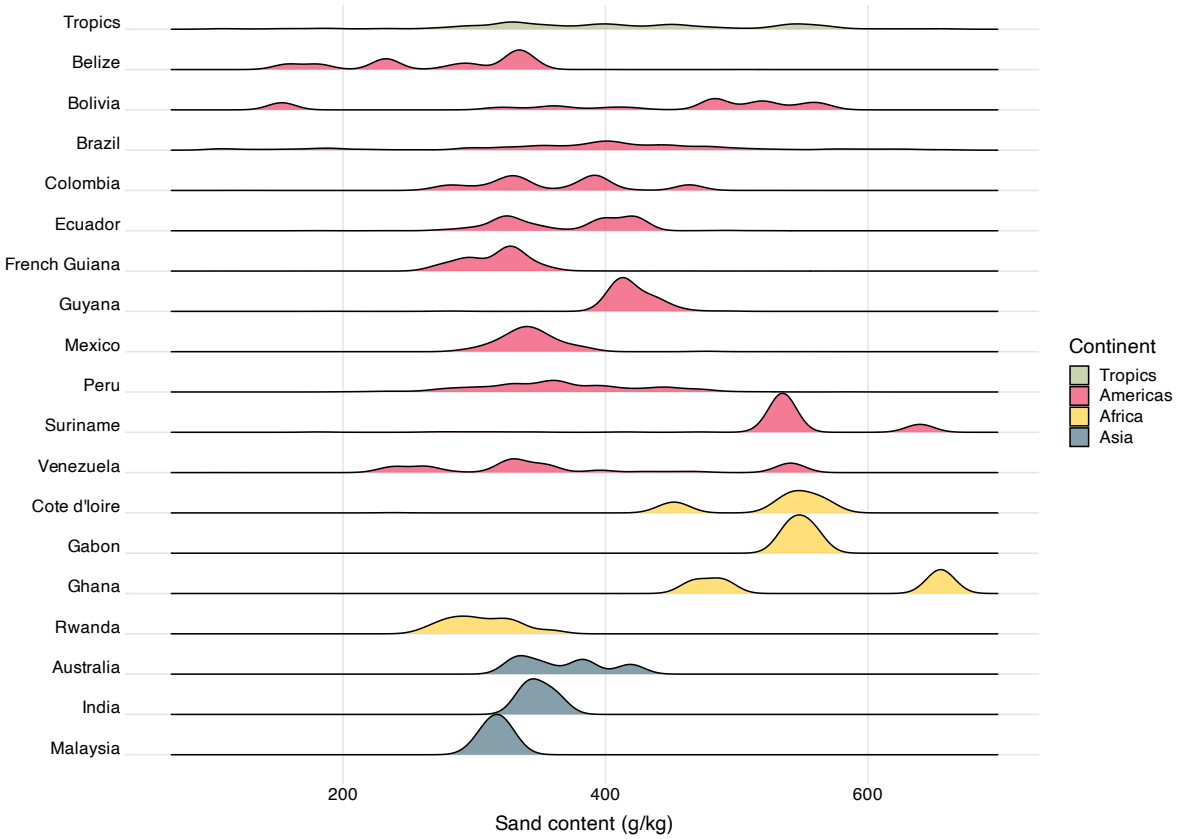

Fig. S4.35. Density distribution plot of sand content for each sampling country where plant functional traits were collected. The top ridgeline graph indicated sand content across tropical forests.

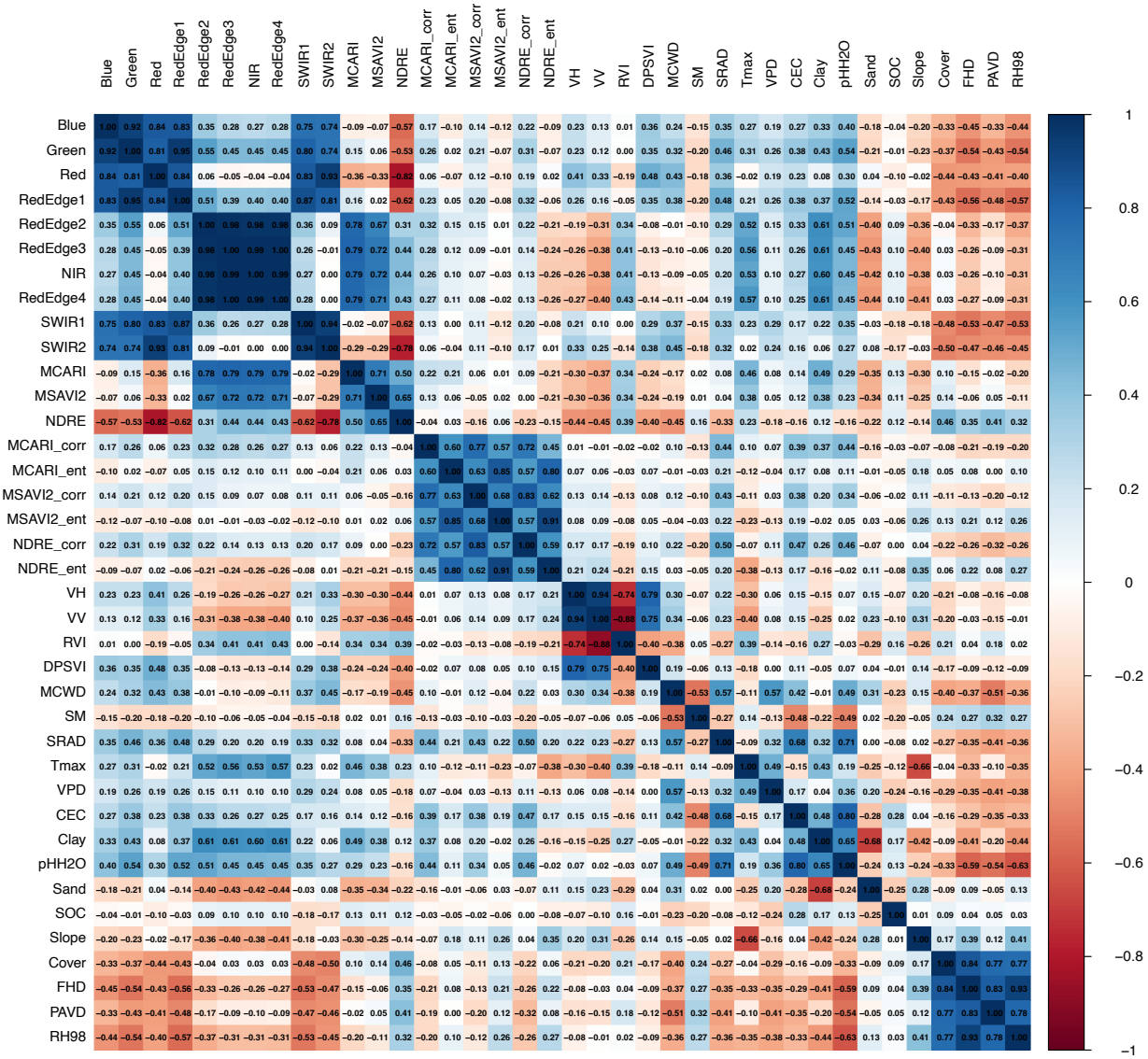

Fig. S4.36. Correlation heatmap of all variables used in this study. SWIR: shortwave infrared, MCARI: modified chlorophyll absorption in reflectance index, MSAVI2: modified soil adjusted vegetation index 2, NDRE: normalised difference red-edge index, MCARI_corr: correlation of MCARI, MCARI_ent: entropy of MCARI, RVI: Radar Vegetation Index, DPSVI: Dual Polarisation SAR Vegetation Index, MCWD: maximum climatological water deficit, SM: soil moisture, SRAD: downward surface shortwave radiation, Tmax: maximum temperature, VPD: vapour pressure deficit, CEC: cation exchange capacity, pHH_2O: soil pH in water, SOC: soil organic carbon, Cover: canopy cover, FHD: foliage height diversity, PAVD: plant area volume density, RH98: the 98th percentile relative height.

4.8.2. Tables

Table S4.1. Moran's *I* test and empirical variogram analysis results.

Type	Trait	Observed	Expected	SD	*P*-value	Distance (km)
Photosynthetic	A_{max}	0.27	-3.62E-05	1.14E-03	<0.01	1.86
	A_{sat}	0.23	-3.65E-05	1.14E-03	<0.01	0.18
Morphological	Leaf dry mass	0.28	-3.68E-05	1.23E-03	<0.01	3.06
	Leaf fresh mass	0.15	-4.62E-05	1.41E-03	<0.01	1.79
	Leaf area	0.29	-3.40E-05	1.22E-03	<0.01	0.5
	Leaf water content	0.23	-4.29E-05	1.31E-03	<0.01	2.13
	SLA	0.29	-3.41E-05	1.23E-03	<0.01	0.15
	Thickness	0.18	-3.52E-05	1.23E-03	<0.01	1.94
	Wood density	0.31	-3.62E-05	1.14E-03	<0.01	1.07
Nutrient	C	0.33	-3.41E-05	1.24E-03	<0.01	0.17
	Ca	0.39	-3.40E-05	1.20E-03	<0.01	2.09
	K	0.36	-3.40E-05	1.20E-03	<0.01	2.32
	Mg	0.19	-3.40E-05	1.19E-03	<0.01	0.17
	N	0.41	-3.34E-05	1.22E-03	<0.01	0.15
	P	0.54	-3.34E-05	1.22E-03	<0.01	3.06

Table S4.2. Leave-one-cluster-out cross-validation results. Here we showed mean R^2 and RMSE values for each trait.

Type	Trait	R^2	RMSE
Photosynthetic	A_{max}	0.31	3.23
	A_{sat}	0.24	1.47
Morphological	Leaf dry mass	0.26	2.82
	Leaf fresh mass	0.11	6.36
	Leaf area	0.22	90.53
	Leaf water content	0.24	4.90
	SLA	0.27	24.40
	Thickness	0.12	10.23
	Wood density	0.42	0.08
Nutrient	C	0.33	1.51
	Ca	0.47	0.34
	K	0.28	0.32
	Mg	0.36	0.09
	N	0.38	0.33
	P	0.53	0.02

Table S4.3. Leave-one-plot-out cross-validation results. Here we showed mean R^2 and RMSE values for each trait.

Type	Trait	R^2	RMSE

Photosynthetic	A_{max}	0.32	3.14
	A_{sat}	0.23	1.48
Morphological	Leaf dry mass	0.26	2.41
	Leaf fresh mass	0.17	7.40
	Leaf area	0.20	224.90
	Leaf water content	0.29	5.26
	SLA	0.31	25.49
	Thickness	0.23	10.40
	Wood density	0.46	0.08
Nutrient	C	0.40	1.58
	Ca	0.48	0.34
	K	0.35	0.29
	Mg	0.41	0.11
	N	0.39	0.33
	P	0.60	0.03

Table S4.4. Leave-one-country-out cross-validation results. Here we showed mean R^2 and RMSE values for each trait.

Type	Trait	R^2	RMSE
Photosynthetic	A_{max}	0.20	3.93
	A_{sat}	0.17	1.88
Morphological	Leaf dry mass	0.23	5.30
	Leaf fresh mass	0.08	8.13
	Leaf area	0.16	226.15
	Leaf water content	0.16	5.65
	SLA	0.21	31.02
	Thickness	0.18	12.72
	Wood density	0.28	0.10
Nutrient	C	0.31	2.23
	Ca	0.34	0.47
	K	0.19	0.33
	Mg	0.33	0.14
	N	0.26	0.46
	P	0.45	0.04

Table S4.5. Leave-one-continent-out cross-validation results.

Type	Trait	LOO-CV method	R^2	RMSE
Photosynthetic	A_{max}	Americas out	0.03	4.37
	A_{sat}		0.01	2.70
Morphological	Leaf dry mass		3.89E-03	6.03
	Leaf fresh mass		4.57E-03	9.59
	Leaf area		3.27E-03	233.11

	Leaf water content		0.03	6.07
	SLA		0.02	34.55
	Thickness		0.02	10.98
	Wood density		0.12	0.14
Nutrient	C		0.04	2.39
	Ca		0.03	0.78
	K		0.02	0.52
	Mg		0.05	0.15
	N		0.04	0.46
	P		0.09	0.05
Photosynthetic	A_{max}		0.10	5.17
	A_{sat}		0.01	2.78
Morphological	Leaf dry mass		0.06	1.38
	Leaf fresh mass		2.45E-03	3.60
	Leaf area		0.03	146.01
	Leaf water content		0.22	4.83
	SLA		0.13	23.96
	Thickness	Africa out	0.05	5.36
	Wood density		0.09	0.11
Nutrient	C		0.06	2.88
	Ca		0.33	0.86
	K		0.09	0.34
	Mg		0.08	0.10
	N		0.31	0.61
	P		0.19	0.05
Photosynthetic	A_{max}		0.06	6.63
	A_{sat}		3.15E-03	2.57
Morphological	Leaf dry mass		0.02	3.91
	Leaf fresh mass		1.15E-03	10.19
	Leaf area		0.02	291.39
	Leaf water content		0.01	14.54
	SLA		0.09	36.63
	Thickness	Asia out	0.06	18.19
	Wood density		0.06	0.10
Nutrient	C		0.02	3.27
	Ca		0.17	0.57
	K		0.06	0.45
	Mg		0.06	0.17
	N		0.19	0.74
	P		0.21	0.04

Table S4.6. Functional trait distribution and variation at continental scale.

Type	Trait	Continent	Mean	Median	SD	Min	Max
Photosynthetic	A_{max}	Africa	14.94	14.18	3.91	8.54	23.97
		Americas	12.89	12.54	2.69	8.43	22.49
		Asia	14.61	13.72	3.73	8.52	23.84

	A_{sat}	Africa	6.01	5.69	1.37	3.61	8.93
		Americas	5.38	5.22	1.12	2.95	8.21
		Asia	5.61	5.37	1.23	3.61	8.56
Morphological	Leaf dry mass	Africa	1.19	1.14	0.43	0.53	2.24
		Americas	0.92	0.83	0.34	0.38	1.73
		Asia	1.07	1.02	0.37	0.51	1.93
	Leaf fresh mass	Africa	3.11	2.81	1.43	1.83	6.27
		Americas	2.48	2.16	1.16	1.04	5.62
		Asia	2.85	2.57	1.29	1.36	5.92
	Leaf area	Africa	129.98	128.37	46.07	48.84	210.91
		Americas	99.94	90.00	38.21	50.17	204.03
		Asia	108.12	101.88	38.86	52.35	207.80
	Leaf water content	Africa	54.82	54.21	3.77	34.46	68.34
		Americas	53.88	52.98	4.40	41.34	71.92
		Asia	58.82	58.41	4.53	48.18	69.73
	SLA	Africa	137.90	138.71	16.25	102.42	171.99
		Americas	127.58	126.05	15.45	96.49	166.57
		Asia	120.34	116.48	15.47	97.18	159.17
	Thickness	Africa	0.27	0.25	0.08	0.08	0.87
		Americas	0.32	0.26	0.15	0.28	1.13
		Asia	0.28	0.26	0.06	0.20	0.72
	Wood density	Africa	0.61	0.61	0.09	0.43	0.83
		Americas	0.62	0.61	0.09	0.40	0.92
		Asia	0.57	0.58	0.09	0.37	0.76
Nutrient	C	Africa	46.17	46.16	1.62	39.74	55.68
		Americas	47.59	47.83	1.48	43.00	54.31
		Asia	45.63	45.53	1.46	36.20	48.93
	Ca	Africa	1.22	1.46	0.48	0.45	2.06
		Americas	0.74	0.65	0.29	0.21	1.57
		Asia	0.90	0.83	0.33	0.37	1.89
	K	Africa	0.94	0.99	0.15	0.41	1.34
		Americas	0.66	0.62	0.18	0.26	1.27
		Asia	0.86	0.85	0.18	0.35	1.17
	Mg	Africa	0.24	0.24	0.03	0.18	0.32
		Americas	0.23	0.23	0.03	0.11	0.27
		Asia	0.24	0.25	0.03	0.19	0.30
	N	Africa	1.99	2.00	0.25	1.41	2.88
		Americas	2.00	2.08	0.23	1.25	2.45
		Asia	1.84	1.87	0.29	0.78	2.21
	P	Africa	0.12	0.12	0.02	0.07	0.20
		Americas	0.09	0.09	0.02	0.02	0.15
		Asia	0.10	0.10	0.02	0.06	0.16

Table S4.7. One-way analysis of variance and post-hoc Tukey honestly significant difference test results.

Type	Trait	Comparison	Difference	LowerCI	UpperCI	*P*-adjusted
Photosynthetic	A_{max}	Americas-Africa	-2.04	-2.15	-1.93	0.00
		Asia-Africa	-0.33	-0.60	-0.06	0.01
		Asia-Americas	1.71	1.46	1.97	0.00

	A_{sat}	Americas-Africa	-0.63	-0.69	-0.57	0.00
		Asia-Africa	-0.40	-0.51	-0.30	0.00
		Asia-Americas	0.23	0.14	0.31	0.00
Morphological	Leaf dry mass	Americas-Africa	-0.26	-0.27	-0.25	0.00
		Asia-Africa	-0.11	-0.15	-0.08	0.00
		Asia-Americas	0.15	0.12	0.18	0.00
	Leaf fresh mass	Americas-Africa	-0.63	-0.67	-0.59	0.00
		Asia-Africa	-0.26	-0.37	-0.15	0.00
		Asia-Americas	0.37	0.26	0.48	0.00
	Leaf area	Americas-Africa	-30.04	-31.33	-28.74	0.00
		Asia-Africa	-21.86	-25.52	-18.19	0.00
		Asia-Americas	8.18	4.65	11.71	0.00
	LWC	Americas-Africa	-0.94	-1.36	-0.52	0.00
		Asia-Africa	3.99	3.46	4.53	0.00
		Asia-Americas	4.94	4.59	5.28	0.00
	SLA	Americas-Africa	-10.33	-10.78	-9.87	0.00
		Asia-Africa	-17.56	-18.95	-16.17	0.00
		Asia-Americas	-7.23	-8.59	-5.88	0.00
	Thickness	Americas-Africa	0.05	0.04	0.05	0.00
		Asia-Africa	0.00	-0.01	0.01	0.56
		Asia-Americas	-0.04	-0.05	-0.03	0.00
	Wood density	Americas-Africa	0.01	0.00	0.01	0.23
		Asia-Africa	-0.04	-0.05	-0.03	0.00
		Asia-Americas	-0.04	-0.05	-0.04	0.00
Nutrient	C	Americas-Africa	1.42	1.35	1.49	0.00
		Asia-Africa	-0.54	-0.66	-0.42	0.00
		Asia-Americas	-1.96	-2.06	-1.86	0.00
	Ca	Americas-Africa	-0.49	-0.50	-0.47	0.00
		Asia-Africa	-0.32	-0.35	-0.30	0.00
		Asia-Americas	0.16	0.14	0.19	0.00
	K	Americas-Africa	-0.28	-0.29	-0.28	0.00
		Asia-Africa	-0.08	-0.09	-0.07	0.00
		Asia-Americas	0.20	0.19	0.22	0.00
	Mg	Americas-Africa	-0.01	-0.01	0.00	0.00
		Asia-Africa	0.00	0.00	0.01	0.02
		Asia-Americas	0.01	0.01	0.01	0.00
	N	Americas-Africa	0.00	-0.01	0.02	0.89
		Asia-Africa	-0.15	-0.17	-0.13	0.00
		Asia-Americas	-0.15	-0.17	-0.14	0.00
	P	Americas-Africa	-0.03	-0.03	-0.03	0.00
		Asia-Africa	-0.02	-0.02	-0.02	0.00
		Asia-Americas	0.01	0.00	0.01	0.00

Table S4.8. Vegetation indices derived from Sentinel-2 spectral bands.

Vegetation index	Equations	Descriptions

MCARI	$MCARI = [(RedEdge - Red) - 0.2 \times (RedEdge - Green)] \times \frac{RedEdge}{Red}$	Modified chlorophyll absorption in reflectance index (Daughtry et al., 2000)
MSAVI2	$MSAVI2 = \frac{1}{2}(2 \times NIR + 1 - \sqrt{(2 \times NIR + 1)^2 - 8 \times (NIR - Red)})$	Modified soil adjusted vegetation index 2 (Qi et al., 1994)
NDRE	$NDRE = \frac{NIR - RedEdge}{NIR + RedEdge}$	Normalised difference red-edge index (Fitzgerald et al., 2010)

Table S4.9. Texture features derived from grey level co-occurrence matrix. In the equations below, N_g is the number of grey levels, *i* and *j* are the grey values in the image, *P(i,j)* denotes the co-occurring probability of two pixels separated by the specified offset having grey values *i* and *j*, while μ_i and μ_j stand for mean values of grey values *i* and *j* that are defined as $\mu_i = \sum_{i=1}^{N_g} iP(i,j)$ and $\mu_j = \sum_{j=1}^{N_g} jP(i,j)$, respectively, σ_i and σ_i standard deviations of grey values i and j that can be determined by $\sigma_i = \sqrt{\sum_{i=1}^{N_g}(i - \mu_i)^2 \cdot P(i,j)}$ and $\sigma_j = \sqrt{\sum_{j=1}^{N_g}(j - \mu_j)^2 \cdot P(i,j)}$, respectively.

Texture feature	Equations	Descriptions
Correlation	$Correlation = \sum_{i=1}^{N_g}\sum_{j=1}^{N_g} P(i,j) \cdot \frac{(i-\mu_i)(j-\mu_j)}{\sigma_i\sigma_j}$	Measures the correlation between pairs of pixels (Haralick et al., 1973)
Entropy	$Entropy = -\sum_{i=1}^{N_g}\sum_{j=1}^{N_g} P(i,j) \cdot log_2(P(i,j))$	Measures the randomness of a grey-level distribution (Zhu et al., 1997)

Table S4.10. Tuned hyperparameter values for Random forests by functional trait. ntree: number of trees, mtry: number of variables considered at each split.

Trait	ntree	mtry
A_{max}	500	10

A_{sat}	650	10
Leaf dry mass	1000	14
Leaf fresh mass	750	9
Leaf area	550	13
Leaf water content	500	11
Specific leaf area (SLA)	500	4
Leaf thickness	350	4
Wood density	600	10
Leaf carbon (C) content	850	11
Leaf calcium (Ca) content	600	8
Leaf potassium (K) content	500	17
Leaf magnesium (Mg) content	950	15
Leaf nitrogen (N) content	800	12
Leaf phosphorus (P) content	1000	16

4.8.3. SAR metrics calculation

4.8.3.1. Radar Vegetation Index

Kim and van Zyl (2009) proposed the Radar Vegetation Index (RVI) to measure soil moisture for both bare and vegetated surfaces using quad-polarisation SAR data, and the RVI was defined as follows:

$$RVI = \frac{8\sigma_{HV}^0}{\sigma_{HH}^0 + \sigma_{VV}^0 + 2\sigma_{HV}^0} \quad (1)$$

where σ_{HV}^0, σ_{HH}^0, and σ_{VV}^0 denotes linear backscattering coefficients of HV, HH, and VV polarisation, respectively.

The original RVI could be only generated from quad-polarisation. The RVI was thus adjusted to adapt to SAR data within only two cross-polarisation channels by assuming that $\sigma_{HH}^0 \approx \sigma_{VV}^0$ (Trudel et al., 2012):

$$RVI_{HH} = \frac{4\sigma^0_{HV}}{\sigma^0_{HH} + \sigma^0_{HV}} \quad (2)$$

where RVI_{HH} is the modification of the *RVI* and especially for SAR data within HH and HV dual-polarisation channels.

Similarly, Nasirzadehdizaji et al. (2019) modified the RVI for Sentinel-1 dual-polarisation (VV-VH) data:

$$RVI_{VV} = \frac{4\sigma^0_{VH}}{\sigma^0_{VV} + \sigma^0_{VH}} \quad (3)$$

where RVI_{VV} denotes the modification of the RVI for SAR data within VV and VH dual-polarisation channels.

4.8.3.2. Dual Polarisation SAR Vegetation Index

Periasamy (2018) proposed the Dual Polarisation SAR Vegetation Index (DPSVI) to retrieve terrestrial biomass in both dry and wet seasons finding its results related to those obtained when using the NDVI calculated from Sentinel-2 optical data and field observed biomass. The DPSVI can be calculated by equation 4:

$$DPSVI = \sigma^0_{VH} \cdot \frac{[((\sigma^0_{VV})_{max} \cdot \sigma^0_{VH} - \sigma^0_{VV} \cdot \sigma^0_{VH} + (\sigma^0_{VH})^2) + ((\sigma^0_{VV})_{max} \cdot \sigma^0_{VV} - (\sigma^0_{VV})^2 + \sigma^0_{VH} \cdot \sigma^0_{VV})]}{\sqrt{2}\sigma^0_{VV}} =$$

$$\frac{(\sigma^0_{VV})_{max} - \sigma^0_{VV} + \sigma^0_{VH}}{\sqrt{2}} \cdot \frac{\sigma^0_{VV} + \sigma^0_{VH}}{\sigma^0_{VV}} \cdot \sigma^0_{VH} \quad (4)$$

where $(\sigma^0_{VV})_{max}$ is the maximum backscattering coefficient in the VV polarisation channel of SAR data.

4.8.4. References

Haralick, R. M., Shanmugam, K., & Dinstein, I. (1973). Textural Features for Image Classification. *IEEE Transactions on Systems, Man, and Cybernetics*, *SMC-3*(6), 610–621. IEEE Transactions on Systems, Man, and Cybernetics. https://doi.org/10.1109/TSMC.1973.4309314

Kim, Y., & van Zyl, J. J. (2009). A Time-Series Approach to Estimate Soil Moisture Using Polarimetric Radar Data. *IEEE Transactions on Geoscience and Remote Sensing*, *47*(8), 2519–2527. IEEE Transactions on Geoscience and Remote Sensing. https://doi.org/10.1109/TGRS.2009.2014944

Trudel, M., Charbonneau, F., & Leconte, R. (2012). Using RADARSAT-2 polarimetric and ENVISAT-ASAR dual-polarization data for estimating soil moisture over agricultural fields. *Canadian Journal of Remote Sensing*, *38*(4), 514–527. https://doi.org/10.5589/m12-043

Zhu, S. C., Wu, Y. N., & Mumford, D. (1997). Minimax Entropy Principle and Its Application to Texture Modeling. *Neural Computation*, *9*(8), 1627–1660. Neural Computation. https://doi.org/10.1162/neco.1997.9.8.1627

4.9. Declarations of competing interest

The authors declare that they have no known competing financial interests or personal relationships that could have appeared to influence the work reported in this paper.

4.10. Acknowledgements

Xiongjie Deng receives the Pay It Forward Scholarship (by China Oxford Scholarship Fund, Oxford) and the New Blackfriars Scholarship (by Blackfriars Hall, Oxford). Yadvinder Malhi is supported by the Frank Jackson Foundation. Jesús Aguirre-Gutiérrez is funded by the NERC (Grants: NE/T011084/1; NE/Z504191/1), the Leverhulme Trust (RPG-2024-342), and the Royal Society (RG\R1\251370).

4.11. Data availability

Because of the data sovereignty from the original data owners, raw data on vegetation censuses and trait data are not publicly available but can be requested by contacting all researchers.

Chapter 5 Quantifying the functional composition and potential resilience hotspots across a large latitudinal and environmental gradient in South American forests (Paper 2)

5.1. Preface

Building on **Paper 1**, which demonstrated the efficiency and robustness of mapping multiple plant functional trait community-weighted means (CWMs) by fusing passive and active remotely sensed data using the Random forests regression algorithm, this chapter extends that approach. Here, we apply the Random forests regression to multispectral and LiDAR data to estimate not only CWMs but also community-weighted variances (CWVs) of leaf and stem morphological, nutrient, hydraulic, and photosynthetic traits. We further explore the resulting functional diversity and redundancy across temperate forests in South America, aiming to reveal key environmental drivers and spatial patterns of ecosystem resilience along a broad latitudinal gradient.

5.1.1. Highlights

This study presents the first 10-m resolution maps of functional trait composition, diversity, and redundancy for Chilean temperate forests, achieving high mapping accuracy by integrating remotely sensed data with the Random forests regression. We identify hydrological stress and soil properties as key drivers shaping trait composition, diversity, and redundancy, and highlight a biodiversity hotspot characterised by high functional diversity and redundancy, suggesting resilience to environmental change.

This chapter titled "Quantifying the functional composition and potential resilience hotspots across a large latitudinal and environmental gradient in South American forests" has been published in the peer-reviewed journal *International Journal of Applied Earth Observation and Geoinformation* on 1 July 2025.

5.1.2. Author information and contribution statement

Xiongjie Deng[1]*, Danny E. Carvajal[2,3], Rocío Urrutia-Jalabert[4,5,6,7], Waira S. Machida[8], Alice Rosen[1,9], Huanyuan Zhang-Zheng[1,10], David Galbraith[11], Sandra Díaz[12,13], Yadvinder Malhi[1,10], Jesús Aguirre-Gutiérrez[1,10]

[1]Environmental Change Institute, School of Geography and the Environment, University of Oxford, Oxford, OX1 3QY, UK
[2]Departamento de Biología, Universidad de La Serena, Casilla 554, La Serena, Chile
[3]Instituto de Ecología y Biodiversidad (IEB), Santiago, Chile
[4]Facultad de Ciencias Agropecuarias y Medioambiente, Universidad de la Frontera, Temuco, Chile
[5]Millennium Nucleus of Patagonian limit of Life (LiLi)
[6]Center for Climate and Resilience Research CR2, Santiago, Chile
[7]Instituto de Conservación Biodiversidad y Territorio, Facultad de Ciencias Forestales y Recursos Naturales, Universidad Austral de Chile, Valdivia, Chile
[8]Departamento de Ecologia, Instituto de Ciências Biológicas, Universidade Federal de Goiás, Brasil
[9]Department of Biology, University of Oxford, Oxford, OX1 3RB, UK
[10]Leverhulme Centre for Nature Recovery, University of Oxford, Oxford, OX1 3QY, UK
[11]School of Geography, University of Leeds, Leeds, UK
[12]Consejo Nacional de investigaciones Científicas y Técnicas, Instituto Multidisciplinario de Biología Vegetal (IMBIV), Córdoba, Argentina
[13]Facultad de Ciencias Exactas, Físicas y Naturales, Universidad Nacional de Córdoba, Córdoba, Argentina

Xiongjie Deng: Writing – original draft, Writing – review & editing, Methodology, Investigation, Software, Formal analysis, Conceptualisation. **Danny E. Carvajal:** Writing – review & editing, Methodology, Field data collection. **Rocío Urrutia-Jalabert:** Writing – review & editing, Methodology, Field data collection. **Waira S. Machida:** Methodology. **Alice Rosen:** Writing – review & editing, Methodology. **Huanyuan Zhang-Zheng:** Writing – review & editing, Methodology. **David Galbraith:** Writing – review & editing, Methodology. **Sandra Díaz:** Writing – review & editing. **Yadvinder Malhi:** Writing – review & editing, Methodology, Supervision, Field data collection. **Jesús Aguirre-Gutiérrez:** Writing – review & editing, Methodology, Investigation, Conceptualisation, Supervision, Field data collection.

5.2. Abstract

Accurately inferring plant functional trait composition, diversity, and redundancy across space and time is pivotal for understanding environmental change impacts on forests' biodiversity and functioning. Here, we provided the first large-scale and high-resolution (10 m) mapping of functional biodiversity in in South American temperate forests (30°S to 53°S). Specifically, we tested the capabilities of combining *in-situ* and remote sensing approaches to deliver accurate estimates of functional trait composition, diversity, and redundancy of temperate forest vegetation in South America considering leaf and stem morphological, nutrient, hydraulic, and photosynthetic traits. We identified hydrological stress, soil properties, and topography as key drivers of plant functional trait distribution and variation. Further, hydrological stress and soil properties were key determinants of functional diversity and redundancy across a large latitudinal gradient. Functional diversity peaked across Mediterranean forests, occupying between 30°S to 35°S. Functional diversity and redundancy were both high at latitudes between 35°S and 42°S, coinciding with Valdivian rainforests. Conversely, functional redundancy peaked between 42°S and 48°S, corresponding to Austral forests. Towards the southernmost extent of the study area, functional diversity and redundancy were both low between 48°S and 53°S, corresponding to the Magellanic subpolar forests. Our results highlight areas in South American temperate forests where both plant functional diversity and redundancy were maximal, hence potentially pointing towards areas more resilient to environmental change, and demonstrate the novel contributions of this study in integrating high-resolution trait mapping with ecological assessment of ecosystem stability.

Keywords: Remote sensing; Functional traits; Functional diversity; Functional redundancy; Temperate forests; Trait-environment relationships

5.3. Introduction

Temperate forests show remarkable diversity in terms of species, soil composition, and the carbon dynamics within their ecosystems (Malhi et al., 1999, 2024). In particular, due to their geographic isolation, temperate forests in Chile are highly endemic at species and higher taxonomic levels (Smith-Ramírez, 2004), and thus have become a priority for conservation

(Echeverría et al., 2006). These temperate forests also provide essential contributions to people (Isbell et al., 2017), protecting watersheds, and absorbing and storing large amounts of carbon (Chen et al., 2023; Perez-Quezada et al., 2021; Urrutia-Jalabert, Malhi, & Lara, 2015). These forests therefore contribute to long-term carbon sequestration (Oliver et al., 2015) and further influence temperature, humidity, and precipitation patterns (Ellis & Eaton, 2021). However, these forests are under persistent threat from replacement by other land covers and uses, such as crops and exotic plantations, degradation (Echeverría et al., 2006), unsustainable logging, warming, and precipitation decrease (Miranda et al., 2017; Perez-Quezada et al., 2023; Urrutia-Jalabert, Malhi, Barichivich, et al., 2015). As a result, the interactions that underpin ecosystem functions and benefits to people have become progressively fragile (Donohue et al., 2016). Therefore, it is essential to understand how ecosystem functioning and biodiversity vary across environmental gradients and respond to key environmental drivers in such temperate forests. This knowledge is crucial for anticipating long-term ecosystem resilience and nature's contributions to people (Bjorkman et al., 2018; Cardinale et al., 2012).

Previous studies exploring relationships between biodiversity and the environment predominantly relied on taxonomic methods to assess the impact of biodiversity on ecosystem functioning (Meyer & Kröncke, 2019). In contrast to taxonomic methods, trait-based approaches focus on functional traits, i.e., traits that represent their morphological, physiological, biochemical or phenological characteristics. These traits are thought to be highly relevant to plant responses to the environmental stress and their impact on wider ecosystem properties (Díaz et al., 2013). By analysing functional traits, we can better understand how plants adjust or adapt to different environmental conditions (Kergunteuil et al., 2019), explain productivity in forests (Zhang-Zheng, Adu-Bredu, et al., 2024; Zhang-Zheng, Deng, et al., 2024), and shed light on the role of plants in ecosystem processes (Díaz et al., 2013). Two metrics are widely used to quantify functional trait composition: the community-weighted mean (CWM) and community-weighted variance (CWV). CWM and CWV correspond to the average and variance in trait values within a community, weighted by the relative abundance (Laliberté & Legendre, 2010) or basal area (Aguirre-Gutiérrez et al., 2025; Pla et al., 2012) of each species. CWM represents the dominant trait values within a community and reflects the average functional characteristics shaped by the most abundant species, while CWV measures the trait diversity within the community and indicates the range and variability of functional strategies present.

Functional diversity is a vital component of biodiversity that captures the range and distribution of plant functional traits across spatial scales (Díaz et al., 2013; Ma et al., 2019). It is a determinant of ecosystem processes (Hooper et al., 2005), ecosystem resilience to environmental change (Aguirre-Gutiérrez et al., 2025; Folke et al., 2004), and provision of nature's benefits to people (Díaz et al., 2007; Laliberté & Legendre, 2010). As a commonly used functional diversity metric, functional dispersion quantifies the extent of trait dissimilarity within plant communities (M. Cadotte et al., 2013), elucidating how divergent or convergent species are in a community in terms of their functional traits. It is expected that higher functional dispersion (i.e., variation in plant trait values in the community) would render higher resilience to environmental change as at least some species should be able to thrive under the changing conditions (Hooper et al., 2005).

In addition, functional redundancy is the degree to which multiple species within an ecosystem show similar functional attributes and therefore are assumed to perform similar ecological roles or functions. This potentially suggests that when one species disappears, other species with similar trait values would be able to carry out the same ecosystem functions than the species lost (Rosenfeld, 2002). Ecosystems with low functional redundancy may be more vulnerable to environmental changes because there are fewer functionally similar species able to fill the roles of the species that are lost (Rosenfeld, 2002). Hence, functional redundancy is thought to be important for ecosystem stability and resilience in the face of disturbances, including extreme climatic events (Oliver et al., 2015). Therefore, assessing both functional diversity and redundancy in an ecosystem is particularly relevant for understanding forest resilience to environmental change (Carmona et al., 2016; F. D. Schneider et al., 2017).

Trait-based approaches have been valuable in describing and predicting ecosystem functions at the individual-to-plot scales. However, their upscaling to whole ecosystems and beyond has proven challenging (Suding et al., 2008). Still, recent advances in remote sensing techniques have allowed upscaling of some functional traits to global scales and the assessment of functional diversity continuously in space for relatively small areas (Hauser et al., 2021; Helfenstein et al., 2022; F. D. Schneider et al., 2017). Remote sensing platforms, including light detection and ranging (LiDAR), multispectral, and image spectroscopy data from both drone and satellite sensors, enable continuous and repeatable data acquisition that can be used to model and map functional traits across ecosystems (Aguirre-Gutiérrez et al., 2025; R. Wang & Gamon, 2019). Specifically, high-resolution LiDAR and spectral (including multispectral and image spectroscopy) data acquired from drone platforms can be used to characterise forest

structural attributes (e.g., canopy height) and canopy reflectance properties, respectively, both of which are closely linked to functional traits (Asner et al., 2017; Camarretta et al., 2020; Kamoske et al., 2021). These detailed measurements at local scales offer critical insights into trait-environment relationships but are often spatially constrained. By integrating such plot-scale observations with coarser-resolution satellite-based remote sensing data, it becomes possible to bridge the spatial "scale-gap" (Thomson et al., 2021) to extend trait-based ecological information from individual plots to entire landscapes or regions (Jetz et al., 2016; Thomson et al., 2021; R. Wang & Gamon, 2019). The multiscale integration of remote sensing and trait-based ecology represents a scalable and essential approach for understanding functional biodiversity across complex landscapes, particularly in data-poor regions such as the temperate forests of South America (Kier et al., 2005; Sheffield et al., 2018).

Despite the capabilities of remote sensing approaches to upscale and predict some functional attributes, there is a lack of understanding about mapping and predicting variability in plant functional traits distribution (Butler et al., 2017) and plant functional diversity and redundancy at large spatial scales (Hortal et al., 2015), particularly in temperate forests beyond North America and Western Europe (Echeverría-Londoño et al., 2018). Besides remotely sensed imagery, environmental variables are also crucial for mapping plant functional traits and inferring functional diversity and redundancy as they shape the conditions under which plants grow and interact (Fortunel et al., 2014; Krishnadas et al., 2018; Wieczynski et al., 2019). Variation in climate, soil properties, topography, and hydrological stress directly influence the expression and performance of plant functional traits. These traits, in turn, determine how plants interact with each other and their environment, affecting overall community structure and ecosystem processes (Díaz et al., 2013; Zirbel et al., 2017). Variation in these biotic and abiotic drivers underpin the adaptation capacity of plants, and it could be expected that higher variation in ecological niches would also lead to a wide array of vegetation functional trait adaptation.

Here, we combined leaf and stem trait data measured *in-situ* from 8104 individual trees across 16 permanent forest plots in Chile with multi-scale remotely sensed data from multiple platforms and diverse environmental variables to model and predict community-level plant functional composition across a large latitudinal and environmental gradient using the Random forests algorithm. Trait data included leaf and stem morphological traits, leaf nutrients, hydraulic, and photosynthetic traits. The plots were distributed across a large latitudinal gradient extending from Mediterranean climate at ~30°S to cold temperate climate at ~53°S,

covering a large annual rainfall (450-4500 mm) and mean annual temperature gradient (5.7-13°C). Our main objectives were to 1) test if and to what extent functional trait composition, diversity, and redundancy can be inferred using remotely sensed data; 2) evaluate how community-level tree functional trait composition, diversity, and redundancy vary across the latitudinal and environmental gradients using both field-based data and spatially explicit model predictions; and 3) identify and quantify the main environmental drivers of distributions of functional trait composition, diversity, and redundancy. We expect higher tree trait variation and higher functional diversity and lower redundancy in areas with more varied climate, topography and soil conditions. Conversely, we expect lower trait variation and higher functional redundancy in areas where climates are more restrictive, or more extreme for plant growth, such as in very cold or very warm areas often impacted by drought.

5.4. Methods and materials

5.4.1. Study area

The study area spans the temperate forests of Chile, South America, which covers a broad latitudinal gradient from approximately 30°S to 53°S. This range encompasses diverse forest ecosystems, including Mediterranean forests (~30°S to ~35°S) (Cueto et al., 2025), Valdivian rainforests (~35°S to ~42°S) (NAHUELHUAL et al., 2007), Austral forests (~42°S to ~48°S) (Huertas Herrera et al., 2023), and Magellanic subpolar forests (~48°S to ~53°S) (Rozzi et al., 2023). The local climate varies considerably along this gradient, with a wide range of environmental conditions, including significant variation in annual precipitation (450-4500 mm) and mean annual temperature (5.7-13°C). In the northernmost Mediterranean zone, the climate is characterised by hot, dry summers and mild, wet winters (Kaiser et al., 2008). Between 35°S and 42°S, the climate transitions to a temperate rainforest type, typical of the Valdivian rainforests, where consistent high annual rainfall (often exceeding 3000 mm) and cooler temperatures create a humid environment (Tecklin et al., 2011). Further south, from 42°S to 53°S, the climate shifts to colder, wetter conditions in the Austral forests and

Magellanic subpolar forests, which experience frequent rainfall and cold spells (Le Roux, 2012; Rozzi et al., 2023).

5.4.2. Field measurements

We conducted vegetation censuses of 8104 individuals (identified to species level) with diameter at breast height ≥10 cm across 16 vegetation plots in seven sites along a wide latitudinal and elevational gradient (from 327.34 to 1251.71 m). Specifically, there are three 0.36-ha plots in Las Cabras (CAB), three 0.36-ha plots in Radal Siete Tazas (RAD), two 1-ha plots in San Pablo de Tregua (SPT), two 0.6-ha plots in Alerce Costero National Park (ALE), two 1-ha plots in Correntoso (COR), two 1-ha plots in Trapananda National Reserve (TRA), and two 1-ha plots in Magallanes National Reserve (MAG) (Fig. 5.1A, B and Supplementary Tables S5.1 and S5.2). These plots largely represent temperate forests, but the CAB plots are also representative of drier and shrubby vegetation. Here, for simplicity we refer to all of them as "forests". The field data collection was carried out between 10 February 2020 and 25 January 2022. To get a holistic view of community dynamics and acquire a comprehensive assessment of functional diversity and redundancy within temperate forests, we measured and calculated a diverse set of leaf and stem functional traits spanning four functional categories (Supplementary Tables S5.3 to S5.6). These included: eight morphological traits: leaf fresh weight (FW, g), leaf dry weight (DW, g), leaf area (LA, cm^2), specific leaf area (SLA, $cm^2\ g^{-1}$), leaf mass per area (LMA, $g\ cm^{-2}$), leaf dry matter content (LDMC, $mg\ g^{-1}$), trunk wood density (TWD, $g\ cm^{-3}$), and branch wood density (BWD, $g\ cm^{-3}$). SLA and LMA were derived from directly measured traits (i.e., LA and FW), although SLA and LMA are mathematically inverses, they offer different insights. SLA is commonly used in growth analyses due to its positive linear relationship with relative growth rate, whereas LMA is more intuitive when analysing structural investment in leaves (Poorter et al., 2009). Six nutrients (i.e., leaf chemical traits): calcium (Ca, %), potassium (K, %), magnesium (Mg, %), nitrogen (N, %), and phosphorus (P, %) content in leaves, and the ratio of leaf nitrogen content and leaf phosphorus content (N/P, unitless). Five hydraulic traits: water potential at which 50% and 88% of hydraulic conductivity is lost (P50 and P88, MPa), minimum water potential (WPmd, MPa), and safety margin for P50 and P88 (SM50 and SM88, MPa). Five photosynthetic traits: temperature at the carbon compensation point (TmaxL, °C), temperature of optimum photosynthesis (Topt, °C), photosynthetic rate at optimum temperature (Aopt, $\mu mol\ CO_2\ m^{-2}\ s^{-1}$), breadth of the temperature optimum (TspanL, °C), and temperature at which the maximum

quantum yield of the photosystem II declines to 50% (T50, °C). Together, these traits offer insights into different aspects of plant function: physical structure, nutrient cycling and ecosystem productivity, water transport strategies, and the efficiency of energy capture and utilisation. Plant traits were collected for the most abundant species, so that we have a coverage of at least 80% of the plot's basal area with trait values.

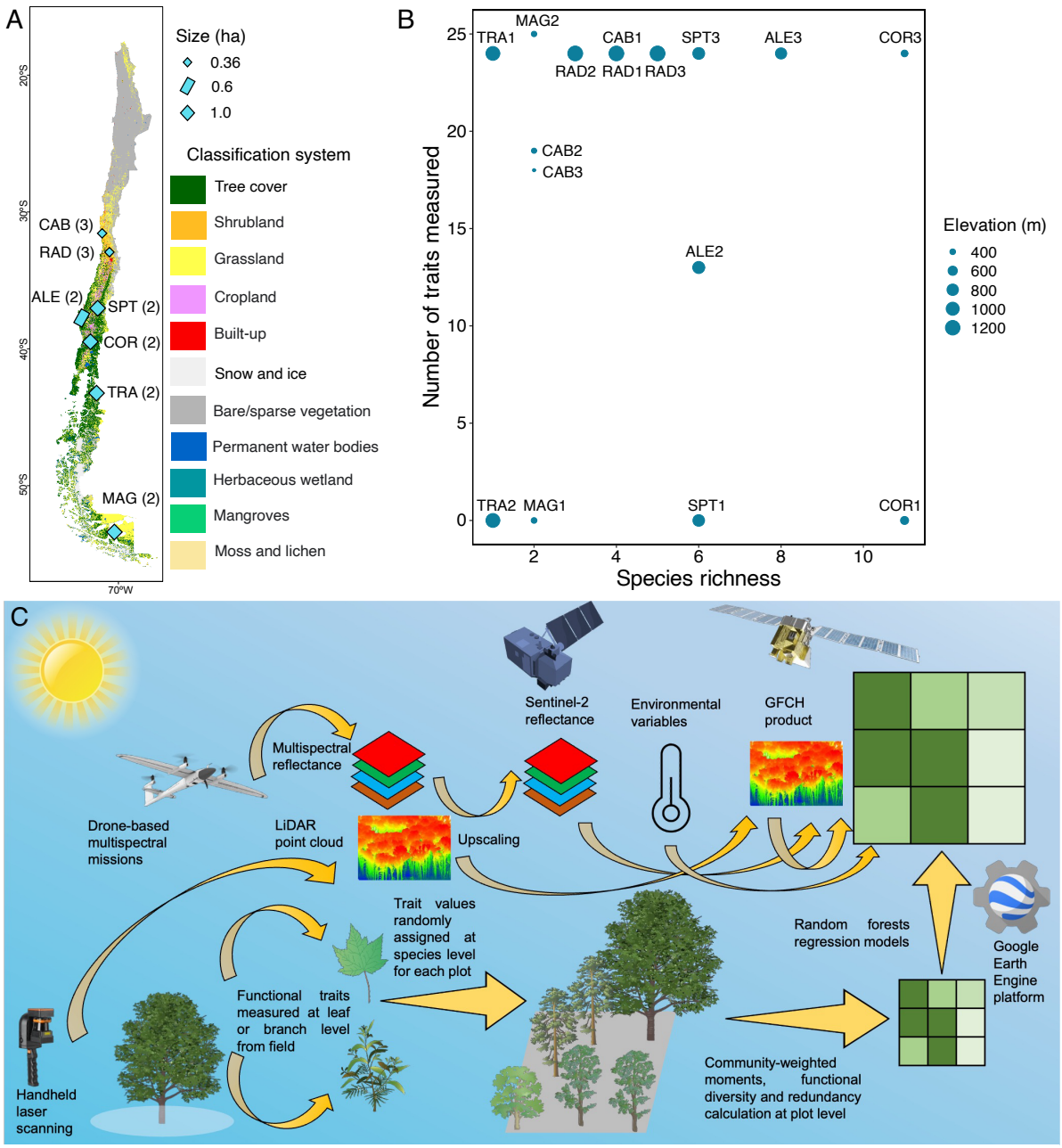
A
Size (ha)
0.36
0.6
1.0
Classification system
Tree cover
Shrubland
Grassland
Cropland
Built-up
Snow and ice
Bare/sparse vegetation
Permanent water bodies
Herbaceous wetland
Mangroves
Moss and lichen
CAB (3)
RAD (3)
ALE (2)
SPT (2)
COR (2)
TRA (2)
MAG (2)
20°S
30°S
40°S
50°S
70°W
B
Number of traits measured
Species richness
Elevation (m)
400
600
800
1000
1200
TRA1
MAG2
CAB1
SPT3
ALE3
COR3
RAD2
RAD1
RAD3
CAB2
CAB3
ALE2
TRA2
MAG1
SPT1
COR1
C
Sentinel-2 reflectance
Environmental variables
GFCH product
Multispectral reflectance
Drone-based multispectral missions
LiDAR point cloud
Upscaling
Trait values randomly assigned at species level for each plot
Functional traits measured at leaf or branch level from field
Handheld laser scanning
Random forests regression models
Google Earth Engine platform
Community-weighted moments, functional diversity and redundancy calculation at plot level
D
Field data collection
Model training and validation
Upscaling to the ecosystem
Biodiversity metrics
Drone images
Traits
Random forests
Important variables
Satellite imagery
Wall-to-wall mapping
CWM
CWV
FDis
FRed

Fig. 5.1. General workflow of the methodological framework used in this study. (**A**) Geographic distribution of the seven study sites along the Chilean latitudinal gradient. Site locations are shown by cyan rectangles with black boundaries. The number in brackets after the abbreviated site name corresponds to the number of plots in that site. Plot sizes within each site are shown by the size of the cyan rectangle (0.36 ha, 0.6 ha, or 1.0 ha plots). Note that all the rectangles are magnified for visualisation purposes. The background map is based on the WorldCover v200 land use and land cover product. (**B**) Detailed information on species richness and the number of traits measured in the field for each plot. The size of each dot indicates the elevation of the plot. Note: there is no trait measurement in plots COR1, MAG1, SPT1, and TRA2, but the species identified in these plots also exist in other plots. (**C**) Mapping plant functional trait composition, diversity, and redundancy with remote sensing and trait-based methods. This process integrates field-collected trait data with advanced remote sensing technologies. In the field, we collected leaf and stem samples from individual trees, and these samples were subsequently analysed in the lab to measure and calculate plant functional traits (see Supplementary: Sampling design and Trait measurements). We also obtained drone-level multispectral images and handheld LiDAR data for most forest plots. For plots without drone multispectral images (SPT1, ALE2, COR1, COR3, and MAG1) or handheld LiDAR data (COR1 and COR3), Planet SuperDove multispectral images and the global forest canopy height (GFCH) product were used. Trait community-weighted means and variances were calculated, representing trait averages and variability, and functional diversity and redundancy were derived from these traits at plot level. We used Random forests regression to establish the link between multispectral, LiDAR, environmental variables and functional traits. To extend these insights from plot to landscape level, we utilised satellite-based remotely sensed data, including Sentinel-2 (multispectral reflectance), the GFCH product (LiDAR-derived canopy height), environmental variables including TerraClimate (climatic variables), SoilGrids (soil properties), SRTM (topography), and ECOSTRESS (hydrological stress). (**D**) Simplified schematic of the main steps: field data collection, model development with Random forests, upscaling with satellite data, and generation of trait maps across Chile.

5.4.3. Plot level remote sensing: multispectral images and laser scanning

We implemented drone missions to obtain high-resolution multispectral images (~5 cm pixel) using the MicaSense Altum multispectral camera across 11 plots, and handheld LiDAR data using the ZEB1 3D handheld laser scanner from GeoSLAM across 14 plots. For the plots

without drone multispectral or handheld LiDAR data due to environmental constraints, we obtained analysis-ready SuperDove multispectral (3 m, containing either five or eight bands, see Supplementary Table S5.7) satellite images from PlanetLabs (https://www.planet.com/) and also extracted canopy height information from the global forest canopy height (GFCH) product (Potapov et al., 2021) (Supplementary Table S5.8). To make the high-resolution datasets comparable with coarser satellite and GFCH product, we harmonised them at the plot level. Specifically, the drone imagery was spectrally subset to match the closest SuperDove bands (red, green, blue, red-edge, and NIR) and spatially aggregated to the plot scale, yielding mean reflectance values directly comparable to Planet SuperDove satellite imagery (3 m). Similarly, handheld LiDAR data were processed to generate plot-level canopy height distributions, from which mean height values were extracted. These were then compared with and made consistent with canopy height estimates derived from the GFCH product. By harmonising all measurements to the same plot-level ecological unit, we ensured that remote sensing predictors from different platforms were comparable for trait prediction analyses.

We processed the six-band MicaSense Altum-PT multispectral images using the Pix4Dmapper software (https://www.pix4d.com/product/pix4dmapper-photogrammetry-software/), following the workflow outlined in the MicaSense Pix4D processing guide (https://support.micasense.com/hc/en-us/articles/115000831714-How-to-Process-MicaSense-Sensor-Data-in-Pix4D). Note that we kept the blue, green, red, red edge, and near-infrared (NIR) bands due to their consistent presence in both drone images and SuperDove satellite images. Additionally, we calculated four vegetation indices, the normalised difference vegetation index (NDVI) (Myneni et al., 1995), normalised difference red edge index (NDRE) (Gitelson & Merzlyak, 1994), soil-adjusted vegetation index (SAVI) (Huete, 1988), and modified soil-adjusted vegetation index (MSAVI) (Qi et al., 1994) to model the functional trait composition, diversity, and redundancy (Supplementary Table S5.9). These indices were selected because they are sensitive to vegetation structure, canopy greenness, and photosynthetic activity, which are closely related to plant functional traits. NDVI and NDRE are widely used indicators of chlorophyll content and photosynthetic potential, making them relevant for modelling traits linked to productivity and leaf function (Aguirre-Gutiérrez et al., 2025; Helfenstein et al., 2022; Sun et al., 2024). SAVI and MSAVI adjust for soil background effects and are especially useful in areas with varying vegetation cover, which helps to better capture spatial heterogeneity relevant to functional trait distributions and biodiversity metrics (Aguirre-Gutiérrez et al., 2025; Hussain et al., 2020; Sun et al., 2024; Z. Wang et al., 2016).

For the LiDAR data, we generated canopy height from the LiDAR point cloud using the LAStools processing software (https://rapidlasso.de/) or directly from the GFCH product.

5.4.4. Environmental variables

We obtained variables related to climate, soil properties, topography, and hydrological stress. For climatic data, we collected three long-term monthly climatic variables and calculated their mean values (1983 to 2022), namely temperature, vapour pressure deficit (VPD), and climatological water deficit (CWD), using the TerraClimate dataset (Abatzoglou et al., 2018) at a spatial resolution of ~4 km (https://www.climatologylab.org/terraclimate.html). Furthermore, we calculated the maximum climatological water deficit (MCWD), which is defined as the most negative value of CWD, to describe the accumulated water stress that occurs across a dry season (Malhi et al., 2009):

$$CWD_{(n)}=CWD_{(n-1)}+P_{(n)}-E_{(n)} \quad (1)$$

$$Max(CWD_{(n)})=0 \quad (2)$$

$$CWD_{(0)}=CWD_{(12)} \quad (3)$$

$$MCWD=Min(CWD_{(0)}, CWD_{(1)}, ..., CWD_{(12)}) \quad (4)$$

where n (n=1, 2, …, 12) is the index of a month over a calendar year, and P and E are precipitation (mm/month) and evapotranspiration (mm/month). We set $CWD_{(6)}=0$ as June is normally the wettest month in Chile (Araya-Osses et al., 2020) and therefore assume the soil is saturated and applied this calculation to the mean annual cycle of precipitation (Malhi et al., 2009). We also calculated the additive inverse of MCWD whereby positive MCWD values are an intuitive indication of increases in water stress.

We gathered soil data from the SoilGrids database (https://soilgrids.org/) at a spatial resolution of 250 m (Hengl et al., 2017). All soil variables were extracted for the top 30 cm layer and averaged across depth intervals (0-5 cm, 5-15 cm, and 15-30 cm) using depth-weighted means (Quick & Chadwick, 2011). The following five variables were summarised at the plot level: cation exchange capacity at pH 7 (CEC, in mmol(c)/kg), pH in water (pHH_2O, pH×10), soil organic carbon (SOC, in dg/kg), clay and sand content (both in g/kg). These variables capture key aspects of soil fertility and structure. Specifically, CEC reflects the soil's ability to retain and exchange nutrients, directly influencing plant nutrient availability. pHH_2O reveals soil acidity or alkalinity, which affects nutrient solubility and species tolerance. SOC

represents the amount of organic matter, often linked to soil health and stress conditions. Finally, soil texture (clay and sand content) affects water-holding capacity, drainage, and root penetration, which are critical for plant growth and habitat suitability.

For topographic data, we obtained the digital elevation model from the shuttle radar topography mission (Farr et al., 2007) at 30 m (https://cmr.earthdata.nasa.gov/search/concepts/C1000000240-LPDAAC_ECS.html) and derived slope and aspect.

Lastly, using the ECOsystem Spaceborne Thermal Radiometer Experiment on Space Station (ECOSTRESS) (Fisher et al., 2020) we extracted evapotranspiration (ET), evaporative stress index (ESI), and water use efficiency (WUE) as indicators of hydrological stress. Specifically, we accessed 4383, 3917, and 4095 tiles for ET, ESI, and WUE, respectively, through AppEEARS at ~70 m spatial resolution (https://appeears.earthdatacloud.nasa.gov/) from 01 November 2019 to 31 January 2023.

5.4.5. Predicting community level traits and functional diversity and redundancy with satellite remote sensing

We used Sentinel-2 multispectral data (10 m) from the European Space Agency (Drusch et al., 2012) and the GFCH product (30 m) for predicting functional trait composition, diversity, and redundancy across forest areas in Chile. The Sentinel-2 mission comprises a constellation of two identical satellites, Sentinel-2A and Sentinel-2B, operating synergistically to capture imagery of the Earth's surface. These satellites are equipped with a multispectral instrument, capturing data across 13 spectral bands, ranging from visible to infrared wavelengths. This extensive spectral coverage allows for detailed analysis of vegetation health and land cover changes, making Sentinel-2 images invaluable for applications in ecology, forestry, and climate studies.

Specifically, we used the COPERNICUS/S2_SR_HARMONIZED collection available through Google Earth Engine (https://earthengine.google.com/) cloud computing platform (Gorelick et al., 2017), which provides atmospherically corrected and harmonised Level-2A surface reflectance data. As part of additional pre-processing, we masked cloud and cirrus pixels using the QA60 band (bits 10 and 11), and rescaled reflectance values to a 0-1 range by dividing by 10000. A median composite was generated from cloud-free images between 10 February 2020 and 25 January 2022 and clipped to the study area for analysis.

5.4.6. Identification of trait-trait correlations

We tested correlations between all functional traits (Supplementary Fig. S5.1) and proposed the mean absolute within-category correlation index (MACI) that is defined as follows to identify key functional traits:

$$\mathrm{MACI}=\frac{\sum_{m=1}^{M}\sum_{n=1}^{M}|C_{m,n}|}{M} \tag{5}$$

where M is the total number of different functional traits in the same category (i.e., morphological, nutrient, hydraulic, and photosynthetic traits), and in an $M\times M$ correlation matrix, m and n indicate the ordinal numbers of traits, where $C_{m,n}$ stands for the correlation value between the mth and the nth functional traits within the same trait category.

By setting the threshold as 0.9, functional traits whose MACI values were greater than 0.9 were excluded as they were highly correlated with other traits in the same category. The use of MACI provided a quantitative measure of trait correlation within the same functional category and ensured that the retained traits represent independent aspects of plant function, which reduces multicollinearity in downstream analyses and improves the robustness and interpretability of trait-based modelling. Based on this criterion, we selected: 1) morphological (Mor) traits: FW, DW, LA, SLA, and TWD; 2) leaf nutrients (Nutr): N, P, Ca, and Mg content in leaves; 3) hydraulic (Hydr) traits: P50, P88, and WPmd, and 4) photosynthetic (Pho) traits: TmaxL, Topt, TspanL, and T50.

5.4.7. Calculating functional trait composition

We calculated the community weighted mean (CWM) and variance (CWV) of every functional trait using the individual's basal area as the weighting factor. Specifically, CWM and CWV are defined as follows:

$$\mathrm{CWM}=\frac{\sum_{i=1}^{N}\mathrm{BA}_i\times \mathrm{t}_i}{\sum_{i=1}^{N}\mathrm{BA}_i} \tag{6}$$

$$\mathrm{CWV}=\frac{\sum_{i=1}^{N}\mathrm{BA}_i\times(\mathrm{t}_i-\mathrm{CWM})^2}{\sum_{i=1}^{N}\mathrm{BA}_i} \tag{7}$$

where N is the total number of tree individuals in a community (i.e., a single plot), and BA_i and t_i denote the basal area and trait value of the ith individual, respectively.

5.4.8. Calculating functional diversity and redundancy

We calculated functional dispersion as a measure of functional diversity. Functional dispersion (FDis) (Laliberté & Legendre, 2010) is defined as the mean distance in multidimensional trait space of individual species to the centroid of all species. FDis quantifies the effective number of functionally distinct species for a given level of species dispersion and measures the spread and variability of species within the trait space. We calculated FDis across the four functional trait categories (morphology, nutrients, hydraulics, and photosynthesis) using the "dbFD" function of the R "FD" package (Laliberté et al., 2014):

$$\mathrm{FDis}=\frac{\sum_{i=1}^{N}\mathrm{BA}_i\times z_i}{\sum_{i=1}^{N}\mathrm{BA}_i} \tag{8}$$

where BA_i is the basal area of species i in a plot, and z_i stands for the distance of species i in a plot to the weighted centroid of the N individual species in the trait space.

In addition, functional redundancy (FRed) measures the extent to which species within a community share similar functional roles and helps infer the resilience and stability of ecosystems by indicating whether there are backup species that can compensate for the loss of others in terms of functional roles (Ricotta et al., 2016). To calculate FRed across the four functional trait categories, we employed the "uniqueness" function of the R "adiv" package (Pavoine, 2020). Specifically, in a community composed of N species:

$$\mathrm{FUni}=\frac{\sum_{i=1}^{N}p_i\times\sum_{j=1}^{N}p_j\delta_{ij}}{\sum_{j=1}^{N}p_j(1-p_i)} \tag{9}$$

$$\mathrm{FRed}=1-\mathrm{FUni} \tag{10}$$

where FUni is functional uniqueness that refers to the distinctiveness of species with similar traits measured at community level. p_i (where $0<p_i\leq 1$ and $\sum_{i=1}^{N}p_i=1$) represents the relative abundance of species i, and δ_{ij} denotes the pairwise functional dissimilarity between species i and j, where $\delta_{ij}=\delta_{ji}$ and $\delta_{ii}=0$.

5.4.9. Predicting functional trait composition, diversity, and redundancy at plot level

We modelled CWM, CWV, functional diversity, and redundancy as a function of climate, soil, topography and the remotely sensed data described above. For all remotely sensed predictors, we calculated their mean and variance at the plot level. The data were then divided into seven

categories: 1) spectral bands: blue, green, red, NIR, and red edge, 2) vegetation indices: NDVI, NDRE, SAVI, and MSAVI, 3) LiDAR, 4) climate: temperature, VPD, and MCWD, 5) hydrological stress: ET, ESI, and WUE, 6) topography: slope and aspect, and 7) soil: CEC, clay, sand, pHH_2O, and SOC. To simplify the model and avoid overfitting, we also tested the correlation between all variable's mean values (Supplementary Fig. S5.2) and applied the MACI to each of them, dropping those whose MACI values were greater than 0.9. Eventually, mean and variance values of red, red edge, NIR, NDVI, NDRE, SAVI, MSAVI, height, MCWD, temperature, ET, ESI, WUE, slope, aspect, CEC, clay, sand, pHH_2O, and SOC were selected.

We then used machine learning (Random forests regression (Breiman, 2001)) to model the CWM, CWV, functional diversity, and redundancy as a function of the above-mentioned variables. To optimise the two key parameters of the Random forests regression, namely the number of trees and the number of variables randomly selected at each split, we tested different combinations. The number of trees ranged from 5 to 100 with a step of 5, and the number of variables ranged from 1 (the minimum number of input bands) to 20 (the maximum number of input bands). To evaluate model performance, we split the dataset into 70% for training and the remaining 30% for testing. We then calculated the mean absolute error (MAE), root mean square error (RMSE), and coefficient of determination (R^2) to comprehensively evaluate the performance of all models. We also evaluated our models based on a leave-one-out cross-validation approach using the "caret" package in R (Kuhn, 2008). The optimal model is determined as the one with minimum RMSE value.

5.4.10. Key drivers of functional trait composition, diversity, and redundancy

To uncover key drivers of functional trait composition, diversity, and redundancy, we tested the importance of each input variable (VarImp) from the models created above. VarImp was calculated using the decrease in node impurities (i.e., the mean reduction in residual sum of squares), as implemented in the varImp function of the R "caret" package (Kuhn, 2008). We also calculated mean VarImp scores of each of the seven groups of input data to explore how different variables contribute to mapping functional traits and assessing FDis and FRed, after normalising the individual variable importance scores to express their relative contribution.

5.4.11. Scaling up from plots to the full study area

To scale predictions from the 16 study plots to the full extent of temperate forests in Chile, we firstly identified forest sites across the study area by generating a forest mask using the "tree cover" class from the 10-m WorldCover v200 land use and land cover product (https://worldcover2021.esa.int/) (Zanaga et al., 2022). Then, we collated Sentinel-2 multispectral images from 2019 to 2023 and conducted pre-processing and applied all the optimal parameters gained from above to the Random forests regression via the Google Earth Engine (https://earthengine.google.com/) cloud computing platform (Gorelick et al., 2017) to predict functional trait composition, diversity, and redundancy (Fig. 5.1C). To minimise the risk of estimation artefacts, the seven calibration sites with 16 plots were selected to cover the main latitudinal and climatic gradients of temperate forests in Chile, and predictions were restricted to forested areas within the same environmental space as the calibration data. These steps ensure that the scaling procedure is robust while acknowledging that predictions in under-sampled areas remain more uncertain and would benefit from additional field trait data.

5.5. Results

5.5.1. Spatial distribution of functional trait composition, diversity, and redundancy

We obtained spatial predictions of the trait community-weighted mean (CWM) and variance (CWV) for each functional trait (Fig. 5.2, all trait maps see Supplementary Figs. S5.3 to S5.10), as well as functional diversity (FDis) and redundancy (FRed) across the study area within forested regions. A bivariate map showing the joint distribution of FDis and FRed was presented in Fig. 5.3 (separate maps were provided in Supplementary Figs. S5.11 and S5.12). Our models for CWM had an average R^2=0.61, while for CWV they had an average R^2 of 0.44 (Supplementary Tables S5.10 to S5.13). The average R^2 for assessing the FDis and FRed were 0.48 and 0.52, respectively (Supplementary Table S5.14).

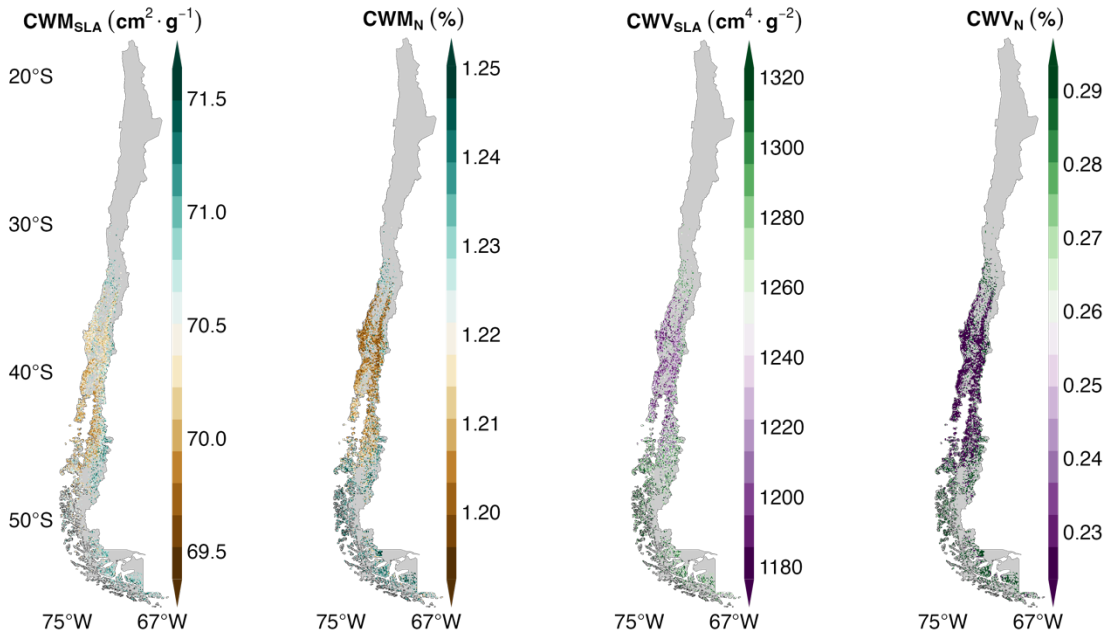

Fig. 5.2. Spatial distribution of community-weighted mean (CWM) and variance (CWV) for specific leaf area (SLA) and leaf nitrogen (N) content across Chilean temperate forests. CWM maps indicate the dominant trait values within forest communities, and CWV maps reflect trait variability. CWM and CWV maps of all traits are included in Supplementary Figs. S5.3 to S5.10.

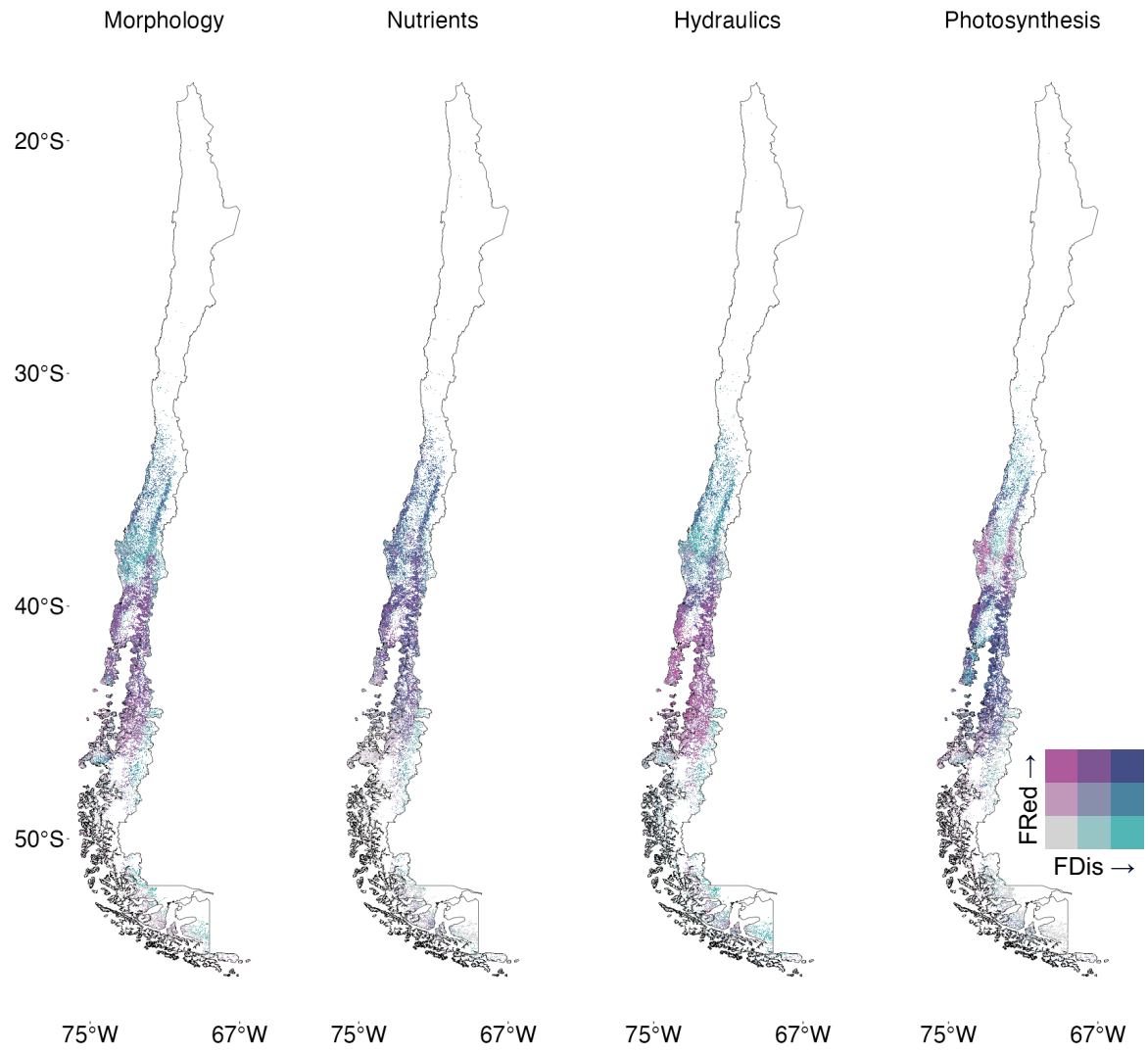

Fig. 5.3. Bivariate maps of functional diversity (FDis) and redundancy (FRed) for morphologic, nutrient, hydraulic, and photosynthetic traits within Chilean temperate forest ecosystems. In the legend located in the bottom right, the horizontal axis represents the range of FDis values, while the vertical axis similarly represents the range of FRed values. The colour gradient shows the joint distribution of FDis and FRed: grey=low diversity and redundancy; turquoise=high diversity, low redundancy; magenta=high redundancy, low diversity; navy=high in both metrics. These maps highlight areas where forests may be more resilient (high FDis and FRed) versus areas potentially vulnerable to environmental change (low FDis and FRed). Individual maps on spatial distribution of FDis and FRed are shown in Supplementary Figs. S5.11 and S5.12.

For functional traits, there was a noticeable pattern in the latitudinal distribution between approximately 35°S and 42°S, where CWM and CWV values for almost all functional traits were relatively low compared to neighbouring regions, which indicated less notable trait

extremes and moderate functional variation. We also found distinct spatial distribution patterns of FDis and FRed across the gradient explored. Notably, we observed a latitudinal gradient wherein both FDis and FRed were high within a narrow band, primarily between latitudes 35°S and 42°S, suggesting that forests here simultaneously hosted diverse functional strategies and redundant trait groups. Within this range, FDis exhibited a range from 0.86 to 2.06 with a mean value of 1.13 (mean values of 1.22, 1.21, 0.83, and 1.27 for $FDis_{Mor}$, $FDis_{Nutr}$, $FDis_{Hydr}$, and $FDis_{Pho}$, respectively, Supplementary Fig. S5.11). Similarly, FRed ranged from 0.31 to 0.63 with a mean of 0.46 (mean values of 0.44, 0.46, 0.48, and 0.46 for $FRed_{Mor}$, $FRed_{Nutr}$, $FRed_{Hydr}$, and $FRed_{Pho}$, respectively, Supplementary Fig. S5.12). There was a divergence in the dominance of the different metrics. Specifically, FDis was higher, with the mean value peaking at 1.29 (mean values of 1.53, 1.13, 1.30, and 1.21 for $FDis_{Mor}$, $FDis_{Nutr}$, $FDis_{Hydr}$, and $FDis_{Pho}$, respectively, Supplementary Fig. S5.11) between latitudes 30°S and 35°S. In contrast, within the latitudinal range of 42°S to 48°S, FRed dominated across the four trait groups with the mean value reaching 0.54 (mean values of 0.56, 0.52, 0.54, and 0.52 for $FRed_{Mor}$, $FRed_{Nutr}$, $FRed_{Hydr}$, and $FRed_{Pho}$, respectively, Supplementary Fig. S5.12). Finally, both FDis and FRed were low between 48°S to 53°S, with mean FDis being 0.71 (mean values of 0.65, 0.81, 0.66, and 0.71 for $FDis_{Mor}$, $FDis_{Nutr}$, $FDis_{Hydr}$, and $FDis_{Pho}$, respectively, Supplementary Fig. S5.11) and mean FRed being 0.23 (mean values of 0.24, 0.23, 0.20, and 0.24 for $FRed_{Mor}$, $FRed_{Nutr}$, $FRed_{Hydr}$, and $FRed_{Pho}$, respectively, Supplementary Fig. S5.12).

5.5.2. Drivers of functional trait composition, diversity, and redundancy across the latitudinal gradient

Variable importance (VarImp) analyses (Figs. 5.4 and 5.5) showed that hydrological stress and soil properties consistently drived functional trait composition, diversity, and redundancy across trait categories. For CWM (Fig. 5.4 and Supplementary Figs. S5.13 to S5.16), the top-ranking variable for predicting CWM_{Mor} and CWM_{Nutr} was hydrological stress (mean VarImp=31.99 for CWM_{Mor} and mean VarImp=36.22 for CWM_{Nutr}), while soil properties contributed the most in predicting CWM_{Hydr} (mean VarImp=23.32) and CWM_{Pho} (mean VarImp=36). Climate followed closely after hydrological stress and soil properties for predicting CWM_{Nutr} (mean VarImp=21.74) and CWM_{Hydr} (mean VarImp=19.20). For CWV (Fig. 5.4 and Supplementary Figs. S5.13 to S5.16), soil properties were identified as the most important variable in the case of morphology, nutrients, and hydraulics (mean VarImp=41.60, 24.97, and 33.99 for CWV_{Mor}, CWV_{Nutr}, and CWV_{Hydr}, respectively). Notably, topography

ranked first in predicting CWV_{Pho} (mean VarImp=23.67), and it was also the second most important predictor for CWV_{Mor} (mean VarImp=28.65) and CWV_{Nutr} (mean VarImp=21.23).

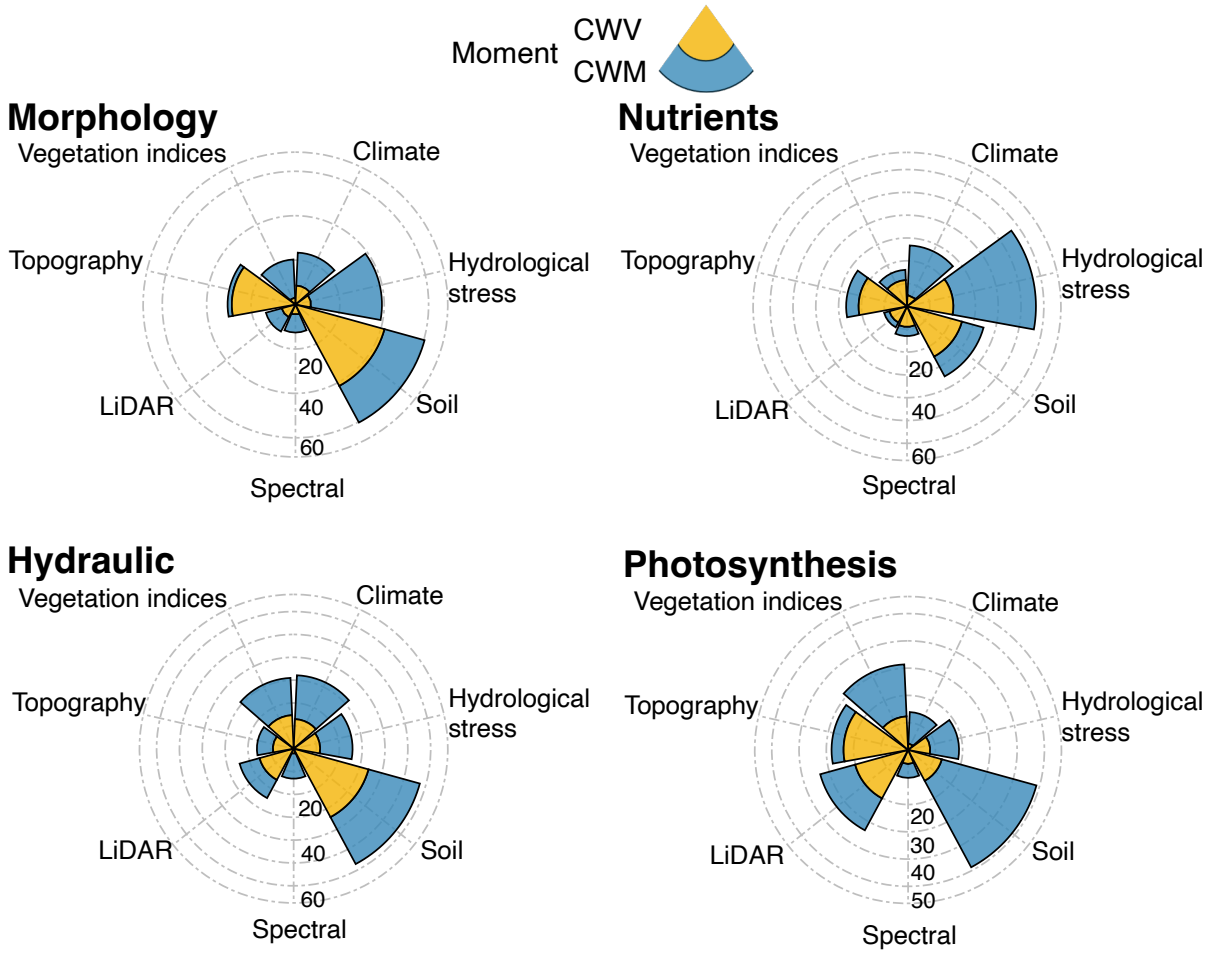

Fig. 5.4. Mean variable importance of input data groups for predicting community-weighted mean (CWM) and community-weighted variance (CWV) of the four categories of functional traits. In each of the polar stacked bar charts, the seven input data types were assigned to specific spokes, along which stacked bars were drawn. The height of each segment within the stacked bar corresponded to the importance of the variable it represented. Different colours were used to distinguish between CWM and CWV. Numbers alongside the grey radial axis denote scale values reflecting normalised importance scores, with the maximum scale adjusted to the highest observed group mean importance score.

Hydrological stress and soil properties emerged as the predominant drivers of FDis and FRed (Fig. 5.5) across all trait groups, with notable mean VarImp of 27.97 and 21.28 for FDis, and 28.13 and 22.88 for FRed, respectively. Moreover, hydrological stress was the only type of variable whose importance scores were consistently high for driving both FDis and FRed in

all trait groups, while plant canopy height contributed little to predicting FRed of morphology, nutrients, and photosynthesis.

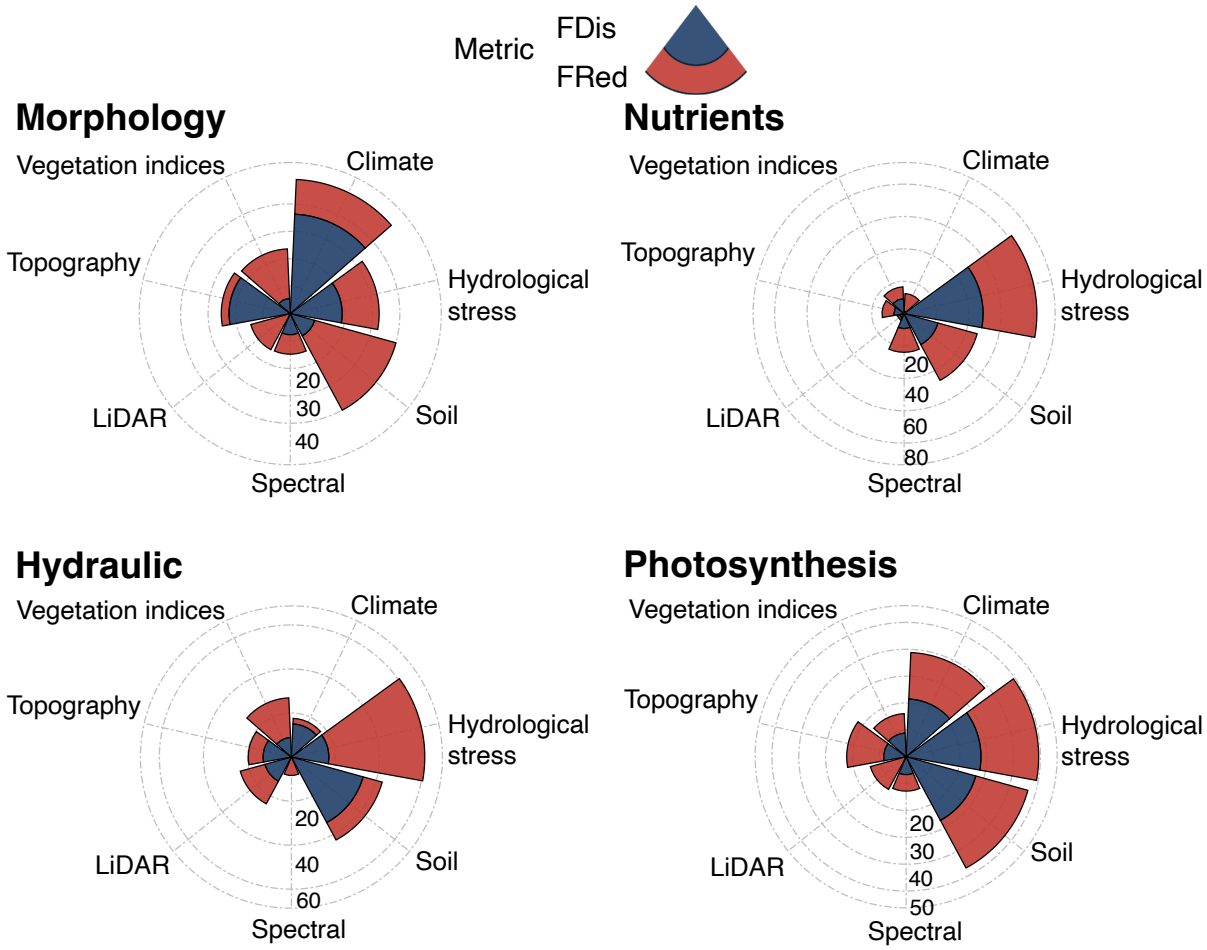

Fig. 5.5. Mean variable importance of input data groups for predicting functional diversity (FDis) and redundancy (FRed) of the four categories of functional traits. In each of the polar stacked bar charts, the seven input data types were assigned to specific spokes, along which stacked bars were drawn. The height of each segment within the stacked bar corresponded to the importance of the variable it represented. Different colours were used to distinguish between FDis and FRed. Numbers alongside the grey radial axis denote scale values reflecting normalised importance scores, with the maximum scale adjusted to the highest observed group mean importance score.

Soil properties (VarImp=30.81 for FDis) and climate (VarImp=36.27 for FRed) emerged as the primary drivers in terms of morphology. For leaf nutrients, the importance of hydrological stress (VarImp=33.29 for FDis and VarImp=48.76 for FRed) and soil properties (VarImp=25.15 for FDis and VarImp=21.58 for FRed) was prominent. When considering

hydraulic traits, hydrological stress (VarImp=43.60) and soil properties (VarImp=33.75) were found as the most important drivers of FDis and FRed, respectively. Lastly, photosynthetic FDis and FRed were notably driven by hydrological stress (VarImp=21.50 for FDis and VarImp=27.84 for FRed) and soil properties (VarImp=20.15 for FDis and VarImp=26.87 for FRed). Additionally, climate also demonstrated high importance in driving FDis (VarImp=17.32) and FRed (VarImp=21.48) of photosynthesis as it ranked third closely to soil properties for both metrics.

5.6. Discussion

5.6.1. Inferring plant functional trait composition, diversity, and redundancy using remote sensing approaches

The integration of plot-level *in-situ* plant functional traits with remotely sensed data acquired across multiple spatial scales and platforms provides not only a comprehensive understanding of trait distributions and variances, but also holistic insights into functional diversity and redundancy (inferred by FDis and FRed in this study). Using multispectral drone imagery and handheld LiDAR scans acquired at the plot-level, we obtain detailed spectral and structural information of forest functional composition at fine scales. Then, we use the satellite data to upscale our results to the extent of the full study area. In doing so, we demonstrate the potential to scale up plot-level ecological understanding with high accuracy across large latitudinal and environmental extents.

The ability to scale up from plot-level data to large spatial extents with remote sensing allows us to generate maps that predict the spatial distribution and variation of plant functional trait composition, diversity, and redundancy across vast areas. By combining multispectral and LiDAR data with *in-situ* measurements, remote sensing proves to be a high-resolution and cost-effective means to monitor and predict the distribution and variability of trait composition, diversity, and redundancy with optimal predictive accuracies (Objective 1). These spatially explicit predictions further allow us to evaluate how functional trait composition, diversity, and redundancy vary across broad latitudinal and environmental gradients (Objective 2), and to identify the most important environmental drivers shaping their distribution and variation across the landscape (Objective 3). Together, these outcomes highlight the potential of integrating field-based trait data and multi-source remote sensing to advance landscape-scale assessments of biodiversity and forest function. These predictions are crucial for assessing how

climate change, extreme weather events, and other environmental stressors may affect forest resilience (Helfenstein et al., 2022), and are therefore not only vital for conservation and forest management strategies but also for developing responses to mitigate the impacts of environmental change.

The uncertainty of our spatial predictions varies across functional trait groups and metrics. Overall, nutrient-related traits exhibit the highest uncertainty across both trait composition (CWM and CWV) and functional diversity (FDis) and redundancy (FRed), as indicated by their comparatively lower predictive performance. This likely reflects both the inherent spatial heterogeneity of leaf nutrients and their sensitivity to micro-environmental factors that are not fully captured by the remotely sensed and environmental predictors used in this study. In contrast, morphological, hydraulic, and photosynthetic traits tend to be more reliably predicted, suggesting stronger links with canopy structure, spectral signals, and large-scale environmental gradients. From an ecological perspective, the higher uncertainty for nutrient traits implies that spatial maps of functional composition, diversity, and redundancy should be interpreted with caution when considering nutrient-driven ecosystem functions, such as productivity and nutrient cycling.

5.6.2. Variation of plant functional traits across latitudinal and environmental gradients

The intermediate region of the study area includes the Mediterranean-Temperate transition zone (35.5°-39.5°S), as well as a rainy, temperate climate zone south of 40°S (up to 48°S), characterised by a temperate climate with dry summers and warm temperatures (Sarricolea et al., 2017). Despite the overall favourable climatic conditions, including cold to moderate temperatures and sufficient moisture (Cavieres et al., 2007), the reduced trait variability within plant communities suggests a regime characterised by ecological homogenisation (Gámez-Virués et al., 2015). Forests in this area are characteristic of the temperate type with mostly evergreen species (Pérez et al., 2003). The dominance of species with similar functional traits in this area may be attributed to the convergence of environmental factors, such as soil properties (Grime, 2006) and topographic features (Schmitt et al., 2020), which limits the dominance of more diverse functional strategies among plant species. Furthermore, more moderate temperatures, compared to the north and south of this area, and the absence of a pronounced dry season, especially toward the south, may contribute to the stabilisation of plant communities (Isbell et al., 2015) and the reduction in trait variability (Dell et al., 2011) by

minimising the influence of seasonal water availability on species composition and functional trait distributions.

In the central portion of the study area (spanning from approximately 30°S to 35°S), several functional traits, i.e., FW, DW, TWD, P50, and P88, consistently exhibit both high CWM and CWV values, likely driven by the Mediterranean climatic conditions of this region (Garreaud et al., 2020). Considering that this pattern mainly appears in morphological and hydraulic traits that are paramount for species survival and reproduction in Mediterranean climates with prolonged drought, high temperatures, and winter rainfall, high CWM indicates prevalent trait values optimised for these climatic conditions (Bruelheide et al., 2018). Small, thick leaves and deep root systems, which enhance water retention and uptake efficiency, are characteristic of this type of climate (Wasson et al., 2012). Concurrently, high trait variance suggests species' abilities to fine-tune these traits to specific microhabitats (Denelle et al., 2019) or respond to localised variations in resource availability (Candeias & Fraterrigo, 2020), contributing to the community's ecological diversity and resilience within the Mediterranean ecosystems.

Conversely, in the southern portion of the study area, the observed increase in both CWM and CWV values for most traits reflects a shift in ecological dynamics within a cold oceanic (temperate/subpolar) climate regime, spanning from approximately 42°S to 53°S. This higher trait variability suggests an ecological setting characterised by colder temperatures and maritime influences (Vilà-Cabrera et al., 2015). The dominance of traits with higher CWM values indicates a commonness of functional strategies adapted to the colder environmental conditions (Bjorkman et al., 2018) typical of this southernmost region. Traits related to temperature responses, such as TmaxL and Topt, exhibited notably higher CWM values, indicating the persistence of certain functional strategies adapted to the cooler temperatures (Laughlin et al., 2018). Additionally, the dominance of cold-adapted species and the presence of diverse ecological niches shaped by maritime influences contribute to the higher trait variability observed in the southern region. One important caveat is the widespread presence of *Pinus radiata* plantations in central and southern Chile, which may partially influence trait-environment relationships. Although areas classified as forests were prioritised in this study, residual plantation effects cannot be fully excluded, particularly in transitional landscapes.

5.6.3. Understanding plant functional diversity and redundancy across temperate forests

Functional diversity and redundancy complement each other in capturing different aspects of community structure and functioning. High diversity with low redundancy may indicate a community with diverse strategies, while low diversity coupled with high redundancy may suggest a more functionally homogeneous community (Mouchet et al., 2010). In our study, we observe distinct latitudinal patterns where some regions exhibit high diversity with high redundancy, while others show imbalances between the two metrics (Table 5.1).

Table 5.1. Latitudinal patterns of functional diversity (FDis) and functional redundancy (FRed), and corresponding ecological interpretation in South American temperate forests.

Latitudinal range (°S)	FDis	FRed	Ecological interpretation
30-35	High	Moderate	Adaptable but sensitive to species loss; Mediterranean drought adaptations
35-42	High	High	High ecological resilience; transition zone with diverse functional strategies
42-48	Moderate	High	Convergent functional strategies; vulnerable to novel disturbances but stable under current climate
48-53	Low	Low	Extremely vulnerable; high-latitude cold-adapted refugia

As expected, we reveal a combination of both high FDis and FRed emerging from dense tree cover and high species diversity in the intermediate region of the study area. This region is a biodiversity hotspot (Echeverría et al., 2006; Myers et al., 2000), where favourable climatic conditions and varied habitats facilitate the coexistence of a diverse array of plant species with distinct functional traits (Kraft et al., 2015). In light of the transition from the Mediterranean climate in the north to the more temperate rainy climate in the south, the observed high FDis signifies the presence of a wide range of functional strategies among plant communities, while the concurrent high FRed suggests a robustness in ecosystem functioning and resilience to ongoing environmental changes and human disturbances (Oliver et al., 2015). This balance between FDis and FRed suggests a high-resilience system, well-adjusted to a mild climate with ample moisture (Correia et al., 2018). However, considering this region's status as a highly threatened area in which forests have experienced extensive conversion to exotic forest plantations (Braun et al., 2017; Miranda et al., 2017), the high FDis and FRed emphasises the

importance of preserving ecological integrity. With reduced trait variability and increased environmental homogenisation in this transitional zone, conservation efforts could target restoration, habitat connectivity enhancement, and community engagement to mitigate degradation.

The high FDis observed across ~30°S and ~35°S, characterised by Mediterranean climate with long dry and hot summers, demonstrates the remarkable adaptation of the regional flora to the harsh environmental conditions. The observed extensive variability in plant functional traits reflects the diverse strategies adopted by species to thrive in water-limited environments (Ruiz-Benito et al., 2017). Such adaptations likely contribute to the high taxonomic diversity observed in this region, as plant species have evolved specialised traits, i.e., SLA and P50 (Costa-Saura et al., 2016), to optimise resource acquisition and utilisation and constrain plant gas exchange under drought conditions (Vilagrosa et al., 2014). Our findings highlight the ecological significance of Mediterranean ecosystems as hotspots of biodiversity and contribute to the overall resilience of the continent's flora.

In addition, our findings carry implications for understanding ecological dynamics and biodiversity conservation across the continent, particularly under recent environmental disturbances. For example, extreme fire weather was observed in connection with climate change and El Niño in 2017 (De la Barrera et al., 2018) and 2023 (Bowman et al., 2019; Cordero et al., 2024), while large-scale forest browning has been linked to the severe megadrought since 2010 (Miranda et al., 2023). Regions with high FDis are likely to be more resilient to these stressors, as diverse functional strategies buffer ecosystem functioning against environmental fluctuations. In contrast, areas with high FRed but low FDis, such as those between approximately 42°S to 48°S, suggest a prevalence of similar functional traits among coexisting species (M. W. Cadotte et al., 2011), indicating convergent adaptation to the harsh environmental conditions, particularly in the latitudes up to approximately 48°S. While this functional similarity allows species to persist under current climates, it also implies that many species occupy similar ecological niches, which increases ecosystem vulnerability to climatic disturbances (Mouillot et al., 2013). If climate change disrupts these niches, it could lead to the simultaneous loss of multiple species that perform overlapping functions, thereby threatening ecosystem functioning. Maintaining current functional biodiversity and improving landscape connectivity should be priorities in conservation to strengthen ecosystem stability and resilience. In the southernmost forests, both FDis and FRed decrease sharply, largely due to naturally low species richness in the high-latitude, cold-adapted forests (e.g., one dominant tree

species in TRA forest, two in MAG forest), further exacerbating their susceptibility to environmental change. Therefore, these ecosystems, though low in diversity, are ecologically significant as refugia for cold-adapted species and as reservoirs of unique genetic resources (Morelli et al., 2020), making their conservation under climate change especially critical. The combination of harsh environmental conditions and limited number of species makes it particularly susceptible to climatic shifts and extreme events (Forzieri et al., 2021), pest and disease outbreaks (Estay et al., 2019), and invasive species. Conservation efforts should focus on protecting intact habitats and minimising further disturbances. Our findings highlight the importance of considering functional diversity and redundancy metrics alongside traditional metrics of species richness and abundance in conservation planning, particularly in regions prone to climate extremes.

5.6.4. Study limitations and future directions

While our study benefits from a broad latitudinal and environmental gradient, we acknowledge that the relatively low number of field plots with *in-situ* trait measurements and high-resolution drone/LiDAR data presents a limitation, and the approach used in this study inevitably introduces higher uncertainty in regions not directly represented by the calibration sites and plots. While these plots were selected to capture a range of environmental and vegetation conditions, the relatively small sample size may introduce uncertainty when extrapolating trait-based models to broader scales. The significant relationships observed are likely driven by the substantial ecological variation across the study area, encompassing Mediterranean to cold-temperate climate zones and diverse forest types. Nonetheless, increasing the number of plots, especially in underrepresented areas such as shrublands or transitional forest zones, could improve the resolution and generality of the derived relationships, and may help capture additional patterns and interactions between functional traits and environmental drivers that may not be fully represented with the current sample size. Predictions of underrepresented areas should be interpreted with caution. Future studies would benefit from integrating additional sampling efforts, possibly through coordinated long-term ecological networks, to improve the spatial representativeness and robustness of model predictions.

In addition, we use a random 70/30 training-testing split and leave-one-out cross-validation within the training set to evaluate model performance. These approaches are commonly applied in trait prediction and remote sensing studies where field data are limited

and sampling is systematic or random (Camino et al., 2018; Z. Wang et al., 2019; Zhang et al., 2022). While these methods can still be affected by spatial autocorrelation, recent findings suggest that they remain robust under certain conditions (Mushagalusa et al., 2024). We acknowledge, however, that spatial structure remains an important consideration in ecological modelling and have therefore highlighted this issue as a limitation in our study. Future work may benefit from incorporating spatial cross-validation strategies to further improve predictive robustness (Roberts et al., 2017).

Furthermore, the dominance of *Pinus radiata* plantations poses a potential limitation for interpreting trait-environment patterns, as they may mask or bias the functional signal of native forests. While the use of the WorldCover dataset helpes reduce this effect, future efforts should expand trait inventories in strictly native forests and improve land-cover discrimination between native forests and plantations.

Finally, Random forests predictions rely on the available training data, and the relatively low predictive accuracy for certain traits, particularly nutrients, highlights the need for additional measurements to improve model robustness. Future directions should focus on incorporating dynamic vegetation models to simulate trait responses under climate change scenarios, expanding trait coverage to include root, reproductive, and wood traits, and linking functional trait composition, diversity, and redundancy maps to socio-ecological resilience by considering human impacts, plantation areas, and land use changes. Integrating long-term disturbance data, such as fire, drought, and pest outbreaks, would further enhance our understanding of functional resilience across temperate forest ecosystems.

5.7. Conclusion

The large latitudinal gradient we studied serves as an invaluable setting to explore trait-environment relationships and key factors that drive functional trait composition, diversity, and redundancy of tree communities. This study demonstrates the first large-scale and high-resolution mapping of plant functional traits in this region and enables an integrated assessment of functional diversity and redundancy across broad spatial scales in South America. Our approach provides an opportunity for mapping plant functional traits and assessing plant functional diversity and redundancy at broad scales.

We identify a transitional zone, the intermediate latitudinal range between approximately 35°S and 42°S, which may represent a critical threshold where forests are more

likely to maintain stability of key ecosystem functions under climate change. This is due to the combination of high trait functional diversity and redundancy, which together provide complementary strategies and insurance effects. The co-occurrence of diverse functional traits and redundant functional groups suggests an ecosystem that possesses both the capacity to adapt to changing conditions and the resilience to withstand disturbances. While we refer to this as contributing to ecosystem "resilience", it is important to note that resilience here is inferred through the potential for functional diversity and redundancy to buffer variability in ecosystem processes, rather than measured directly.

In the northern region (approximately 30°S to 35°S), high functional diversity but low functional redundancy suggests adaptability to environmental changes but potential vulnerability to species loss, which could destabilise ecosystem functioning. Conservation strategies in this zone should prioritise maintaining the local flora to ensure both high functional diversity and redundancy, thereby enhancing the stability of ecosystem functions. Conversely, in the southern region (between approximately 42°S to 48°S), forests exhibit high functional redundancy but low functional diversity, indicating adaptation to harsh Subantarctic conditions. However, the concentration of species with similar traits may increase vulnerability to climate change, as multiple species could be affected by the same disturbance. Conservation efforts here should prioritise maintaining existing functional biodiversity and promoting landscape connectivity to support ecosystem stability and forest resilience. From approximately 48°S to 53°S, both functional diversity and redundancy are low, due to extremely low species richness in high-latitude forests. These ecosystems are especially vulnerable to change but remain critical as refugia for cold-adapted species and reservoirs of unique genetic diversity. Conservation should focus on protecting intact habitats and minimising additional disturbance.

5.8. References

Abatzoglou, J. T., Dobrowski, S. Z., Parks, S. A., & Hegewisch, K. C. (2018). TerraClimate, a high-resolution global dataset of monthly climate and climatic water balance from 1958–2015. *Scientific Data*, *5*(1), 170191. https://doi.org/10.1038/sdata.2017.191

Aguirre-Gutiérrez, J., Rifai, S. W., Deng, X., ter Steege, H., Thomson, E., Corral-Rivas, J. J., Guimaraes, A. F., Muller, S., Klipel, J., Fauset, S., Resende, A. F., Wallin, G., Joly, C. A., Abernethy, K., Adu-Bredu, S., Alexandre Silva, C., de Oliveira, E. A., Almeida, D. R. A., Alvarez-Davila, E., … Malhi, Y. (2025). Canopy functional trait variation across Earth's tropical forests. *Nature*, 1–8. https://doi.org/10.1038/s41586-025-08663-2

Araya-Osses, D., Casanueva, A., Román-Figueroa, C., Uribe, J. M., & Paneque, M. (2020). Climate change projections of temperature and precipitation in Chile based on statistical downscaling. *Climate Dynamics*, *54*, 4309–4330.

Asner, G. P., Martin, R. E., Knapp, D. E., Tupayachi, R., Anderson, C. B., Sinca, F., Vaughn, N. R., & Llactayo, W. (2017). Airborne laser-guided imaging spectroscopy to map forest trait diversity and guide conservation. *Science*, *355*(6323), 385–389. https://doi.org/10.1126/science.aaj1987

Bjorkman, A. D., Myers-Smith, I. H., Elmendorf, S. C., Normand, S., Rüger, N., Beck, P. S. A., Blach-Overgaard, A., Blok, D., Cornelissen, J. H. C., Forbes, B. C., Georges, D., Goetz, S. J., Guay, K. C., Henry, G. H. R., HilleRisLambers, J., Hollister, R. D., Karger, D. N., Kattge, J., Manning, P., … Weiher, E. (2018). Plant functional trait change across a warming tundra biome. *Nature*, *562*(7725), 57–62. https://doi.org/10.1038/s41586-018-0563-7

Bowman, D. M., Moreira-Muñoz, A., Kolden, C. A., Chávez, R. O., Muñoz, A. A., Salinas, F., González-Reyes, Á., Rocco, R., De la Barrera, F., & Williamson, G. J. (2019). Human–

environmental drivers and impacts of the globally extreme 2017 Chilean fires. *Ambio*, *48*, 350–362.

Braun, A. C., Troeger, D., Garcia, R., Aguayo, M., Barra, R., & Vogt, J. (2017). Assessing the impact of plantation forestry on plant biodiversity: A comparison of sites in Central Chile and Chilean Patagonia. *Global Ecology and Conservation*, *10*, 159–172.

Breiman, L. (2001). Random forests. *Machine Learning*, *45*, 5–32.

Bruelheide, H., Dengler, J., Purschke, O., Lenoir, J., Jiménez-Alfaro, B., Hennekens, S. M., Botta-Dukát, Z., Chytrý, M., Field, R., Jansen, F., Kattge, J., Pillar, V. D., Schrodt, F., Mahecha, M. D., Peet, R. K., Sandel, B., van Bodegom, P., Altman, J., Alvarez-Dávila, E., … Jandt, U. (2018). Global trait–environment relationships of plant communities. *Nature Ecology & Evolution*, *2*(12), 1906–1917. https://doi.org/10.1038/s41559-018-0699-8

Butler, E. E., Datta, A., Flores-Moreno, H., Chen, M., Wythers, K. R., Fazayeli, F., Banerjee, A., Atkin, O. K., Kattge, J., & Amiaud, B. (2017). Mapping local and global variability in plant trait distributions. *Proceedings of the National Academy of Sciences*, *114*(51), E10937–E10946.

Cadotte, M., Albert, C. H., & Walker, S. C. (2013). The ecology of differences: Assessing community assembly with trait and evolutionary distances. *Ecology Letters*, *16*(10), 1234–1244.

Cadotte, M. W., Carscadden, K., & Mirotchnick, N. (2011). Beyond species: Functional diversity and the maintenance of ecological processes and services. *Journal of Applied Ecology*, *48*(5), 1079–1087.

Camarretta, N., A. Harrison, P., Lucieer, A., M. Potts, B., Davidson, N., & Hunt, M. (2020). From Drones to Phenotype: Using UAV-LiDAR to Detect Species and Provenance

Variation in Tree Productivity and Structure. *Remote Sensing*, *12*(19), Article 19. https://doi.org/10.3390/rs12193184

Camino, C., González-Dugo, V., Hernández, P., Sillero, J. C., & Zarco-Tejada, P. J. (2018). Improved nitrogen retrievals with airborne-derived fluorescence and plant traits quantified from VNIR-SWIR hyperspectral imagery in the context of precision agriculture. *International Journal of Applied Earth Observation and Geoinformation*, *70*, 105–117. https://doi.org/10.1016/j.jag.2018.04.013

Candeias, M., & Fraterrigo, J. (2020). Trait coordination and environmental filters shape functional trait distributions of forest understory herbs. *Ecology and Evolution*, *10*(24), 14098–14112.

Cardinale, B. J., Duffy, J. E., Gonzalez, A., Hooper, D. U., Perrings, C., Venail, P., Narwani, A., Mace, G. M., Tilman, D., & Wardle, D. A. (2012). Biodiversity loss and its impact on humanity. *Nature*, *486*(7401), 59–67.

Carmona, C. P., De Bello, F., Mason, N. W. H., & Lepš, J. (2016). Traits Without Borders: Integrating Functional Diversity Across Scales. *Trends in Ecology & Evolution*, *31*(5), 382–394. https://doi.org/10.1016/j.tree.2016.02.003

Cavieres, L. A., Badano, E. I., Sierra-Almeida, A., & Molina-Montenegro, M. A. (2007). Microclimatic modifications of cushion plants and their consequences for seedling survival of native and non-native herbaceous species in the high Andes of central Chile. *Arctic, Antarctic, and Alpine Research*, *39*(2), 229–236.

Chen, J., Shao, Z., Deng, X., Huang, X., & Dang, C. (2023). Vegetation as the catalyst for water circulation on global terrestrial ecosystem. *Science of The Total Environment*, *895*, 165071. https://doi.org/10.1016/j.scitotenv.2023.165071

Cordero, R. R., Feron, S., Damiani, A., Carrasco, J., Karas, C., Wang, C., Kraamwinkel, C. T., & Beaulieu, A. (2024). Extreme fire weather in Chile driven by climate change and El

Niño–Southern Oscillation (ENSO). *Scientific Reports*, *14*(1), 1974. https://doi.org/10.1038/s41598-024-52481-x

Correia, D. L. P., Raulier, F., Bouchard, M., & Filotas, É. (2018). Response diversity, functional redundancy, and post-logging productivity in northern temperate and boreal forests. *Ecological Applications*, *28*(5), 1282–1291. https://doi.org/10.1002/eap.1727

Costa-Saura, J. M., Martínez-Vilalta, J., Trabucco, A., Spano, D., & Mereu, S. (2016). Specific leaf area and hydraulic traits explain niche segregation along an aridity gradient in Mediterranean woody species. *Perspectives in Plant Ecology, Evolution and Systematics*, *21*, 23–30.

Cueto, D. A., Alaniz, A. J., Hidalgo-Corrotea, C., Vergara, P. M., Carvajal, M. A., & Barrios-Saravia, A. (2025). Chilean Mediterranean forest on the verge of collapse? Evidence from a comprehensive risk analysis. *Science of The Total Environment*, *964*, 178557. https://doi.org/10.1016/j.scitotenv.2025.178557

De la Barrera, F., Barraza, F., Favier, P., Ruiz, V., & Quense, J. (2018). Megafires in Chile 2017: Monitoring multiscale environmental impacts of burned ecosystems. *Science of the Total Environment*, *637*, 1526–1536.

Dell, A. I., Pawar, S., & Savage, V. M. (2011). Systematic variation in the temperature dependence of physiological and ecological traits. *Proceedings of the National Academy of Sciences*, *108*(26), 10591–10596.

Denelle, P., Violle, C., & Munoz, F. (2019). Distinguishing the signatures of local environmental filtering and regional trait range limits in the study of trait–environment relationships. *Oikos*, *128*(7), 960–971.

Díaz, S., Lavorel, S., De Bello, F., Quétier, F., Grigulis, K., & Robson, T. M. (2007). Incorporating plant functional diversity effects in ecosystem service assessments. *Proceedings of the National Academy of Sciences*, *104*(52), 20684–20689.

Díaz, S., Purvis, A., Cornelissen, J. H. C., Mace, G. M., Donoghue, M. J., Ewers, R. M., Jordano, P., & Pearse, W. D. (2013). Functional traits, the phylogeny of function, and ecosystem service vulnerability. *Ecology and Evolution*, *3*(9), 2958–2975. https://doi.org/10.1002/ece3.601

Docherty, E. M., Gloor, E., Sponchiado, D., Gilpin, M., Pinto, C. A. D., Junior, H. M., Coughlin, I., Ferreira, L., Junior, J. A. S., da Costa, A. C. L., Meir, P., & Galbraith, D. (2023). Long-term drought effects on the thermal sensitivity of Amazon forest trees. *Plant, Cell & Environment*, *46*(1), 185–198. https://doi.org/10.1111/pce.14465

Donohue, I., Hillebrand, H., Montoya, J. M., Petchey, O. L., Pimm, S. L., Fowler, M. S., Healy, K., Jackson, A. L., Lurgi, M., & McClean, D. (2016). Navigating the complexity of ecological stability. *Ecology Letters*, *19*(9), 1172–1185.

Drusch, M., Del Bello, U., Carlier, S., Colin, O., Fernandez, V., Gascon, F., Hoersch, B., Isola, C., Laberinti, P., & Martimort, P. (2012). Sentinel-2: ESA's optical high-resolution mission for GMES operational services. *Remote Sensing of Environment*, *120*, 25–36.

Echeverría, C., Coomes, D., Salas, J., Rey-Benayas, J. M., Lara, A., & Newton, A. (2006). Rapid deforestation and fragmentation of Chilean temperate forests. *Biological Conservation*, *130*(4), 481–494.

Echeverría-Londoño, S., Enquist, B. J., Neves, D. M., Violle, C., Boyle, B., Kraft, N. J., Maitner, B. S., McGill, B., Peet, R. K., & Sandel, B. (2018). Plant functional diversity and the biogeography of biomes in North and South America. *Frontiers in Ecology and Evolution*, *6*, 219.

Ellis, C. J., & Eaton, S. (2021). Microclimates hold the key to spatial forest planning under climate change: Cyanolichens in temperate rainforest. *Global Change Biology*, *27*(9), 1915–1926.

Estay, S. A., Chávez, R. O., Rocco, R., & Gutiérrez, A. G. (2019). Quantifying massive outbreaks of the defoliator moth Ormiscodes amphimone in deciduous Nothofagus-dominated southern forests using remote sensing time series analysis. *Journal of Applied Entomology*, *143*(7), 787–796.

Farr, T. G., Rosen, P. A., Caro, E., Crippen, R., Duren, R., Hensley, S., Kobrick, M., Paller, M., Rodriguez, E., & Roth, L. (2007). The shuttle radar topography mission. *Reviews of Geophysics*, *45*(2).

Fisher, J. B., Lee, B., Purdy, A. J., Halverson, G. H., Dohlen, M. B., Cawse-Nicholson, K., Wang, A., Anderson, R. G., Aragon, B., Arain, M. A., Baldocchi, D. D., Baker, J. M., Barral, H., Bernacchi, C. J., Bernhofer, C., Biraud, S. C., Bohrer, G., Brunsell, N., Cappelaere, B., … Hook, S. (2020). ECOSTRESS: NASA's Next Generation Mission to Measure Evapotranspiration From the International Space Station. *Water Resources Research*, *56*(4), e2019WR026058. https://doi.org/10.1029/2019WR026058

Folke, C., Carpenter, S., Walker, B., Scheffer, M., Elmqvist, T., Gunderson, L., & Holling, C. S. (2004). Regime shifts, resilience, and biodiversity in ecosystem management. *Annu. Rev. Ecol. Evol. Syst.*, *35*, 557–581.

Fortunel, C., Paine, C. E. T., Fine, P. V. A., Kraft, N. J. B., & Baraloto, C. (2014). Environmental factors predict community functional composition in Amazonian forests. *Journal of Ecology*, *102*(1), 145–155. https://doi.org/10.1111/1365-2745.12160

Forzieri, G., Girardello, M., Ceccherini, G., Spinoni, J., Feyen, L., Hartmann, H., Beck, P. S., Camps-Valls, G., Chirici, G., & Mauri, A. (2021). Emergent vulnerability to climate-driven disturbances in European forests. *Nature Communications*, *12*(1), 1081.

Gámez-Virués, S., Perović, D. J., Gossner, M. M., Börschig, C., Blüthgen, N., De Jong, H., Simons, N. K., Klein, A.-M., Krauss, J., & Maier, G. (2015). Landscape simplification

filters species traits and drives biotic homogenization. *Nature Communications*, *6*(1), 8568.

Garreaud, R. D., Boisier, J. P., Rondanelli, R., Montecinos, A., Sepúlveda, H. H., & Veloso-Aguila, D. (2020). The central Chile mega drought (2010–2018): A climate dynamics perspective. *International Journal of Climatology*, *40*(1), 421–439.

Gitelson, A., & Merzlyak, M. N. (1994). Spectral Reflectance Changes Associated with Autumn Senescence of *Aesculus hippocastanum* L. and *Acer platanoides* L. Leaves. Spectral Features and Relation to Chlorophyll Estimation. *Journal of Plant Physiology*, *143*(3), 286–292. https://doi.org/10.1016/S0176-1617(11)81633-0

Gorelick, N., Hancher, M., Dixon, M., Ilyushchenko, S., Thau, D., & Moore, R. (2017). Google Earth Engine: Planetary-scale geospatial analysis for everyone. *Remote Sensing of Environment*, *202*, 18–27. https://doi.org/10.1016/j.rse.2017.06.031

Grime, J. P. (2006). Trait convergence and trait divergence in herbaceous plant communities: Mechanisms and consequences. *Journal of Vegetation Science*, *17*(2), 255–260.

Hauser, L. T., Féret, J.-B., An Binh, N., Van Der Windt, N., Sil, Â. F., Timmermans, J., Soudzilovskaia, N. A., & Van Bodegom, P. M. (2021). Towards scalable estimation of plant functional diversity from Sentinel-2: In-situ validation in a heterogeneous (semi-)natural landscape. *Remote Sensing of Environment*, *262*, 112505. https://doi.org/10.1016/j.rse.2021.112505

Helfenstein, I. S., Schneider, F. D., Schaepman, M. E., & Morsdorf, F. (2022). Assessing biodiversity from space: Impact of spatial and spectral resolution on trait-based functional diversity. *Remote Sensing of Environment*, *275*, 113024. https://doi.org/10.1016/j.rse.2022.113024

Hengl, T., Mendes de Jesus, J., Heuvelink, G. B., Ruiperez Gonzalez, M., Kilibarda, M., Blagotić, A., Shangguan, W., Wright, M. N., Geng, X., & Bauer-Marschallinger, B.

(2017). SoilGrids250m: Global gridded soil information based on machine learning. *PLoS One*, *12*(2), e0169748.

Hooper, D. U., Chapin III, F. S., Ewel, J. J., Hector, A., Inchausti, P., Lavorel, S., Lawton, J. H., Lodge, D. M., Loreau, M., & Naeem, S. (2005). Effects of biodiversity on ecosystem functioning: A consensus of current knowledge. *Ecological Monographs*, *75*(1), 3–35.

Hortal, J., de Bello, F., Diniz-Filho, J. A. F., Lewinsohn, T. M., Lobo, J. M., & Ladle, R. J. (2015). Seven shortfalls that beset large-scale knowledge of biodiversity. *Annual Review of Ecology, Evolution, and Systematics*, *46*, 523–549.

Huertas Herrera, A., Toro-Manríquez, M. D. R., Salinas Sanhueza, J., Rivas Guíñez, F., Lencinas, M. V., & Martínez Pastur, G. (2023). Relationships among livestock, structure, and regeneration in Chilean Austral Macrozone temperate forests. *Trees, Forests and People*, *13*, 100426. https://doi.org/10.1016/j.tfp.2023.100426

Huete, A. R. (1988). A soil-adjusted vegetation index (SAVI). *Remote Sensing of Environment*, *25*(3), 295–309. https://doi.org/10.1016/0034-4257(88)90106-X

Hussain, S., Gao, K., Din, M., Gao, Y., Shi, Z., & Wang, S. (2020). Assessment of UAV-Onboard Multispectral Sensor for Non-Destructive Site-Specific Rapeseed Crop Phenotype Variable at Different Phenological Stages and Resolutions. *Remote Sensing*, *12*(3), Article 3. https://doi.org/10.3390/rs12030397

Isbell, F., Craven, D., Connolly, J., Loreau, M., Schmid, B., Beierkuhnlein, C., Bezemer, T. M., Bonin, C., Bruelheide, H., & De Luca, E. (2015). Biodiversity increases the resistance of ecosystem productivity to climate extremes. *Nature*, *526*(7574), 574–577.

Isbell, F., Gonzalez, A., Loreau, M., Cowles, J., Díaz, S., Hector, A., Mace, G. M., Wardle, D. A., O'Connor, M. I., & Duffy, J. E. (2017). Linking the influence and dependence of people on biodiversity across scales. *Nature*, *546*(7656), 65–72.

Jetz, W., Cavender-Bares, J., Pavlick, R., Schimel, D., Davis, F. W., Asner, G. P., Guralnick, R., Kattge, J., Latimer, A. M., & Moorcroft, P. (2016). Monitoring plant functional diversity from space. *Nature Plants*, *2*(3), 1–5.

Kaiser, J., Schefuß, E., Lamy, F., Mohtadi, M., & Hebbeln, D. (2008). Glacial to Holocene changes in sea surface temperature and coastal vegetation in north central Chile: High *versus* low latitude forcing. *Quaternary Science Reviews*, *27*(21), 2064–2075. https://doi.org/10.1016/j.quascirev.2008.08.025

Kamoske, A. G., Dahlin, K. M., Serbin, S. P., & Stark, S. C. (2021). Leaf traits and canopy structure together explain canopy functional diversity: An airborne remote sensing approach. *Ecological Applications*, *31*(2), e02230. https://doi.org/10.1002/eap.2230

Kergunteuil, A., Humair, L., Münzbergová, Z., & Rasmann, S. (2019). Plant adaptation to different climates shapes the strengths of chemically mediated tritrophic interactions. *Functional Ecology*, *33*(10), 1893–1903.

Kier, G., Mutke, J., Dinerstein, E., Ricketts, T. H., Küper, W., Kreft, H., & Barthlott, W. (2005). Global patterns of plant diversity and floristic knowledge. *Journal of Biogeography*, *32*(7), 1107–1116. https://doi.org/10.1111/j.1365-2699.2005.01272.x

Kraft, N. J., Godoy, O., & Levine, J. M. (2015). Plant functional traits and the multidimensional nature of species coexistence. *Proceedings of the National Academy of Sciences*, *112*(3), 797–802.

Krishnadas, M., Beckman, N. G., Zuluaga, J. C. P., Zhu, Y., Whitacre, J., Wenzel, J. W., Queenborough, S. A., & Comita, L. S. (2018). Environment and past land use together predict functional diversity in a temperate forest. *Ecological Applications*, *28*(8), 2142–2152. https://doi.org/10.1002/eap.1802

Kuhn, M. (2008). Building Predictive Models in R Using the caret Package. *Journal of Statistical Software*, *28*, 1–26. https://doi.org/10.18637/jss.v028.i05

Laliberté, E., & Legendre, P. (2010). A distance-based framework for measuring functional diversity from multiple traits. *Ecology*, *91*(1), 299–305. https://doi.org/10.1890/08-2244.1

Laliberté, E., Legendre, P., Shipley, B., & Laliberté, M. E. (2014). Package 'fd'. *Measuring Functional Diversity from Multiple Traits, and Other Tools for Functional Ecology*, *1*, 0–12.

Laughlin, D. C., Strahan, R. T., Adler, P. B., & Moore, M. M. (2018). Survival rates indicate that correlations between community-weighted mean traits and environments can be unreliable estimates of the adaptive value of traits. *Ecology Letters*, *21*(3), 411–421.

Le Roux, J. P. (2012). A review of Tertiary climate changes in southern South America and the Antarctic Peninsula. Part 2: Continental conditions. *Sedimentary Geology*, *247–248*, 21–38. https://doi.org/10.1016/j.sedgeo.2011.12.001

Ma, X., Mahecha, M. D., Migliavacca, M., van der Plas, F., Benavides, R., Ratcliffe, S., Kattge, J., Richter, R., Musavi, T., Baeten, L., Barnoaiea, I., Bohn, F. J., Bouriaud, O., Bussotti, F., Coppi, A., Domisch, T., Huth, A., Jaroszewicz, B., Joswig, J., … Wirth, C. (2019). Inferring plant functional diversity from space: The potential of Sentinel-2. *Remote Sensing of Environment*, *233*, 111368. https://doi.org/10.1016/j.rse.2019.111368

Malhi, Y., Aragão, L. E. O. C., Galbraith, D., Huntingford, C., Fisher, R., Zelazowski, P., Sitch, S., McSweeney, C., & Meir, P. (2009). Exploring the likelihood and mechanism of a climate-change-induced dieback of the Amazon rainforest. *Proceedings of the National Academy of Sciences*, *106*(49), 20610–20615. https://doi.org/10.1073/pnas.0804619106

Malhi, Y., Baldocchi, D., & Jarvis, P. (1999). The carbon balance of tropical, temperate and boreal forests. *Plant, Cell & Environment*, *22*(6), 715–740.

Malhi, Y., Christmann, T., Deng, X., Zhang-Zheng, H., Moore, S., & Riutta, T. (2024). Forest carbon budgets and climate change. In *Routledge Handbook of Forest Ecology* (2nd ed.). Routledge.

Meyer, J., & Kröncke, I. (2019). Shifts in trait-based and taxonomic macrofauna community structure along a 27-year time-series in the south-eastern North Sea. *PLOS ONE*, *14*(12), e0226410. https://doi.org/10.1371/journal.pone.0226410

Miranda, A., Altamirano, A., Cayuela, L., Lara, A., & González, M. (2017). Native forest loss in the Chilean biodiversity hotspot: Revealing the evidence. *Regional Environmental Change*, *17*(1), 285–297. https://doi.org/10.1007/s10113-016-1010-7

Miranda, A., Syphard, A. D., Berdugo, M., Carrasco, J., Gómez-González, S., Ovalle, J. F., Delpiano, C. A., Vargas, S., Squeo, F. A., Miranda, M. D., Dobbs, C., Mentler, R., Lara, A., & Garreaud, R. (2023). Widespread synchronous decline of Mediterranean-type forest driven by accelerated aridity. *Nature Plants*, *9*(11), 1810–1817. https://doi.org/10.1038/s41477-023-01541-7

Morelli, T. L., Barrows, C. W., Ramirez, A. R., Cartwright, J. M., Ackerly, D. D., Eaves, T. D., Ebersole, J. L., Krawchuk, M. A., Letcher, B. H., Mahalovich, M. F., Meigs, G. W., Michalak, J. L., Millar, C. I., Quiñones, R. M., Stralberg, D., & Thorne, J. H. (2020). Climate-change refugia: Biodiversity in the slow lane. *Frontiers in Ecology and the Environment*, *18*(5), 228–234. https://doi.org/10.1002/fee.2189

Mouchet, M. A., Villéger, S., Mason, N. W. H., & Mouillot, D. (2010). Functional diversity measures: An overview of their redundancy and their ability to discriminate community assembly rules. *Functional Ecology*, *24*(4), 867–876. https://doi.org/10.1111/j.1365-2435.2010.01695.x

Mouillot, D., Graham, N. A. J., Villéger, S., Mason, N. W. H., & Bellwood, D. R. (2013). A functional approach reveals community responses to disturbances. *Trends in Ecology & Evolution*, *28*(3), 167–177. https://doi.org/10.1016/j.tree.2012.10.004

Mushagalusa, C. A., Fandohan, A. B., & Glèlè Kakaï, R. (2024). Random forest and spatial cross-validation performance in predicting species abundance distributions. *Environmental Systems Research*, *13*(1), 23. https://doi.org/10.1186/s40068-024-00352-9

Myers, N., Mittermeier, R. A., Mittermeier, C. G., da Fonseca, G. A. B., & Kent, J. (2000). Biodiversity hotspots for conservation priorities. *Nature*, *403*(6772), 853–858. https://doi.org/10.1038/35002501

Myneni, R. B., Hall, F. G., Sellers, P. J., & Marshak, A. L. (1995). The interpretation of spectral vegetation indexes. *IEEE Transactions on Geoscience and Remote Sensing*, *33*(2), 481–486. https://doi.org/10.1109/TGRS.1995.8746029

NAHUELHUAL, L., DONOSO, P., LARA, A., NÚÑEZ, D., OYARZÚN, C., & NEIRA, E. (2007). VALUING ECOSYSTEM SERVICES OF CHILEAN TEMPERATE RAINFORESTS. *Environment, Development and Sustainability*, *9*(4), 481–499. https://doi.org/10.1007/s10668-006-9033-8

Oliver, T. H., Heard, M. S., Isaac, N. J. B., Roy, D. B., Procter, D., Eigenbrod, F., Freckleton, R., Hector, A., Orme, C. D. L., Petchey, O. L., Proença, V., Raffaelli, D., Suttle, K. B., Mace, G. M., Martín-López, B., Woodcock, B. A., & Bullock, J. M. (2015). Biodiversity and Resilience of Ecosystem Functions. *Trends in Ecology & Evolution*, *30*(11), 673–684. https://doi.org/10.1016/j.tree.2015.08.009

Osazuwa-Peters, O., & Zanne, A. (2011). Wood density protocol. *URL Http://Www. Publish. Csiro. Au/Prometheuswiki/Tiki-Pagehistory. Php*, *3*, 199–217.

Pavoine, S. (2020). adiv: An r package to analyse biodiversity in ecology. *Methods in Ecology and Evolution*, *11*(9), 1106–1112. https://doi.org/10.1111/2041-210X.13430

Pereira, L., Bittencourt, P. R. L., Oliveira, R. S., Junior, M. B. M., Barros, F. V., Ribeiro, R. V., & Mazzafera, P. (2016). Plant pneumatics: Stem air flow is related to embolism – new perspectives on methods in plant hydraulics. *New Phytologist*, *211*(1), 357–370. https://doi.org/10.1111/nph.13905

Pereira, L., Bittencourt, P. R. L., Pacheco, V. S., Miranda, M. T., Zhang, Y., Oliveira, R. S., Groenendijk, P., Machado, E. C., Tyree, M. T., Jansen, S., Rowland, L., & Ribeiro, R. V. (2020). The Pneumatron: An automated pneumatic apparatus for estimating xylem vulnerability to embolism at high temporal resolution. *Plant, Cell & Environment*, *43*(1), 131–142. https://doi.org/10.1111/pce.13647

Pérez, C. A., Armesto, J. J., Torrealba, C., & Carmona, M. R. (2003). Litterfall dynamics and nitrogen use efficiency in two evergreen temperate rainforests of southern Chile. *Austral Ecology*, *28*(6), 591–600. https://doi.org/10.1046/j.1442-9993.2003.01315.x

Pérez-Harguindeguy, N., Díaz, S., Garnier, E., Lavorel, S., Poorter, H., Jaureguiberry, P., Bret-Harte, M. S., Cornwell, W. K., Craine, J. M., Gurvich, D. E., Urcelay, C., Veneklaas, E. J., Reich, P. B., Poorter, L., Wright, I. J., Ray, P., Enrico, L., Pausas, J. G., De Vos, A. C., … Cornelissen, J. H. C. (2013). New handbook for standardised measurement of plant functional traits worldwide. *Australian Journal of Botany*, *61*(3), 167. https://doi.org/10.1071/BT12225

Perez-Quezada, J. F., Barichivich, J., Urrutia-Jalabert, R., Carrasco, E., Aguilera, D., Bacour, C., & Lara, A. (2023). Warming and Drought Weaken the Carbon Sink Capacity of an Endangered Paleoendemic Temperate Rainforest in South America. *Journal of Geophysical Research: Biogeosciences*, *128*(4), e2022JG007258. https://doi.org/10.1029/2022JG007258

Perez-Quezada, J. F., Urrutia, P., Olivares-Rojas, J., Meijide, A., Sánchez-Cañete, E. P., & Gaxiola, A. (2021). Long term effects of fire on the soil greenhouse gas balance of an old-growth temperate rainforest. *Science of The Total Environment*, *755*, 142442. https://doi.org/10.1016/j.scitotenv.2020.142442

Pla, L., Casanoves, F., & Di Rienzo, J. (2012). *Quantifying Functional Biodiversity*. Springer Netherlands. https://doi.org/10.1007/978-94-007-2648-2

Poorter, H., Niinemets, Ü., Poorter, L., Wright, I. J., & Villar, R. (2009). Causes and consequences of variation in leaf mass per area (LMA): A meta-analysis. *New Phytologist*, *182*(3), 565–588. https://doi.org/10.1111/j.1469-8137.2009.02830.x

Potapov, P., Li, X., Hernandez-Serna, A., Tyukavina, A., Hansen, M. C., Kommareddy, A., Pickens, A., Turubanova, S., Tang, H., Silva, C. E., Armston, J., Dubayah, R., Blair, J. B., & Hofton, M. (2021). Mapping global forest canopy height through integration of GEDI and Landsat data. *Remote Sensing of Environment*, *253*, 112165. https://doi.org/10.1016/j.rse.2020.112165

Qi, J., Chehbouni, A., Huete, A. R., Kerr, Y. H., & Sorooshian, S. (1994). A modified soil adjusted vegetation index. *Remote Sensing of Environment*, *48*(2), 119–126. https://doi.org/10.1016/0034-4257(94)90134-1

Quick, D. J., & Chadwick, O. A. (2011). Accumulation of salt-rich dust from Owens Lake playa in nearby alluvial soils. *Aeolian Research*, *3*(1), 23–29. https://doi.org/10.1016/j.aeolia.2011.03.004

Ricotta, C., De Bello, F., Moretti, M., Caccianiga, M., Cerabolini, B. E. L., & Pavoine, S. (2016). Measuring the functional redundancy of biological communities: A quantitative guide. *Methods in Ecology and Evolution*, *7*(11), 1386–1395. https://doi.org/10.1111/2041-210X.12604

Roberts, D. R., Bahn, V., Ciuti, S., Boyce, M. S., Elith, J., Guillera-Arroita, G., Hauenstein, S., Lahoz-Monfort, J. J., Schröder, B., Thuiller, W., Warton, D. I., Wintle, B. A., Hartig, F., & Dormann, C. F. (2017). Cross-validation strategies for data with temporal, spatial, hierarchical, or phylogenetic structure. *Ecography*, *40*(8), 913–929. https://doi.org/10.1111/ecog.02881

Rosenfeld, J. S. (2002). Functional redundancy in ecology and conservation. *Oikos*, *98*(1), 156–162. https://doi.org/10.1034/j.1600-0706.2002.980116.x

Rouault, E., Warmerdam, F., Schwehr, K., Kiselev, A., Butler, H., Łoskot, M., Szekeres, T., Tourigny, E., Landa, M., Miara, I., Elliston, B., Chaitanya, K., Plesea, L., Morissette, D., Jolma, A., Dawson, N., Baston, D., de Stigter, C., & Miura, H. (2024). GDAL. *Zenodo*. https://doi.org/10.5281/zenodo.13330875

Rozzi, R., Rosenfeld, S., Armesto, J. J., Mansilla, A., Núñez-Ávila, M., & Massardo, F. (2023). Ecological Connections Across the Marine-Terrestrial Interface in Chilean Patagonia. In J. C. Castilla, J. J. Armesto Zamudio, M. J. Martínez-Harms, & D. Tecklin (Eds.), *Conservation in Chilean Patagonia: Assessing the State of Knowledge, Opportunities, and Challenges* (pp. 323–354). Springer International Publishing. https://doi.org/10.1007/978-3-031-39408-9_13

Ruiz-Benito, P., Ratcliffe, S., Jump, A. S., Gómez-Aparicio, L., Madrigal-González, J., Wirth, C., Kändler, G., Lehtonen, A., Dahlgren, J., Kattge, J., & Zavala, M. A. (2017). Functional diversity underlies demographic responses to environmental variation in European forests. *Global Ecology and Biogeography*, *26*(2), 128–141. https://doi.org/10.1111/geb.12515

Sarricolea, P., Herrera-Ossandon, M., & Meseguer-Ruiz, Ó. (2017). Climatic regionalisation of continental Chile. *Journal of Maps*, *13*(2), 66–73. https://doi.org/10.1080/17445647.2016.1259592

Schmitt, S., Hérault, B., Ducouret, É., Baranger, A., Tysklind, N., Heuertz, M., Marcon, É., Cazal, S. O., & Derroire, G. (2020). Topography consistently drives intra- and inter-specific leaf trait variation within tree species complexes in a Neotropical forest. *Oikos*, *129*(10), 1521–1530. https://doi.org/10.1111/oik.07488

Schneider, C. A., Rasband, W. S., & Eliceiri, K. W. (2012). NIH Image to ImageJ: 25 years of image analysis. *Nature Methods*, *9*(7), 671–675. https://doi.org/10.1038/nmeth.2089

Schneider, F. D., Morsdorf, F., Schmid, B., Petchey, O. L., Hueni, A., Schimel, D. S., & Schaepman, M. E. (2017). Mapping functional diversity from remotely sensed morphological and physiological forest traits. *Nature Communications*, *8*(1), 1441. https://doi.org/10.1038/s41467-017-01530-3

Sheffield, J., Wood, E. F., Pan, M., Beck, H., Coccia, G., Serrat-Capdevila, A., & Verbist, K. (2018). Satellite Remote Sensing for Water Resources Management: Potential for Supporting Sustainable Development in Data-Poor Regions. *Water Resources Research*, *54*(12), 9724–9758. https://doi.org/10.1029/2017WR022437

Smith-Ramírez, C. (2004). The Chilean coastal range: A vanishing center of biodiversity and endemism in South American temperate rainforests. *Biodiversity & Conservation*, *13*(2), 373–393. https://doi.org/10.1023/B:BIOC.0000006505.67560.9f

Suding, K. N., Lavorel, S., Chapin Iii, F. S., Cornelissen, J. H. C., Díaz, S., Garnier, E., Goldberg, D., Hooper, D. U., Jackson, S. T., & Navas, M.-L. (2008). Scaling environmental change through the community-level: A trait-based response-and-effect framework for plants. *Global Change Biology*, *14*(5), 1125–1140. https://doi.org/10.1111/j.1365-2486.2008.01557.x

Sun, W., Chen, D., Li, Z., Li, S., Cheng, S., Niu, X., Cai, Y., Shi, Z., Wu, C., Yang, G., & Yang, X. (2024). Monitoring wetland plant diversity from space: Progress and perspective.

International Journal of Applied Earth Observation and Geoinformation, *130*, 103943. https://doi.org/10.1016/j.jag.2024.103943

Tecklin, D., DellaSala, D. A., Luebert, F., & Pliscoff, P. (2011). Valdivian Temperate Rainforests of Chile and Argentina. In D. A. DellaSala (Ed.), *Temperate and Boreal Rainforests of the World: Ecology and Conservation* (pp. 132–153). Island Press/Center for Resource Economics. https://doi.org/10.5822/978-1-61091-008-8_5

Thomson, E. R., Spiegel, M. P., Althuizen, I. H. J., Bass, P., Chen, S., Chmurzynski, A., Halbritter, A. H., Henn, J. J., Jónsdóttir, I. S., Klanderud, K., Li, Y., Maitner, B. S., Michaletz, S. T., Niittynen, P., Roos, R. E., Telford, R. J., Enquist, B. J., Vandvik, V., Macias-Fauria, M., & Malhi, Y. (2021). Multiscale mapping of plant functional groups and plant traits in the High Arctic using field spectroscopy, UAV imagery and Sentinel-2A data. *Environmental Research Letters*, *16*(5), 055006. https://doi.org/10.1088/1748-9326/abf464

Urrutia-Jalabert, R., Malhi, Y., Barichivich, J., Lara, A., Delgado-Huertas, A., Rodríguez, C. G., & Cuq, E. (2015). Increased water use efficiency but contrasting tree growth patterns in Fitzroya cupressoides forests of southern Chile during recent decades. *Journal of Geophysical Research: Biogeosciences*, *120*(12), 2505–2524. https://doi.org/10.1002/2015JG003098

Urrutia-Jalabert, R., Malhi, Y., & Lara, A. (2015). The Oldest, Slowest Rainforests in the World? Massive Biomass and Slow Carbon Dynamics of Fitzroya cupressoides Temperate Forests in Southern Chile. *PLOS ONE*, *10*(9), e0137569. https://doi.org/10.1371/journal.pone.0137569

Vilà-Cabrera, A., Martínez-Vilalta, J., & Retana, J. (2015). Functional trait variation along environmental gradients in temperate and Mediterranean trees. *Global Ecology and Biogeography*, *24*(12), 1377–1389. https://doi.org/10.1111/geb.12379

Vilagrosa, A., Hernández, E. I., Luis, V. C., Cochard, H., & Pausas, J. G. (2014). Physiological differences explain the co-existence of different regeneration strategies in Mediterranean ecosystems. *New Phytologist*, *201*(4), 1277–1288. https://doi.org/10.1111/nph.12584

Wang, R., & Gamon, J. A. (2019). Remote sensing of terrestrial plant biodiversity. *Remote Sensing of Environment*, *231*, 111218. https://doi.org/10.1016/j.rse.2019.111218

Wang, Z., Townsend, P. A., Schweiger, A. K., Couture, J. J., Singh, A., Hobbie, S. E., & Cavender-Bares, J. (2019). Mapping foliar functional traits and their uncertainties across three years in a grassland experiment. *Remote Sensing of Environment*, *221*, 405–416. https://doi.org/10.1016/j.rse.2018.11.016

Wang, Z., Wang, T., Darvishzadeh, R., Skidmore, A. K., Jones, S., Suarez, L., Woodgate, W., Heiden, U., Heurich, M., & Hearne, J. (2016). Vegetation Indices for Mapping Canopy Foliar Nitrogen in a Mixed Temperate Forest. *Remote Sensing*, *8*(6), Article 6. https://doi.org/10.3390/rs8060491

Wasson, A. P., Richards, R. A., Chatrath, R., Misra, S. C., Prasad, S. V. S., Rebetzke, G. J., Kirkegaard, J. A., Christopher, J., & Watt, M. (2012). Traits and selection strategies to improve root systems and water uptake in water-limited wheat crops. *Journal of Experimental Botany*, *63*(9), 3485–3498. https://doi.org/10.1093/jxb/ers111

Wieczynski, D. J., Boyle, B., Buzzard, V., Duran, S. M., Henderson, A. N., Hulshof, C. M., Kerkhoff, A. J., McCarthy, M. C., Michaletz, S. T., Swenson, N. G., Asner, G. P., Bentley, L. P., Enquist, B. J., & Savage, V. M. (2019). Climate shapes and shifts functional biodiversity in forests worldwide. *Proceedings of the National Academy of Sciences*, *116*(2), 587–592. https://doi.org/10.1073/pnas.1813723116

Zanaga, D., Van De Kerchove, R., Daems, D., De Keersmaecker, W., Brockmann, C., Kirches, G., Wevers, J., Cartus, O., Santoro, M., Fritz, S., Lesiv, M., Herold, M., Tsendbazar, N.-

E., Xu, P., Ramoino, F., & Arino, O. (2022). *ESA WorldCover 10 m 2021 v200* [Dataset]. Zenodo. https://doi.org/10.5281/zenodo.7254221

Zhang, Y.-W., Wang, T., Guo, Y., Skidmore, A., Zhang, Z., Tang, R., Song, S., & Tang, Z. (2022). Estimating Community-Level Plant Functional Traits in a Species-Rich Alpine Meadow Using UAV Image Spectroscopy. *Remote Sensing*, *14*(14), Article 14. https://doi.org/10.3390/rs14143399

Zhang-Zheng, H., Adu-Bredu, S., Duah-Gyamfi, A., Moore, S., Addo-Danso, S. D., Amissah, L., Valentini, R., Djagbletey, G., Anim-Adjei, K., Quansah, J., Sarpong, B., Owusu-Afriyie, K., Gvozdevaite, A., Tang, M., Ruiz-Jaen, M. C., Ibrahim, F., Girardin, C. A. J., Rifai, S., Dahlsjö, C. A. L., … Malhi, Y. (2024). Contrasting carbon cycle along tropical forest aridity gradients in West Africa and Amazonia. *Nature Communications*, *15*(1), 3158. https://doi.org/10.1038/s41467-024-47202-x

Zhang-Zheng, H., Deng, X., Aguirre-Gutiérrez, J., Stocker, B. D., Thomson, E., Ding, R., Adu-Bredu, S., Duah-Gyamfi, A., Gvozdevaite, A., Moore, S., Oliveras Menor, I., Prentice, I. C., & Malhi, Y. (2024). Why models underestimate West African tropical forest primary productivity. *Nature Communications*, *15*(1), 9574. https://doi.org/10.1038/s41467-024-53949-0

Zirbel, C. R., Bassett, T., Grman, E., & Brudvig, L. A. (2017). Plant functional traits and environmental conditions shape community assembly and ecosystem functioning during restoration. *Journal of Applied Ecology*, *54*(4), 1070–1079. https://doi.org/10.1111/1365-2664.12885

5.9. Supplementary materials

5.9.1. Figures

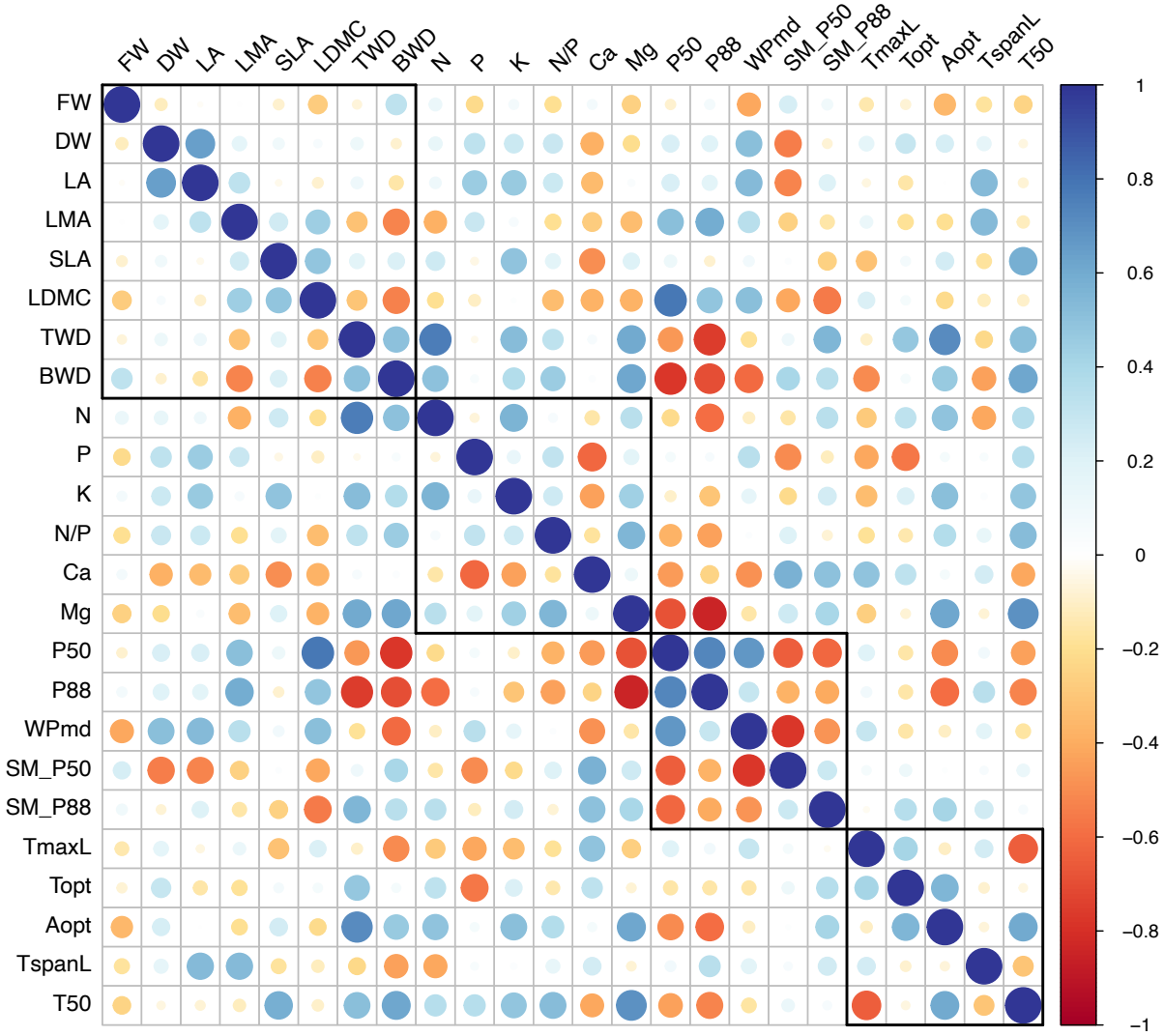

Fig. S5.1. Trait within-category correlation.

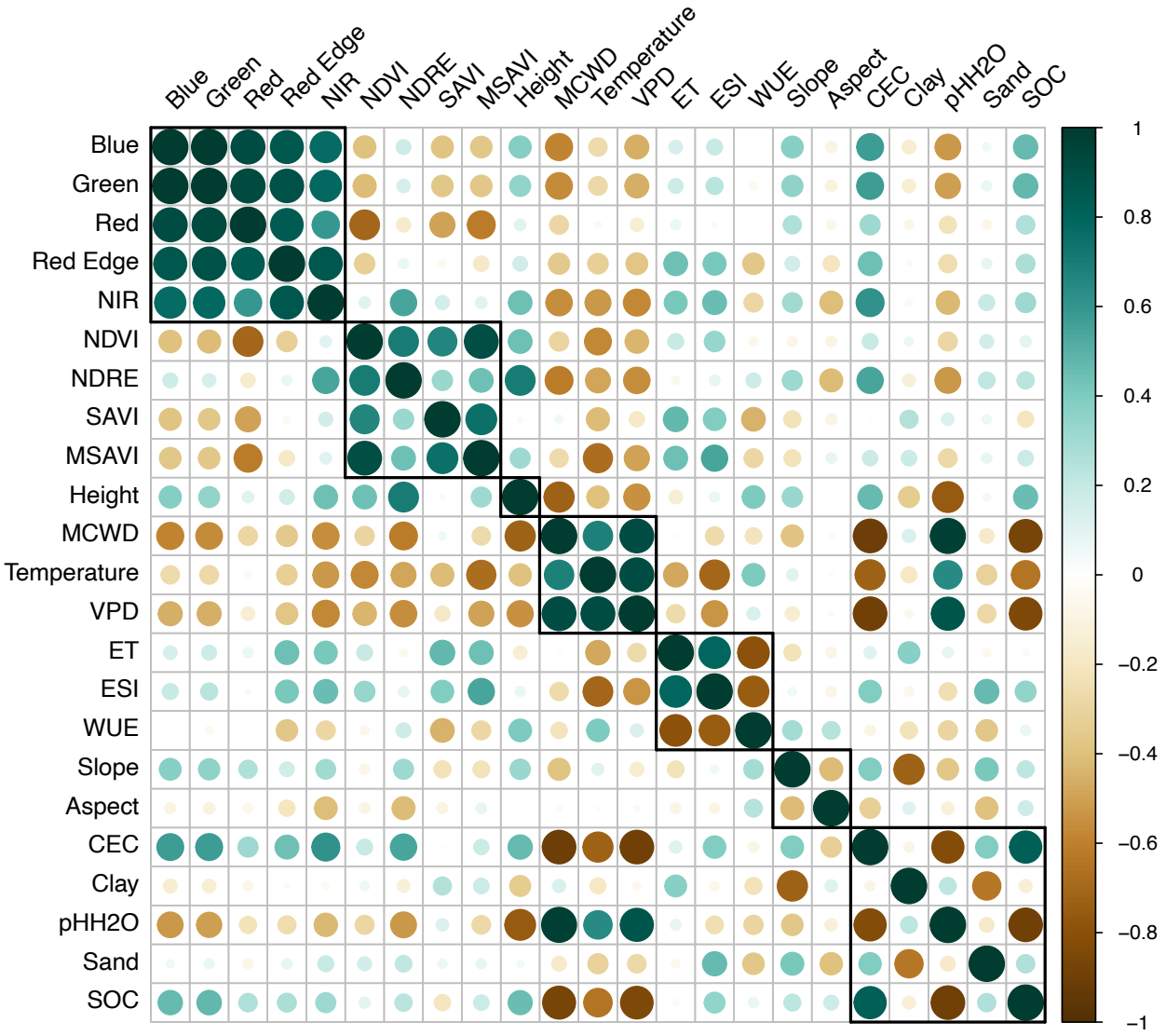

Fig. S5.2. Input band within-category correlation.

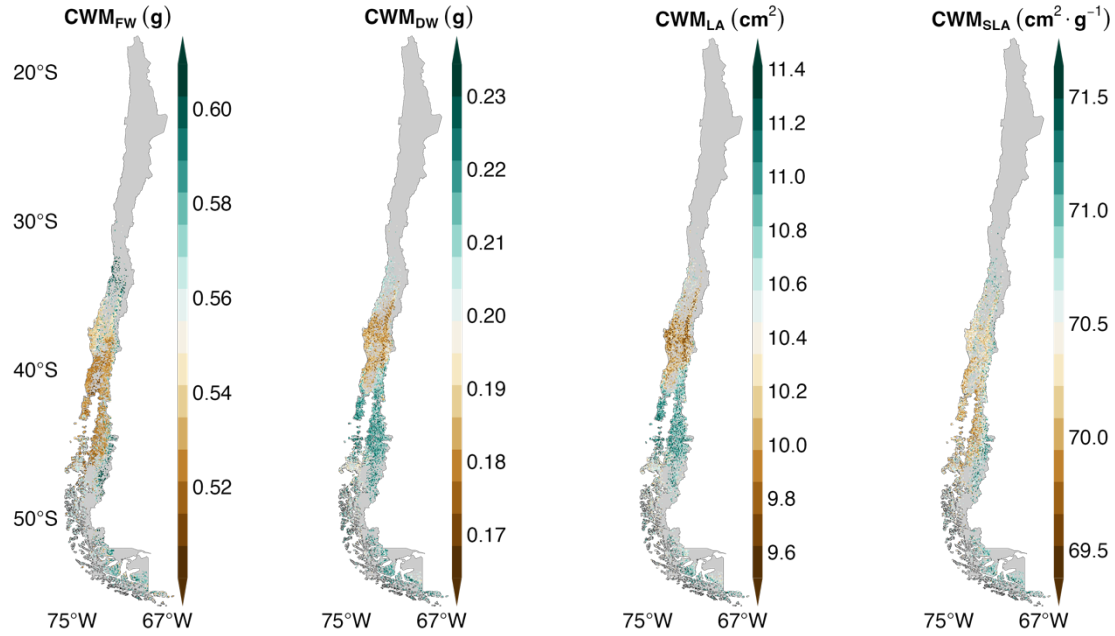

Fig. S5.3. Distribution maps of CWM of FW, DW, LA, and SLA.

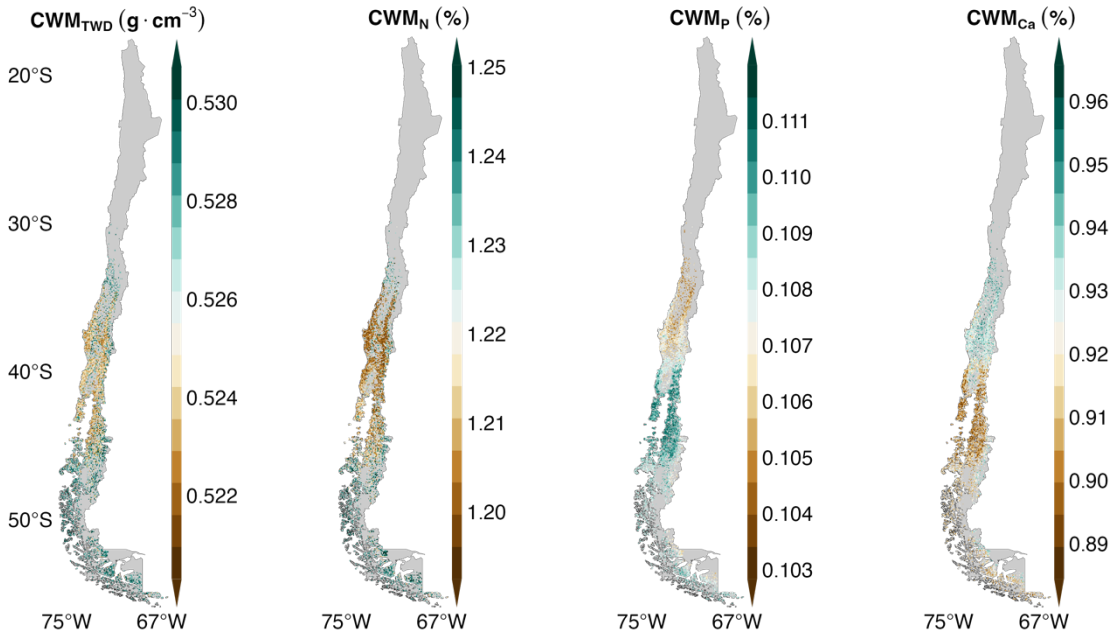

Fig. S5.4. Distribution maps of CWM of TWD, N, P, and Ca.

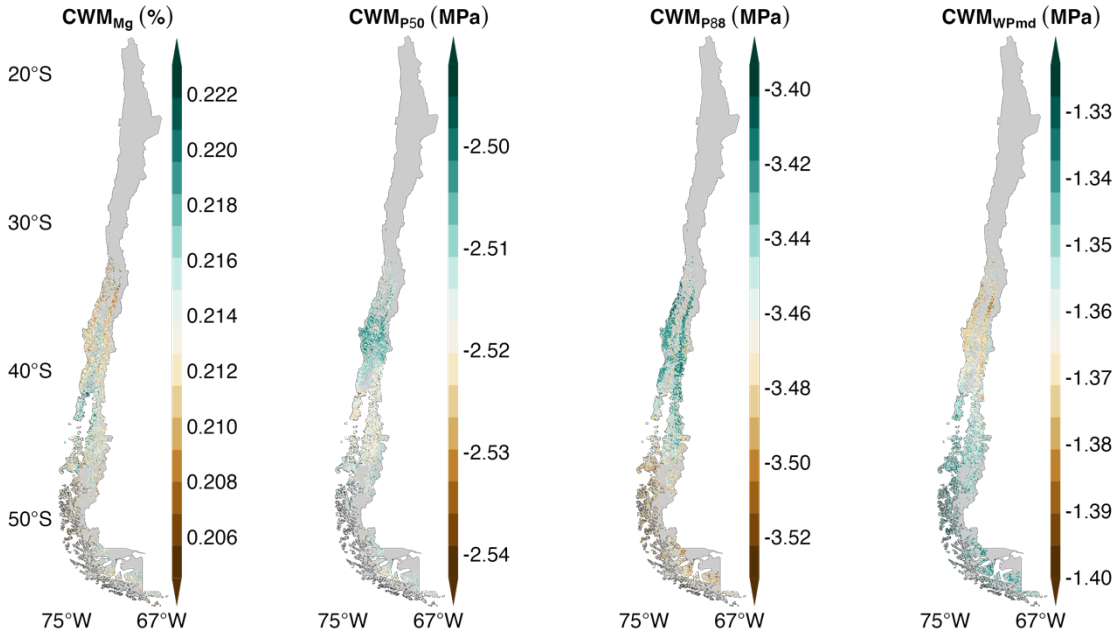

Fig. S5.5. Distribution maps of CWM of Mg, P50, P88, and WPmd.

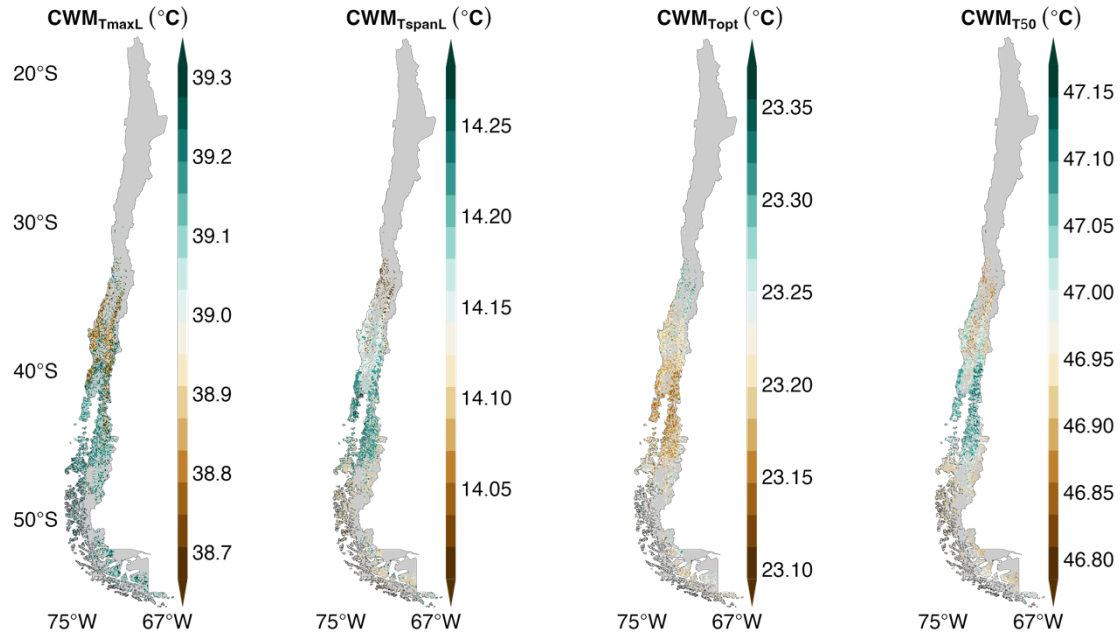

Fig. S5.6. Distribution maps of CWM of TmaxL, TspanL, Topt, and T50.

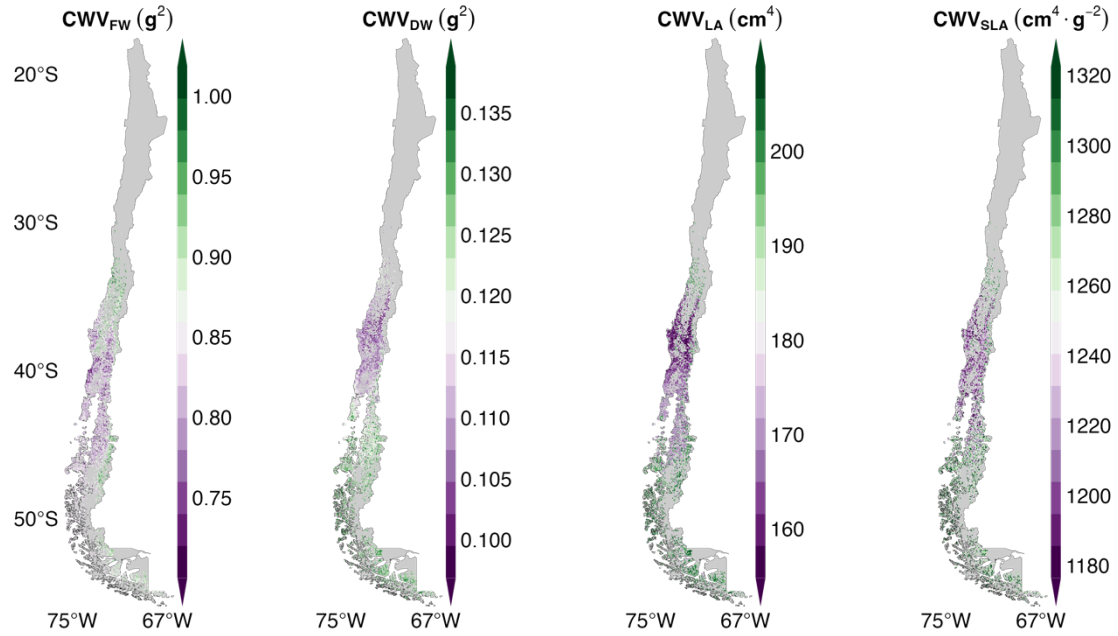

Fig. S5.7. Distribution maps of CWV of FW, DW, LA, and SLA.

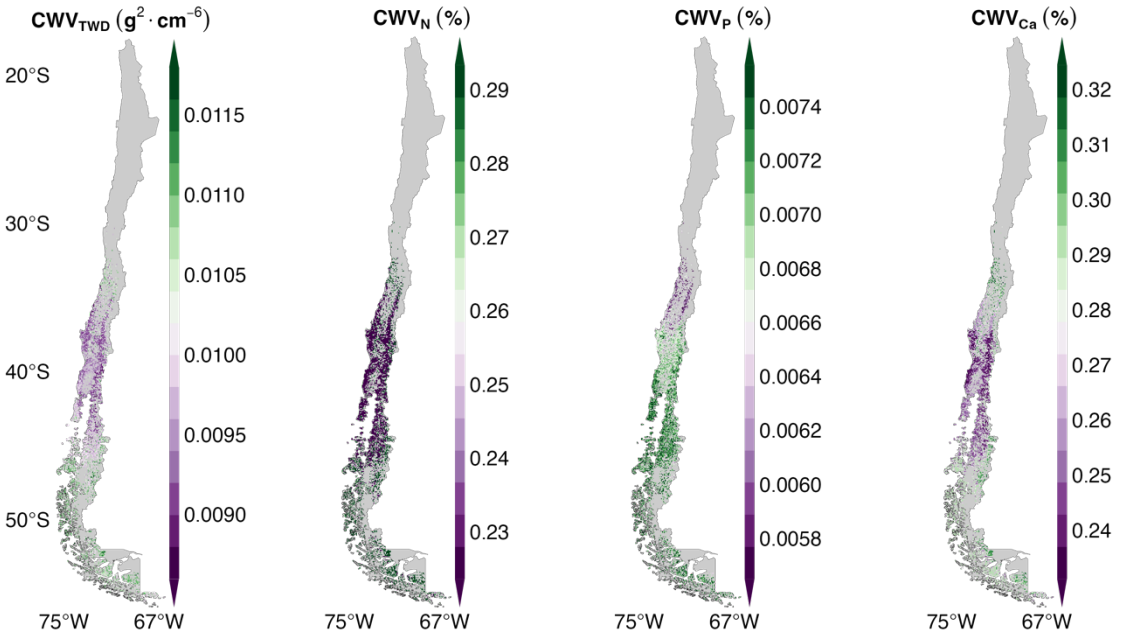

Fig. S5.8. Distribution maps of CWV of TWD, N, P, and Ca.

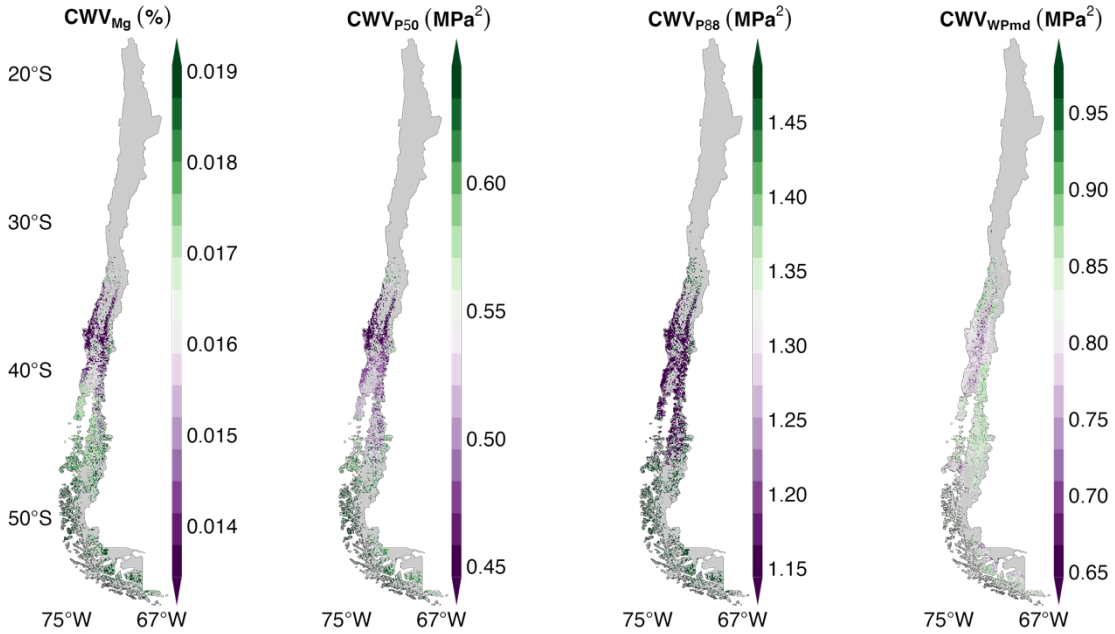

Fig. S5.9. Distribution maps of CWV of Mg, P50, P88, and WPmd.

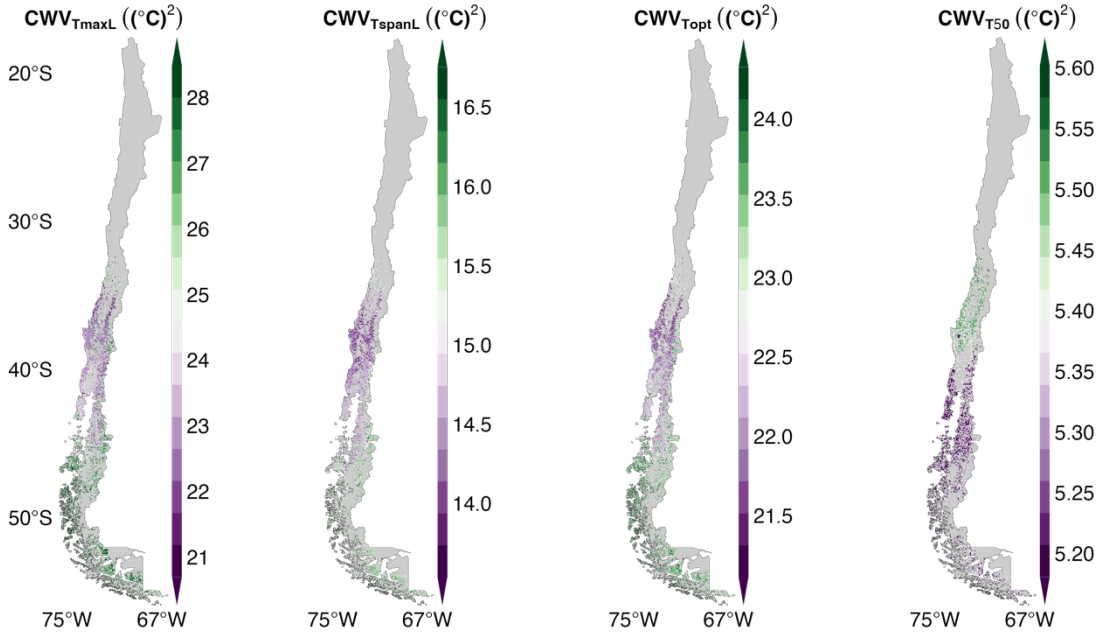

Fig. S5.10. Distribution maps of CWV of TmaxL, TspanL, Topt, and T50.

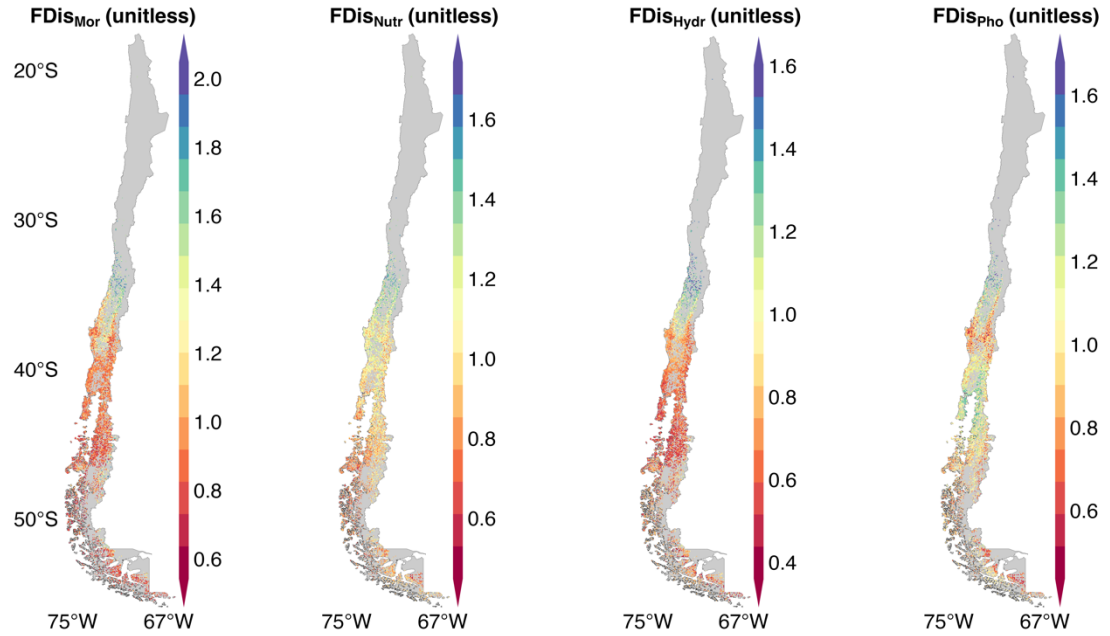

Fig. S5.11. Distribution maps of FDis of morphological, nutrients, hydraulic, and photosynthetic traits.

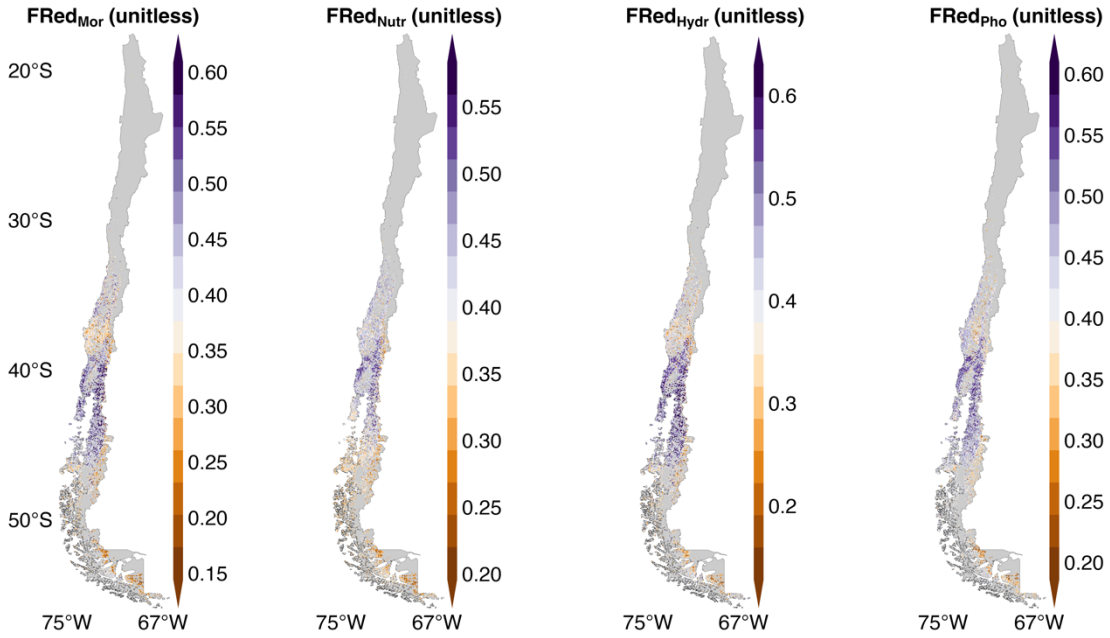

Fig. S5.12. Distribution maps of FRed of morphological, nutrients, hydraulic, and photosynthetic traits.

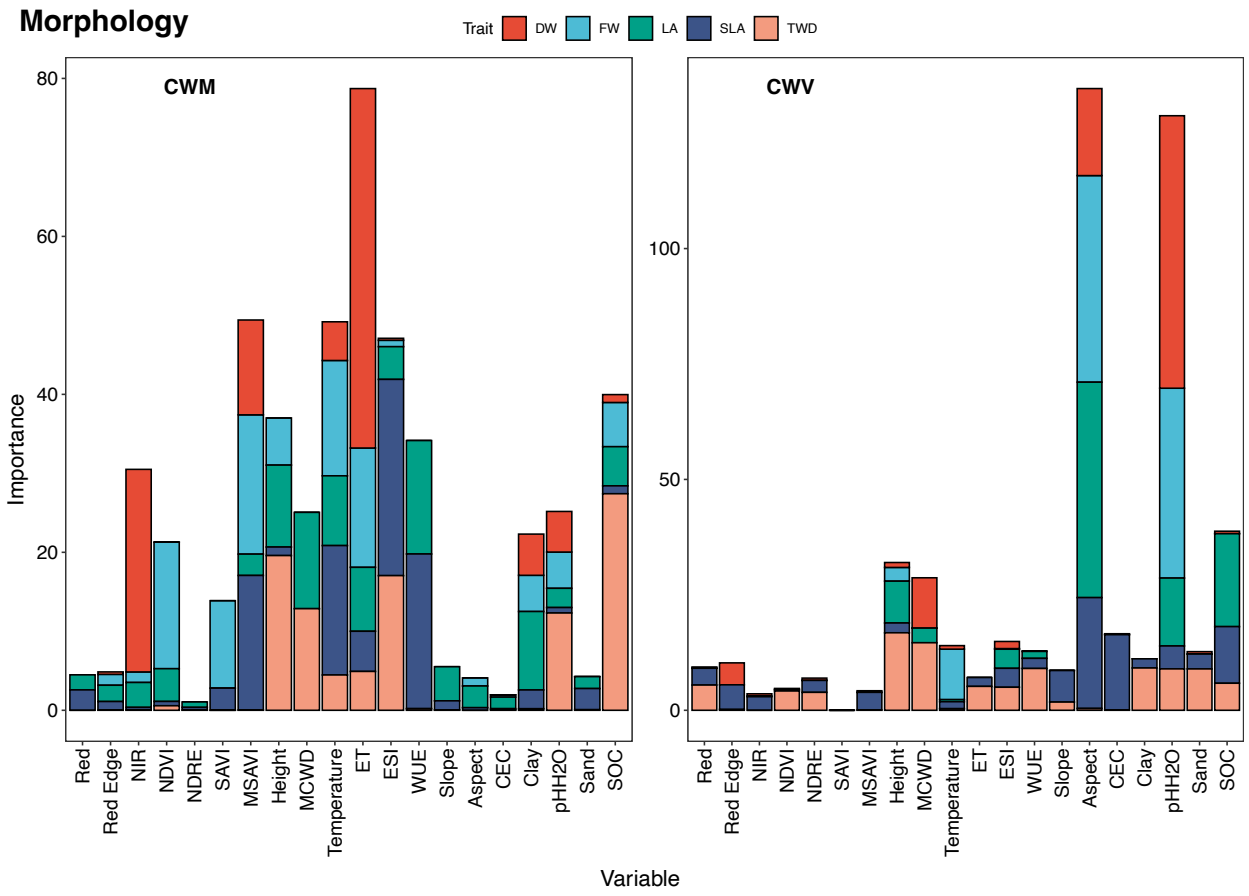

Fig. S5.13. The contribution of each variable in predicting morphological traits. Variable importance of all variables inputted into Random forests regression for predicting the two community-weighted moments of morphological traits. Each panel contains two stacked bar charts, representing the variable importance of all variables in predicting CWM and CWV of functional traits, respectively. All stacked bar charts are arranged in the order of spectral bands, vegetation indices, plant canopy height, climatic covariates, hydrological stress, topography, and soil properties. Each stacked bar denotes the importance of an input variable for predicting functional traits with different segments corresponding to distinct functional traits. Colours are used to differentiate the five morphological traits, refer to the legend for the corresponding colour-key associations.

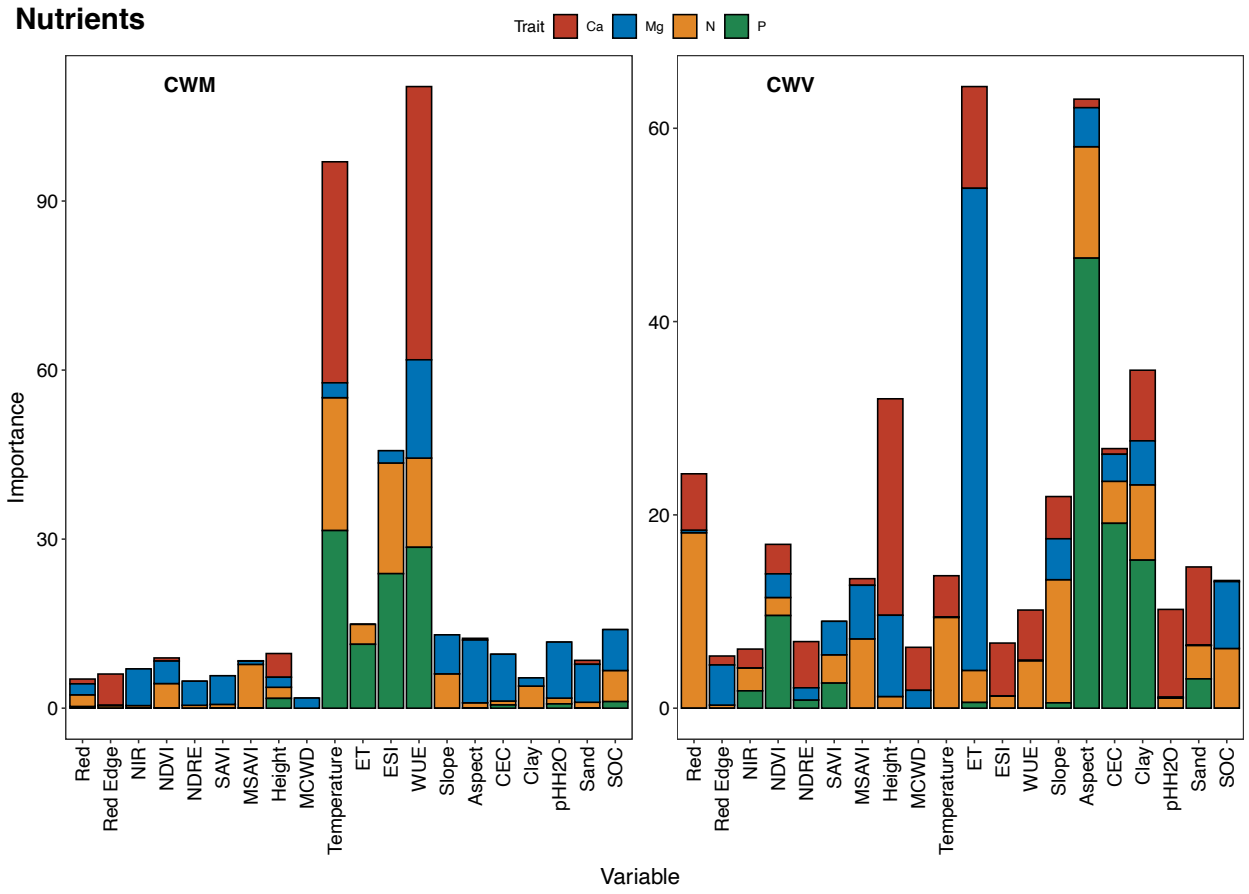

Fig. S5.14. The contribution of each variable in predicting nutrient traits. Variable importance of all variables inputted into Random forests regression for predicting the two community-weighted moments of nutrient traits. Each panel contains two stacked bar charts, representing the variable importance of all variables in predicting CWM and CWV of functional traits, respectively. All stacked bar charts are arranged in the order of spectral bands, vegetation indices, plant canopy height, climatic covariates, hydrological stress, topography, and soil properties. Each stacked bar denotes the importance of an input variable for predicting functional traits with different segments corresponding to distinct functional traits. Colours are used to differentiate the four nutrient traits, refer to the legend for the corresponding colour-key associations.

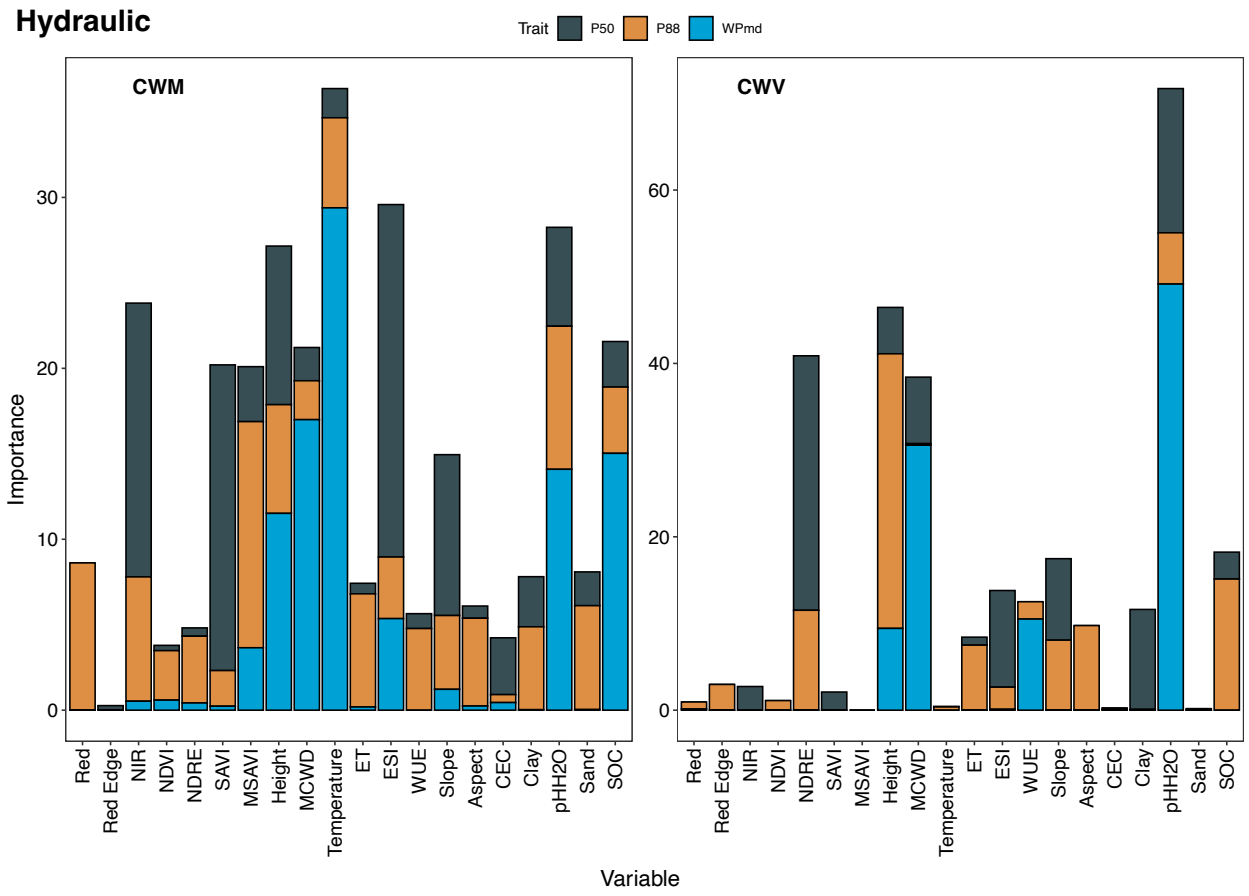

Fig. S5.15. The contribution of each variable in predicting hydraulic traits. Variable importance of all variables inputted into Random forests regression for predicting the two community-weighted moments of hydraulic traits. Each panel contains two stacked bar charts, representing the variable importance of all variables in predicting CWM and CWV of functional traits, respectively. All stacked bar charts are arranged in the order of spectral bands, vegetation indices, plant canopy height, climatic covariates, hydrological stress, topography, and soil properties. Each stacked bar denotes the importance of an input variable for predicting functional traits with different segments corresponding to distinct functional traits. Colours are used to differentiate the three hydraulic traits, refer to the legend for the corresponding colour-key associations.

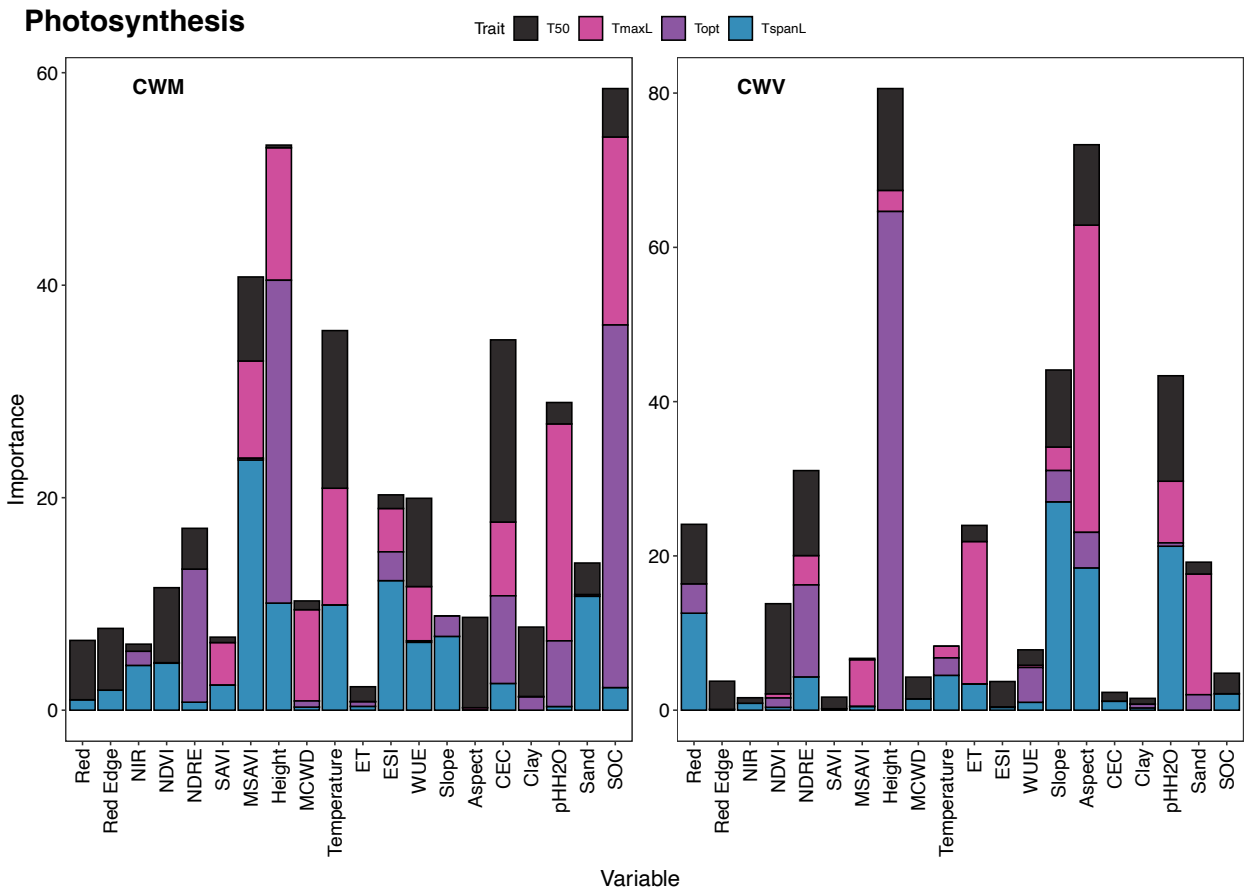

Fig. S5.16. The contribution of each variable in predicting photosynthetic traits. Variable importance of all variables inputted into Random forests regression for predicting the two community-weighted moments of photosynthetic traits. Each panel contains two stacked bar charts, representing the variable importance of all variables in predicting CWM and CWV of functional traits, respectively. All stacked bar charts are arranged in the order of spectral bands, vegetation indices, plant canopy height, climatic covariates, hydrological stress, topography, and soil properties. Each stacked bar denotes the importance of an input variable for predicting functional traits with different segments corresponding to distinct functional traits. Colours are used to differentiate the four photosynthetic traits, refer to the legend for the corresponding colour-key associations.

5.9.2. Sampling design

At each of the seven study sites, we installed two or three permanent plots to estimate tree abundance (Supplementary Table S5.1). The dominant tree species (in basal area) at each site were: *Lithraea caustica* and *Peumus boldus* in CAB, *Austrocedrus chilensis, Nothofagus dombeyi* and *Nothofagus obliqua* in RAD, *Laureliopsis philippiana, Nothofagus dombeyi* and *Saxegothaea conspicua* in SPT, *Drimys winteri, Fitzroya cupressoides* and *Nothofagus betuloides* in ALE, *Drimys winteri, Laureliopsis philippiana* and *Nothofagus betuloides* in COR, *Nothofagus pumilio* in TRA and *Nothofagus pumilio* and *Nothofagus antarctica* in MAG (Supplementary Table S5.1).

5.9.3. Trait measurements

All traits were measured in adult individuals (between 20 cm and 80 cm diameter at breast height-DBH) of the most abundant tree species at each site. Measurements were taken during the Austral Spring and Summer seasons (from November to February).

Leaf morphological traits were measured in 10 randomly selected individuals per species per site, according to *s*tandardised protocols (Pérez-Harguindeguy et al., 2013). Within one or two hours (h) after collection, one to five (depending on leaf size) fully expanded leaves per individual were scanned (Scanner Epson Perfection V850) and their fresh weight (FW; g) was measured using an analytical balance (ADAM PGL 203). Leaves were then oven-dried at 60 °C for 48 h to measure their dry weight (DW; g). Leaf area (LA; cm^2) was calculated using ImageJ (C. A. Schneider et al., 2012), specific leaf area (SLA; the ratio of leaf area to leaf dry mass [$cm^2\ g^{-1}$]), leaf mass per area (LMA; the ratio of leaf dry mass to leaf area [$g\ cm^{-2}$]), and leaf dry matter content (LDMC; the ratio of leaf dry mass to fresh mass [$mg\ g^{-1}$]) were also calculated. For trunk wood density estimates, an increment core of approximately 10 cm length (5 mm diameter) was collected using an increment borer, and a 5 cm branch section was cut for branch wood density. The branch section was cut from a large branch collected for hydraulic vulnerability measurements (see below). Wood density (WD; the ratio of oven dry mass to green volume [$g\ cm^{-3}$]) was calculated using shorter wood sections (i.e., 3 cm length), from where green volume was calculated (after removing branch's bark) using the water displacement method (Osazuwa-Peters & Zanne, 2011). Wood pieces were then oven-dried at 60 °C for 48 h to measure their dry weight.

For leaf nutrients, four individuals were sampled per species per site. Fully expanded leaves were collected from tree branches (the same used for photosynthetic traits measurements), oven-dried at 60 °C for 48 h, and stored in paper bags until analysis. Nitrogen content (N [%]), phosphorus content (P [%]), potassium content (K [%]), calcium content (Ca [%]), magnesium content (Mg [%]), and the N/P ratio were quantified at the Laboratorio de Nutrición y Suelos Forestales at the Universidad Austral de Chile.

The stem P50 and P88, were determined in five trees per site through xylem vulnerability to air entry curves, that relate the xylem water potential measured with a Scholander pressure bomb and the percent loss of hydraulic function (i.e. the percentage of air discharged) using a pneumatron apparatus V 1.0 (Pereira et al., 2016, 2020). For this purpose, long branches approximately 1 m long were collected early in the morning from the top or sun exposed areas of the trees using a big shot and a handmade knife. Smaller branches, that were cut under water, were used to record the air flowing out of the stems. For the development of the curve, measurements (air discharged and water potentials) were repeatedly taken after variable dehydration times (15 minutes at the beginning, then 30 minutes and up to one hour), and a sigmoidal curve was used to fit the data and calculate the P50 and P88 for each tree (Pereira et al., 2016).

The hydraulic safety margin (MPa) was calculated as the difference between the stem P50 and P88 and the minimum xylem water potential, measured in five trees per site at the end of the summer.

Photosynthesis temperature response curves (A-T curves) were performed in long branches of four trees per site, collected following the same protocol mentioned above. Measurements were taken between 10:00 and 15:00 h on fully expanded leaves using an open gas exchange system (Li- 6400XT, Li-Cor Inc., Lincoln, NE, USA) set at 1000 mmol photons m^{-2} s^{-1} (10% blue), at an ambient CO_2 concentration (400 mmol CO_2 mol^{-1}) and at 13 different ambient/block temperatures (9°C, 12°C, 15°C, 18°C, 21°C, 24°C, 27°C, 30°C, 33°C, 36°C, 40°C, 45°C and 50°C). The temperature at carbon compensation point (TmaxL, °C), temperature of optimum photosynthesis (Topt, °C), photosynthesis rate at optimum temperature (Aopt, µmol CO_2 m^{-2} s^{-1}), and the breadth of temperature optimum (TspanL, °C) in each temperature response curve, were determined using a standard quadratic equation (Docherty et al., 2023). The temperature at which the maximum quantum yield of photosystem II declines to 50% (T50, °C) was estimated through heat thermal tolerance assays in five trees per site. 35 leaves (5 per temperature treatment) were collected per individual and were covered

with moist tissue paper and put into sealed plastic bags. Leaves were then immersed in a temperature-controlled water bath preset to the desired temperature (30 °C, 40 °C, 45 °C, 47 °C, 50 °C and 55°C) for 15 min. A set of leaves were not immersed in temperature treatments, which were used as a control (ambient temperature of about 18 to 20°C). After each temperature treatment, leaves in their plastic bags were placed into opaque containers for dark adaptation at room temperature for 30 min, before chlorophyll fluorescence (Fv/Fm) was measured with a handheld chlorophyll fluorometer. T50 was estimated using a four-parameter logistic curve (Docherty et al., 2023).

5.9.4. Processing workflow for plot-level remotely sensed data

The main steps for processing multispectral drone images with the Pix4D software included image radiometric correction and calibration (no correction for the long-wave infrared (LWIR) band because the thermal imager in Altum was already radiometrically calibrated) using reflectance panel and sunshine sensor data, and generation of reflectance maps for each spectral band. We then merged the reflectance maps into one multi-layer virtual raster (.vrt file) using the gdalbuildvrt programme of the Geospatial Data Abstraction Library (Rouault et al., 2024) in the command line for each plot. Finally, we loaded the .vrt file into the QGIS software and exported it as a raster (.tif file) for each plot. When using the LAStools software to process handheld LiDAR data, we first removed outliers with the LASview tool. Ground points were classified with the LASground_new tool using hyperfine search criteria to accurately identify ground points. We then extracted canopy height for all returns above a 2-m threshold with the LASheight tool following default settings, thus separating canopy from understory vegetation, and we removed duplicate returns with the LASduplicate tool.

5.9.5. Tables

Table S5.1. Total tree species richness and relative abundance (estimated from basal area) at each site. Site acronyms: CAB-Las Cabras, RAD-Radal Siete Tazas, SPT-San Pablo de Tregua, ALE-Alerce Costero National Park, COR-Correntoso, TRA-Trapananda National Reserve, MAG-Magallanes National Reserve.

	Sites						
	CAB	RAD	SPT	ALE	COR	TRA	MAG
Number of plots	3	3	2	2	2	2	2

Total tree-species richness		2	5	6	8	11	1	2
Plot size (ha)		0.36	0.36	1	0.6	1	1	1
Tree species	Tree acronyms	Relative abundance						
Austrocedrus chilensis	Ac	-	0.10929	-	-	-	-	-
Amomyrtus luma	Al	-	-	0.00912	-	0.06949	-	-
Amomyrtus meli	Am	-	-	0.00065	-	-	-	-
Caldcuvia paniculata	Cp	-	-	-	-	0.01847	-	-
Drimys winteri	Dw	-	-	-	0.03431	0.14052	-	-
Eucryphia cordifolia	Ec	-	-	-	-	0.05042	-	-
Fitzroya cupressoides	Fc	-	-	-	0.9021	-	-	-
Lithraea caustica	Lc	0.6271	-	-	-	-	-	-
Lomatia ferruginea	Lf	-	-	-	-	0.00115	-	-
Lomatia hirsuta	Lh	-	0.02135	-	-	-	-	-
Laureliopsis phillipiana	Lp	-	-	0.43608	-	0.29146	-	-
Maytenus boaria	Mb	-	0.0004	-	-	-	-	-
Myrceugenia planipes	Mp	-	-	0.02338	-	0.01259	-	-
Nothofagus antarctica	Na						-	0.1477
Nothofagus betuloides	Nb	-	-	-	0.02941	0.23699	-	-
Nothofagus dombeyi	Nd	-	0.68858	0.05351	0.00406	-	-	-
Nothofagus nitida	Nn	-	-	-	0.00733	-	-	-
Nothofagus obliqua	No	-	0.18041	-	-	-	-	-
Nothofagus pumilio	Np						1	0.8523
Ovidia pillopillo	Op	-	-	-	8.50E-05	-	-	-
Peumus boldus	Pb	0.3728	-	-	-	-	-	-
Podocarpus nubigenus	Pn	-	-	-	-	0.00674	-	-
Pilgerodendron uviferum	Pu	-	-	-	0.01619	-	-	-
Saxegothaea conspicua	Sc	-	-	0.47727	-	0.15959	-	-
Weinmannia trichosperma	Wt	-	-	-	0.00297	0.01259	-	-

Table S5.2. Information on plot locations, elevations, and sizes.

Site	Plot ID	Longitude (˚)	Latitude (˚)	Elevation (m)	Size (ha)
Las Cabras	CAB1	-71.192	-34.211	388.45	0.36
	CAB2	-71.193	-34.212	386.41	0.36
	CAB3	-71.193	-34.213	358.7	0.36
Radal 7 Tazas	RAD1	-70.97	-35.48	1233.53	0.36
	RAD2	-70.969	-35.479	1245.03	0.36
	RAD3	-70.969	-35.478	1244.595	0.36
San Pablo de Tregua	SPT1	-72.074	-39.598	876.293	1
	SPT3	-72.098	-39.604	774	1
Alerce Costero	ALE2	-73.445	-40.171	820	0.6
	ALE3	-73.443	-40.173	841.586	0.6

Correntoso	COR1	-72.65	-41.521	513.025	1
	COR3	-72.646	-41.522	442	1
Trapananda National Reserve	TRA1	-71.762	-45.338	1102	1
	TRA2	-71.764	-45.34	1108.75	1
Magallanes National Reserve	MAG1	-71.032	-53.142	401.376	1
	MAG2	-71.026	-53.143	392.472	1

Table S5.3. Description of all morphological traits measured and calculated in Chile and the reasons why they were measured in this study.

Trait	Abbreviation	Unit	Description	Trait selection justification
Leaf fresh weight	FW	g	Mass of a fresh leaf	Higher FW suggests robust growth and favourable environmental conditions, while lower values may indicate stress or resource limitations
Leaf dry weight	DW	g	Mass of a dry leaf	DW assesses the plant's biomass allocation and long-term growth strategies and resource-use efficiency
Specific leaf area	SLA	$cm^2\ g^{-1}$	A ratio indicating how much leaf area a plant builds with a given amount of leaf biomass	SLA correlates with whole plant growth and reflects the trade-off between resource acquisition and conservation
Leaf area	LA	cm^2	Area of leaves	LA quantifies the surface area available for photosynthesis, providing a direct measure of the plant's potential to capture solar energy and contribute to ecosystem productivity
Leaf mass per area	LMA	$g\ cm^{-2}$	The ratio between leaf dry mass and leaf area	Higher LMA suggests thicker, denser leaves with potentially lower photosynthetic rates, and lower LMA indicates thinner, more photosynthetically active leaves
Leaf dry matter content	LDMC	$mg\ g^{-1}$	The ratio of leaf dry mass to fresh mass	LDMC evaluates the proportion of dry matter in the leaf, providing insights into leaf structure, resource-use strategies, and the plant's its ability to retain water
Trunk wood density	TWD	$g\ cm^{-3}$	The dry weight per unit volume of wood, the amount of wood in a unit measured at trunks	TWD assesses the structural and mechanical properties of tree trunks, wood strength, resource allocation strategies, and potential resistance to mechanical stresses and environmental pressures

Branch wood density	BWD	g cm^{-3}	The dry weight per unit volume of wood, the amount of wood in a unit measured at branches	BWD evaluates the structural characteristics of tree branches, branch strength, mechanical stability, and resource allocation within the canopy, influencing overall tree architecture and ecological interactions

Table S5.4. Description of all leaf nutrients measured in Chile and the reasons why they were measured in this study.

Trait	Abbreviation	Unit	Description	Trait selection justification
Leaf calcium content	Ca	%	Calcium content per unit dry leaf mass	
Leaf potassium content	K	%	Potassium content per unit dry leaf mass	
Leaf magnesium content	Mg	%	Magnesium content per unit dry leaf mass	
Leaf nitrogen content	N	%	Nitrogen content per unit dry leaf mass	Leaf nutrients comprehensively assess plant nutritional status, nutrient interactions, and potential impacts ecosystem dynamics
Leaf phosphorus content	P	%	Phosphorus content per unit dry leaf mass	
Ratio of leaf nitrogen and phosphorus content	N/P	Unitless	Ratio of leaf nitrogen and phosphorus content per unit dry leaf mass	

Table S5.5. Description of all hydraulic traits measured in Chile and the reasons why they were measured in this study.

Trait	Abbreviation	Unit	Description	Trait selection justification
P50	P50	MPa	Water potential at which 50% and 88% of hydraulic conductivity is lost	P50 and P88 evaluate the plant's tolerance to water stress and its ability to maintain hydraulic conductivity under drought conditions
P88	P88	MPa		
WPmd	WPmd	MPa	Minimum water potential (midday water potential at the driest month)	WPmd assesses the plant's drought tolerance and capacity to withstand water stress, providing critical information on its ability to maintain water balance during periods of limited water availability
SM_P50	SM50	MPa	Safety Margin P50 and P88	SM50 and SM88 serve as important indicators predicting the vulnerability of plants to drought-induced mortality
SM_P88	SM88	MPa		

Table S5.6. Description of all photosynthetic traits measured in Chile and the reasons why they were measured in this study.

Trait	Abbreviation	Unit	Description	Trait selection justification
TmaxL	TmaxL	°C	Temperature at carbon compensation point	TmaxL assesses the minimum temperature required for a plant to achieve carbon balance, providing insights into a species' thermal tolerance, metabolic performance, and adaptation to specific environmental conditions
Temperature of Optimum Photosynthesis	Topt	°C	Temperature of optimum photosynthesis	Topt evaluates the temperature range at which a plant achieves maximal photosynthetic efficiency, species' thermal adaptation, growth potential, and responsiveness to changing environmental conditions
Photosynthesis rate at optimum temperature	Aopt	μmol CO_2 m^{-2} s^{-1}	Photosynthesis rate at optimum temperature	Aopt assesses the species' potential for carbon assimilation and overall growth performance

TspanL	TspanL	°C	Breadth of temperature optimum	TspanL characterised the range of temperatures over which a plant exhibits optimal photosynthetic rates and the species' ability to perform efficiently across varying environmental conditions
T50	T50	°C	Temperature at which the maximum quantum yield of the photosystem II declines to 50%	T50 assesses the species' vulnerability to temperature-induced reductions in photosynthetic efficiency

Table S5.7. Description of multispectral images collected for each plot. B, G, R, RE, and NIR are abbreviations for the spectral bands blue, green, red, red edge, and near-infrared, respectively.

Plot	Instrument type	Imaging date	Scenes tiles	Spectral bands (centre bandwidth (nm))	Spatial resolution (m)
CAB1	MicaSense Altum-PT	10/01/2020	618	B (475), G (560), R (668), RE (717), NIR (842)	5.28×10^{-2}
CAB2	MicaSense Altum-PT	10/01/2020	1200	B (475), G (560), R (668), RE (717), NIR (842)	5.28×10^{-2}
CAB3	MicaSense Altum-PT	10/01/2020	799	B (475), G (560), R (668), RE (717), NIR (842)	5.28×10^{-2}
RAD3	MicaSense Altum-PT	11/01/2020	1194	B (475), G (560), R (668), RE (717), NIR (842)	5.28×10^{-2}
RAD2	MicaSense Altum-PT	11/01/2020	1356	B (475), G (560), R (668), RE (717), NIR (842)	5.28×10^{-2}
RAD1	MicaSense Altum-PT	11/01/2020	1188	B (475), G (560), R (668), RE (717), NIR (842)	5.28×10^{-2}
SPT1	SuperDove	09/11/2021	2	Coastal blue (431-452), B (465-515), Green I (513-549), G (547-583), Yellow (600-620), R (650-680), RE (697-713), NIR (845-885)	3
SPT3	MicaSense Altum-PT	03/03/2020	390	B (475), G (560), R (668), RE (717), NIR (842)	5.28×10^{-2}
ALE2	SuperDove	18/09/2020	2	B (465-515), G (547-583), R (650-680), RE (697-713), NIR (845-885)	3
ALE3	MicaSense Altum-PT	04/03/2020	468	B (475), G (560), R (668), RE (717), NIR (842)	5.28×10^{-2}
COR1	SuperDove	24/03/2021	1	B (465-515), G (547-583), R (650-680), RE (697-713), NIR (845-885)	3
COR3	SuperDove	24/03/2021	1	B (465-515), G (547-583), R (650-680), RE (697-713), NIR (845-885)	3
TRA1	MicaSense Altum-PT	20/01/2020	498	B (475), G (560), R (668), RE (717), NIR (842)	5.28×10^{-2}

TRA2	MicaSense Altum-PT	20/01/2020	732	B (475), G (560), R (668), RE (717), NIR (842)	5.28×10^{-2}
MAG1	SuperDove	17/01/2023	1	Coastal blue (431-452), B (465-515), Green I (513-549), G (547-583), Yellow (600-620), R (650-680), RE (697-713), NIR (845-885)	3
MAG2	MicaSense Altum-PT	07/03/2020	780	B (475), G (560), R (668), RE (717), NIR (842)	5.28×10^{-2}

Table S5.8. Description of LiDAR data collected for each plot.

Plot	Instrument type	Imaging date	Scanner points per second	Spatial resolution (m)
CAB1	ZEB1 handheld 3D scanner	06/01/2020	43000	0.01-0.03 (environment dependant)
CAB2	ZEB1 handheld 3D scanner	06/01/2020	43000	0.01-0.03 (environment dependant)
CAB3	ZEB1 handheld 3D scanner	06/01/2020	43000	0.01-0.03 (environment dependant)
RAD3	ZEB1 handheld 3D scanner	17/01/2020	43000	0.01-0.03 (environment dependant)
RAD2	ZEB1 handheld 3D scanner	17/01/2020	43000	0.01-0.03 (environment dependant)
RAD1	ZEB1 handheld 3D scanner	17/01/2020	43000	0.01-0.03 (environment dependant)
SPT1	ZEB1 handheld 3D scanner	28/02/2020	43000	0.01-0.03 (environment dependant)
SPT3	ZEB1 handheld 3D scanner	28/02/2020	43000	0.01-0.03 (environment dependant)
ALE2	ZEB1 handheld 3D scanner	29/02/2020	43000	0.01-0.03 (environment dependant)
ALE3	ZEB1 handheld 3D scanner	29/02/2020	43000	0.01-0.03 (environment dependant)
COR1	Global Forest Canopy Height	/	/	30
COR3	Global Forest Canopy Height	/	/	30
TRA1	ZEB1 handheld 3D scanner	15/01/2020	43000	0.01-0.03 (environment dependant)
TRA2	ZEB1 handheld 3D scanner	15/01/2020	43000	0.01-0.03 (environment dependant)
MAG1	ZEB1 handheld 3D scanner	02/03/2020	43000	0.01-0.03 (environment dependant)

MAG2	ZEB1 handheld 3D scanner	03/03/2020	43000	0.01-0.03 (environment dependant)

Table S5.9. Vegetation indices generated from spectral bands.

Vegetation index	Abbreviation	Equation	Description
Normalised Difference Vegetation Index	NDVI	$\frac{\rho_{NIR}-\rho_{Red}}{\rho_{NIR}+\rho_{Red}}$	Used to estimate the amount and health of vegetation
Normalised Difference Red Edge Index	NDRE	$\frac{\rho_{NIR}-\rho_{Red\ Edge}}{\rho_{NIR}+\rho_{Red\ Edge}}$	Particularly useful for assessing subtle changes in vegetation health and stress
Soil-Adjusted Vegetation Index	SAVI	$1.5\times\frac{\rho_{NIR}-\rho_{Red}}{\rho_{NIR}+\rho_{Red}+0.5}$	An improvement over NDVI, designed to minimise the influence of soil brightness
Modified Soil-Adjusted Vegetation Index	MSAVI	$\frac{2\times\rho_{NIR}+1-\sqrt{(2\times\rho_{NIR}+1)^2-8\times(\rho_{NIR}-\rho_{Red})}}{2}$	Aiming to provide a more accurate representation of vegetation cover

Table S5.10. Model performance for mapping the two community-weighted moments of morphological traits. The bold numbers indicate the highest R^2 values.

Trait	FW	DW	LA	SLA	TWD

Moment	CWM	CWV	CWM	CWV	CWM	CWV	CWM	CWV	CWM	CWV
R^2	0.50	**0.64**	0.58	0.59	0.33	0.51	0.82	0.40	**0.92**	0.37
RMSE	0.18	0.19	0.07	0.03	4.04	57.25	18.71	565.68	0.05	0.00
MAE	0.14	0.14	0.05	0.02	3.14	47.72	15.48	453.34	0.04	0.00

Table S5.11. Model performance for mapping the two community-weighted moments of nutrient traits. The bold numbers indicate the highest R^2 values.

Trait	N		P		Ca		Mg	
Moment	CWM	CWV	CWM	CWV	CWM	CWV	CWM	CWV
R^2	0.75	0.27	**0.77**	0.39	0.36	**0.44**	0.25	0.15
RMSE	0.28	0.05	0.05	0.00	0.23	0.15	0.07	0.01
MAE	0.25	0.04	0.03	0.00	0.17	0.09	0.06	0.01

Table S5.12. Model performance for mapping the two community-weighted moments of hydraulic traits. The bold numbers indicate the highest R^2 values.

Trait	P50		P88		WPmd	
Moment	CWM	CWV	CWM	CWV	CWM	CWV

R^2	0.54	0.27	0.77	0.14	**0.97**	**0.96**
RMSE	0.36	0.30	0.49	0.53	0.20	0.39
MAE	0.29	0.25	0.42	0.46	0.16	0.21

Table S5.13. Model performance for mapping the two community-weighted moments of photosynthetic traits. The bold numbers indicate the highest R^2 values.

Trait	TmaxL		Topt		TspanL		T50	
Moment	CWM	CWV	CWM	CWV	CWM	CWV	CWM	CWV
R^2	0.57	0.54	**0.68**	**0.77**	0.34	0.18	0.57	0.38
RMSE	2.08	5.49	1.83	2.59	1.04	2.49	1.26	1.88
MAE	1.41	3.69	1.47	1.66	0.76	1.60	0.91	1.42

Table S5.14. Model performance for assessing the four groups of FDis and FRed. The bold numbers indicate the highest R^2 values.

Group	Morphology		Nutrients		Hydraulic		Photosynthesis	
Metric	FDis	FRed	FDis	FRed	FDis	FRed	FDis	FRed
R^2	0.36	0.52	0.23	0.48	**0.69**	0.54	0.64	**0.56**

RMSE	0.91	0.16	0.55	0.17	0.41	0.18	0.44	0.16
MAE	0.69	0.12	0.45	0.13	0.32	0.15	0.33	0.13

5.9.6. References

Docherty, E. M., Gloor, E., Sponchiado, D., Gilpin, M., Pinto, C. A. D., Junior, H. M., Coughlin, I., Ferreira, L., Junior, J. A. S., da Costa, A. C. L., Meir, P., & Galbraith, D. (2023). Long-term drought effects on the thermal sensitivity of Amazon forest trees. *Plant, Cell & Environment*, *46*(1), 185–198. https://doi.org/10.1111/pce.14465

Osazuwa-Peters, O., & Zanne, A. (2011). Wood density protocol. *URL Http://Www. Publish. Csiro. Au/Prometheuswiki/Tiki-Pagehistory. Php*, *3*, 199–217.

Pereira, L., Bittencourt, P. R. L., Oliveira, R. S., Junior, M. B. M., Barros, F. V., Ribeiro, R. V., & Mazzafera, P. (2016). Plant pneumatics: Stem air flow is related to embolism – new perspectives on methods in plant hydraulics. *New Phytologist*, *211*(1), 357–370. https://doi.org/10.1111/nph.13905

Pereira, L., Bittencourt, P. R. L., Pacheco, V. S., Miranda, M. T., Zhang, Y., Oliveira, R. S., Groenendijk, P., Machado, E. C., Tyree, M. T., Jansen, S., Rowland, L., & Ribeiro, R. V. (2020). The Pneumatron: An automated pneumatic apparatus for estimating xylem vulnerability to embolism at high temporal resolution. *Plant, Cell & Environment*, *43*(1), 131–142. https://doi.org/10.1111/pce.13647

Pérez-Harguindeguy, N., Díaz, S., Garnier, E., Lavorel, S., Poorter, H., Jaureguiberry, P., Bret-Harte, M. S., Cornwell, W. K., Craine, J. M., Gurvich, D. E., Urcelay, C., Veneklaas, E. J., Reich, P. B., Poorter, L., Wright, I. J., Ray, P., Enrico, L., Pausas, J. G., De Vos, A. C., … Cornelissen, J. H. C. (2013). New handbook for standardised measurement of plant functional traits worldwide. *Australian Journal of Botany*, *61*(3), 167. https://doi.org/10.1071/BT12225

Schneider, C. A., Rasband, W. S., & Eliceiri, K. W. (2012). NIH Image to ImageJ: 25 years of image analysis. *Nature Methods*, *9*(7), 671–675. https://doi.org/10.1038/nmeth.2089

5.10. Declarations of competing interest

The authors declare that they have no known competing financial interests or personal relationships that could have appeared to influence the work reported in this paper.

5.11. Acknowledgements

Xiongjie Deng receives the Pay It Forward Scholarship (by China Oxford Scholarship Fund, Oxford) and the New Blackfriars Scholarship (by Blackfriars Hall, Oxford). Danny E. Carvajal is funded by the Fondecyt postdoctoral Grant 3230154 and Proyecto Basal FB210006 (Instituto de Ecología y Biodiversidad, IEB). Rocío Urrutia-Jalabert is funded by the Fondecyt Regular Grant 1240500, the ANID-Millennium Science Initiative-Center Code NCN2024_040, the ANID/FONDAP 1523A0002 project (Center for Climate and Resilience Research CR2). The data collection for this project was funded by the Natural Environment Research Council (NERC) CONICYT ARBOLES project (Grant: NE/S011811/1). Sandra Díaz is funded by an Oxford Martin School Fellowship. Yadvinder Malhi is supported by the Frank Jackson Foundation. Jesús Aguirre-Gutiérrez is funded by the NERC (Grants: NE/T011084/1; NE/Z504191/1), the Leverhulme Trust (RPG-2024-342), and the Royal Society (RG\R1\251370).

5.12. Data availability

Data will be made available on request.

Chapter 6 Trait-based analysis of Mexican forest resilience to extreme climate change (Paper 3)

6.1. Preface

As the final chapter of this thesis, this study builds on the trait-mapping framework and spatial analyses of functional diversity and redundancy established in **Papers 1** and **2** to explore how these biodiversity metrics contribute to forest carbon resilience, defined here as the ability of forests to maintain or accumulate carbon, reflected in carbon stocks, gains, losses, and net carbon sink. Focusing on temperate and tropical forests in Mexico, we assess how initial functional diversity and redundancy measured at the start of monitoring in morphological and nutrient traits influences temporal changes in carbon stocks and dynamics under increasing climatic stress. This chapter shifts from spatial prediction to ecological interpretation, aiming to understand the stabilising role of biodiversity in maintaining carbon stocks and dynamics under climate change.

6.1.1. Highlights

Using repeated forest inventory data, we examined how initial functional diversity and climate stressors shape temporal changes in carbon stocks, gains, losses, and net carbon sink. In temperate forests, higher morphological trait diversity enhanced carbon accumulation and stability, buffering the impacts of drought and temporal stress. Nutrient trait diversity, by contrast, was linked to reduced carbon resilience, likely due to traits favouring fast growth over drought tolerance. Interaction analyses revealed that morphological diversity mitigated, while nutrient diversity amplified, climate-related carbon losses. These stabilising effects were not evident in tropical forests, possibly due to trait saturation or data limitations.

This paper is prepared for submission to *Nature Climate Change*, which requires the Method section to be placed at the end of the manuscript in accordance with the journal's author guidelines.

6.1.2. Author information and contribution statement

Xiongjie Deng[1*], José Javier Corral-Rivas[2], Maria Guadalupe Nava-Miranda[3,4], Huanyuan Zhang-Zheng[1,5], Yadvinder Malhi[1,5], Jesús Aguirre-Gutiérrez[1,5]

[1]Environmental Change Institute, School of Geography and the Environment, University of Oxford, Oxford, OX1 3QY, UK

[2]Facultad de Ciencias Forestales y Ambientales, Universidad Juárez del Estado de Durango, Durango 34120, Mexico

[3]Escuela Politécnica Superior de Ingeniería, Campus Terra, Universidad de Santiago de Compostela, 27002 Lugo, Spain

[4]Colegio de Ciencias y Humanidades, Universidad Juárez del Estado de Durango, Durango 34120, Mexico

[5]Leverhulme Centre for Nature Recovery, University of Oxford, Oxford, OX1 3QY, UK

Xiongjie Deng: Writing – original draft, Writing – review & editing, Methodology, Investigation, Software, Formal analysis, Conceptualisation. **José Javier Corral-Rivas:** Writing – review & editing, Field data collection. **Maria Guadalupe Nava-Miranda:** Writing – review & editing, Field data collection. **Huanyuan Zhang-Zheng:** Writing – review & editing, Methodology. **Yadvinder Malhi:** Writing – review & editing, Supervision. **Jesús Aguirre-Gutiérrez:** Writing – review & editing, Methodology, Conceptualisation, Supervision.

6.2. Abstract

Understanding the mechanisms that sustain forest carbon stocks and dynamics under climate change is critical for forecasting ecosystem resilience. Here, we use repeated forest inventory data from temperate and tropical forest plots in Mexico to assess how functional diversity and redundancy in morphological and nutrient traits at the beginning of monitoring (hereafter initial) and climatic stressors influence forest carbon resilience, defined as the forest's ability to maintain or accumulate carbon, reflected in temporal changes in carbon stocks, gains, losses, and net carbon sink. We find that in temperate forests, higher initial morphological functional diversity (FD_{Mor}) consistently enhances the stability of carbon-related processes, supporting greater carbon accumulation, higher gains, lower losses, and a stronger net sink, thereby buffering against the negative effects of increasing drought severity and temporal stress. In contrast, nutrient-based functional diversity (FD_{Nutr}) is associated with declines in carbon stability, likely reflecting trait combinations favouring fast growth but lower drought tolerance.

Interaction effects reveal that high FD_{Mor} restrains the adverse impacts of both climate and time on carbon fluxes, whereas high FD_{Nutr} amplifies them. In tropical forests, neither functional trait diversity nor climate variables shows strong or consistent associations with carbon resilience, possibly due to limited data, trait saturation, or overriding climatic constraints. These results highlight that the stabilising effect of functional trait diversity on forest carbon stocks and dynamics is particularly pronounced in temperate forests under increasing drought stress.

Keywords: Functional diversity; Carbon resilience; Warming; Drought stress; Climate change; Temperate forests; Tropical forests

6.3. Main

Forests are critical components of the global carbon cycle, they act as major carbon sinks that regulate atmospheric CO_2 levels and influence global climate patterns (Pan et al., 2011). Forest ecosystems are not only central to carbon storage and nutrient cycling (Malhi et al., 2024) but also provide a host of other essential services, including biodiversity support and water regulation (Chen et al., 2023). However, the growing intensity of climate change, particularly through extreme droughts, threatens the resilience of forest ecosystems worldwide (Malhi et al., 2020). Extreme droughts disrupt key carbon flux processes by limiting photosynthesis, reducing biomass growth, and increasing tree mortality, leading to substantial carbon losses from forest ecosystems (Doughty et al., 2015; Schlesinger et al., 2016). As drought stress intensifies, forests may experience declines in carbon gains due to suppressed productivity, while simultaneously facing increased carbon emissions through tree death and decomposition (Anderegg et al., 2013). In the most severe cases, these combined effects can shift forests from being net carbon sinks to becoming net carbon sources, thereby accelerating atmospheric CO_2 accumulation (Anderegg et al., 2013; Anderegg, Trugman, Badgley, Konings, et al., 2020; Yang et al., 2018). Measures of carbon stocks and dynamics (carbon gains, carbon losses, and net carbon sink) thus provide integrative indicators of forest functioning and resilience (defined as the ability of forests to absorb disturbances and reorganise under change while maintaining critical functions and structure (Scheffer, 2009)) under drought. However, predicting how this carbon dynamics respond to climatic extremes remains challenging without an understanding of the ecological and functional properties that confer stability to forest ecosystems.

Recent advances in trait-based ecology have highlighted the pivotal role of community functional trait diversity (FD) and redundancy (FR) in mediating forest responses to environmental stress (Sakschewski et al., 2016; Wieczynski et al., 2019; B. F. Oliveira et al., 2022; Hisano et al., 2024) such as drought. Functional traits, such as leaf area, wood density, and hydraulic traits, provide an aggregate measure of the dominant ecological strategies within a community, which directly influence drought tolerance (Anderegg et al., 2016, 2019; Serra-Maluquer et al., 2022). In addition, FD captures the range of trait values within a community and reflects the spectrum of ecological strategies that species employ in response to environmental challenges, and FD can reveal information about ecosystem functioning and the susceptibility of a forest ecosystem to climate change (Anderegg et al., 2018; Schneider et al., 2017) and disturbances (Durán et al., 2019; Jetz et al., 2016). There is a strong positive relationship between FD and forest stability and, by extension, resilience (Schmitt et al., 2020a). Higher FD can enhance ecosystem resilience by promoting complementary responses among coexisting species, which helps stabilise ecosystem functions such as carbon uptake and biomass retention during periods of stress (Hisano et al., 2024; Oliver et al., 2015; Schmitt et al., 2020b). On the other hand, FR reflects the degree to which multiple species share similar functional traits (Rosenfeld, 2002), and potentially act as an insurance mechanism to maintain ecosystem functioning despite the loss of individual species (Biggs et al., 2020), and thus buffer ecosystem functioning during disturbances: when one species declines or dies under stress, others with similar functional roles can compensate and maintain community-level processes (Ricotta et al., 2016) such as primary production and carbon sequestration. In systems subject to increasing climatic variability, such insurance effects are likely to be critical for long-term ecosystem stability.

While functional trait diversity and redundancy are not direct measures of resilience, they represent mechanisms that can promote the stability of ecosystem processes in the face of disturbance and directional change. From a conservation perspective, this means that maintaining or restoring functional trait diversity and redundancy can directly support climate mitigation goals by safeguarding carbon storage and ensuring continued forest functioning under intensifying climatic stress. Although these trait-based metrics are known to be vital in shaping forest resilience, there is a limited body of work linking functional trait metrics directly to carbon fluxes, and few studies have directly tested whether higher functional diversity and redundancy actually enhance resistance or resilience in terms of forest carbon stocks and

dynamics, particularly in the context of extreme droughts (Prentice et al., 2014; Sakschewski et al., 2016).

Known as one of the main world megadiverse countries, Mexico hosts 10 to 12 percent of the global biodiversity, with its forests spanning a wide range of ecosystems from tropical rainforests to temperate pine-oak forests. These forests play a critical role in carbon storage, nutrient cycling, climate regulation, and the maintenance of biodiversity (Fuller et al., 2007; Galicia & Zarco-Arista, 2014). However, Mexican forests are increasingly threatened by and vulnerable to the impacts of climate change. In particular they are currently undergoing one of the most extensive and severe droughts in decades (Dobler-Morales & Bocco, 2021). Despite their ecological importance, the resilience of these forests to such extreme climatic events remains poorly understood yet warrants urgent investigation. Understanding how Mexican forests respond to prolonged droughts, and the functional attributes that influence their capacity to withstand and recover from such droughts, is essential for informing conservation and management strategies. Maintaining high functional diversity increases an ecosystem's overall capacity to adapt to changing environmental conditions, safeguarding its long-term stability, and high functional redundancy ensures that crucial services like carbon sequestration continue even if some species decline due to climate impacts. By promoting and protecting functional diversity and redundancy, we are essentially increasing an ecosystem's adaptive capacity.

In biodiverse regions such as Mexico, where droughts are intensifying, it is crucial to examine how functional trait diversity and redundancy interact to influence carbon stocks and dynamics. Tropical and temperate forests are key to global biodiversity and carbon storage but are also among the most vulnerable to climate extremes (Bennett et al., 2023; Hubau et al., 2020; Millar & Stephenson, 2015). While numerous studies have observed the impacts of drought on forest structure and biomass (Bennett et al., 2021, 2023; Hubau et al., 2020; Maia et al., 2020), few have examined how community trait diversity and redundancy directly affect forest carbon fluxes under extreme drought conditions. This gap is especially pronounced in high-biodiversity countries like Mexico, where forest resilience remains largely unquantified in functional and carbon terms.

Here, we assess how functional trait diversity and redundancy mediate the carbon resilience of Mexican forests under intensifying drought stress. We compiled and analysed repeated forest census data from 293 forest plots (each 0.25 ha) across Mexico, including 278 temperate forest plots and 15 tropical forest plots, spanning the period from 2007 to 2021. Across these plots, we tracked over 13056 trees with diameter at breast height (DBH) greater

than 5 cm. Each plot was censused 2 to 3 times, with mean census intervals of 6.77 years, which enabled estimates of carbon stocks, gains, losses, and net sink strength over time. To characterise community functioning, we compiled data on morphological traits and leaf nutrients. Using these trait values, we calculated FD and FR separately for morphological traits and nutrients. Climatic conditions at each plot were characterised using mean annual maximum temperature (T_{max}, in °C), vapour pressure deficit (VPD, in kPa), and maximum climatological water deficit (MCWD, in mm), with spatial patterns and plot locations shown in Fig.6.1a-c, the climatic space occupied by the plots illustrated in Fig. 6.1d, and the long-term trends of these climate variables over the study period displayed in Fig. 6.1e.

This study tests the hypothesis that higher initial functional diversity enhances forest resilience to extreme climatic events, particularly droughts, by buffering carbon losses and maintaining positive net carbon balances. By linking community trait diversity metrics directly to observed carbon fluxes, we aim to evaluate how trait-based ecosystem properties shape both the resistance (reduced loss during drought) and recovery (subsequent gains) of forests. Unlike previous studies focused primarily on tropical systems, our analysis includes a large number of temperate Mexican forests, offering a broader perspective on how forest functional structure mediates carbon responses across diverse climatic contexts. Through this approach, we contribute novel insights into the mechanisms of forest resilience and the potential for functional trait-based metrics to inform forest conservation and climate mitigation strategies.

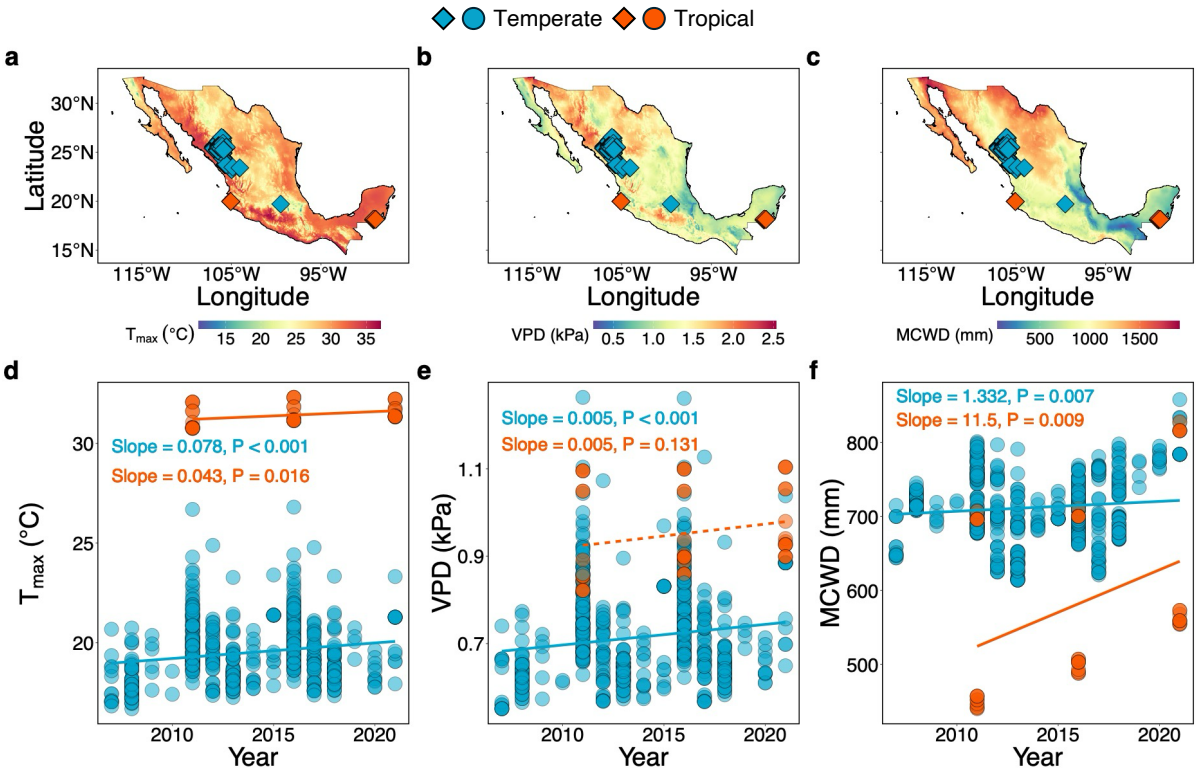

Fig. 6.1. Spatial patterns and long-term trends of warming and drought stress across temperate and tropical forests in Mexico. a-c, Spatial distributions of mean maximum temperature (T_{max}, °C, **a**), vapour pressure deficit (VPD, kPa, **b**), and maximum climatological water deficit (MCWD, mm, **c**) across Mexico over the study period (2007–2021), overlaid with the locations of temperate (blue squares) and tropical (orange squares) forest inventory plots. Note that all the squares are magnified for visualisation purposes. **d-f**, Temporal trends in T_{max} (**d**), VPD (**e**), and MCWD (**f**) from 2007 to 2021 for temperate (blue) and tropical (orange) forest plots. Each point represents an annual observation at a plot, and regression lines indicate the average trend for each forest type: solid lines represent statistically significant trends (P<0.05), while dashed lines denote non-significant trends (P>0.05).

6.4. Results

6.4.1. Intensifying warming and drought across Mexican forests

Between 2007 and 2021, both temperate and tropical forests in Mexico experienced statistically significant and concurrent warming and increasing drought stress, although the magnitude and significance of these changes varied by forest type. In temperate forests, maximum temperature (T_{max}) rose at a rate of 0.078 °C per year (P<0.001, Fig. 6.1d), while tropical forests exhibited a more modest but still significant increase of 0.043 °C per year (P=0.016, Fig. 6.1d). These

trends resulted in cumulative warming of approximately 1.09 °C and 0.60 °C over the 14-year period in temperate and tropical forests in Mexico, respectively.

Vapour pressure deficit (VPD), a measure of atmospheric aridity, also increased across both biomes, although significance differed. In temperate forests, VPD rose by 0.005 kPa per year (P<0.001, Fig. 6.1e), totalling an approximate rise of 0.07 kPa. In tropical forests, the rate of VPD increase was similar (0.005 kPa per year), but not statistically significant (P=0.131, Fig. 6.1e). Seasonal drought intensity, as reflected by the maximum climatological water deficit (MCWD), intensified in both biomes. Tropical forests showed the strongest increase, with MCWD deepening by 11.5 mm per year (P=0.009, Fig. 6.1f), accumulating to a total increase of ~161 mm over the study period. Temperate forests also experienced a significant rise in drought severity, with MCWD increasing by 1.332 mm per year (P=0.007, Fig. 6.1f), corresponding to an overall increase of ~18.6 mm.

6.4.2. Long-term trends and future projections of carbon stocks and dynamics

Over the period from 2007 to 2021, carbon stocks in temperate forests showed a significant long-term increase, with an estimated slope of 2.122 Mg C ha^{-1} yr^{-1} (P<0.001, Fig. 6.2a). Tropical forests also exhibited a significantly positive trend in carbon stocks with a slope of 2.475 Mg C ha^{-1} yr^{-1} (P=0.009, Fig. 6.2a). Carbon dynamics, in contrast, revealed more complex patterns. In temperate forests, carbon gains declined significantly over time (slope=-0.318 Mg C ha^{-1} yr^{-2}, P<0.001, Fig. 6.2c), while carbon losses remained stable (slope=-0.008 Mg C ha^{-1} yr^{-2}, P=0.817, Fig. 6.2d), although the result was statistically non-significant. In tropical forests, carbon gains also showed a significantly declining trend (slope=-0.184 Mg C ha^{-1} yr^{-2}, P=0.042, Fig. 6.2c). Carbon losses, in contrast, exhibited a slight upward trend (slope=0.07 Mg C ha^{-1} yr^{-2}, P=0.394, Fig. 6.2d), although again not statistically significant.

These trends resulted in a decrease in the net carbon sink over time, particularly in temperate forests (slope=-0.31 Mg C ha^{-1} yr^{-2}, P<0.001, Fig. 6.2b). Although tropical forests showed a similar declining trend in net carbon sink (slope=-0.254 Mg C ha^{-1} yr^{-2}, Fig. 6.2b), this trend was not statistically significant (P=0.09). Extrapolations from the observed trends predicted that temperate forests would reach carbon sink saturation by approximately 2025, while tropical forests were expected to follow by 2029. These projections suggested that, under current trajectories, both forest types may lose their capacity to act as net carbon sinks before the end of this decade (Fig. 6.2b).

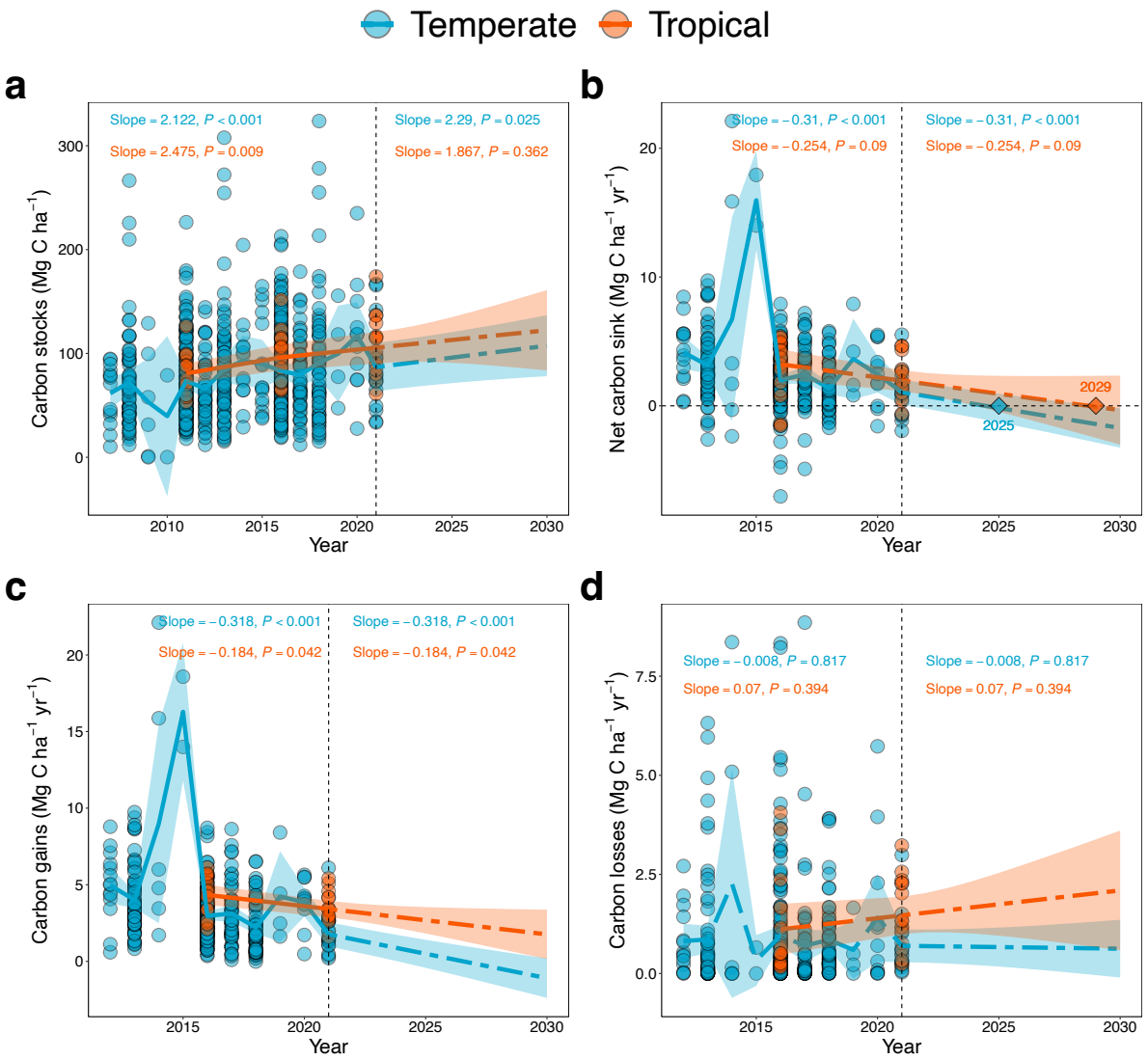

Fig. 6.2. Long-term trends and projected trajectories of carbon stocks and dynamics in Mexican forests. a-d, Annual trends for temperate (blue) and tropical (orange) forests in aboveground carbon stocks (**a**), net carbon sink (**b**), carbon gains (**b**), and carbon losses (**d**) between 2007 and 2021, and extrapolated projections of prior trends to 2030. Solid lines indicate statistically significant trends (P<0.05), and dashed lines indicate non-significant trends (P>0.05). Two-dashed lines denote extrapolated trajectories from 2021 to 2030 based on observed trends. Projections in panel (**b**) suggest that temperate forests may reach carbon sink saturation by 2025, with tropical forests following by 2029.

6.4.3. Functional and climatic drivers of carbon resilience

Our analysis revealed biome-specific patterns in how FD influenced the rate of change in forest carbon stocks and dynamics. In temperate forests, higher initial morphological FD (FD_{Mor}) was

consistently associated with enhanced carbon resilience. Specifically, greater FD_{Mor} was significantly associated with faster increases in carbon stocks (slope=1.878 Mg C ha^{-1} yr^{-1}, P<0.001, Fig. 6.3a), greater net carbon sink (slope=1.028 Mg C ha^{-1} yr^{-2}, P<0.001, Fig. 6.3b), increased carbon gains (slope=0.604 Mg C ha^{-1} yr^{-2}, P<0.001, Fig. 6.3c), and reduced carbon losses (slope=-0.441 Mg C ha^{-1} yr^{-2}, P<0.001, Fig. 6.3d). In contrast, tropical forests showed no significant relationship between FD_{Mor} and any carbon metric (Fig. 6.3a-d). Nutrient-based FD (FD_{Nutr}) revealed an unexpected negative association with the change rate of carbon stocks and dynamics in temperate forests. Higher initial FD_{Nutr} was significantly linked to reduced carbon stocks (slope=-3.440 Mg C ha^{-1} yr^{-1}, P<0.001, Fig. 6.4a), diminished net carbon sink (slope=-1.826 Mg C ha^{-1} yr^{-2}, P<0.001, Fig. 6.4b), lower carbon gains (slope=-1.017 Mg C ha^{-1} yr^{-2}, P<0.001, Fig. 6.4c), and higher carbon losses (slope=0.907 Mg C ha^{-1} yr^{-2}, P=0.006, Fig. 6.4d). Again, these patterns were not reflected in tropical forests, where FD_{Nutr} showed no significant associations with any carbon metric (Fig. 6.4a-d). Beyond FD, morphological FR showed no significant associations with changes in carbon stocks or dynamics in either temperate or tropical forests (Supplementary Fig. S6.1).

In addition to functional attributes, we assessed how climatic stress (mean annual MCWD and VPD) influenced the temporal change rates of carbon stocks and dynamics. MCWD exhibited significant negative associations with multiple carbon metrics in temperate forests. Higher drought severity (i.e., greater MCWD) was associated with declining carbon stocks (slope=-0.03 Mg C ha^{-1} yr^{-1}, P<0.001, Fig. 6.5a), decreasing net carbon sink (slope=-0.006 Mg C ha^{-1} yr^{-2}, P=0.016, Fig. 6.5b), and increasing carbon losses (slope=0.004 Mg C ha^{-1} yr^{-2}, P=0.015, Fig. 6.5d). Carbon gains, however, were not significantly affected (P=0.278, Fig. 6.5c). In contrast, tropical forests showed no significant relationships between MCWD and any carbon metric (Fig. 6.5a-d). By comparison, VPD did not show statistically significant associations with changes in carbon stocks or dynamics in either biome (Supplementary Fig. S6.2). In temperate forests, trends were weak and non-significant across all metrics (Supplementary Fig. S6.2), while in tropical forests, despite a relatively large positive slope for carbon stocks (slope=13.89 Mg C ha^{-1} yr^{-1}, Supplementary Fig. S6.2a), the relationship was non-significant (P=0.597, Supplementary Fig. S6.2a).

Our analysis also revealed significant interaction effects between FD components and both climatic (MCWD) and temporal (Year) variables in temperate forests (Supplementary Figs. S6.3 to S6.6). Specifically, higher FD_{Mor} significantly buffered the negative impact of increasing drought severity (MCWD) on the rate of carbon stock change (interaction=2.29,

P<0.001, Supplementary Fig. S6.3a), and the decline of carbon stock change rate was steepest at low FD_{Mor} but remained most stable under high FD_{Mor} (Supplementary Fig. S6.3a). Similarly, FD_{Mor} moderated temporal trends (Year), with the positive trend of carbon stocks change rate only observed at high FD_{Mor} (interaction=0.73, P<0.001, Supplementary Fig. S6.3c), while stocks declined under low and median FD_{Mor} (Supplementary Fig. S6.3c). For the change rate of carbon dynamics, high FD_{Mor} significantly restrained declines in temporal net carbon sink, carbon gains and increases in carbon losses (interactions ranging from -0.94 to 2.63, all P<0.001, Supplementary Figs. S6.4 to S6.6). Conversely, FD_{Nutr} showed the opposite pattern. Greater FD_{Nutr} exacerbated negative effects of both MCWD (interaction=-1.44, P<0.001, Supplementary Figs. S6.3e, S6.4e, S6.5e, and S6.6e) and Year (interactions ranging from -0.77 to -1.08, all P<0.001, Supplementary Figs. S6.3g, S6.4g, S6.5g, and S6.6g) on the change rate of carbon stocks and carbon dynamics. No significant interaction effects were observed in tropical forests (all P>0.05, Supplementary Figs. S6.7 to S6.10).

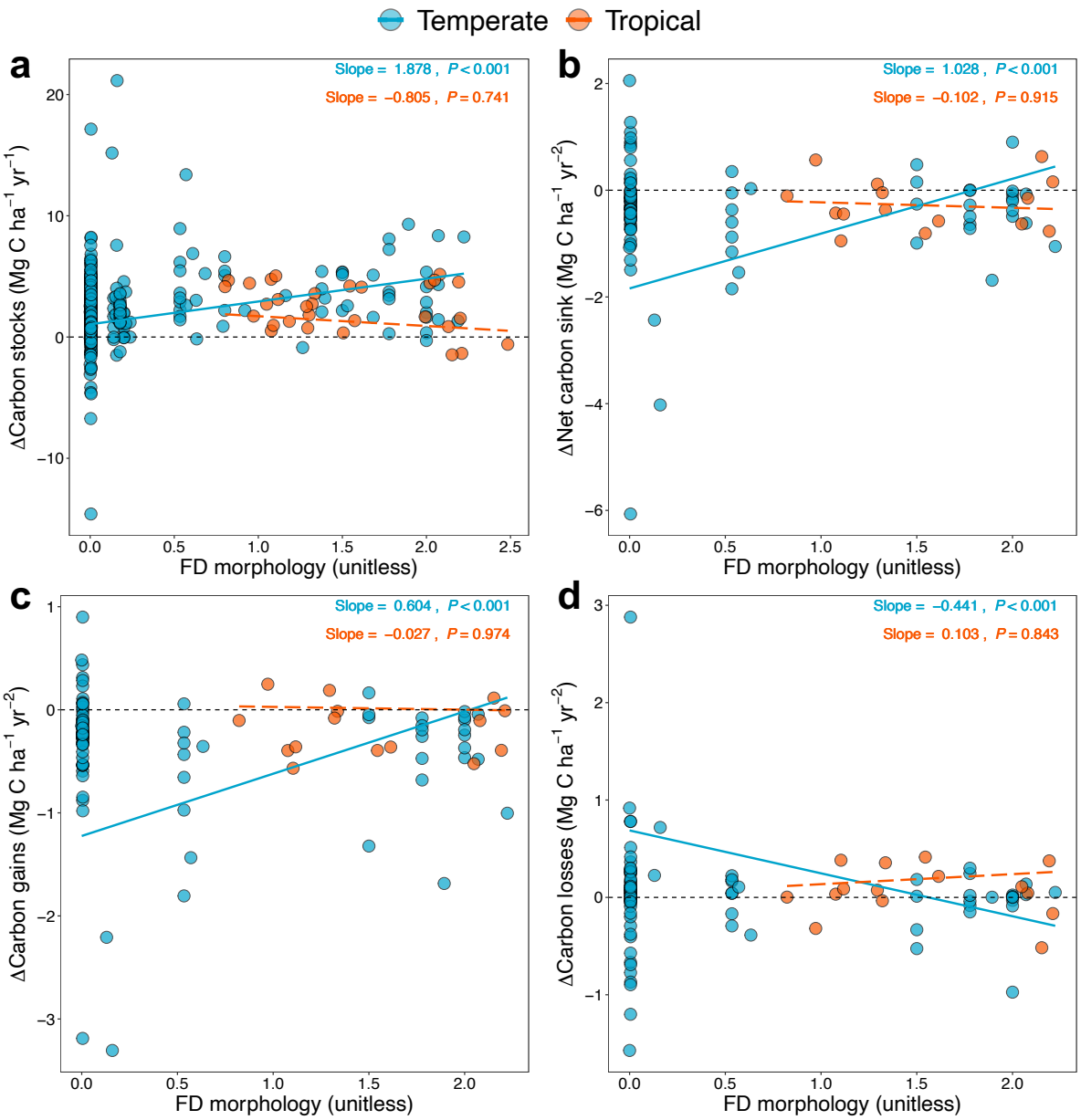

Fig. 6.3. Effects of morphological functional diversity (FD) on changes in forest carbon stocks and dynamics. Relationships between initial morphological functional diversity and the change rate of carbon stocks (**a**), net carbon sink (**b**), carbon gains (**c**), and carbon losses (**d**) in temperate (blue) and tropical (orange) forests. Each point represents a census interval for a plot, and regression lines indicate biome-specific trends. Solid lines denote statistically significant relationships (P<0.05), and dashed lines indicate non-significance (P>0.05).

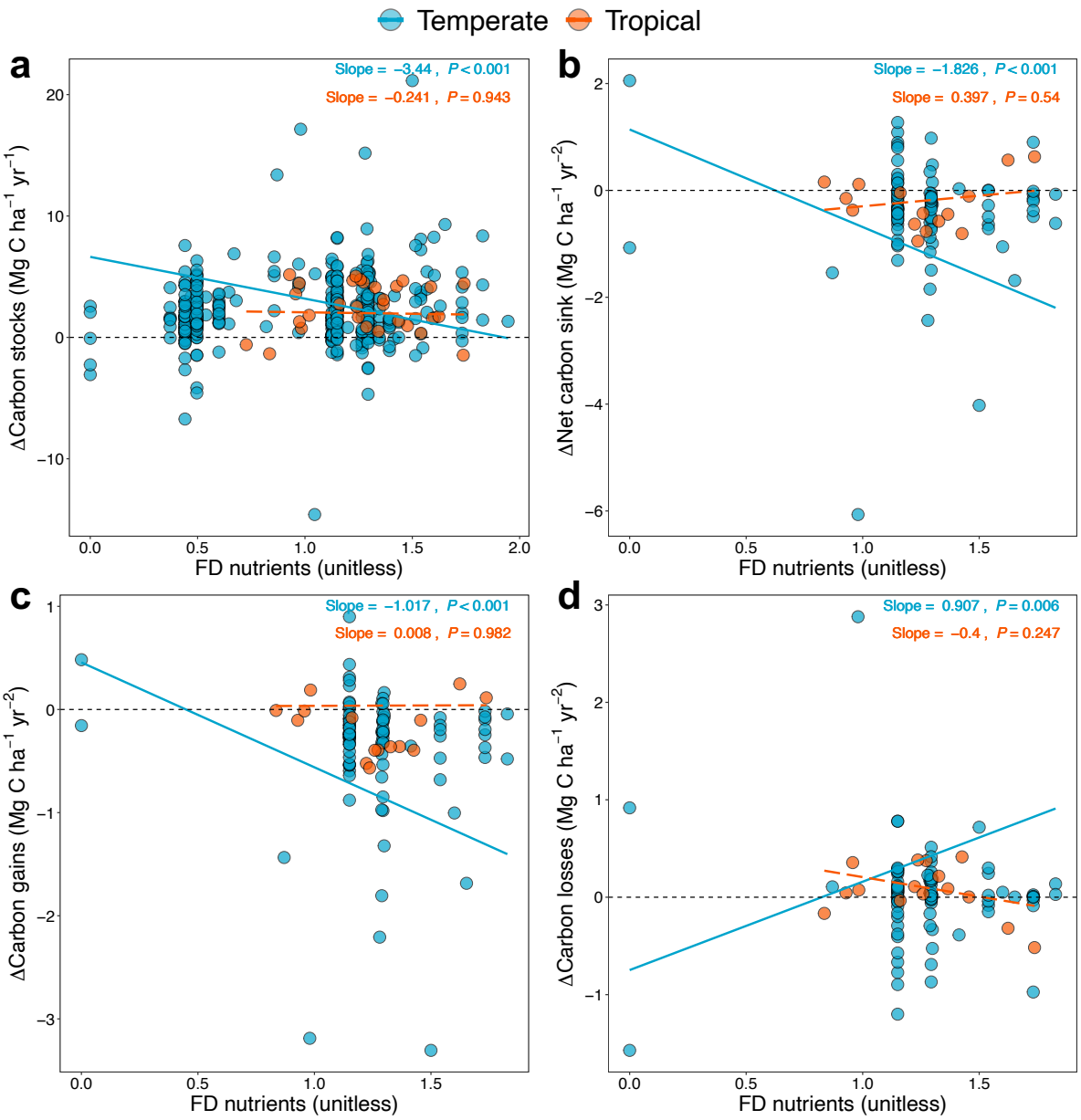

Fig. 6.4. Effects of nutrient-based functional diversity (FD) on changes in forest carbon stocks and dynamics. Relationships between initial nutrient-based functional diversity and the change rate of carbon stocks (**a**), net carbon sink (**b**), carbon gains (**c**), and carbon losses (**d**) in temperate (blue) and tropical (orange) forests. Each point represents a census interval for a plot, and regression lines indicate biome-specific trends. Solid lines denote statistically significant relationships (P<0.05), and dashed lines indicate non-significance (P>0.05).

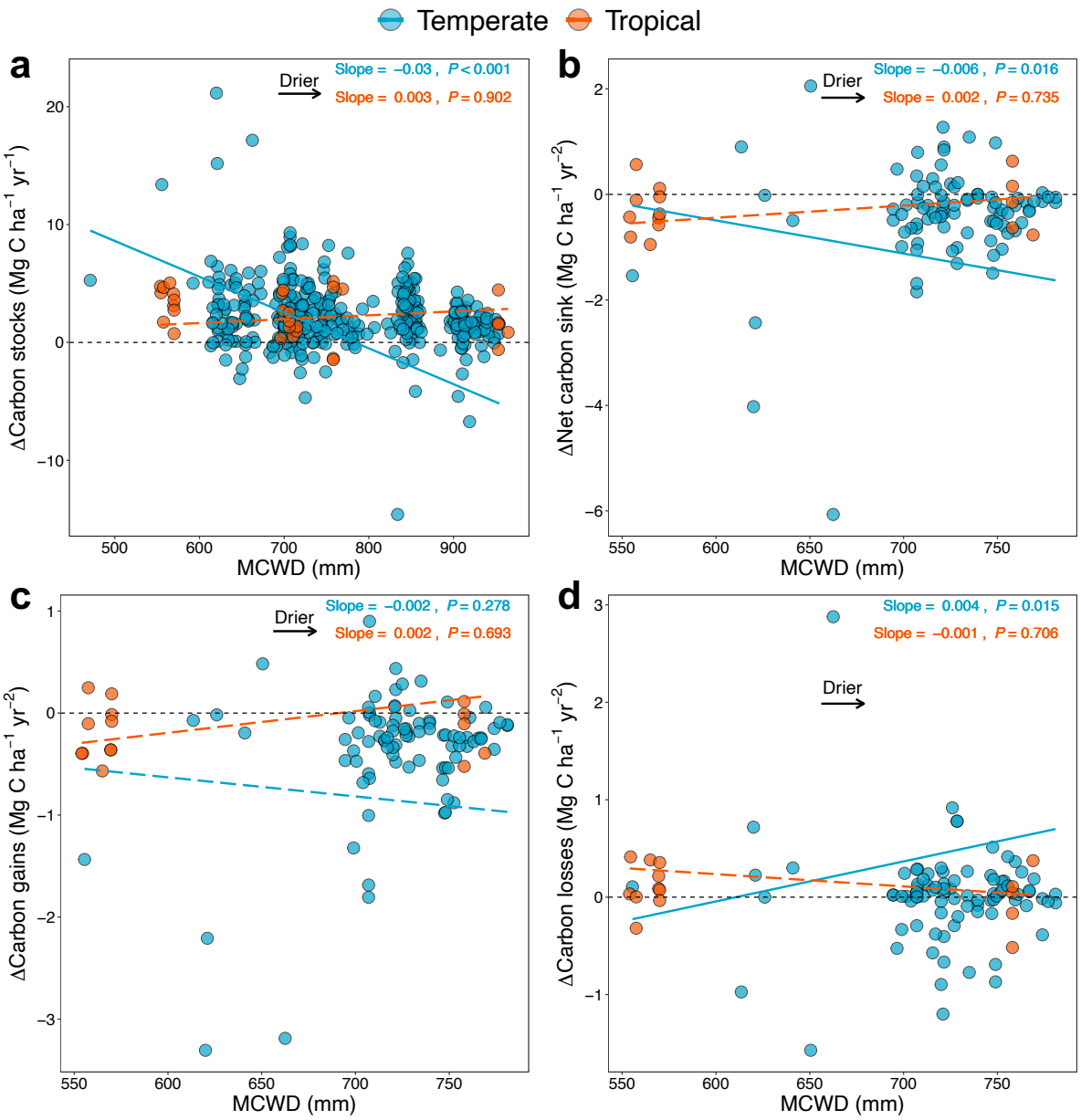

Fig. 6.5. Effects of mean maximum cumulative water deficit (MCWD) on changes in forest carbon stocks and dynamics. Relationships between mean MCWD and the change rate of carbon stocks (**a**), net carbon sink (**b**), carbon gains (**c**), and carbon losses (**d**) in temperate (blue) and tropical (orange) forests. Each point represents a census interval for a plot, and regression lines represent statistically significant (solid) or non-significant (dashed) trends (P<0.05 and P>0.05, respectively).

6.5. Discussion

6.5.1. Warming and drying trends reshape Mexican forest climates

Our biome-specific yet concurrent trends in temperature and drought-related metrics indicate that both temperate and tropical forest types are undergoing increasingly stressful climatic conditions from 2007 to 2021. Tropical forests are showing greater absolute increases in seasonal drought severity (MCWD), while temperate forests are experiencing more statistically robust warming (T_{max}) and atmospheric drying (VPD). The positive and highly significant trends in T_{max}, VPD, and MCWD are consistent with broader regional (De la Barreda et al., 2020; Overpeck & Udall, 2020) and global (Trenberth et al., 2014; Zscheischler & Seneviratne, 2017) climate trends. These shifts reflect rising atmospheric heat extremes (T_{max}), declining atmospheric moisture (VPD), and worsening soil water deficits and diminished water availability (MCWD), which together exacerbate thermal stress, increase evaporative demand, and reduce plant water supply, and ultimately driving suppressing forest stress and increasing tree mortality (Bauman et al., 2022; Esquivel-Muelbert et al., 2020).

In tropical forests, while the warming trend is weaker and VPD changes are not statistically significant, MCWD increases, which suggests intensifying dry-season water deficits. This deepening MCWD trend is particularly concerning, as it reflects increasing seasonal drought stress (Bauman et al., 2022; Malhi et al., 2009). Even in the absence of strong VPD signals, severe dry season deficits alone can diminish tropical forest resilience and carbon balance by disrupting water transport and increasing vulnerability to disturbance (Stan & Sanchez-Azofeifa, 2019).

The cumulative effects of these climate shifts differ between forest types. In temperate forests, T_{max} increases by approximately 1.09 °C, accompanied by a 0.07 kPa rise in VPD and an intensification of seasonal drought measured by an increase of 18.65 mm in MCWD between 2007 and. Higher temperatures can increase respiration costs and tree mortality risks (Anderegg et al., 2013), while elevated VPD impairs stomatal function and reduces photosynthesis (Grossiord et al., 2020). Over time, such conditions can reduce productivity and alter competitive dynamics (McDowell et al., 2020). In contrast, tropical forests experience a 0.60 °C rise in T_{max}, with VPD increasing by 0.07 kPa, a similar magnitude to temperate forests, though not statistically significant. However, seasonal drought severity (MCWD) deepens substantially by 161 mm, indicating a much greater increase in cumulative dry season water deficits. Although tropical species often display traits adapted to periodic water stress, the scale of drought intensification raises concerns about long-term resilience (R. S. Oliveira et al., 2021). These compounding stressors are likely to push many forest systems beyond physiological thresholds (Betts et al., 2008; Lesk et al., 2022), especially in water-limited or transitional

ecosystems. Under high temperatures and elevated VPD, stomatal closure reduces transpiration, which can conserve soil moisture in the short term but concurrently intensifies land surface warming (Grossiord et al., 2020; Jalakas et al., 2021; Lesk et al., 2022) and further amplifies forest stress and feedback to regional climate (Anderegg, Trugman, Badgley, Anderson, et al., 2020; Bonan, 2008), and increasing MCWD signifies intensifying seasonal drought stress, potentially triggering hydraulic failure and carbon starvation (Bennett et al., 2021, 2023; Tavares et al., 2023). Over time, these pressures can reshape species composition (Morin et al., 2018), reduce forest productivity (Xu et al., 2019), and compromise long-term carbon storage and sequestration capacity (Liu et al., 2024), which poses significant challenges for the resilience of both temperate and tropical forests under future climate trajectories (Forzieri et al., 2022).

6.5.2. Shifting carbon stocks and declining carbon sink strength

Our analyses reveal contrasting carbon trajectories between forest types. Temperate forests experience significant carbon accumulation from 2007 to 2021, while tropical forests show a marginal and non-significant increase. These patterns may reflect a legacy of past land-use recovery (Poorter et al., 2016, 2021), shifts in disturbance regimes (Pugh et al., 2019), or periods of climatic favourability in some forest zones (Eggers et al., 2008). However, despite the growth in biomass carbon for both forest types, they exhibit declining net carbon sinks over the same time, driven by reductions in carbon gains (in the case of tropical forests) and slight increases in carbon losses, which suggests potential early signals of carbon sink saturation (Brienen et al., 2015; Hubau et al., 2020; Maia et al., 2020), where forests continue to sequester carbon but at a diminishing rate. This decoupling suggests that while total stocks may still be rising, the rate of accumulation is slowing due to declining gains (e.g., growth and recruitment) and slightly rising or stable losses (e.g., mortality and turnover), particularly in tropical forests. This finding aligns with the previous studies (Brienen et al., 2015; Hubau et al., 2020; Maia et al., 2020; Mo et al., 2023). As forests mature with increasing competition, growth rates often slow (Anderson-Teixeira et al., 2022) and structural limitations like hydraulic constraints reduce net productivity (McDowell et al., 2022). Simultaneously, increasing stress from warming and drought can exacerbate mortality (Marchin et al., 2022; McDowell et al., 2022), even in forests with rising total biomass carbon. Thus, carbon gains and losses may begin to converge. This dynamic is critical to recognise, as it reflects a shift from an expanding carbon

sink to a potentially saturating or unstable one, with important implications for future climate mitigation capacity.

Potentially the most critical finding is the projected collapse of net carbon sinks by 2025 in temperate forests (Fig. 6.2b) and 2029 in tropical forests (Fig. 6.2b). While it is expected that mature forests eventually approach carbon balance over long timescales, the concern here is the accelerated pace of this transition under intensifying drought and climate stress. Instead of stabilising around neutrality, this convergence toward net-zero sequestration or negative net carbon uptake, where emissions from mortality consistently exceed gains from growth, signals a potential tipping point, beyond which these forests may transition from carbon sinks to sources. Similar early declines have been reported across the Amazon (Brienen et al., 2015; Gatti et al., 2021; Hubau et al., 2020) and Africa (Bennett et al., 2021), where increasing drought and warming have undermined carbon uptake capacity, which suggests a broader pattern of vulnerability in tropical and subtropical biomes. As Mexican forests are approaching these critical thresholds, feedback to the regional climate system is likely to intensify. Diminished carbon uptake weakens the land carbon sink and accelerates atmospheric CO_2 accumulation (Ruehr et al., 2023). Moreover, climate-induced forest degradation can increase albedo and reduce evapotranspiration (Lawton et al., 2001; Zeng et al., 2021), reinforcing warming and aridification at the land surface (Lawrence & Vandecar, 2015; Lawton et al., 2001; Zeng et al., 2021). This biophysical feedback further amplifies local climate extremes and may reduce the effectiveness of forests in buffering against broader climate variability (Coe et al., 2013; Staal et al., 2018). Thus, the critical issue is not that carbon sink collapse will eventually occur, but that climate change may accelerate and lock in this transition, undermining both local and global climate regulation. Our results suggest that, without targeted conservation, adaptive management, and mitigation strategies to enhance resilience and functionality, Mexican forests may follow the same trajectory toward becoming persistent carbon source under continuing climate change.

6.5.3. Functional trait diversity and climatic stress shape forest carbon resilience

Our results highlight the critical role of FD in mediating components of forest carbon resilience, particularly in temperate forests. Higher initial FD_{Mor} emerges as a strong positive driver of changes in carbon stocks, net carbon sink, and carbon gains in temperate forests, while simultaneously reducing carbon losses. These findings support our hypothesis that higher

initial FD enhances forest carbon stability. Morphologically diverse communities may support greater niche complementarity or facilitation (Bulleri et al., 2016) in light capture, water use, and mechanical support (Sapijanskas et al., 2014), allowing coexisting species to optimise resource acquisition and maintain productivity under environmental stress (Cadotte et al., 2011), thus enhancing biomass accumulation and buffering against stressors (Aoyama et al., 2023). The observed increases in the change rate of carbon stocks and net carbon sink, alongside higher carbon gains and reduced carbon losses, indicate that FD_{Mor} contributes to buffering carbon dynamics against drought and warming (Lavorel et al., 2015; Lloret et al., 2012), thereby enhancing the stability of these particular carbon-cycle processes. Furthermore, interaction effects between FD_{Mor} and MCWD show that forests with higher FD_{Mor} exhibit more stable trajectories in carbon stock change under intensifying drought, whereas forests with lower FD_{Mor} experience steeper declines. Similarly, the FD_{Mor}×Year interaction indicate that forests with low or median FD_{Mor} see decreasing carbon stocks over time, while those with high FD_{Mor} exhibit increasing stocks. For net carbon sink, gains, and losses, high FD_{Mor} also moderate negative temporal trends, including in net sink, carbon gains, and carbon losses, further supporting its resilience-enhancing role. However, we caution that this evidence applies specifically to carbon-related metrics and does not encompass other ecosystem functions or broader dimensions of resilience. Thus, while FD_{Mor} clearly supports more stable carbon dynamics under climatic stress in Mexican temperate forests, further research is required to determine whether such effects extend to other processes (e.g., regeneration, recruitment, or nutrient cycling).

In contrast, FD_{Nutr} shows the opposite pattern in temperate forests. Higher initial FD_{Nutr} is significantly associated with declining change rate of carbon stocks, net carbon sink, and carbon gains, and increasing change rate of carbon losses in temperate forests. The divergent effects of FD_{Nutr} on carbon resilience likely reflect underlying trade-offs inherent in leaf economic strategies under climatic stress, such as exacerbating drought conditions. Acquisitive species with nutrient-rich leaves (high nitrogen and phosphorus content) (Homeier et al., 2021) may benefit from fast resource uptake and photosynthesis during wet seasons, which in turn prioritise rapid growth, but they often have lower water-use efficiency, thus they require more water to produce biomass compared to conservative species that are typically low in leaf nutrients and high in drought tolerance, and their low drought tolerance makes them vulnerable under intensifying stress (Camarero et al., 2024; Chaturvedi et al., 2021). Thus, higher FD_{Nutr} may amplify stress exposure rather than buffer it, especially when coupled with increasing

drought severity and long-term climatic stress. This pattern highlights how different trait dimensions can diverge in their contributions to resilience: while FD_{Mor} enhances carbon stability, FD_{Nutr} may intensify ecological trade-offs that destabilise carbon cycling under drought. In addition, higher FD_{Nutr} amplifies negative effects of both MCWD and time, indicating potential vulnerability in communities dominated by acquisitive strategies.

By contrast, tropical forests do not show significant associations between initial FD and carbon resilience. One likely explanation is that tropical forests already harbour much higher baseline levels of FD, so the marginal benefits of additional FD may saturate and provide diminishing returns. Moreover, higher biodiversity has been linked to higher tree mortality (Searle et al., 2022), which may offset potential stability benefits of trait complementarity. In addition, the lack of observed resilience effects may result from the overwhelming intensity of heat waves and drought conditions as captured by T_{max} and MCWD, which can constrain physiological plasticity (Bjorkman et al., 2018) and suppress the buffering capacity of trait variation. Together, these mechanisms suggest that in tropical forests, either ecological saturation of FD effects or overriding climatic stress limits the capacity of FD to enhance carbon resilience.

FR in morphological traits does not significantly explain changes in carbon stocks or dynamics in either biome, potentially because high redundancy implies limited variation in functional traits across communities, which weakens the biodiversity-ecosystem functioning relationship. As previous studies have suggested, when FD is saturated, i.e., FD is high but not variable, its explanatory power for ecosystem functioning diminishes, even if species richness remains high (Cadotte et al., 2011).

Climatic stressors, particularly seasonal drought intensity (MCWD), are more consistently linked to carbon resilience than atmospheric drought (VPD). In temperate forests, higher MCWD values, which indicate greater cumulative seasonal water deficits, are associated with declining rates of carbon stocks, net carbon sink, and carbon losses. These relationships highlight the importance of soil water availability during the dry season in regulating forest carbon balance. Unlike short-term fluctuations in atmospheric moisture, MCWD captures the prolonged intensity of water limitation (Malhi et al., 2009), which directly affects tree hydraulic function, photosynthetic capacity, and mortality risk (Bauman et al., 2022). Severe seasonal drought can impair plant water transport and reduce carbon assimilation, particularly for species lacking deep rooting or conservative water-use strategies (Powers et al., 2020). As such,

MCWD represents a strong integrative stressor that constrains forest productivity and enhances vulnerability to mortality and biomass decline, especially in water-limited temperate systems.

6.5.4. Limitations, core insights, and applied relevance

This study has several limitations that should be acknowledged when interpreting the findings. First, there is a sampling imbalance between temperate and tropical forests. Temperate forests in western Mexico are represented by most plots, which provides robust statistical power and strong confidence in the patterns we report. In contrast, tropical forests (15 plots) and isolated southern temperate plots are underrepresented, which increases uncertainty and limits the ability to detect consistent biodiversity-climate-carbon relationships in those ecosystems. Nonetheless, retaining tropical and southern temperate plots was important for providing baseline context, highlighting data gaps, and identifying regions where additional sampling is needed. From an applied perspective, this highlights that conservation and management efforts in Mexico should prioritise temperate forests, where results are most reliable, while also recognising the ecological significance of tropical and southern temperate forests and the urgent need for improved monitoring in these regions.

Second, the climatic drivers were characterised using TerraClimate data. Although TerraClimate provides long-term and spatially consistent estimates of T_{max}, VPD, and MCWD, its ~4 km resolution cannot fully capture local microclimatic variation. Plot-level conditions are influenced by fine-scale topography, soil properties, and canopy structure, which can strongly mediate drought severity and temperature extremes. As such, while TerraClimate metrics provide robust regional drivers, they may misrepresent the exact climatic conditions experienced by individual forest plots, which adds uncertainty to the strength of biodiversity-climate-carbon relationships.

Third, our carbon flux estimates are subject to methodological assumptions. Tree-level carbon stocks were derived from forest-type-specific allometric equations, converted to carbon using a fixed factor (45.6% of biomass), and adjusted for census interval bias with the "*CIC1*" correction. While these approaches are widely used and provide comparability across studies, they inevitably introduce uncertainties in absolute values of carbon stocks and fluxes. In particular, the reliance on general forest-type allometries may oversimplify species-specific differences in tree form and biomass allocation. Using species-specific allometric equations would likely improve accuracy. Nonetheless, because the same methods were applied

consistently across all sites and forest types, relative differences and comparative patterns among forests can be interpreted with confidence.

Despite these limitations, three core ecological insights emerge with confidence, particularly from the well-sampled western temperate forests:

(1) The stabilising role of FD_{Mor} in enhancing carbon stock accumulation and buffering carbon-cycle processes against drought and warming.

(2) The destabilising influence of FD_{Nutr}, likely reflecting ecological trade-offs between acquisitive and conservative plant strategies under climatic stress.

(3) The moderating effect of drought severity, with intensifying water deficits constraining carbon resilience.

Together, these insights provide an applied foundation for conservation and management in Mexico. They suggest that temperate forests should be prioritised for conservation due to both their strong representation in the dataset and their demonstrated role in maintaining stable carbon dynamics under climate stress. At the same time, the ecological significance of tropical and southern temperate forests highlights the need for expanded monitoring networks and improved trait and climate data in underrepresented regions. These efforts will be critical for designing targeted conservation and restoration strategies that enhance functional diversity, mitigate drought vulnerability, and maintain the long-term carbon resilience of Mexico's forests.

6.6. Methods

An overview of the study design and analytical sequence was provided in the schematic workflow (Fig. 6.6). Detailed procedures for each step were described in the following subsections.

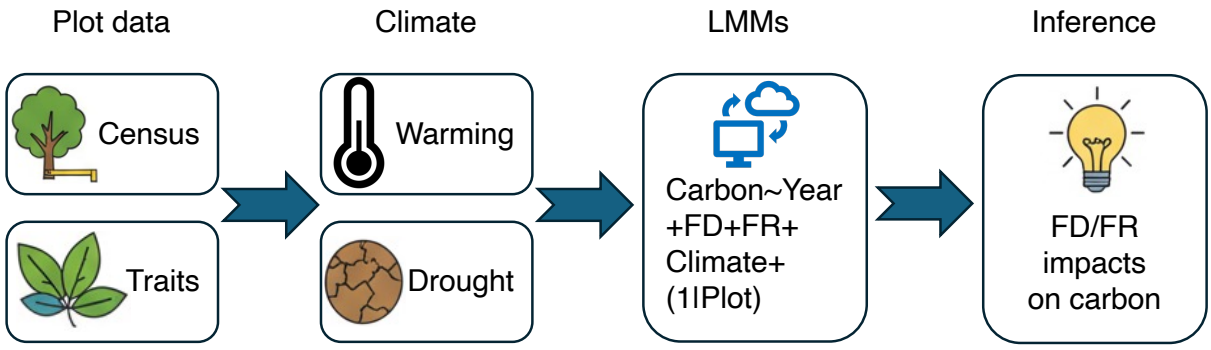

Fig. 6.6. Schematic workflow of the study design and analytical framework. Forest inventory data and functional traits were collected from temperate and tropical plots to generate carbon stocks and dynamics (stocks, gains, losses, and net sink) and functional trait diversity and redundancy, respectively, and climate variables were extracted from TerraClimate as climatic stress indicators. These inputs were then linked to forest carbon stocks and dynamics using linear mixed-effects models (LMMs) to investigate the impact of functional diversity and redundancy on forest carbon resilience. FD: functional diversity, FR: functional redundancy.

6.6.1. Plot data collection and selection

We compiled and selected repeated forest census data and wood density (in g cm^{-3}) from 293 structurally intact (Brienen et al., 2015; Hubau et al., 2020) (free of fire and anthropogenic disturbances) forest plots (0.25 ha, totalling 73.25 ha) across Mexico, spanning the period from 2007 to 2021. These plots were part of the Monitoreo Nacional Forestal network (http://fcfposgrado.ujed.mx/monafor/inicio/), established by the Mexican National Forestry Commission to support sustainable forest management and long-term ecological monitoring. Each plot was censused 2 to 3 times, with mean census interval length of 6.77 years. Specifically, our data comprised 690 census intervals nested within 293 plots, including temperate forest plots (645 census intervals nested within 278 plots, Fig. 6.1a) and tropical forest plots (45 census intervals nested within 15 plots, Fig. 6.1a). Across these plots, we tracked over 13056 trees with DBH≥5 cm, representing 194 species with plot-level species richness ranging from 1 to 45 (mean=9.65). Tree measurements followed the protocol of Corral-Rivas et al. (2009). Note that the uneven sampling between temperate and tropical forest plots created an imbalance, with temperate forests being better represented. Such imbalance limited the statistical power to detect relationships in tropical forests and southern temperate forests and therefore resulted from these subsets should be interpreted with caution. We retained the tropical and southern plots because they extended the ecological and climatic coverage of the study and allowed broader contextual comparisons. However, our main inferences and conclusions were drawn from the well-sampled temperate forests of western Mexico, where robust representation ensured higher reliability of the results.

6.6.2. Carbon stocks and dynamics estimation

6.6.2.1. Tree aboveground carbon and carbon stocks estimation

To estimate aboveground carbon (AGC, in Mg C) for each individual tree, we applied forest-type-specific allometric equations (Chave et al., 2014; Segura & Kanninen, 2005) published previously to calculate aboveground biomass, which was then converted to carbon based on the assumption that AGC constitutes 45.6% of total aboveground biomass (Martin et al., 2018). The following equations were used to estimate AGC for trees in temperate and tropical forests, respectively:

$$AGC = 0.456 \times [0.0291 \times (DBH^{1.74165} \times H^{1.16614}) + 0.02029 \times (DBH^{1.33299} \times H^{0.92887}) + 0.02508 \times (DBH^{1.83773} \times H^{0.54626}) + 0.05227 \times (DBH^{1.28231} \times H^{0.43275})] \times 0.001 \quad (1)$$

$$AGC = 0.456 \times [0.0673 \times (WD \times DBH^2 \times H)^{0.976}] \times 0.001 \quad (2)$$

where AGC (in Mg C) was the AGC in living biomass for a tree, WD (in in g cm^{-3}), DBH (in cm), and H (in m) denoted wood density, diameter at breast height, and tree height of this tree. Plot-level carbon stocks (in Mg C ha^{-1}) in each census were estimated as the sum of the AGC of all living trees, scaled by plot area, which was 0.25 ha in this study.

6.6.2.2. Carbon dynamics estimation

Carbon gains (in Mg C ha^{-1} yr^{-1}) were calculated as the sum of the AGC accumulated by surviving trees (i.e., the difference in AGC between two censuses) plus the AGC of newly recruited trees, which was defined as individuals that reached DBH≥5 cm at the end of the interval (assuming DBH=0 at the start). The total gain was then divided by the census interval length (in years) and scaled to per-hectare values. Similarly, carbon losses (in Mg C ha^{-1} yr^{-1}) were estimated as the sum of AGC from all trees that died during a census interval, divided by the interval length and plot area. As both carbon gains and losses were sensitive to census interval bias, particularly due to the underestimation of unobserved growth and mortality events over longer intervals, we applied a correction following a method denoted "CIC_1" (Talbot et al., 2014). This adjustment accounted for unrecorded growth of trees that died within the interval and recruits that grew and died between two censuses. Finally, net carbon sink (in Mg C ha^{-1} yr^{-1}) was calculated as carbon gains minus carbon losses.

6.6.3. Functional trait diversity and redundancy

6.6.3.1. Functional diversity

We focused on key morphological and leaf nutrient traits directly related to plant ecological strategies and drought responses. We collected data on five morphological traits including leaf dry mass (in g), specific leaf area (in cm^2 g^{-1}), leaf area (in cm^2), leaf thickness (in mm), and wood density (in g cm^{-3}), and three leaf nutrient traits including leaf carbon (in %), nitrogen (in %), and phosphorus (in %) content. These trait data were obtained through a combination of direct field measurements in Mexico and species-level data from trait databases including TRY (https://www.try-db.org/TryWeb/Home.php) (Kattge et al., 2011, 2020) and the Botanical Information and Ecology Network (https://bien.nceas.ucsb.edu/bien/) (Enquist et al., 2016). We quantified FD separately for morphological traits and nutrients using functional dispersion (Laliberté & Legendre, 2010). FD_{Mor} and FD_{Nutr} were calculated separately based on the dbFD function from the R package FD (Lalibert et al., 2014):

$$FD = \frac{\sum_{i=1}^{n} BA_i \times z_i}{\sum_{i=1}^{n} BA_i} \quad (3)$$

where BA_i was the basal area of species i in a plot, and z_i stood for the distance of species i in a plot to the weighted centroid of the n individual species in the trait space.

6.6.3.2. Functional redundancy

Similarly, we calculated FR separately for morphological traits and nutrients. We used the uniqueness function from the R package adiv (Pavoine, 2020). Specifically, for a community of n species:

$$FU = \frac{\sum_{i=1}^{n} p_i \times \sum_{j=1}^{n} p_j \delta_{ij}}{\sum_{j=1}^{n} p_j (1 - p_i)} \quad (4)$$

$$FR = 1 - FU \quad (5)$$

where FU was functional uniqueness at community level, p_i with $0<p_i\leq 1$ and $\sum_{i=1}^{n} p_i = 1$ represented the relative abundance of a given species i, and δ_{ij} denoted the pairwise functional dissimilarity between species i and j ($\delta_{ij} = \delta_{ji}$ and $\delta_{ii} = 0$).

6.6.4. Climatic variables and drought estimation

We extracted monthly climatic data experienced by each plot during the monitoring period from the TerraClimate dataset (https://www.climatologylab.org/terraclimate.html) (Abatzoglou et al., 2018) that provided global climatic and hydrological data at ~4 km. For

each forest plot in Mexico, we obtained monthly maximum temperature (T_{max}, in °C) and vapour pressure deficit (VPD, in kPa) from 2007 to 2021. These variables were extracted using plot-level coordinates and aggregated to derive annual means for each census interval. We calculated mean annual T_{max} and mean annual VPD for each interval by averaging the monthly values over the years encompassed by the census periods.

To quantify drought intensity, we calculated the maximum climatological water deficit (MCWD, in mm), a metric that captured the peak severity of dry-season water deficit within a year (Malhi et al., 2009). MCWD was computed following the methodology of previous studies (Aragão et al., 2007; Malhi et al., 2009), modified for use with TerraClimate data. Specifically, the estimation of monthly climatological water deficit (CWD) for each census interval was initiate by identifying the wettest month of the first year, and was calculated iteratively for each plot using monthly precipitation (Pr, in mm) and an assumed constant monthly evapotranspiration (ET) of 100 mm as used in previous research (Bennett et al., 2023; Hubau et al., 2020; Malhi et al., 2009; Phillips et al., 2009):

$$CWD_{(n)} = CWD_{(n-1)} + ET - Pr_{(n)} \quad (6)$$

$$min[CWD_{(n)}] = 0 \quad (7)$$

$$if\ CWD_{(n)} < 0, then\ CWD_{(n)} = 0 \quad (8)$$

$$CWD_{(0)} = CWD_{(12)} \quad (9)$$

$$MCWD = max[CWD_{(0)}, CWD_{(1)}, \ldots, CWD_{(12)}] \quad (10)$$

where $CWD_{(n)}$ and $Pr_{(n)}$ represented the water deficit and precipitation in month n (n=1, 2, …, 12), and ET was evapotranspiration set as 100 mm. We set $CWD_{(7)}$=0 as July was typically the wettest month in Mexico (Murray-Tortarolo, 2021), and negative $CWD_{(n)}$ values were also set to zero to indicate the absence of drought conditions (Aragão et al., 2014; Hubau et al., 2020), which ensured that water deficits accumulated only during dry periods, while the deficit reset annually from the peak wet season. The MCWD for each year was then defined as the most positive (i.e., driest) monthly CWD value within the year. In this case, larger MCWD values directly reflected more intense water stress.

We selected T_{max} and VPD as indicators of heat and atmospheric dryness stress, respectively, while MCWD served as a temperature-independent measure of water deficit. These climatic variables allowed us to independently evaluate the effects of warming and drought on forest carbon stocks and dynamics. We highlighted that for the first census of each

plot, we used the average climatic values of these three variables from the five years preceding the census date to represent baseline environmental conditions prior to initial measurements (Maia et al., 2020). The spatial patterns and long-term trends of these environmental variables across the study region were displayed in Fig. 6.1a–c and Fig. 6.1d–e, respectively.

6.6.5. Statistical modelling of carbon stocks and dynamics trend estimation

We applied weighting in the carbon dynamics models to account for residual variation due to interval duration (Hubau et al., 2020; Maia et al., 2020). Specifically, we used the cube root of the census interval length as the weighting factor. Since all plots had the same area, no spatial weighting was applied. Carbon stocks models were also unweighted due to uniform plot size and consistent census timing. We organised the modelling approach into two primary sections:

6.6.5.1. Long-term trends in carbon stocks and dynamics

We first modelled each carbon metric (stocks, gains, losses, and net sink) as a function of time using bivariate linear mixed-effects models (LMMs). The year used in each model corresponded to the midpoint of the census interval, except for carbon stocks, where the census year was used directly (Maia et al., 2020).

6.6.5.2. Multivariate drivers of long-term changes in carbon stocks and dynamics

We used LMMs to estimate the rate of change in these variables over time, considering potential drivers including temporal trends (calendar year), FD, FR, and climatic variables (mean annual T_{max} and VPD, and MCWD) of each plot. To compute the rate of change in carbon stocks, we used the difference in carbon stocks between two consecutive census years divided by the time between censuses (Hisano et al., 2024). Therefore, ΔCarbon stocks=(Carbon stocks$_b$-Carbon stocks$_a$)/(Year$_b$-Year$_a$), where Carbon stocks$_b$ is the carbon stocks at the later census year Year$_b$, Carbon stocks$_a$ is the carbon stock at the previous census year Year$_a$. For carbon dynamics variables (gains, losses, and net sink), we used values already expressed in per-year units and modelled them against the midpoint year of the census interval rather than using the census year directly as the temporal variable (Brienen et al., 2015; Hisano et al., 2024; Hubau et al., 2020; Maia et al., 2020). Thus, ΔCarbon dynamics=(Carbon dynamics$_b$-Carbon dynamics$_a$)/(Mid$_b$-Mid$_a$), where Carbon dynamics$_b$ is the per-year carbon

gains, losses, or net carbon sink during the later census interval, Carbon dynamics$_a$ is the corresponding value during the previous interval, and Mid$_b$ and Mid$_a$ are the midpoints (in decimal years) of the respective census intervals.

Prior to model fitting, we calculated pairwise Pearson correlation coefficients among all predictors (Supplementary Fig. S6.11) and only included variables with $|r|<0.8$ to reduce multicollinearity and redundancy in the models. Eventually, predictors included in the global LMMs were year, FD_{Mor} and FD_{Nutr}, morphological FR (FR_{Mor}), VPD, and MCWD. These predictors included in the final models were standardised with scaling and centring (mean=0, SD=1) to facilitate comparison of effect sizes. Because field measurements were repeatedly taken from the same plots over time, we accounted for temporal non-independence by incorporating random effects into our modelling framework, we used LMMs with plot identity as a random effect to account for temporal autocorrelation (Hisano et al., 2024; Hubau et al., 2020; Maia et al., 2020). Random slopes were not included due to limited census intervals in some plots (Brienen et al., 2015; Hubau et al., 2020; Maia et al., 2020), which prevented model convergence.

To explore the roles of climatic and functional drivers of long-term changes in carbon stocks and dynamics, we fitted global LMMs using the lmer function from the lme4 package and applied the restricted maximum likelihood estimation (Bates et al., 2015), with fixed effects for time, functional attributes (FD and FR), and climatic conditions (VPD and MCWD), we also included interaction terms to evaluate how FD and FR varied through time and under different climatic conditions:

$$\Delta Carbon\ stocks \sim Intercept + Year + FD_{Mor} + FD_{Nutr} + FR_{Mor} + VPD + MCWD + Year \times (FD_{Mor} + FD_{Nutr}) + VPD \times (FD_{Mor} + FD_{Nutr}) + MCWD \times (FD_{Mor} + FD_{Nutr}) + (1|Plot) \quad (11)$$

$$\Delta Carbon\ dynamics \sim Intercept + Year + FD_{Mor} + FD_{Nutr} + FR_{Mor} + VPD + MCWD + Year \times (FD_{Mor} + FD_{Nutr}) + VPD \times (Year + FD_{Mor} + FD_{Nutr}) + MCWD \times (Year + FD_{Mor} + FD_{Nutr}) + (1|Plot) \quad (12)$$

where ΔCarbon stocks (in Mg C ha^{-1} yr^{-1}) and ΔCarbon dynamics (in Mg C ha^{-1} yr^{-2}) were the rate of change of carbon stocks and carbon dynamics including carbon gains, losses, and net carbon sink. Year in model (12) and (13) were the census year of the later time point and the midpoint year of the census interval, respectively. Note that Year was not included in models for tropical forests due to the limited unique number of years. FD_{Mor}, FD_{Nutr}, and FR_{Mor} were

morphological FD, nutrient-related FD, and morphological FR in the first census as we aimed to investigate if higher initial FD and FR enhance forest carbon resilience to climate change. VPD and MCWD were mean vapour pressure deficit and mean maximum climatological water deficit over the census interval. We included two groups of interaction terms, with the first group comprising interactions between time and initial FD and FR, and the second group including interactions between climatic stressors (VPD and MCWD) and time and initial FD and FR. The first interaction terms tested whether forests with higher initial FD and/or FR showed stronger or weaker carbon change over time, i.e., whether functional resilience mechanisms buffered or amplified carbon change over time, while the second interaction terms assessed whether the effects of time and FD and FR on carbon stocks and dynamics depended on climate stress, specifically atmospheric aridity (VPD) and water availability (MCWD), e.g., they allowed us to assess whether the forest resilience associated with initial FD and FR was more (or less) effective under drier and more water-limited conditions. (1|Plot) stood for the random effect of plot identity , which accounted for repeated measurements and unmeasured variation (e.g., local disturbances, historical management, microclimate differences, and other unknow factors (Hisano et al., 2024; Maia et al., 2020)) from the same plot over time.

We also evaluated spatial autocorrelation in residuals of global models using the Moran's *I* test based on the coordinates of the plots via the ncf package (Bjornstad & Cai, 2022) at the 0.05 significance level. The minimum *P* value obtained was 0.059, indicating no significant spatial autocorrelation.

The most informative and best-ranked simplified models were identified using an information theoretic approach based on second-order Akaike Information Criterion (AICc), implemented via the dredge function from the MuMIn package (Bartoń, 2025). We selected all models within $\Delta AICc \leq 4$ of the top-ranked model and ensured reliable estimates by only including predictors with variance inflation factor<4. Model coefficients were averaged across the best set of models using multimodel inference based on the model.avg function from the MuMIn package (Bartoń, 2025), and the final results were based on the conditional averaged coefficients. We considered predictors significant at the 0.05 level.

6.7. References

Abatzoglou, J. T., Dobrowski, S. Z., Parks, S. A., & Hegewisch, K. C. (2018). TerraClimate, a high-resolution global dataset of monthly climate and climatic water balance from 1958–2015. *Scientific Data*, *5*(1), 170191. https://doi.org/10.1038/sdata.2017.191

Anderegg, W. R. L., Kane, J. M., & Anderegg, L. D. L. (2013). Consequences of widespread tree mortality triggered by drought and temperature stress. *Nature Climate Change*, *3*(1), 30–36. https://doi.org/10.1038/nclimate1635

Anderegg, W. R. L., Klein, T., Bartlett, M., Sack, L., Pellegrini, A. F. A., Choat, B., & Jansen, S. (2016). Meta-analysis reveals that hydraulic traits explain cross-species patterns of drought-induced tree mortality across the globe. *Proceedings of the National Academy of Sciences*, *113*(18), 5024–5029. https://doi.org/10.1073/pnas.1525678113

Anderegg, W. R. L., Konings, A. G., Trugman, A. T., Yu, K., Bowling, D. R., Gabbitas, R., Karp, D. S., Pacala, S., Sperry, J. S., Sulman, B. N., & Zenes, N. (2018). Hydraulic diversity of forests regulates ecosystem resilience during drought. *Nature*, *561*(7724), 538–541. https://doi.org/10.1038/s41586-018-0539-7

Anderegg, W. R. L., Trugman, A. T., Badgley, G., Anderson, C. M., Bartuska, A., Ciais, P., Cullenward, D., Field, C. B., Freeman, J., Goetz, S. J., Hicke, J. A., Huntzinger, D., Jackson, R. B., Nickerson, J., Pacala, S., & Randerson, J. T. (2020). Climate-driven risks to the climate mitigation potential of forests. *Science*, *368*(6497), eaaz7005. https://doi.org/10.1126/science.aaz7005

Anderegg, W. R. L., Trugman, A. T., Badgley, G., Konings, A. G., & Shaw, J. (2020). Divergent forest sensitivity to repeated extreme droughts. *Nature Climate Change*, *10*(12), 1091–1095. https://doi.org/10.1038/s41558-020-00919-1

Anderegg, W. R. L., Trugman, A. T., Bowling, D. R., Salvucci, G., & Tuttle, S. E. (2019). Plant functional traits and climate influence drought intensification and land–

atmosphere feedbacks. *Proceedings of the National Academy of Sciences*, *116*(28), 14071–14076. https://doi.org/10.1073/pnas.1904747116

Anderson-Teixeira, K. J., Herrmann, V., Rollinson, C. R., Gonzalez, B., Gonzalez-Akre, E. B., Pederson, N., Alexander, M. R., Allen, C. D., Alfaro-Sánchez, R., Awada, T., Baltzer, J. L., Baker, P. J., Birch, J. D., Bunyavejchewin, S., Cherubini, P., Davies, S. J., Dow, C., Helcoski, R., Kašpar, J., … Zuidema, P. A. (2022). Joint effects of climate, tree size, and year on annual tree growth derived from tree-ring records of ten globally distributed forests. *Global Change Biology*, *28*(1), 245–266. https://doi.org/10.1111/gcb.15934

Aoyama, L., Shaw, E. A., White, C. T., Suding, K. N., & Hallett, L. M. (2023). Functional diversity buffers biomass production across variable rainfall conditions through different processes above- versus below-ground. *Functional Ecology*, *37*(9), 2371–2385. https://doi.org/10.1111/1365-2435.14394

Aragão, L. E. O. C., Malhi, Y., Roman-Cuesta, R. M., Saatchi, S., Anderson, L. O., & Shimabukuro, Y. E. (2007). Spatial patterns and fire response of recent Amazonian droughts. *Geophysical Research Letters*, *34*(7). https://doi.org/10.1029/2006GL028946

Aragão, L. E. O. C., Poulter, B., Barlow, J. B., Anderson, L. O., Malhi, Y., Saatchi, S., Phillips, O. L., & Gloor, E. (2014). Environmental change and the carbon balance of Amazonian forests. *Biological Reviews*, *89*(4), 913–931. https://doi.org/10.1111/brv.12088

Bartoń, K. (2025). *MuMIn: Multi-Model Inference* (Version 1.48.11) [Computer software]. https://cran.r-project.org/web/packages/MuMIn/index.html

Bates, D., Mächler, M., Bolker, B., & Walker, S. (2015). Fitting Linear Mixed-Effects Models Using lme4. *Journal of Statistical Software*, *67*, 1–48. https://doi.org/10.18637/jss.v067.i01

Bauman, D., Fortunel, C., Delhaye, G., Malhi, Y., Cernusak, L. A., Bentley, L. P., Rifai, S. W., Aguirre-Gutiérrez, J., Menor, I. O., Phillips, O. L., McNellis, B. E., Bradford, M., Laurance, S. G. W., Hutchinson, M. F., Dempsey, R., Santos-Andrade, P. E., Ninantay-Rivera, H. R., Chambi Paucar, J. R., & McMahon, S. M. (2022). Tropical tree mortality has increased with rising atmospheric water stress. *Nature*, *608*(7923), 528–533. https://doi.org/10.1038/s41586-022-04737-7

Bennett, A. C., Dargie, G. C., Cuni-Sanchez, A., Tshibamba Mukendi, J., Hubau, W., Mukinzi, J. M., Phillips, O. L., Malhi, Y., Sullivan, M. J. P., Cooper, D. L. M., Adu-Bredu, S., Affum-Baffoe, K., Amani, C. A., Banin, L. F., Beeckman, H., Begne, S. K., Bocko, Y. E., Boeckx, P., Bogaert, J., … Lewis, S. L. (2021). Resistance of African tropical forests to an extreme climate anomaly. *Proceedings of the National Academy of Sciences*, *118*(21), e2003169118. https://doi.org/10.1073/pnas.2003169118

Bennett, A. C., Rodrigues de Sousa, T., Monteagudo-Mendoza, A., Esquivel-Muelbert, A., Morandi, P. S., Coelho de Souza, F., Castro, W., Duque, L. F., Flores Llampazo, G., Manoel dos Santos, R., Ramos, E., Vilanova Torre, E., Alvarez-Davila, E., Baker, T. R., Costa, F. R. C., Lewis, S. L., Marimon, B. S., Schietti, J., Burban, B., … Phillips, O. L. (2023). Sensitivity of South American tropical forests to an extreme climate anomaly. *Nature Climate Change*, *13*(9), 967–974. https://doi.org/10.1038/s41558-023-01776-4

Betts, R. A., Malhi, Y., & Roberts, J. T. (2008). The future of the Amazon: New perspectives from climate, ecosystem and social sciences. *Philosophical Transactions of the Royal*

Society B: Biological Sciences, *363*(1498), 1729–1735. https://doi.org/10.1098/rstb.2008.0011

Biggs, C. R., Yeager, L. A., Bolser, D. G., Bonsell, C., Dichiera, A. M., Hou, Z., Keyser, S. R., Khursigara, A. J., Lu, K., Muth, A. F., Negrete Jr., B., & Erisman, B. E. (2020). Does functional redundancy affect ecological stability and resilience? A review and meta-analysis. *Ecosphere*, *11*(7), e03184. https://doi.org/10.1002/ecs2.3184

Bjorkman, A. D., Myers-Smith, I. H., Elmendorf, S. C., Normand, S., Rüger, N., Beck, P. S. A., Blach-Overgaard, A., Blok, D., Cornelissen, J. H. C., Forbes, B. C., Georges, D., Goetz, S. J., Guay, K. C., Henry, G. H. R., HilleRisLambers, J., Hollister, R. D., Karger, D. N., Kattge, J., Manning, P., … Weiher, E. (2018). Plant functional trait change across a warming tundra biome. *Nature*, *562*(7725), 57–62. https://doi.org/10.1038/s41586-018-0563-7

Bjornstad, O. N., & Cai, J. (2022). *ncf: Spatial Covariance Functions* (Version 1.3-2) [Computer software]. https://cran.r-project.org/web/packages/ncf/index.html

Bonan, G. B. (2008). Forests and Climate Change: Forcings, Feedbacks, and the Climate Benefits of Forests. *Science*, *320*(5882), 1444–1449. https://doi.org/10.1126/science.1155121

Brienen, R. J. W., Phillips, O. L., Feldpausch, T. R., Gloor, E., Baker, T. R., Lloyd, J., Lopez-Gonzalez, G., Monteagudo-Mendoza, A., Malhi, Y., Lewis, S. L., Vásquez Martinez, R., Alexiades, M., Álvarez Dávila, E., Alvarez-Loayza, P., Andrade, A., Aragão, L. E. O. C., Araujo-Murakami, A., Arets, E. J. M. M., Arroyo, L., … Zagt, R. J. (2015). Long-term decline of the Amazon carbon sink. *Nature*, *519*(7543), 344–348. https://doi.org/10.1038/nature14283

Bulleri, F., Bruno, J. F., Silliman, B. R., & Stachowicz, J. J. (2016). Facilitation and the niche: Implications for coexistence, range shifts and ecosystem functioning. *Functional Ecology*, *30*(1), 70–78. https://doi.org/10.1111/1365-2435.12528

Cadotte, M. W., Carscadden, K., & Mirotchnick, N. (2011). Beyond species: Functional diversity and the maintenance of ecological processes and services. *Journal of Applied Ecology*, *48*(5), 1079–1087. https://doi.org/10.1111/j.1365-2664.2011.02048.x

Camarero, J. J., Pizarro, M., Gernandt, D. S., & Gazol, A. (2024). Smaller conifers are more resilient to drought. *Agricultural and Forest Meteorology*, *350*, 109993. https://doi.org/10.1016/j.agrformet.2024.109993

Chaturvedi, R. K., Tripathi, A., Raghubanshi, A. S., & Singh, J. S. (2021). Functional traits indicate a continuum of tree drought strategies across a soil water availability gradient in a tropical dry forest. *Forest Ecology and Management*, *482*, 118740. https://doi.org/10.1016/j.foreco.2020.118740

Chave, J., Réjou-Méchain, M., Búrquez, A., Chidumayo, E., Colgan, M. S., Delitti, W. B. C., Duque, A., Eid, T., Fearnside, P. M., Goodman, R. C., Henry, M., Martínez-Yrízar, A., Mugasha, W. A., Muller-Landau, H. C., Mencuccini, M., Nelson, B. W., Ngomanda, A., Nogueira, E. M., Ortiz-Malavassi, E., … Vieilledent, G. (2014). Improved allometric models to estimate the aboveground biomass of tropical trees. *Global Change Biology*, *20*(10), 3177–3190. https://doi.org/10.1111/gcb.12629

Chen, J., Shao, Z., Deng, X., Huang, X., & Dang, C. (2023). Vegetation as the catalyst for water circulation on global terrestrial ecosystem. *Science of The Total Environment*, *895*, 165071. https://doi.org/10.1016/j.scitotenv.2023.165071

Coe, M. T., Marthews, T. R., Costa, M. H., Galbraith, D. R., Greenglass, N. L., Imbuzeiro, H. M. A., Levine, N. M., Malhi, Y., Moorcroft, P. R., Muza, M. N., Powell, T. L.,

Saleska, S. R., Solorzano, L. A., & Wang, J. (2013). Deforestation and climate feedbacks threaten the ecological integrity of south–southeastern Amazonia. *Philosophical Transactions of the Royal Society B: Biological Sciences*, *368*(1619), 20120155. https://doi.org/10.1098/rstb.2012.0155

Corral-Rivas, J., Vargas, B., Wehenkel, C., Aguirre, C., Álvarez, G., & Rojo, A. (2009). Guía para el establecimiento de sitios de investigación forestal y de suelos en bosques del estado de Durango. *Editorial UJED. Durango, México*.

De la Barreda, B., Metcalfe, S. E., & Boyd, D. S. (2020). Precipitation regionalization, anomalies and drought occurrence in the Yucatan Peninsula, Mexico. *International Journal of Climatology*, *40*(10), 4541–4555. https://doi.org/10.1002/joc.6474

Dobler-Morales, C., & Bocco, G. (2021). Social and environmental dimensions of drought in Mexico: An integrative review. *International Journal of Disaster Risk Reduction*, *55*, 102067. https://doi.org/10.1016/j.ijdrr.2021.102067

Doughty, C. E., Metcalfe, D. B., Girardin, C. a. J., Amézquita, F. F., Cabrera, D. G., Huasco, W. H., Silva-Espejo, J. E., Araujo-Murakami, A., da Costa, M. C., Rocha, W., Feldpausch, T. R., Mendoza, A. L. M., da Costa, A. C. L., Meir, P., Phillips, O. L., & Malhi, Y. (2015). Drought impact on forest carbon dynamics and fluxes in Amazonia. *Nature*, *519*(7541), 78–82. https://doi.org/10.1038/nature14213

Durán, S. M., Martin, R. E., Díaz, S., Maitner, B. S., Malhi, Y., Salinas, N., Shenkin, A., Silman, M. R., Wieczynski, D. J., Asner, G. P., Bentley, L. P., Savage, V. M., & Enquist, B. J. (2019). Informing trait-based ecology by assessing remotely sensed functional diversity across a broad tropical temperature gradient. *Science Advances*, *5*(12), eaaw8114. https://doi.org/10.1126/sciadv.aaw8114

Eggers, J., Lindner, M., Zudin, S., Zaehle, S., & Liski, J. (2008). Impact of changing wood demand, climate and land use on European forest resources and carbon stocks during

the 21st century. *Global Change Biology*, *14*(10), 2288–2303. https://doi.org/10.1111/j.1365-2486.2008.01653.x

Enquist, B. J., Condit, R., Peet, R. K., Schildhauer, M., & Thiers, B. M. (2016). *Cyberinfrastructure for an integrated botanical information network to investigate the ecological impacts of global climate change on plant biodiversity* (No. e2615v2). PeerJ Inc. https://doi.org/10.7287/peerj.preprints.2615v2

Esquivel-Muelbert, A., Phillips, O. L., Brienen, R. J. W., Fauset, S., Sullivan, M. J. P., Baker, T. R., Chao, K.-J., Feldpausch, T. R., Gloor, E., Higuchi, N., Houwing-Duistermaat, J., Lloyd, J., Liu, H., Malhi, Y., Marimon, B., Marimon Junior, B. H., Monteagudo-Mendoza, A., Poorter, L., Silveira, M., … Galbraith, D. (2020). Tree mode of death and mortality risk factors across Amazon forests. *Nature Communications*, *11*(1), 5515. https://doi.org/10.1038/s41467-020-18996-3

Forzieri, G., Dakos, V., McDowell, N. G., Ramdane, A., & Cescatti, A. (2022). Emerging signals of declining forest resilience under climate change. *Nature*, *608*(7923), 534–539. https://doi.org/10.1038/s41586-022-04959-9

Fuller, T., Sánchez-Cordero, V., Illoldi-Rangel, P., Linaje, M., & Sarkar, S. (2007). The cost of postponing biodiversity conservation in Mexico. *Biological Conservation*, *134*(4), 593–600. https://doi.org/10.1016/j.biocon.2006.08.028

Galicia, L., & Zarco-Arista, A. E. (2014). Multiple ecosystem services, possible trade-offs and synergies in a temperate forest ecosystem in Mexico: A review. *International Journal of Biodiversity Science, Ecosystem Services & Management*, *10*(4), 275–288. https://doi.org/10.1080/21513732.2014.973907

Gatti, L. V., Basso, L. S., Miller, J. B., Gloor, M., Gatti Domingues, L., Cassol, H. L. G., Tejada, G., Aragão, L. E. O. C., Nobre, C., Peters, W., Marani, L., Arai, E., Sanches, A. H., Corrêa, S. M., Anderson, L., Von Randow, C., Correia, C. S. C., Crispim, S. P.,

& Neves, R. A. L. (2021). Amazonia as a carbon source linked to deforestation and climate change. *Nature*, *595*(7867), 388–393. https://doi.org/10.1038/s41586-021-03629-6

Grossiord, C., Buckley, T. N., Cernusak, L. A., Novick, K. A., Poulter, B., Siegwolf, R. T. W., Sperry, J. S., & McDowell, N. G. (2020). Plant responses to rising vapor pressure deficit. *New Phytologist*, *226*(6), 1550–1566. https://doi.org/10.1111/nph.16485

Hisano, M., Ghazoul, J., Chen, X., & Chen, H. Y. H. (2024). Functional diversity enhances dryland forest productivity under long-term climate change. *Science Advances*, *10*(17), eadn4152. https://doi.org/10.1126/sciadv.adn4152

Homeier, J., Seeler, T., Pierick, K., & Leuschner, C. (2021). Leaf trait variation in species-rich tropical Andean forests. *Scientific Reports*, *11*(1), 9993. https://doi.org/10.1038/s41598-021-89190-8

Hubau, W., Lewis, S. L., Phillips, O. L., Affum-Baffoe, K., Beeckman, H., Cuní-Sanchez, A., Daniels, A. K., Ewango, C. E. N., Fauset, S., Mukinzi, J. M., Sheil, D., Sonké, B., Sullivan, M. J. P., Sunderland, T. C. H., Taedoumg, H., Thomas, S. C., White, L. J. T., Abernethy, K. A., Adu-Bredu, S., … Zemagho, L. (2020). Asynchronous carbon sink saturation in African and Amazonian tropical forests. *Nature*, *579*(7797), 80–87. https://doi.org/10.1038/s41586-020-2035-0

Jalakas, P., Takahashi, Y., Waadt, R., Schroeder, J. I., & Merilo, E. (2021). Molecular mechanisms of stomatal closure in response to rising vapour pressure deficit. *New Phytologist*, *232*(2), 468–475. https://doi.org/10.1111/nph.17592

Jetz, W., Cavender-Bares, J., Pavlick, R., Schimel, D., Davis, F. W., Asner, G. P., Guralnick, R., Kattge, J., Latimer, A. M., & Moorcroft, P. (2016). Monitoring plant functional diversity from space. *Nature Plants*, *2*(3), 1–5.

Kattge, J., Bönisch, G., Díaz, S., Lavorel, S., Prentice, I. C., Leadley, P., Tautenhahn, S., Werner, G. D. A., Aakala, T., Abedi, M., Acosta, A. T. R., Adamidis, G. C., Adamson, K., Aiba, M., Albert, C. H., Alcántara, J. M., Alcázar C, C., Aleixo, I., Ali, H., … Wirth, C. (2020). TRY plant trait database – enhanced coverage and open access. *Global Change Biology*, *26*(1), 119–188. https://doi.org/10.1111/gcb.14904

Kattge, J., Díaz, S., Lavorel, S., Prentice, I. C., Leadley, P., Bönisch, G., Garnier, E., Westoby, M., Reich, P. B., Wright, I. J., Cornelissen, J. H. C., Violle, C., Harrison, S. P., Van BODEGOM, P. M., Reichstein, M., Enquist, B. J., Soudzilovskaia, N. A., Ackerly, D. D., Anand, M., … Wirth, C. (2011). TRY – a global database of plant traits. *Global Change Biology*, *17*(9), 2905–2935. https://doi.org/10.1111/j.1365-2486.2011.02451.x

Lalibert, E., Legendre, P., & Shipley, B. (2014). Measuring functional diversity from multiple traits, and other tools for functional ecology. *R-Package FD*.

Laliberté, E., & Legendre, P. (2010). A distance-based framework for measuring functional diversity from multiple traits. *Ecology*, *91*(1), 299–305.

Lavorel, S., Colloff, M. J., Mcintyre, S., Doherty, M. D., Murphy, H. T., Metcalfe, D. J., Dunlop, M., Williams, R. J., Wise, R. M., & Williams, K. J. (2015). Ecological mechanisms underpinning climate adaptation services. *Global Change Biology*, *21*(1), 12–31. https://doi.org/10.1111/gcb.12689

Lawrence, D., & Vandecar, K. (2015). Effects of tropical deforestation on climate and agriculture. *Nature Climate Change*, *5*(1), 27–36. https://doi.org/10.1038/nclimate2430

Lawton, R. O., Nair, U. S., Pielke, R. A., & Welch, R. M. (2001). Climatic Impact of Tropical Lowland Deforestation on Nearby Montane Cloud Forests. *Science*, *294*(5542), 584–587. https://doi.org/10.1126/science.1062459

Lesk, C., Anderson, W., Rigden, A., Coast, O., Jägermeyr, J., McDermid, S., Davis, K. F., & Konar, M. (2022). Compound heat and moisture extreme impacts on global crop yields under climate change. *Nature Reviews Earth & Environment*, *3*(12), 872–889. https://doi.org/10.1038/s43017-022-00368-8

Liu, X., Lie, Z., Reich, P. B., Zhou, G., Yan, J., Huang, W., Wang, Y., Peñuelas, J., Tissue, D. T., Zhao, M., Wu, T., Wu, D., Xu, W., Li, Y., Tang, X., Zhou, S., Meng, Z., Liu, S., Chu, G., … Liu, J. (2024). Long-term warming increased carbon sequestration capacity in a humid subtropical forest. *Global Change Biology*, *30*(1), e17072. https://doi.org/10.1111/gcb.17072

Lloret, F., Escudero, A., Iriondo, J. M., Martínez-Vilalta, J., & Valladares, F. (2012). Extreme climatic events and vegetation: The role of stabilizing processes. *Global Change Biology*, *18*(3), 797–805. https://doi.org/10.1111/j.1365-2486.2011.02624.x

Maia, V. A., Santos, A. B. M., de Aguiar-Campos, N., de Souza, C. R., de Oliveira, M. C. F., Coelho, P. A., Morel, J. D., da Costa, L. S., Farrapo, C. L., Fagundes, N. C. A., de Paula, G. G. P., Santos, P. F., Gianasi, F. M., da Silva, W. B., de Oliveira, F., Girardelli, D. T., de Carvalho Araújo, F., Vilela, T. A., Pereira, R. T., … dos Santos, R. M. (2020). The carbon sink of tropical seasonal forests in southeastern Brazil can be under threat. *Science Advances*, *6*(51), eabd4548. https://doi.org/10.1126/sciadv.abd4548

Malhi, Y., Aragão, L. E., Galbraith, D., Huntingford, C., Fisher, R., Zelazowski, P., Sitch, S., McSweeney, C., & Meir, P. (2009). Exploring the likelihood and mechanism of a climate-change-induced dieback of the Amazon rainforest. *Proceedings of the National Academy of Sciences*, *106*(49), 20610–20615.

Malhi, Y., Christmann, T., Deng, X., Zhang-Zheng, H., Moore, S., & Riutta, T. (2024). Forest carbon budgets and climate change. In *Routledge Handbook of Forest Ecology* (2nd ed.). Routledge.

Malhi, Y., Franklin, J., Seddon, N., Solan, M., Turner, M. G., Field, C. B., & Knowlton, N. (2020). Climate change and ecosystems: Threats, opportunities and solutions. *Philosophical Transactions of the Royal Society B: Biological Sciences*, *375*(1794), 20190104. https://doi.org/10.1098/rstb.2019.0104

Marchin, R. M., Backes, D., Ossola, A., Leishman, M. R., Tjoelker, M. G., & Ellsworth, D. S. (2022). Extreme heat increases stomatal conductance and drought-induced mortality risk in vulnerable plant species. *Global Change Biology*, *28*(3), 1133–1146. https://doi.org/10.1111/gcb.15976

Martin, A. R., Doraisami, M., & Thomas, S. C. (2018). Global patterns in wood carbon concentration across the world's trees and forests. *Nature Geoscience*, *11*(12), 915–920. https://doi.org/10.1038/s41561-018-0246-x

McDowell, N. G., Allen, C. D., Anderson-Teixeira, K., Aukema, B. H., Bond-Lamberty, B., Chini, L., Clark, J. S., Dietze, M., Grossiord, C., Hanbury-Brown, A., Hurtt, G. C., Jackson, R. B., Johnson, D. J., Kueppers, L., Lichstein, J. W., Ogle, K., Poulter, B., Pugh, T. A. M., Seidl, R., … Xu, C. (2020). Pervasive shifts in forest dynamics in a changing world. *Science*, *368*(6494), eaaz9463. https://doi.org/10.1126/science.aaz9463

McDowell, N. G., Sapes, G., Pivovaroff, A., Adams, H. D., Allen, C. D., Anderegg, W. R. L., Arend, M., Breshears, D. D., Brodribb, T., Choat, B., Cochard, H., De Cáceres, M., De Kauwe, M. G., Grossiord, C., Hammond, W. M., Hartmann, H., Hoch, G., Kahmen, A., Klein, T., … Xu, C. (2022). Mechanisms of woody-plant mortality under

rising drought, CO2 and vapour pressure deficit. *Nature Reviews Earth & Environment*, *3*(5), 294–308. https://doi.org/10.1038/s43017-022-00272-1

Millar, C. I., & Stephenson, N. L. (2015). Temperate forest health in an era of emerging megadisturbance. *Science*, *349*(6250), 823–826. https://doi.org/10.1126/science.aaa9933

Mo, L., Zohner, C. M., Reich, P. B., Liang, J., de Miguel, S., Nabuurs, G.-J., Renner, S. S., van den Hoogen, J., Araza, A., Herold, M., Mirzagholi, L., Ma, H., Averill, C., Phillips, O. L., Gamarra, J. G. P., Hordijk, I., Routh, D., Abegg, M., Adou Yao, Y. C., … Crowther, T. W. (2023). Integrated global assessment of the natural forest carbon potential. *Nature*, *624*(7990), 92–101. https://doi.org/10.1038/s41586-023-06723-z

Morin, X., Fahse, L., Jactel, H., Scherer-Lorenzen, M., García-Valdés, R., & Bugmann, H. (2018). Long-term response of forest productivity to climate change is mostly driven by change in tree species composition. *Scientific Reports*, *8*(1), 5627. https://doi.org/10.1038/s41598-018-23763-y

Murray-Tortarolo, G. N. (2021). Seven decades of climate change across Mexico. *Atmósfera*, *34*(2), 217–226. https://doi.org/10.20937/atm.52803

Oliveira, B. F., Moore, F. C., & Dong, X. (2022). Biodiversity mediates ecosystem sensitivity to climate variability. *Communications Biology*, *5*(1), 1–9. https://doi.org/10.1038/s42003-022-03573-9

Oliveira, R. S., Eller, C. B., Barros, F. de V., Hirota, M., Brum, M., & Bittencourt, P. (2021). Linking plant hydraulics and the fast–slow continuum to understand resilience to drought in tropical ecosystems. *New Phytologist*, *230*(3), 904–923. https://doi.org/10.1111/nph.17266

Oliver, T. H., Heard, M. S., Isaac, N. J. B., Roy, D. B., Procter, D., Eigenbrod, F., Freckleton, R., Hector, A., Orme, C. D. L., Petchey, O. L., Proença, V., Raffaelli, D., Suttle, K. B., Mace, G. M., Martín-López, B., Woodcock, B. A., & Bullock, J. M. (2015). Biodiversity and Resilience of Ecosystem Functions. *Trends in Ecology & Evolution*, *30*(11), 673–684. https://doi.org/10.1016/j.tree.2015.08.009

Overpeck, J. T., & Udall, B. (2020). Climate change and the aridification of North America. *Proceedings of the National Academy of Sciences*, *117*(22), 11856–11858. https://doi.org/10.1073/pnas.2006323117

Pan, Y., Birdsey, R. A., Fang, J., Houghton, R., Kauppi, P. E., Kurz, W. A., Phillips, O. L., Shvidenko, A., Lewis, S. L., Canadell, J. G., Ciais, P., Jackson, R. B., Pacala, S. W., McGuire, A. D., Piao, S., Rautiainen, A., Sitch, S., & Hayes, D. (2011). A Large and Persistent Carbon Sink in the World's Forests. *Science*, *333*(6045), 988–993. https://doi.org/10.1126/science.1201609

Pavoine, S. (2020). adiv: An r package to analyse biodiversity in ecology. *Methods in Ecology and Evolution*, *11*(9), 1106–1112. https://doi.org/10.1111/2041-210X.13430

Phillips, O. L., Aragão, L. E. O. C., Lewis, S. L., Fisher, J. B., Lloyd, J., López-González, G., Malhi, Y., Monteagudo, A., Peacock, J., Quesada, C. A., van der Heijden, G., Almeida, S., Amaral, I., Arroyo, L., Aymard, G., Baker, T. R., Bánki, O., Blanc, L., Bonal, D., … Torres-Lezama, A. (2009). Drought Sensitivity of the Amazon Rainforest. *Science*, *323*(5919), 1344–1347. https://doi.org/10.1126/science.1164033

Poorter, L., Bongers, F., Aide, T. M., Almeyda Zambrano, A. M., Balvanera, P., Becknell, J. M., Boukili, V., Brancalion, P. H. S., Broadbent, E. N., Chazdon, R. L., Craven, D., de Almeida-Cortez, J. S., Cabral, G. A. L., de Jong, B. H. J., Denslow, J. S., Dent, D. H., DeWalt, S. J., Dupuy, J. M., Durán, S. M., … Rozendaal, D. M. A. (2016). Biomass

resilience of Neotropical secondary forests. *Nature*, *530*(7589), 211–214. https://doi.org/10.1038/nature16512

Poorter, L., Craven, D., Jakovac, C. C., van der Sande, M. T., Amissah, L., Bongers, F., Chazdon, R. L., Farrior, C. E., Kambach, S., Meave, J. A., Muñoz, R., Norden, N., Rüger, N., van Breugel, M., Almeyda Zambrano, A. M., Amani, B., Andrade, J. L., Brancalion, P. H. S., Broadbent, E. N., … Hérault, B. (2021). Multidimensional tropical forest recovery. *Science*, *374*(6573), 1370–1376. https://doi.org/10.1126/science.abh3629

Powers, J. S., Vargas G., G., Brodribb, T. J., Schwartz, N. B., Pérez-Aviles, D., Smith-Martin, C. M., Becknell, J. M., Aureli, F., Blanco, R., Calderón-Morales, E., Calvo-Alvarado, J. C., Calvo-Obando, A. J., Chavarría, M. M., Carvajal-Vanegas, D., Jiménez-Rodríguez, C. D., Murillo Chacon, E., Schaffner, C. M., Werden, L. K., Xu, X., & Medvigy, D. (2020). A catastrophic tropical drought kills hydraulically vulnerable tree species. *Global Change Biology*, *26*(5), 3122–3133. https://doi.org/10.1111/gcb.15037

Prentice, I. C., Dong, N., Gleason, S. M., Maire, V., & Wright, I. J. (2014). Balancing the costs of carbon gain and water transport: Testing a new theoretical framework for plant functional ecology. *Ecology Letters*, *17*(1), 82–91. https://doi.org/10.1111/ele.12211

Pugh, T. A. M., Arneth, A., Kautz, M., Poulter, B., & Smith, B. (2019). Important role of forest disturbances in the global biomass turnover and carbon sinks. *Nature Geoscience*, *12*(9), 730–735. https://doi.org/10.1038/s41561-019-0427-2

Ricotta, C., De Bello, F., Moretti, M., Caccianiga, M., Cerabolini, B. E. L., & Pavoine, S. (2016). Measuring the functional redundancy of biological communities: A quantitative guide. *Methods in Ecology and Evolution*, *7*(11), 1386–1395. https://doi.org/10.1111/2041-210X.12604

Rosenfeld, J. S. (2002). Functional redundancy in ecology and conservation. *Oikos*, *98*(1), 156–162. https://doi.org/10.1034/j.1600-0706.2002.980116.x

Ruehr, S., Keenan, T. F., Williams, C., Zhou, Y., Lu, X., Bastos, A., Canadell, J. G., Prentice, I. C., Sitch, S., & Terrer, C. (2023). Evidence and attribution of the enhanced land carbon sink. *Nature Reviews Earth & Environment*, *4*(8), 518–534. https://doi.org/10.1038/s43017-023-00456-3

Sakschewski, B., von Bloh, W., Boit, A., Poorter, L., Peña-Claros, M., Heinke, J., Joshi, J., & Thonicke, K. (2016). Resilience of Amazon forests emerges from plant trait diversity. *Nature Climate Change*, *6*(11), 1032–1036. https://doi.org/10.1038/nclimate3109

Sapijanskas, J., Paquette, A., Potvin, C., Kunert, N., & Loreau, M. (2014). Tropical tree diversity enhances light capture through crown plasticity and spatial and temporal niche differences. *Ecology*, *95*(9), 2479–2492. https://doi.org/10.1890/13-1366.1

Scheffer, M. (2009). *Critical Transitions in Nature and Society*. Princeton University Press. https://doi.org/10.2307/j.ctv173f1g1

Schlesinger, W. H., Dietze, M. C., Jackson, R. B., Phillips, R. P., Rhoades, C. C., Rustad, L. E., & Vose, J. M. (2016). Forest biogeochemistry in response to drought. *Global Change Biology*, *22*(7), 2318–2328. https://doi.org/10.1111/gcb.13105

Schmitt, S., Maréchaux, I., Chave, J., Fischer, F. J., Piponiot, C., Traissac, S., & Hérault, B. (2020a). Functional diversity improves tropical forest resilience: Insights from a long-term virtual experiment. *Journal of Ecology*, *108*(3), 831–843. https://doi.org/10.1111/1365-2745.13320

Schmitt, S., Maréchaux, I., Chave, J., Fischer, F. J., Piponiot, C., Traissac, S., & Hérault, B. (2020b). Functional diversity improves tropical forest resilience: Insights from a long-term virtual experiment. *Journal of Ecology*, *108*(3), 831–843. https://doi.org/10.1111/1365-2745.13320

Schneider, F. D., Morsdorf, F., Schmid, B., Petchey, O. L., Hueni, A., Schimel, D. S., & Schaepman, M. E. (2017). Mapping functional diversity from remotely sensed morphological and physiological forest traits. *Nature Communications*, *8*(1), 1441. https://doi.org/10.1038/s41467-017-01530-3

Searle, E. B., Chen, H. Y. H., & Paquette, A. (2022). Higher tree diversity is linked to higher tree mortality. *Proceedings of the National Academy of Sciences*, *119*(19), e2013171119. https://doi.org/10.1073/pnas.2013171119

Segura, M., & Kanninen, M. (2005). Allometric Models for Tree Volume and Total Aboveground Biomass in a Tropical Humid Forest in Costa Rica. *Biotropica*, *37*(1), 2–8. https://doi.org/10.1111/j.1744-7429.2005.02027.x

Serra-Maluquer, X., Gazol, A., Anderegg, W. R. L., Martínez-Vilalta, J., Mencuccini, M., & Camarero, J. J. (2022). Wood density and hydraulic traits influence species' growth response to drought across biomes. *Global Change Biology*, *28*(12), 3871–3882. https://doi.org/10.1111/gcb.16123

Staal, A., Tuinenburg, O. A., Bosmans, J. H. C., Holmgren, M., van Nes, E. H., Scheffer, M., Zemp, D. C., & Dekker, S. C. (2018). Forest-rainfall cascades buffer against drought across the Amazon. *Nature Climate Change*, *8*(6), 539–543. https://doi.org/10.1038/s41558-018-0177-y

Stan, K., & Sanchez-Azofeifa, A. (2019). Tropical Dry Forest Diversity, Climatic Response, and Resilience in a Changing Climate. *Forests*, *10*(5), Article 5. https://doi.org/10.3390/f10050443

Talbot, J., Lewis, S. L., Lopez-Gonzalez, G., Brienen, R. J. W., Monteagudo, A., Baker, T. R., Feldpausch, T. R., Malhi, Y., Vanderwel, M., Araujo Murakami, A., Arroyo, L. P., Chao, K.-J., Erwin, T., van der Heijden, G., Keeling, H., Killeen, T., Neill, D., Núñez Vargas, P., Parada Gutierrez, G. A., … Phillips, O. L. (2014). Methods to estimate

aboveground wood productivity from long-term forest inventory plots. *Forest Ecology and Management*, *320*, 30–38. https://doi.org/10.1016/j.foreco.2014.02.021

Tavares, J. V., Oliveira, R. S., Mencuccini, M., Signori-Müller, C., Pereira, L., Diniz, F. C., Gilpin, M., Marca Zevallos, M. J., Salas Yupayccana, C. A., Acosta, M., Pérez Mullisaca, F. M., Barros, F. de V., Bittencourt, P., Jancoski, H., Scalon, M. C., Marimon, B. S., Oliveras Menor, I., Marimon, B. H., Fancourt, M., … Galbraith, D. R. (2023). Basin-wide variation in tree hydraulic safety margins predicts the carbon balance of Amazon forests. *Nature*, *617*(7959), 111–117. https://doi.org/10.1038/s41586-023-05971-3

Trenberth, K. E., Dai, A., van der Schrier, G., Jones, P. D., Barichivich, J., Briffa, K. R., & Sheffield, J. (2014). Global warming and changes in drought. *Nature Climate Change*, *4*(1), 17–22. https://doi.org/10.1038/nclimate2067

Wieczynski, D. J., Boyle, B., Buzzard, V., Duran, S. M., Henderson, A. N., Hulshof, C. M., Kerkhoff, A. J., McCarthy, M. C., Michaletz, S. T., Swenson, N. G., Asner, G. P., Bentley, L. P., Enquist, B. J., & Savage, V. M. (2019). Climate shapes and shifts functional biodiversity in forests worldwide. *Proceedings of the National Academy of Sciences*, *116*(2), 587–592. https://doi.org/10.1073/pnas.1813723116

Xu, C., McDowell, N. G., Fisher, R. A., Wei, L., Sevanto, S., Christoffersen, B. O., Weng, E., & Middleton, R. S. (2019). Increasing impacts of extreme droughts on vegetation productivity under climate change. *Nature Climate Change*, *9*(12), 948–953. https://doi.org/10.1038/s41558-019-0630-6

Yang, Y., Saatchi, S. S., Xu, L., Yu, Y., Choi, S., Phillips, N., Kennedy, R., Keller, M., Knyazikhin, Y., & Myneni, R. B. (2018). Post-drought decline of the Amazon carbon sink. *Nature Communications*, *9*(1), 3172. https://doi.org/10.1038/s41467-018-05668-6

Zeng, Z., Wang, D., Yang, L., Wu, J., Ziegler, A. D., Liu, M., Ciais, P., Searchinger, T. D., Yang, Z.-L., Chen, D., Chen, A., Li, L. Z. X., Piao, S., Taylor, D., Cai, X., Pan, M., Peng, L., Lin, P., Gower, D., … Wood, E. F. (2021). Deforestation-induced warming over tropical mountain regions regulated by elevation. *Nature Geoscience*, *14*(1), 23–29. https://doi.org/10.1038/s41561-020-00666-0

Zscheischler, J., & Seneviratne, S. I. (2017). Dependence of drivers affects risks associated with compound events. *Science Advances*, *3*(6), e1700263. https://doi.org/10.1126/sciadv.1700263

6.8. Supplementary materials

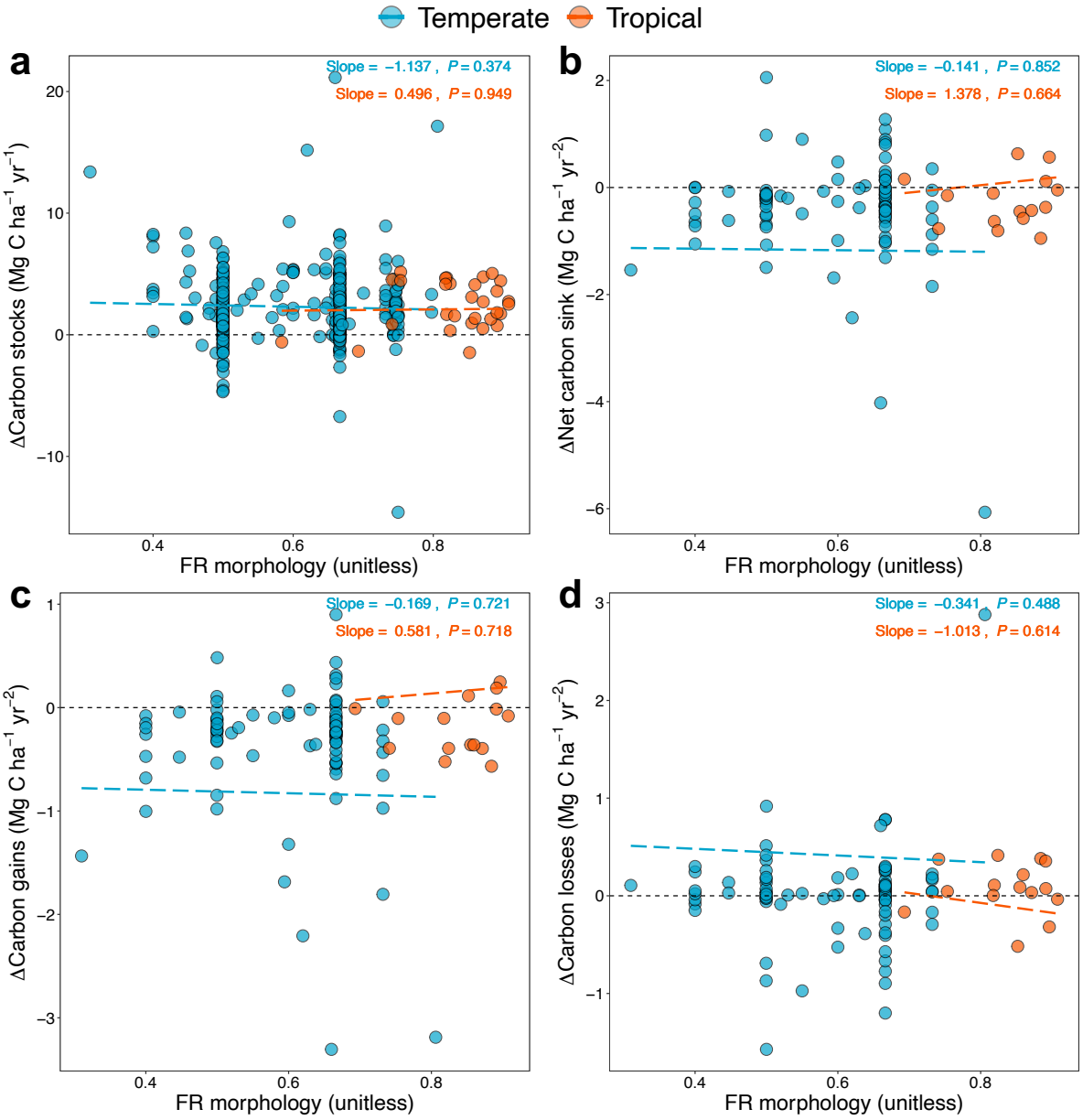

Fig. S6.1. Effects of morphological functional redundancy (FR) on changes in forest carbon stocks and dynamics. Relationships between initial morphological functional redundancy and the change rate of carbon stocks (**a**), net carbon sink (**b**), carbon gains (**c**), and carbon losses (**d**) in temperate (blue) and tropical (orange) forests. Each point represents a census interval for a plot, and regression lines indicate biome-specific trends. Solid lines denote statistically significant relationships (P<0.05), and dashed lines indicate non-significance (P>0.05).

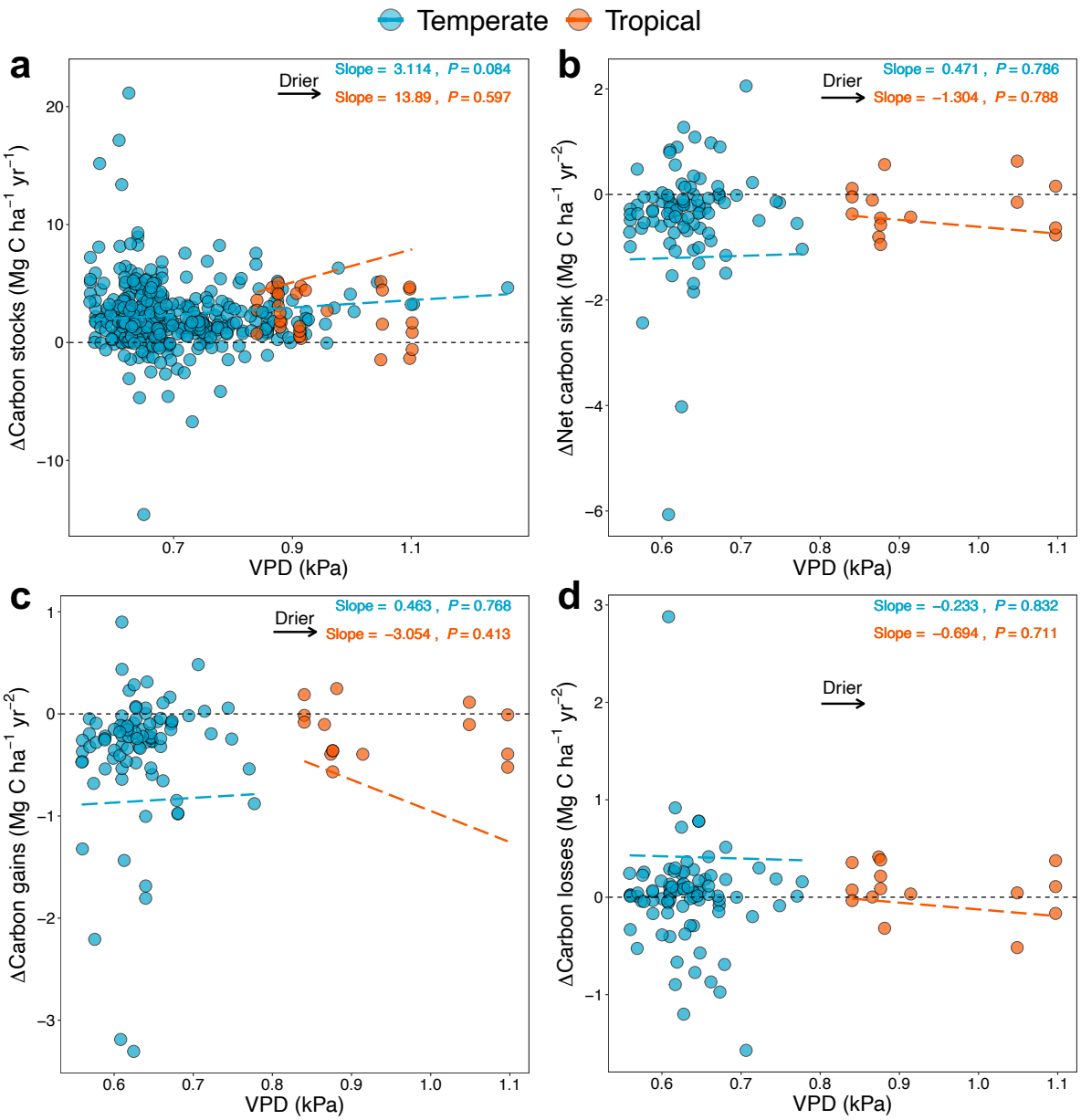

Fig. S6.2. Effects of vapour pressure deficit (VPD) on changes in forest carbon stocks and dynamics. Relationships between mean VPD and the change rate of carbon stocks (**a**), net carbon sink (**b**), carbon gains (**c**), and carbon losses (**d**) in temperate (blue) and tropical (orange) forests. Each point represents a census interval for a plot, and regression lines represent statistically significant (solid) or non-significant (dashed) trends (P<0.05 and P>0.05, respectively).

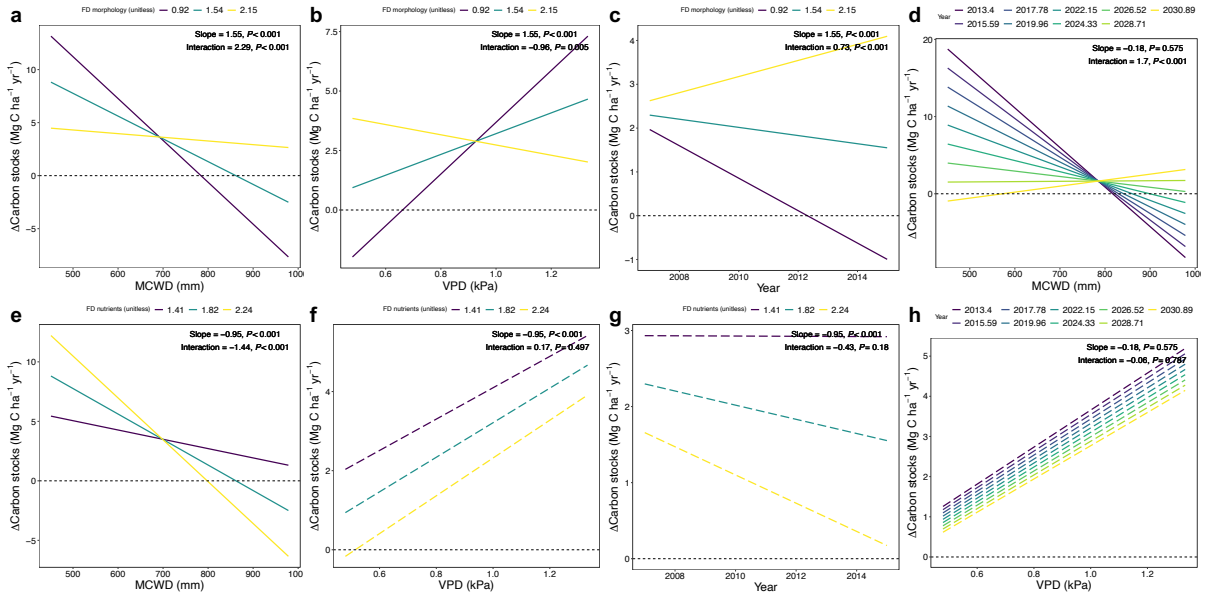

Fig. S6.3. Interaction effects between predictors on the change rate of carbon stocks in temperate forest. (**a**), MCWD as predictor and FD_{Mor} as mediating variable (**b**), VPD as predictor and FD_{Mor} as mediating variable (**c**), Time as predictor and FD_{Mor} as mediating variable (**d**) MCWD as predictor and time as mediating variable (**e**), MCWD as predictor and FD_{Nutr} as mediating variable (**f**), VPD as predictor FD_{Nutr} and as mediating variable (**g**), Time as predictor FD_{Nutr} and as mediating variable (**h**) VPD as predictor and time as mediating variable. Lines represent statistically significant (solid) or non-significant (dashed) interaction effects (P<0.05 and P>0.05, respectively), with different colours indicating multiple mediating variable levels.

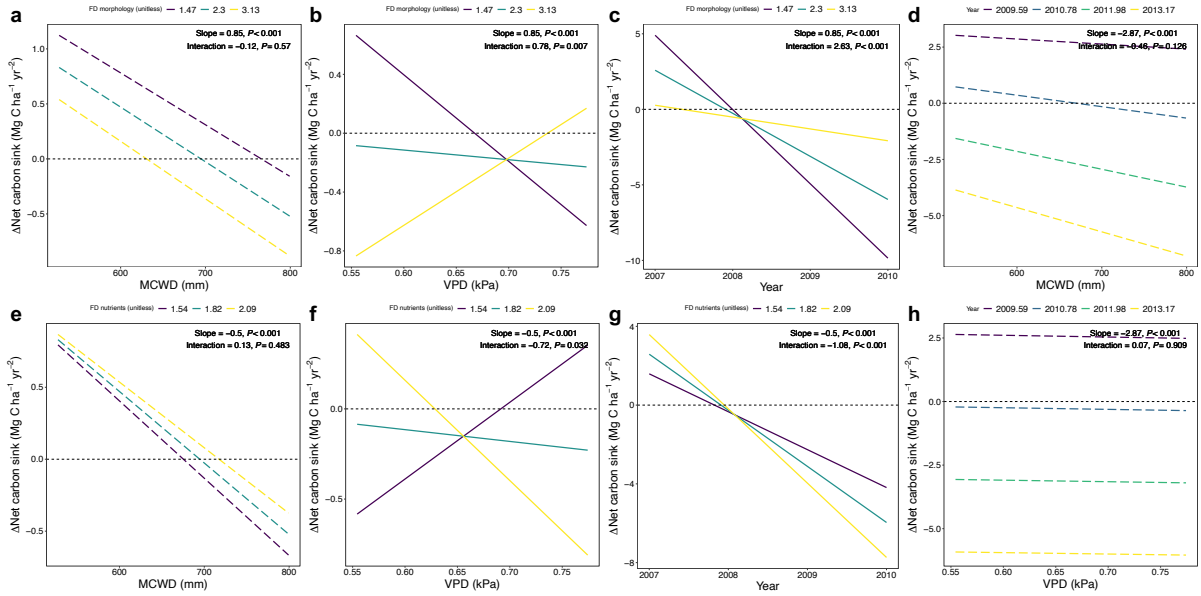

Fig. S6.4. Interaction effects between predictors on the change rate of net carbon sink in temperate forest. (**a**), MCWD as predictor and FD_{Mor} as mediating variable (**b**), VPD as predictor and FD_{Mor} as mediating variable (**c**), Time as predictor and FD_{Mor} as mediating variable (**d**) MCWD as predictor and time as mediating variable (**e**), MCWD as predictor and FD_{Nutr} as mediating variable (**f**), VPD as predictor FD_{Nutr} and as mediating variable (**g**), Time as predictor FD_{Nutr} and as mediating variable (**h**) VPD as predictor and time as mediating variable. Lines represent statistically significant (solid) or non-significant (dashed) interaction effects (P<0.05 and P>0.05, respectively), with different colours indicating multiple mediating variable levels.

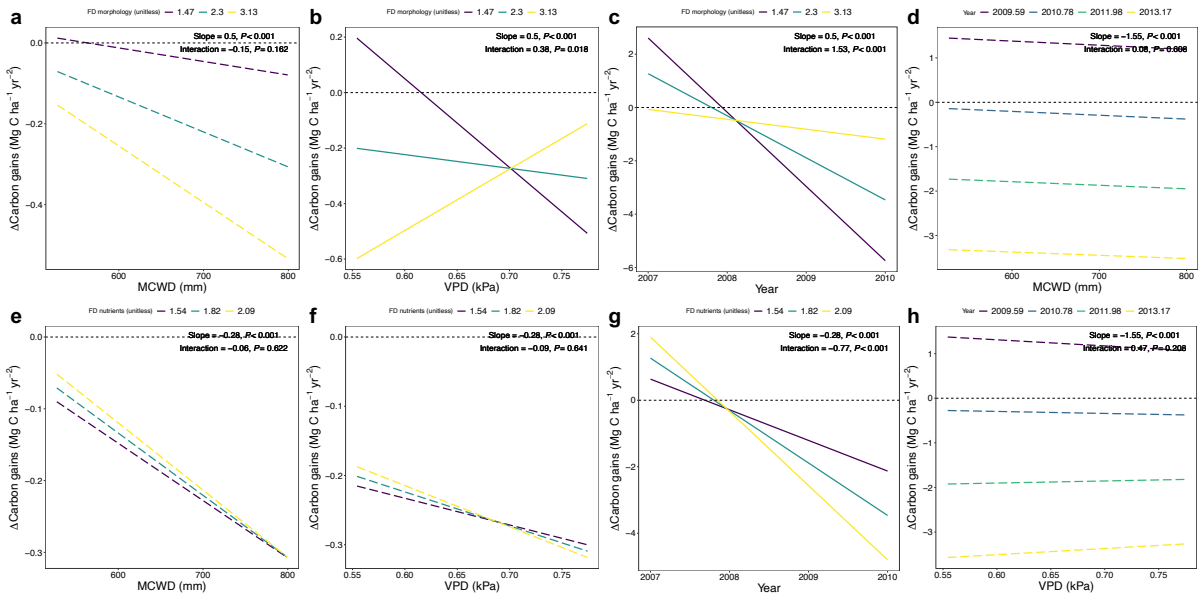

Fig. S6.5. Interaction effects between predictors on the change rate of carbon gains in temperate forest. (**a**), MCWD as predictor and FD_{Mor} as mediating variable (**b**), VPD as predictor and FD_{Mor} as mediating variable (**c**), Time as predictor and FD_{Mor} as mediating variable (**d**) MCWD as predictor and time as mediating variable (**e**), MCWD as predictor and FD_{Nutr} as mediating variable (**f**), VPD as predictor FD_{Nutr} and as mediating variable (**g**), Time as predictor FD_{Nutr} and as mediating variable (**h**) VPD as predictor and time as mediating variable. Lines represent statistically significant (solid) or non-significant (dashed) interaction effects (P<0.05 and P>0.05, respectively), with different colours indicating multiple mediating variable levels.

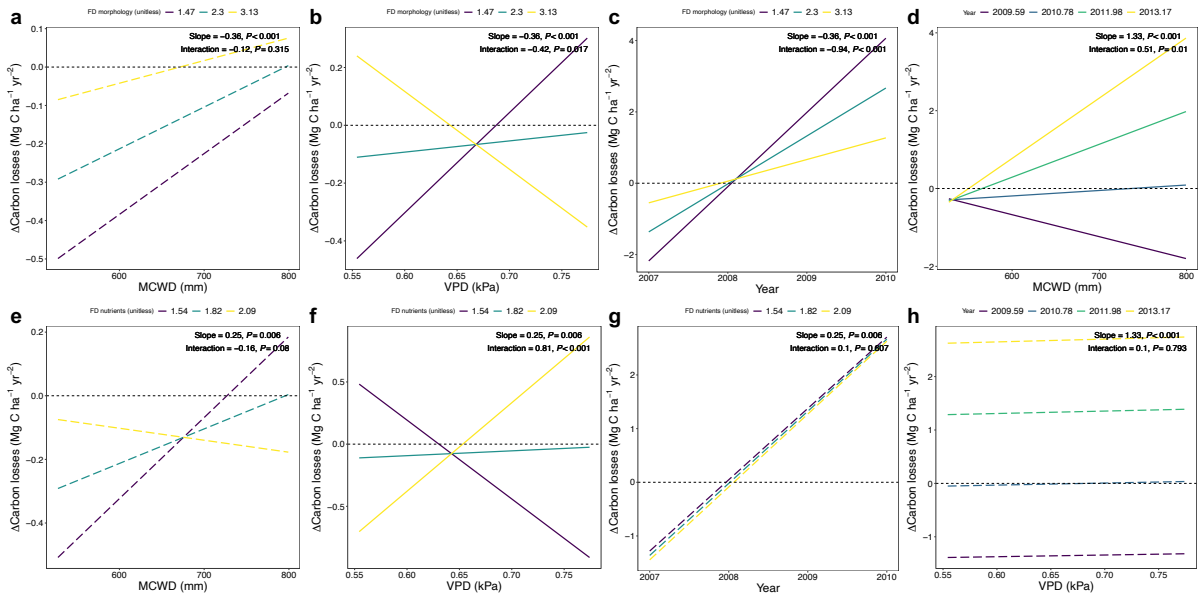

Fig. S6.6. Interaction effects between predictors on the change rate of carbon losses in temperate forest. (**a**), MCWD as predictor and FD_{Mor} as mediating variable (**b**), VPD as predictor and FD_{Mor} as mediating variable (**c**), Time as predictor and FD_{Mor} as mediating variable (**d**) MCWD as predictor and time as mediating variable (**e**), MCWD as predictor and FD_{Nutr} as mediating variable (**f**), VPD as predictor FD_{Nutr} and as mediating variable (**g**), Time as predictor FD_{Nutr} and as mediating variable (**h**) VPD as predictor and time as mediating variable. Lines represent statistically significant (solid) or non-significant (dashed) interaction effects (P<0.05 and P>0.05, respectively), with different colours indicating multiple mediating variable levels.

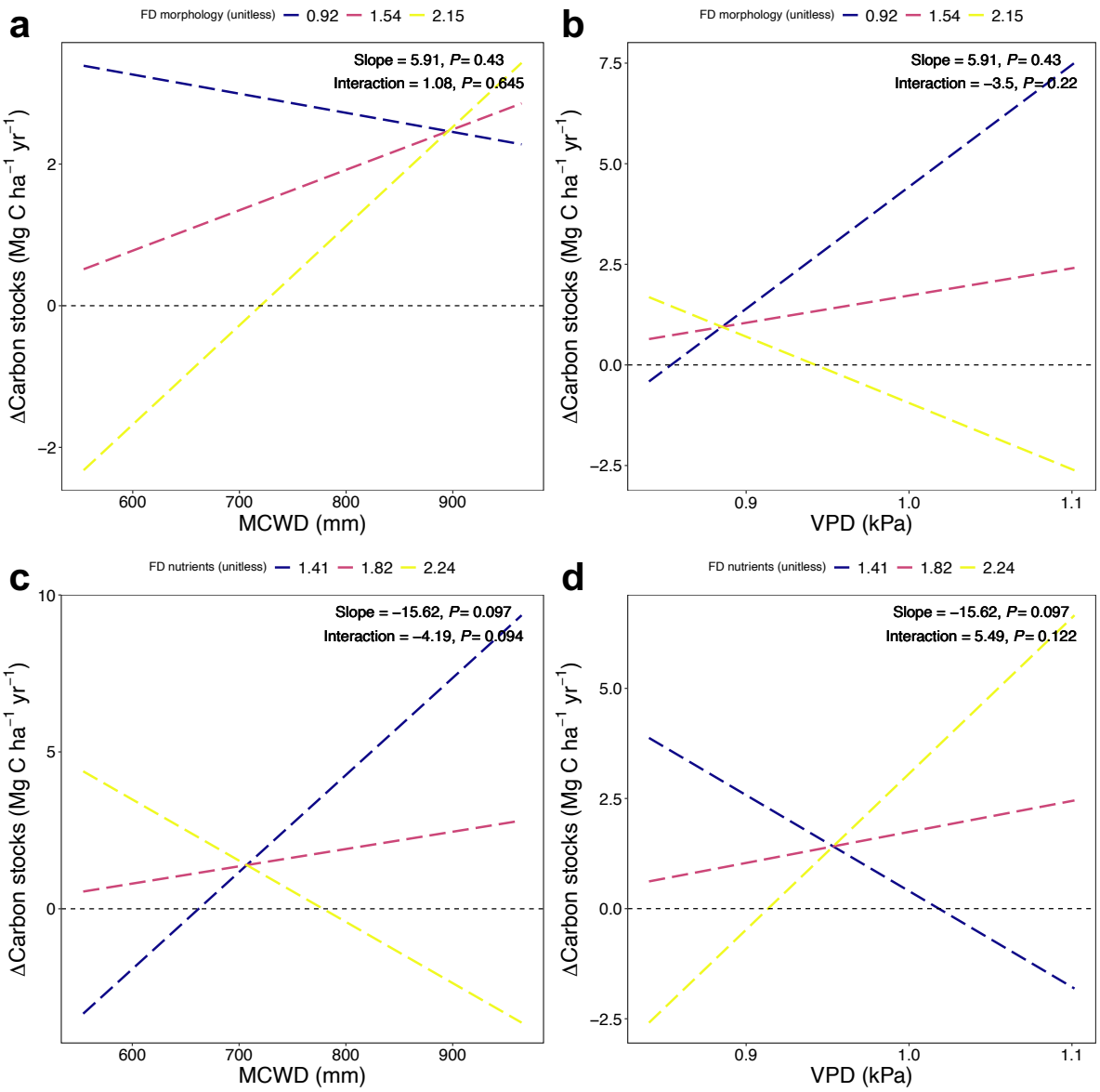

Fig. S6.7. Interaction effects between predictors on the change rate of carbon stocks in temperate forest. (**a**), MCWD as predictor and FD_{Mor} as mediating variable (**b**), VPD as predictor and FD_{Mor} as mediating variable (**c**), MCWD as predictor and FD_{Nutr} as mediating variable (**d**), VPD as predictor FD_{Nutr} and as mediating variable. Lines represent statistically significant (solid) or non-significant (dashed) interaction effects (P<0.05 and P>0.05, respectively), with different colours indicating multiple mediating variable levels.

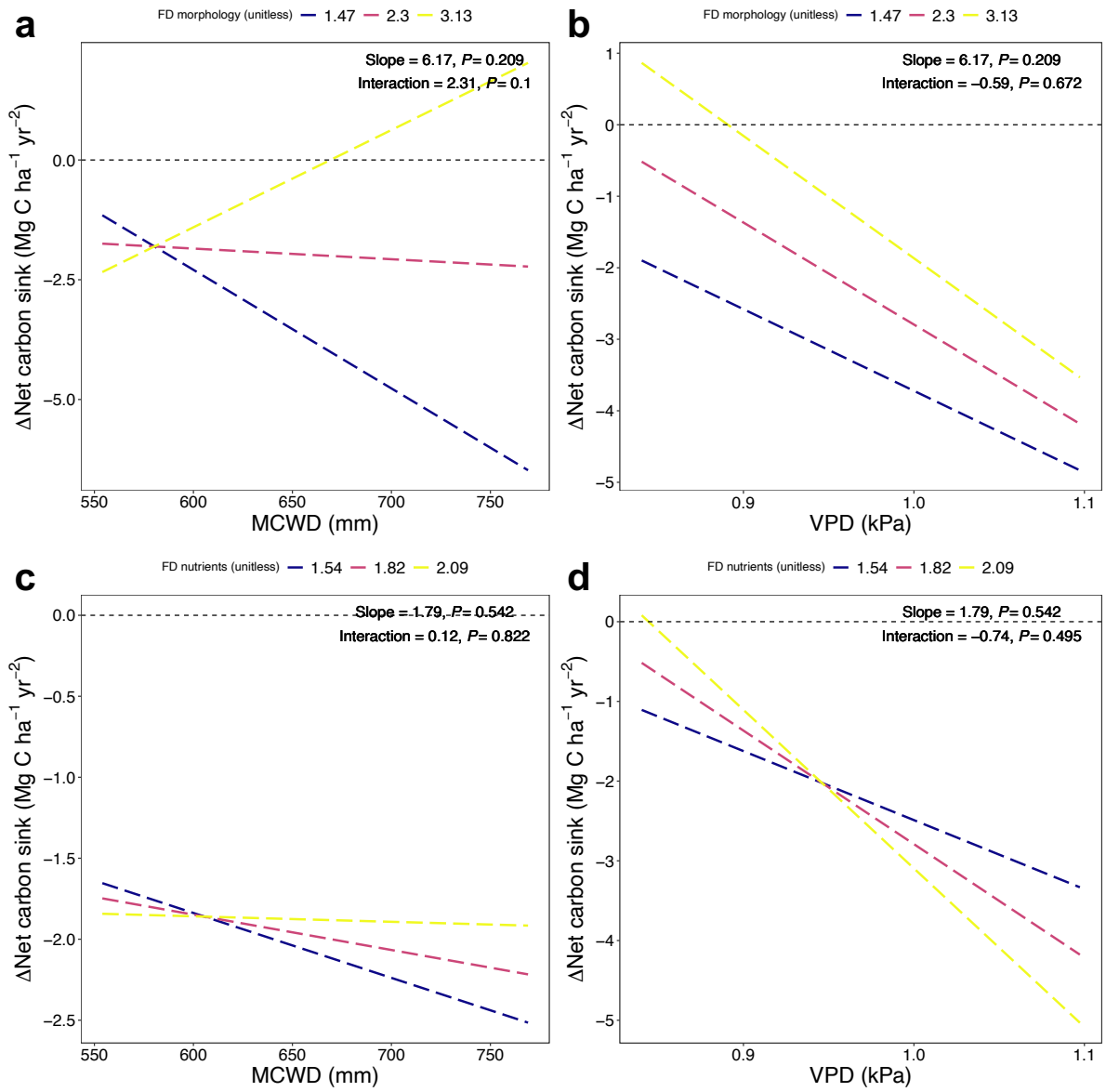

Fig. S6.8. Interaction effects between predictors on the change rate of net carbon sink in temperate forest. (**a**), MCWD as predictor and FD_{Mor} as mediating variable (**b**), VPD as predictor and FD_{Mor} as mediating variable (**c**), MCWD as predictor and FD_{Nutr} as mediating variable (**d**), VPD as predictor FD_{Nutr} and as mediating variable. Lines represent statistically significant (solid) or non-significant (dashed) interaction effects (P<0.05 and P>0.05, respectively), with different colours indicating multiple mediating variable levels.

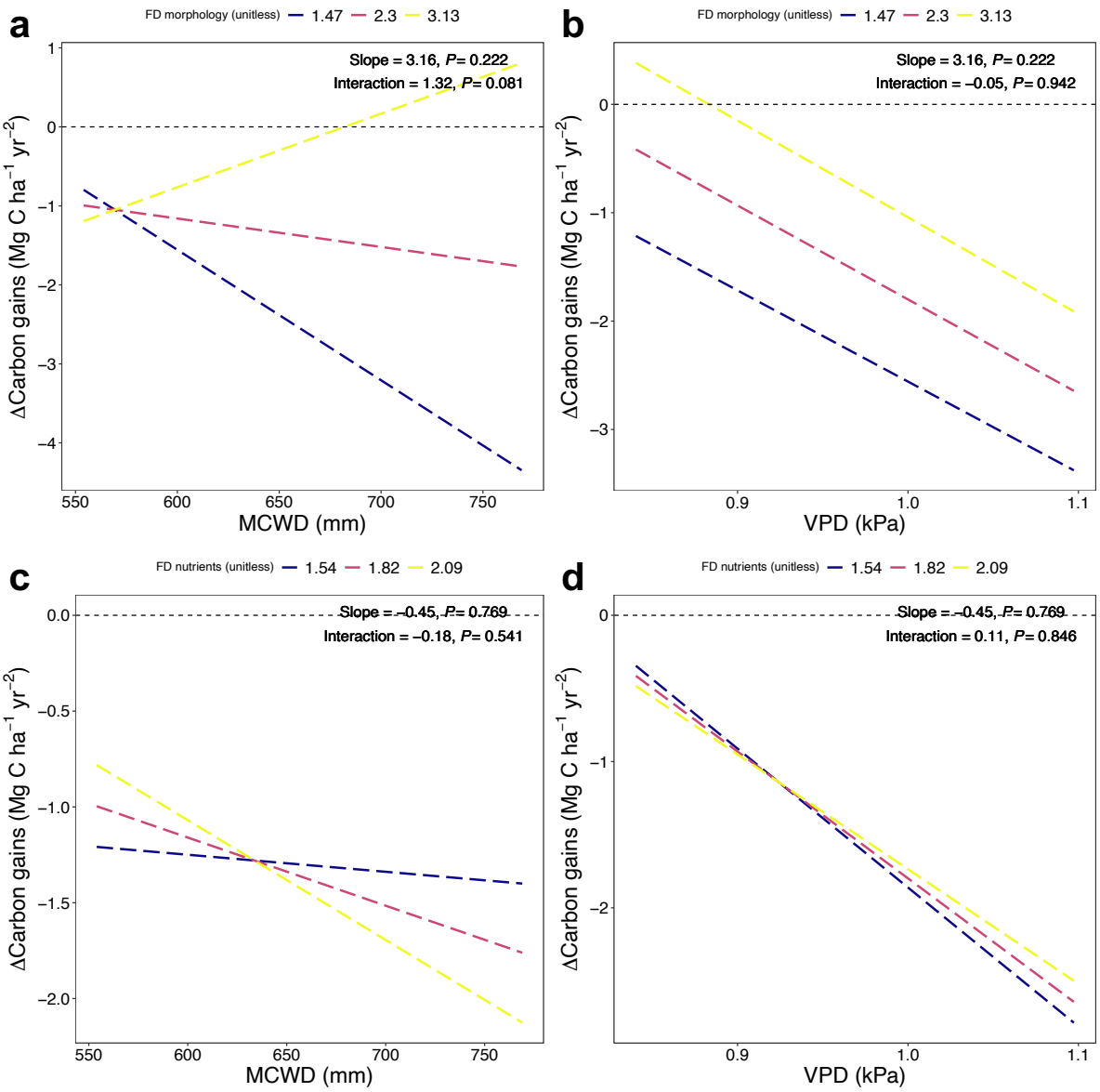

Fig. S6.9. Interaction effects between predictors on the change rate of carbon gains in temperate forest. (**a**), MCWD as predictor and FD_{Mor} as mediating variable (**b**), VPD as predictor and FD_{Mor} as mediating variable (**c**), MCWD as predictor and FD_{Nutr} as mediating variable (**d**), VPD as predictor FD_{Nutr} and as mediating variable. Lines represent statistically significant (solid) or non-significant (dashed) interaction effects (P<0.05 and P>0.05, respectively), with different colours indicating multiple mediating variable levels.

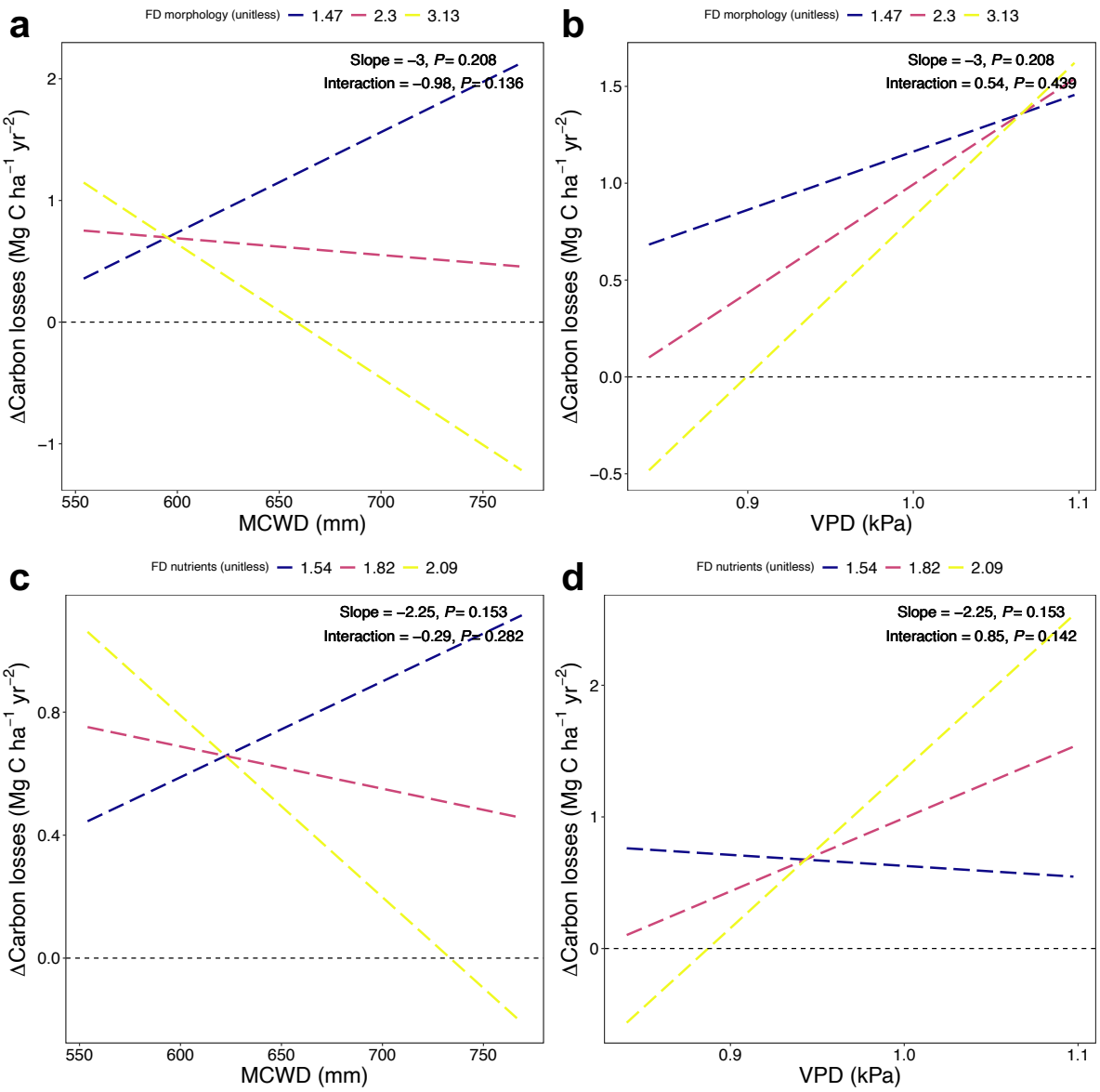

Fig. S6.10. Interaction effects between predictors on the change rate of carbon losses in temperate forest. (**a**), MCWD as predictor and FD_{Mor} as mediating variable (**b**), VPD as predictor and FD_{Mor} as mediating variable (**c**), MCWD as predictor and FD_{Nutr} as mediating variable (**d**), VPD as predictor FD_{Nutr} and as mediating variable. Lines represent statistically significant (solid) or non-significant (dashed) interaction effects (P<0.05 and P>0.05, respectively), with different colours indicating multiple mediating variable levels.

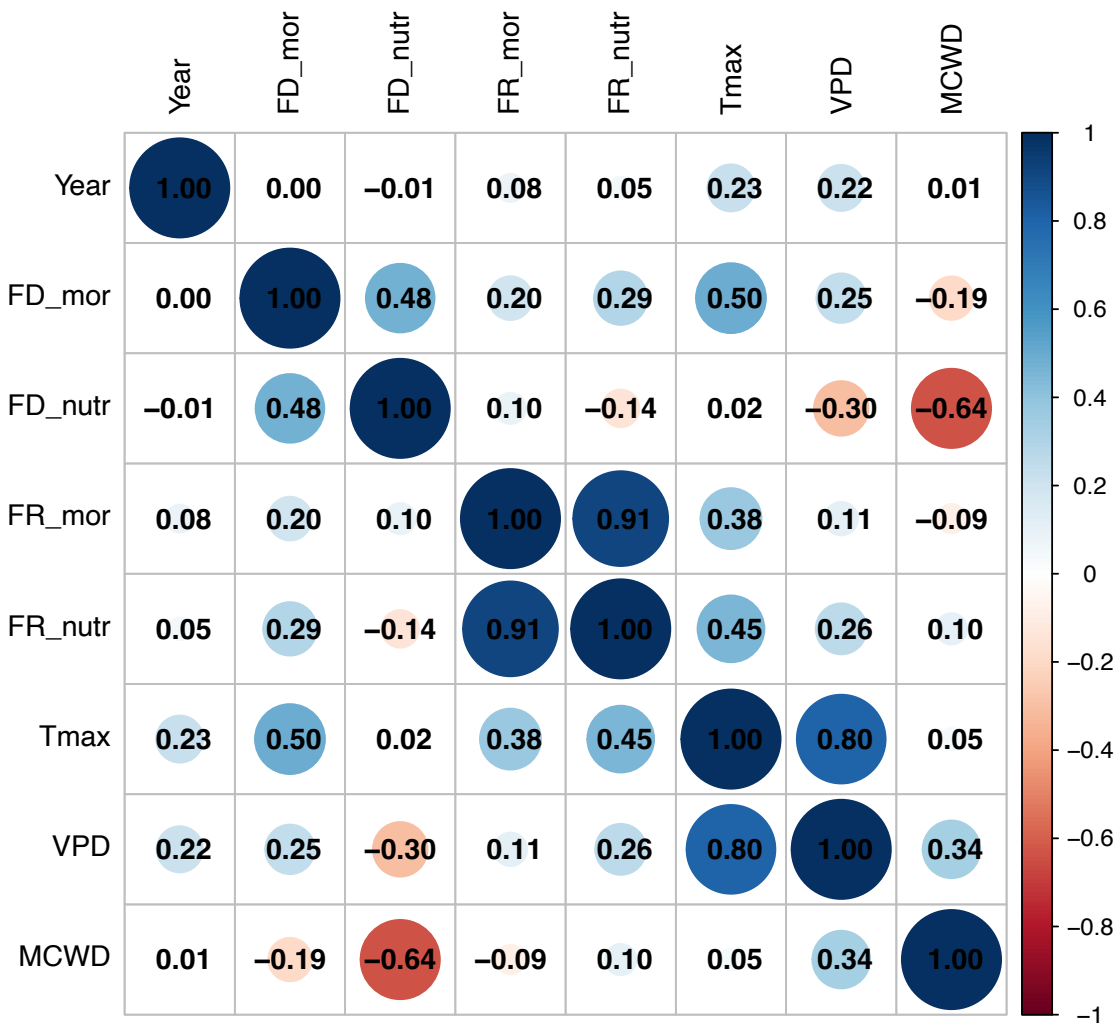

Fig. 6.S11. Heatmap of pairwise correlation between predictors.

6.9. Declarations of competing interest

The authors declare that they have no known competing financial interests or personal relationships that could have appeared to influence the work reported in this paper.

6.10. Acknowledgements

Xiongjie Deng receives the Pay It Forward Scholarship (by China Oxford Scholarship Fund, Oxford) and the New Blackfriars Scholarship (by Blackfriars Hall, Oxford). Yadvinder Malhi is supported by the Frank Jackson Foundation. Jesús Aguirre-Gutiérrez is funded by the NERC (Grants: NE/T011084/1; NE/Z504191/1), the Leverhulme Trust (RPG-2024-342), and the Royal Society (RG\R1\251370). Vegetation censuses were collected via the Monitoreo Nacional Forestal network (http://fcfposgrado.ujed.mx/monafor/inicio/).

6.11. Data availability

Because of the data sovereignty from the original data owners, raw data on vegetation censuses and trait data are not publicly available but can be requested by contacting all researchers.

Chapter 7 Synthesis and conclusion

This chapter revisits the main research questions that guided this work, summaries primary conclusions and novelties, acknowledges the limitations encountered during the research, and proposes promising avenues for future research in this critical field. This thesis has explored how plant functional trait composition, diversity, and redundancy can be assessed using multi-sensor remote sensing, and how these functional characteristics influence forest resilience in the face of increasing environmental stress. Through three integrated studies, it has contributed to advancing our ability to monitor, understand, and predict the ecological functioning of forest ecosystems at broad spatial and temporal scales. The findings highlight both the potential and the complexity of using trait-based approaches and remotely sensed data to address key challenges in forest ecology and global change biology.

7.1. Summary of the primary conclusions

This thesis makes a novel contribution to forest functional ecology by being the first to establish cross-biome linkages between remote sensing, functional traits, and ecosystem resilience. Through innovative remote sensing applications, detailed analyses of functional diversity across environmental gradients, and critical assessments of climate change impacts on forest carbon dynamics, it advances our understanding of how forests function and respond to global change. The key findings from **Chapters 4**, **5**, and **6** are synthesised below.

7.1.1. Remote sensing of large-scale trait mapping

The study in **Chapter 4** represents one of the first attempts to predict multiple functional traits including morphological and photosynthetic traits and leaf nutrients across the tropics using an integrated remote sensing framework. By combining multispectral, SAR, and LiDAR data with environmental variables and employing both machine learning (Random forests) and deep learning (Multilayer Perceptron) algorithms trained on the largest available tropical trait dataset, the research demonstrates that Random forests outperforms Multilayer Perceptron in terms of pan-tropical traits mapping, likely due to their robustness to data complexity, limited sample sizes for deep architectures, and handling nonlinear relationships effectively. The Multilayer Perceptron algorithm's performance may have been constrained by the sample size, which, though substantial, might be insufficient for deep learning algorithms to generalise without

overfitting. The results prove the value of integrating different remote sensing modalities, each capturing unique biophysical dimensions: multispectral for leaf nutrients, and SAR and LiDAR for canopy structure, as the integrated multi-sensor and environmental data approach achieved comparable or improved accuracy for several traits, such as leaf dry mass, leaf water content, and leaf nutrients (Ca, Mg, N, P), when compared to studies relying solely on spectral and environmental data (Aguirre-Gutiérrez et al., 2025).

Another critical aspect of **Chapter 4** is the comprehensive assessment of spatial robustness through a series of cross-validation strategies, including leave-one-plot-out, leave-one-cluster-out, leave-one-country-out, and leave-one-continent-out methods. These tests are designed to evaluate not just model accuracy, but also the generalisability of trait predictions across geographic and ecological boundaries. While overall prediction accuracy is strong under standard validation procedures, performance consistently declines as the spatial scale of exclusion increases. This pattern highlights the presence of strong regional effects and substantial spatial heterogeneity in trait-environment relationships. It suggests that models calibrated in one area may not reliably transfer to distant or ecologically distinct regions, even within the same biome. This spatial sensitivity is particularly important in tropical ecosystems, where high biodiversity, environmental complexity, and limited ground data exacerbate challenges of model transferability (Sequeira et al., 2018; Yates et al., 2018). These findings highlight the importance of incorporating spatial structure explicitly into model development and validation (Rangel et al., 2010; Roberts et al., 2017), and they call for more geographically representative training data if large-scale trait mapping is to be operationalised with confidence.

Importantly, the spatial variability in trait predictions indicates the regional heterogeneity in trait-environment relationships, which complicates the generalisation of models across biomes. Despite this, clear patterns are found that photosynthetic traits are largely shaped by climate, while morphological traits and leaf nutrients show stronger associations with soil and terrain properties. These findings demonstrate the feasibility of predicting multiple functional traits across large and diverse areas and highlight the importance of environmental gradients in shaping functional trait distributions and variations.

Regarding the primary drivers for trait prediction, remotely sensed data, especially multispectral imagery proves most influential. This highlights the capacity of spectral data to capture subtle variations in plant physiology and biochemistry (Kokaly et al., 2009; Thenkabail et al., 2018). SAR data are particularly important for predicting photosynthetic traits, likely due to its sensitivity to vegetation structure and moisture (Lucas et al., 2010). While LiDAR metrics

have lower overall importance, they contribute significantly to SLA prediction, suggesting the relevance of 3D structural information (Omasa et al., 2007). This highlights the synergistic benefits of integrating multiple remotely sensed data. In contrast, broad-scale environmental variables (soil, climate, and terrain) play a relatively minor role in direct trait prediction compared to remotely sensed data, possibly due to scale mismatches in environmental datasets.

7.1.2. Mapping functional trait composition, diversity, and redundancy across environmental gradients

Building on the trait-mapping foundation from **Chapter 4**, **Chapter 5** expands the analysis to include functional diversity and redundancy considering morphology, nutrients, photosynthesis, and hydraulics using the Random forests algorithm. A key achievement is demonstrating the ability to accurately scale up plot-level ecological understanding across extensive latitudinal and environmental gradients. By integrating multispectral drone imagery, handheld LiDAR scans, satellite data, and environmental variables, the study shows how fine-scale field data can be scaled up to landscape levels. This enables spatially explicit assessments of trait composition and functional diversity and redundancy across broad latitudinal gradients in South American temperate forests.

The results reveals clear latitudinal patterns in functional trait composition, diversity, and redundancy across South American temperate forests in Chile, shaped by interacting gradients of climate, soil, and topography. A transitional zone between approximately 35°S and 42°S emerges as a region of particular interest, where both functional diversity and redundancy peak. This co-occurrence suggests that these forests may possess strong resilience to disturbances, with both a wide range of adaptive strategies and functional overlap that can buffer against species loss. In addition, the northern Mediterranean region (~30°S to ~35°S) is characterised by high functional diversity but low redundancy, indicating adaptability to environmental variability but increased vulnerability should key species be lost. In contrast, toward the south, from ~42°S to ~48°S, forests exhibit high redundancy but lower diversity, suggesting ecological convergence under harsher Subantarctic conditions. While redundancy may offer some resilience, the prevalence of similar trait strategies increases the risk of synchronous species decline under future stress. Beyond 48°S, in the southernmost forests, both functional diversity and redundancy are low, reflecting extremely low species richness. These ecosystems are especially vulnerable but play an important role as refugia for cold-

adapted taxa and reservoirs of unique evolutionary history. These findings reinforce the value of functional trait-based metrics for informing conservation priorities and highlight the importance of management strategies to vulnerabilities under climate change.

7.1.3. Integrating methods and addressing limitations

Across **Chapters 4** and **5**, the integration of multi-source remotely sensed images and trait data proves critical. The combination of remote sensor types allows for robust and scalable estimates of functional trait composition, diversity, and redundancy, which is a promising pathway for operational ecological monitoring. However, several limitations must be acknowledged. Sparse field plot data in some regions limit the resolution of spatial models, particularly in shrublands or transitional forests. The presence of spatial autocorrelation also presents challenges for model validation, even when using advanced cross-validation strategies.

Future studies should aim to expand field sampling, especially in underrepresented ecosystems, and employ spatially explicit validation methods. Long-term ecological networks and coordinated monitoring efforts would improve the spatial robustness and transferability of trait models. Methodologically, the continued development of hybrid analytical approaches that combine statistical, machine learning, and physically based models is essential to enhance trait prediction and ecological inference.

7.1.4. Climate change impacts on forest ecosystems and carbon dynamics

Chapter 6 focuses on the impacts of recent warming and drying trends (2007-2021) on Mexican temperate and tropical forests, particularly concerning their carbon stocks and net carbon sink. The findings reveals that both forest types are experiencing increasingly stressful climatic conditions. Tropical forests exhibit greater absolute increases in seasonal drought severity (MCWD), while temperate forests show more statistically robust warming (maximum temperature) and atmospheric drying (VPD). These trends, consistent with broader regional (Méndez & Magaña, 2010; Stahle et al., 2009) and global patterns (Dai, 2011, 2013; Trenberth et al., 2014), exacerbate thermal stress, reduce plant water supply, and ultimately suppress forest growth and increase tree mortality.

Specifically, tropical forests see a sharp increase in MCWD, indicating intensifying dry-season water deficits that can diminish resilience even without strong VPD signals.

Temperate forests experience a significant rise in maximum temperature, VPD, and MCWD between 2007 and 2021. These compounding stressors are likely pushing many forest systems beyond their physiological thresholds, potentially reshaping species composition, reducing productivity, and compromising long-term carbon storage.

Regarding carbon resilience, temperate forests show significant carbon accumulation over the study period, while tropical forests have a non-significant increase. However, both forest types exhibit declining net carbon sinks. This is driven by reductions in carbon gains (especially in tropical forests) and slight increases in carbon losses, suggesting an early signal of carbon sink saturation. This decoupling, where total stocks might rise while the rate of accumulation slows, is attributed to factors like hydraulic constraints and increasing stress-induced mortality. Most alarmingly, the study projects a potential collapse of net carbon sinks by 2025 in these temperate forests and 2029 in the tropical forests, which means they could transition from carbon sinks to carbon sources. This trajectory, similar to trends observed in the Amazon and Africa (Hubau et al., 2020), has severe implications for regional climate feedbacks and suggests Mexican forests may become persistent carbon sources without urgent intervention.

Chapter 6 also investigates the role of functional trait diversity and redundancy in mediating forest carbon resilience. In temperate forests, higher initial morphological functional diversity is strongly linked to positive changes in carbon stocks, net carbon sink, and carbon gains, while also reducing carbon losses. This suggests that diverse structural and morphological traits enhance niche complementarity or facilitation, which allows for optimised resource acquisition and buffering against environmental stress. Conversely, higher nutrient functional diversity in temperate forests is associated with declining carbon stocks, net sink, and gains, and increasing losses. This likely reflects trade-offs where acquisitive species (high nutrients and fast growth) are more vulnerable to drought due to lower water-use efficiency. In the tropical forests studied, neither functional diversity shows significant associations with carbon resilience, possibly due to higher baseline diversity where additional diversity effects level off, or because the intensity of climatic stress overwhelmed any buffering capacity of trait variation. Morphological functional redundancy does not significantly explain carbon dynamics in either biome. Finally, seasonal drought intensity (MCWD) emerges as a more consistent climatic stressor linked to carbon resilience than atmospheric drought (VPD), particularly in temperate forests, highlighting the critical role of soil water availability.

7.2. Collective implications for forest functional ecology and resilience

The collective findings of this thesis demonstrate the transformative potential of integrating multiple remote sensing sensors including spectral, SAR, and LiDAR data with trait-based ecological frameworks to advance our understanding of forest function, biodiversity, and resilience under global change. By enabling the spatially explicit mapping of functional traits such as leaf nutrients, morphological, and photosynthetic traits, as well as derived metrics like functional diversity and redundancy, this work contributes to a transition beyond purely taxonomic approaches toward a more dynamic and trait-based understanding of ecosystems. This integrated perspective is critical for assessing how forests respond to complex environmental gradients and disturbances. The thesis confirms that trait-based monitoring, when coupled with advanced remote sensing technologies, allows for more ecologically meaningful assessments of forest composition, function, and vulnerability.

One of the central contributions of this research is the empirical linkage between specific dimensions of functional diversity and indicators of ecosystem resilience, particularly carbon stocks and carbon dynamics. The consistent positive influence of morphological trait diversity on carbon uptake and stability in temperate forests demonstrates the role of structural variation in maintaining ecosystem function under climatic stress, particularly warming and drought. In contrast, the observed negative associations between nutrient trait diversity and carbon resilience point to important ecological trade-offs, where acquisitive strategies that promote rapid growth may simultaneously reduce resistance to environmental extremes and/or resilience to environmental disturbances. These findings advance our understanding beyond general biodiversity-function relationships by identifying which types of trait variation matter most, and under what conditions. Moreover, the spatial modelling of trait composition across environmental gradients reveals that resilience is not uniformly distributed but rather concentrated in regions with specific combinations of diversity and redundancy, such as the temperate transition zone in Chile identified in **Chapter 5**, while other regions may face increased risks due to functional convergence or low trait richness.

In addition to the theoretical value, the insights carry significant applied implications. The spatial patterns uncovered in **Chapters 4** and **5**, including high-diversity, high-redundancy "resilience hotspots" and low-diversity, low-redundancy "risk zones," provide a foundation for more targeted conservation strategies. For example, maintaining or enhancing morphological diversity in structurally diverse forests could be a practical goal for forest managers aiming to preserve carbon storage and mitigate the impacts of climate change. Similarly, areas with high

functional redundancy but low trait variation may benefit from efforts to promote ecological connectivity or diversify species compositions to reduce vulnerability to current and novel climatic stressors. The detection of declining net carbon sink and projected transitions to net carbon sources in Mexican forests reinforces the urgency of such interventions, highlighting the real-time implications of trait-based monitoring for understanding and responding to climatic tipping points.

Ultimately, this thesis provides both a conceptual and methodological foundation for applying functional ecology principles through remote sensing technologies to the real-world challenges of biodiversity loss and climate change. It offers scalable and transferable approaches for assessing ecosystem condition and resilience, with direct relevance to ecological forecasting, conservation planning, and adaptive management. The demonstrated ability to predict functional trait composition, quantify functional diversity and redundancy, and link these trait-based metrics to ecosystem outcomes such as carbon dynamics suggests that trait-based remote sensing is not only scientifically robust but also policy-informative. As the global forest community increasingly turns to nature-based solutions for climate mitigation and biodiversity conservation (Seddon, Chausson, et al., 2020; Seddon, Daniels, et al., 2020; Seddon et al., 2021), this research supports a transition toward ecosystem monitoring informed by plant functional traits, which moves from observing forests to understanding them in terms of the functions they perform and the resilience they can sustain.

7.3. Limitations of the research

While this thesis presents significant advances in the application of remote sensing and trait-based approaches to forest functional ecology, it is essential to critically evaluate its limitations, as these shape the scope and interpretation of the findings.

The first limitation concerns the distribution, density, and representativeness of plot data. In pan-tropical forests (**Chapter 4**), South American temperate forests (**Chapter 5**), and Mexican forests (**Chapter 6**), plots were unevenly distributed or limited, with dense coverage in certain regions and underrepresentation in others. This imbalance may bias results toward the ecological conditions of better-sampled areas (e.g., tropical Americas and western temperate Mexico), while limiting inference for tropical Africa and Asia, transitional or disturbance-prone systems like shrublands in Chile, and tropical Mexico. Consequently, some

of the observed trait distribution patterns and biodiversity-carbon-climate relationships may reflect regional sampling biases rather than generalisable ecological patterns.

The second limitation lies in the reliance on remote sensing for trait prediction. Although multi-sensor models achieved good performance in **Chapters 4** and **5**, uncertainties remain due to sensor resolution and the reliance on training data that may not fully capture local trait variability. These uncertainties can propagate into large-scale trait maps, especially where predictions are extrapolated beyond the environmental or taxonomic range of training plots. The resulting trait-environment relationships may therefore reflect artefacts of model transferability as much as true ecological gradients, particularly across biomes with distinct evolutionary histories.

Third, generalising results across biomes remains a substantial challenge. As shown in **Chapters 5** and **6**, trait-environment and trait-function relationships are often regionally specific, shaped by local adaptations, disturbance histories, and environmental context. For example, morphological functional diversity enhanced carbon resilience in Mexican temperate forests but not in tropical forests, highlighting that the same trait dimensions may operate differently depending on baseline diversity and climatic stress regimes. This limits the ability to infer universal mechanisms from regionally focused studies and indicates the risk of overextending results beyond the biomes where they were tested.

Finally, the temporal and process scope of the analyses also imposes constraints. The carbon resilience analysis (**Chapter 6**) focused on 2007-2021, a period of accelerating drought and warming, but longer-term dynamics including lagged responses to past disturbances remain unresolved. Moreover, the analyses emphasised climate-driven stressors, while other drivers such as fire, pests, pathogens, and anthropogenic disturbance (Burton et al., 2020; Weed et al., 2013) were not explicitly modelled. These unaccounted factors may interact with climate stress in complex ways, further shaping forest trajectories.

Recognising these limitations is critical not only for contextualising the findings of this thesis but also for guiding future research. Addressing sampling bias through expanded monitoring networks, improving remote sensing calibration with broader and more representative ground data, and testing trait-function relationships across diverse biomes will be essential to strengthen the generality and applied relevance of trait-based approaches in forest ecology under global change.

7.4. Avenues for future research

The findings and limitations of this thesis highlight several directions for future research that can deepen our understanding of forest functional ecology and resilience. One major priority is improving the spatial prediction and interpretation of functional traits. This will require more advanced modelling approaches that explicitly account for spatial autocorrelation and regional heterogeneity, such as spatial cross-validation and geographically weighted machine learning techniques (Hashemi & Karimi, 2020; Wang et al., 2023; Yang et al., 2023). Enhanced environmental datasets, particularly higher-resolution information on soil properties, microclimate, and topography, can help disentangle the influences of environmental gradients from remotely sensed data, thereby improving model accuracy and interpretability. Alongside these technical advances, there remains a need for mechanistic ecological studies that investigate the physiological drivers behind trait distribution and variation patterns, which helps to bridge remotely sensed data with ecological theory (Cavender-Bares et al., 2022; Enquist et al., 2015).

Advancing assessments of functional diversity and redundancy will also require expanded and better-coordinated data infrastructures. Establishing long-term ecological monitoring networks that integrate *in-situ* trait sampling with remote sensing across diverse forest types would improve spatial representativeness and allow for more robust inference (Hauser et al., 2021; Pause et al., 2016). Greater attention should also be given to the development of multi-dimensional trait diversity metrics that move beyond univariate indices (Daly et al., 2018; O'Shaughnessy et al., 2023), as well as to understanding how these metrics change over time in response to disturbance and restoration. Moreover, examine how functional traits relate to key ecosystem services beyond carbon dynamics, such as water cycling, pollination, and/or soil stability, would offer a more complete understanding of ecosystem function and resilience (Faucon et al., 2017; Oliver et al., 2015).

Climate change impacts, and their implications for forest resilience, remain a critical field for future work. Continued long-term monitoring of carbon fluxes in regions identified as at risk of net sink collapse will be essential to assess the validity of early warning signs and to better understand forest responses at or beyond potential tipping points. Further investigation into the mechanisms by which morphological trait diversity promotes carbon resilience, and why nutrient diversity may have contrasting effects, could be addressed through targeted eco-physiological studies or manipulative experiments. In tropical forests, where no clear link between functional diversity and carbon resilience is observed, more focused studies can

explore alternative trait dimensions, such as hydraulic and/or photosynthetic traits (Anderegg et al., 2016, 2018; Hu et al., 2022; Qi et al., 2021), or assess whether extreme stress simply overwhelms the buffering capacity of diversity (Cadotte et al., 2011). Importantly, future studies should aim to account for the interactive effects of multiple stressors, including fire, pests, land use, and climate extremes, to develop a more realistic understanding of ecosystem vulnerability (Gonzalez et al., 2010; Laurance et al., 2011; Stork et al., 2009).

Finally, bridging science and practice will be essential for translating these insights into meaningful conservation and management outcomes. The remote sensing methods and trait-based frameworks developed in this thesis can be developed into operational tools for forest managers to monitor functional diversity and resilience in real time. Field-based experiments designed to test adaptive management interventions, such as fostering morphological diversity to enhance climate resilience, can validate theoretical predictions and inform practical strategies. Integrating socioeconomic dimensions into future research will also be crucial to ensure that resilience-building measures are both ecologically effective and socially just (Cinner & Barnes, 2019), especially in forest ecosystems facing the dual pressures of environmental degradation and climate change. Together, these avenues offer a path toward more resilient forest ecosystems and more informed management in an era of rapid environmental transformation.

7.5. References

Aguirre-Gutiérrez, J., Rifai, S. W., Deng, X., ter Steege, H., Thomson, E., Corral-Rivas, J. J., Guimaraes, A. F., Muller, S., Klipel, J., Fauset, S., Resende, A. F., Wallin, G., Joly, C. A., Abernethy, K., Adu-Bredu, S., Alexandre Silva, C., de Oliveira, E. A., Almeida, D. R. A., Alvarez-Davila, E., … Malhi, Y. (2025). Canopy functional trait variation across Earth's tropical forests. *Nature*, 1–8. https://doi.org/10.1038/s41586-025-08663-2

Anderegg, W. R. L., Klein, T., Bartlett, M., Sack, L., Pellegrini, A. F. A., Choat, B., & Jansen, S. (2016). Meta-analysis reveals that hydraulic traits explain cross-species patterns of drought-induced tree mortality across the globe. *Proceedings of the National Academy of Sciences*, *113*(18), 5024–5029. https://doi.org/10.1073/pnas.1525678113

Anderegg, W. R. L., Konings, A. G., Trugman, A. T., Yu, K., Bowling, D. R., Gabbitas, R., Karp, D. S., Pacala, S., Sperry, J. S., Sulman, B. N., & Zenes, N. (2018). Hydraulic diversity of forests regulates ecosystem resilience during drought. *Nature*, *561*(7724), 538–541. https://doi.org/10.1038/s41586-018-0539-7

Burton, P. J., Jentsch, A., & Walker, L. R. (2020). The Ecology of Disturbance Interactions. *BioScience*, *70*(10), 854–870. https://doi.org/10.1093/biosci/biaa088

Cadotte, M. W., Carscadden, K., & Mirotchnick, N. (2011). Beyond species: Functional diversity and the maintenance of ecological processes and services. *Journal of Applied Ecology*, *48*(5), 1079–1087.

Cavender-Bares, J., Schneider, F. D., Santos, M. J., Armstrong, A., Carnaval, A., Dahlin, K. M., Fatoyinbo, L., Hurtt, G. C., Schimel, D., Townsend, P. A., Ustin, S. L., Wang, Z., & Wilson, A. M. (2022). Integrating remote sensing with ecology and evolution to advance biodiversity conservation. *Nature Ecology & Evolution*, *6*(5), 506–519. https://doi.org/10.1038/s41559-022-01702-5

Cinner, J. E., & Barnes, M. L. (2019). Social Dimensions of Resilience in Social-Ecological Systems. *One Earth*, *1*(1), 51–56. https://doi.org/10.1016/j.oneear.2019.08.003

Dai, A. (2011). Drought under global warming: A review. *WIREs Climate Change*, *2*(1), 45–65. https://doi.org/10.1002/wcc.81

Dai, A. (2013). Increasing drought under global warming in observations and models. *Nature Climate Change*, *3*(1), 52–58. https://doi.org/10.1038/nclimate1633

Daly, A. J., Baetens, J. M., & De Baets, B. (2018). Ecological Diversity: Measuring the Unmeasurable. *Mathematics*, *6*(7), Article 7. https://doi.org/10.3390/math6070119

Enquist, B. J., Norberg, J., Bonser, S. P., Violle, C., Webb, C. T., Henderson, A., Sloat, L. L., & Savage, V. M. (2015). Chapter Nine - Scaling from Traits to Ecosystems: Developing a General Trait Driver Theory via Integrating Trait-Based and Metabolic Scaling Theories. In S. Pawar, G. Woodward, & A. I. Dell (Eds.), *Advances in Ecological Research* (Vol. 52, pp. 249–318). Academic Press. https://doi.org/10.1016/bs.aecr.2015.02.001

Faucon, M.-P., Houben, D., & Lambers, H. (2017). Plant Functional Traits: Soil and Ecosystem Services. *Trends in Plant Science*, *22*(5), 385–394. https://doi.org/10.1016/j.tplants.2017.01.005

Gonzalez, P., Neilson, R. P., Lenihan, J. M., & Drapek, R. J. (2010). Global patterns in the vulnerability of ecosystems to vegetation shifts due to climate change. *Global Ecology and Biogeography*, *19*(6), 755–768. https://doi.org/10.1111/j.1466-8238.2010.00558.x

Hashemi, M., & Karimi, H. A. (2020). Weighted Machine Learning for Spatial-Temporal Data. *IEEE Journal of Selected Topics in Applied Earth Observations and Remote Sensing*, *13*, 3066–3082. https://doi.org/10.1109/JSTARS.2020.2995834

Hauser, L. T., Féret, J.-B., An Binh, N., van der Windt, N., Sil, Â. F., Timmermans, J., Soudzilovskaia, N. A., & van Bodegom, P. M. (2021). Towards scalable estimation of

plant functional diversity from Sentinel-2: In-situ validation in a heterogeneous (semi-)natural landscape. *Remote Sensing of Environment*, *262*, 112505. https://doi.org/10.1016/j.rse.2021.112505

Hu, Y., Xiang, W., Schäfer, K. V. R., Lei, P., Deng, X., Forrester, D. I., Fang, X., Zeng, Y., Ouyang, S., Chen, L., & Peng, C. (2022). Photosynthetic and hydraulic traits influence forest resistance and resilience to drought stress across different biomes. *Science of The Total Environment*, *828*, 154517. https://doi.org/10.1016/j.scitotenv.2022.154517

Hubau, W., Lewis, S. L., Phillips, O. L., Affum-Baffoe, K., Beeckman, H., Cuní-Sanchez, A., Daniels, A. K., Ewango, C. E. N., Fauset, S., Mukinzi, J. M., Sheil, D., Sonké, B., Sullivan, M. J. P., Sunderland, T. C. H., Taedoumg, H., Thomas, S. C., White, L. J. T., Abernethy, K. A., Adu-Bredu, S., … Zemagho, L. (2020). Asynchronous carbon sink saturation in African and Amazonian tropical forests. *Nature*, *579*(7797), 80–87. https://doi.org/10.1038/s41586-020-2035-0

Kokaly, R. F., Asner, G. P., Ollinger, S. V., Martin, M. E., & Wessman, C. A. (2009). Characterizing canopy biochemistry from imaging spectroscopy and its application to ecosystem studies. *Remote Sensing of Environment*, *113*, S78–S91. https://doi.org/10.1016/j.rse.2008.10.018

Laurance, W. F., Dell, B., Turton, S. M., Lawes, M. J., Hutley, L. B., McCallum, H., Dale, P., Bird, M., Hardy, G., Prideaux, G., Gawne, B., McMahon, C. R., Yu, R., Hero, J.-M., Schwarzkopf, L., Krockenberger, A., Douglas, M., Silvester, E., Mahony, M., … Cocklin, C. (2011). The 10 Australian ecosystems most vulnerable to tipping points. *Biological Conservation*, *144*(5), 1472–1480. https://doi.org/10.1016/j.biocon.2011.01.016

Lucas, R., Armston, J., Fairfax, R., Fensham, R., Accad, A., Carreiras, J., Kelley, J., Bunting, P., Clewley, D., Bray, S., Metcalfe, D., Dwyer, J., Bowen, M., Eyre, T., Laidlaw, M., &

Shimada, M. (2010). An Evaluation of the ALOS PALSAR L-Band Backscatter—Above Ground Biomass Relationship Queensland, Australia: Impacts of Surface Moisture Condition and Vegetation Structure. *IEEE Journal of Selected Topics in Applied Earth Observations and Remote Sensing*, *3*(4), 576–593. https://doi.org/10.1109/JSTARS.2010.2086436

Méndez, M., & Magaña, V. (2010). *Regional Aspects of Prolonged Meteorological Droughts over Mexico and Central America*. https://doi.org/10.1175/2009JCLI3080.1

Oliver, T. H., Heard, M. S., Isaac, N. J. B., Roy, D. B., Procter, D., Eigenbrod, F., Freckleton, R., Hector, A., Orme, C. D. L., Petchey, O. L., Proença, V., Raffaelli, D., Suttle, K. B., Mace, G. M., Martín-López, B., Woodcock, B. A., & Bullock, J. M. (2015). Biodiversity and Resilience of Ecosystem Functions. *Trends in Ecology & Evolution*, *30*(11), 673–684. https://doi.org/10.1016/j.tree.2015.08.009

Omasa, K., Hosoi, F., & Konishi, A. (2007). 3D lidar imaging for detecting and understanding plant responses and canopy structure. *Journal of Experimental Botany*, *58*(4), 881–898. https://doi.org/10.1093/jxb/erl142

O'Shaughnessy, K. A., Knights, A. M., Hawkins, S. J., Hanley, M. E., Lunt, P., Thompson, R. C., & Firth, L. B. (2023). Metrics matter: Multiple diversity metrics at different spatial scales are needed to understand species diversity in urban environments. *Science of The Total Environment*, *895*, 164958. https://doi.org/10.1016/j.scitotenv.2023.164958

Pause, M., Schweitzer, C., Rosenthal, M., Keuck, V., Bumberger, J., Dietrich, P., Heurich, M., Jung, A., & Lausch, A. (2016). In Situ/Remote Sensing Integration to Assess Forest Health—A Review. *Remote Sensing*, *8*(6), Article 6. https://doi.org/10.3390/rs8060471

Qi, M., Liu, X., Li, Y., Song, H., Yin, Z., Zhang, F., He, Q., Xu, Z., & Zhou, G. (2021). Photosynthetic resistance and resilience under drought, flooding and rewatering in

maize plants. *Photosynthesis Research*, *148*(1–2), 1–15. https://doi.org/10.1007/s11120-021-00825-3

Rangel, T. F., Diniz-Filho, J. A. F., & Bini, L. M. (2010). SAM: A comprehensive application for Spatial Analysis in Macroecology. *Ecography*, *33*(1), 46–50. https://doi.org/10.1111/j.1600-0587.2009.06299.x

Roberts, D. R., Bahn, V., Ciuti, S., Boyce, M. S., Elith, J., Guillera-Arroita, G., Hauenstein, S., Lahoz-Monfort, J. J., Schröder, B., Thuiller, W., Warton, D. I., Wintle, B. A., Hartig, F., & Dormann, C. F. (2017). Cross-validation strategies for data with temporal, spatial, hierarchical, or phylogenetic structure. *Ecography*, *40*(8), 913–929. https://doi.org/10.1111/ecog.02881

Seddon, N., Chausson, A., Berry, P., Girardin, C. A. J., Smith, A., & Turner, B. (2020). Understanding the value and limits of nature-based solutions to climate change and other global challenges. *Philosophical Transactions of the Royal Society B: Biological Sciences*, *375*(1794), 20190120. https://doi.org/10.1098/rstb.2019.0120

Seddon, N., Daniels, E., Davis, R., Chausson, A., Harris, R., Hou-Jones, X., Huq, S., Kapos, V., Mace, G. M., Rizvi, A. R., Reid, H., Roe, D., Turner, B., & Wicander, S. (2020). Global recognition of the importance of nature-based solutions to the impacts of climate change. *Global Sustainability*, *3*, e15. https://doi.org/10.1017/sus.2020.8

Seddon, N., Smith, A., Smith, P., Key, I., Chausson, A., Girardin, C., House, J., Srivastava, S., & Turner, B. (2021). Getting the message right on nature-based solutions to climate change. *Global Change Biology*, *27*(8), 1518–1546. https://doi.org/10.1111/gcb.15513

Sequeira, A. M. M., Bouchet, P. J., Yates, K. L., Mengersen, K., & Caley, M. J. (2018). Transferring biodiversity models for conservation: Opportunities and challenges. *Methods in Ecology and Evolution*, *9*(5), 1250–1264. https://doi.org/10.1111/2041-210X.12998

Stahle, D. W., Cook, E. R., Díaz, J. V., Fye, F. K., Burnette, D. J., Griffin, D., Soto, R. A., Seager, R., & Heim Jr., R. R. (2009). Early 21st-Century Drought in Mexico. *Eos, Transactions American Geophysical Union*, *90*(11), 89–90. https://doi.org/10.1029/2009EO110001

Stork, N. E., Coddington, J. A., Colwell, R. K., Chazdon, R. L., Dick, C. W., Peres, C. A., Sloan, S., & Willis, K. (2009). Vulnerability and Resilience of Tropical Forest Species to Land-Use Change. *Conservation Biology*, *23*(6), 1438–1447. https://doi.org/10.1111/j.1523-1739.2009.01335.x

Thenkabail, P. S., Lyon, J. G., & Huete, A. (2018). *Biophysical and biochemical characterization and plant species studies*. CRC Press.

Trenberth, K. E., Dai, A., van der Schrier, G., Jones, P. D., Barichivich, J., Briffa, K. R., & Sheffield, J. (2014). Global warming and changes in drought. *Nature Climate Change*, *4*(1), 17–22. https://doi.org/10.1038/nclimate2067

Wang, Y., Khodadadzadeh, M., & Zurita-Milla, R. (2023). Spatial+: A new cross-validation method to evaluate geospatial machine learning models. *International Journal of Applied Earth Observation and Geoinformation*, *121*, 103364. https://doi.org/10.1016/j.jag.2023.103364

Weed, A. S., Ayres, M. P., & Hicke, J. A. (2013). Consequences of climate change for biotic disturbances in North American forests. *Ecological Monographs*, *83*(4), 441–470. https://doi.org/10.1890/13-0160.1

Yang, W., Deng, M., Tang, J., & Luo, L. (2023). Geographically weighted regression with the integration of machine learning for spatial prediction. *Journal of Geographical Systems*, *25*(2), 213–236. https://doi.org/10.1007/s10109-022-00387-5

Yates, K. L., Bouchet, P. J., Caley, M. J., Mengersen, K., Randin, C. F., Parnell, S., Fielding, A. H., Bamford, A. J., Ban, S., Barbosa, A. M., Dormann, C. F., Elith, J., Embling, C. B.,

Ervin, G. N., Fisher, R., Gould, S., Graf, R. F., Gregr, E. J., Halpin, P. N., … Sequeira, A. M. M. (2018). Outstanding Challenges in the Transferability of Ecological Models. *Trends in Ecology & Evolution*, *33*(10), 790–802. https://doi.org/10.1016/j.tree.2018.08.001